Cape Peninsula
University of Technology

IEC 61850 STANDARD-BASED PROTECTION OF THE COUPLING POINT BETWEEN A WIND FARM AND THE POWER GRID

by

Sinawo Nomandela

Thesis submitted in fulfilment of the requirements for the degree

Master of Engineering: Electrical Engineering

in the Faculty of Engineering and the Built Environment

at the Cape Peninsula University of Technology

Supervisor: Mr. Ratshitanga
Co-supervisor: Dr. Mnguni

Bellville
January 2021

DECLARATION

I, Sinawo Nomandela, declare that the contents of this dissertation/thesis represent my own unaided work, and that the dissertation/thesis has not previously been submitted for academic examination towards any qualification. Furthermore, it represents my own opinions and not necessarily those of the Cape Peninsula University of Technology.

21 August 2021

Signed **Date**

ABSTRACT

Power system aims to continuously supply power to customers even at very high demand. The high energy demand causes a decrease in voltages at the substations and this may cause the voltage collapse in the power system, which in turn may cause a total system shutdown if not attended to. Since the increased load demand becomes a major cause of voltage collapse in power systems, additional power sources, namely wind power plants are of recommendation and this is due to their reactive power contribution to the power systems. Wind power plants improve the reliability of the power system by supplying power to the grid when load demand is too high, while at the same time withstanding some of the natural power system disturbances, namely short-circuit faults and sudden increase in load demand.

Power quality is one of the power system requirements when integrating wind power plants into the existing power grid. The general wind power plant operational mode is that a wind generator should be disconnected from the grid when its output voltage goes below or above by ten percent from its rated voltage. Due to uncontrollable wind speed, wind generators produce fluctuating power leading to the tripping off of the generating unit. The fluctuating power from the wind generators appears on the grid side, reducing the reliability of the existing protective devices set for the system.

This thesis makes use of the IEEE Nine-Bus system modelled and simulated using the Real-time Simulation Computer-Aided Design (RSCAD) whose simulations are in real-time with the support of the Real-Time Digital Simulator (RTDS). Using the simulated power system network, contingency studies are conducted in terms of the load demand increase to calculate the additional power requirements. A wind power plant (WPP) is also modelled using the same modelling and simulation platform and coupled into the power system in compensation of the additional load demand. Most importantly, the IEC 61850 standard-based protection scheme is developed for the coupling point of a wind power plant to the power. This protection scheme is adaptive for both load conditions of the system when the wind power plant is coupled into the power system.

Keywords: Distributed Energy Renewables, grid codes, integration, point of common coupling, adaptive protection scheme, IEC 61850 Standard, Intelligent Electronic Device, Real-Time Digital Simulator, Hardware-In-Loop

ACKNOWLEDGEMENTS

I wish to thank:

- I wish to thank my supervisors for their support.
- All the members of the Center for Substation Automation and Energy Management Systems (CSAEMS) for their motivation.

DEDICATION

This thesis is dedicated to my mother Lindiwe Nomandela.

TABLE OF CONTENTS

DECLARATION ii
ABSTRACT iii
ACKNOWLEDGEMENTS i
TABLE OF CONTENTS iii
CHAPTER ONE 1
INTRODUCTION 1
1.1 Introduction 1
1.2 Awareness of the problem 2
1.3 Problem statement 3
1.4 Research aims and objectives 4
1.5 Hypothesis 5
1.6 Delimitation of research 6
1.7 The motivation of the research problem 6
1.8 Assumptions 7
1.9 Research design and methodology 8
1.9.1 Literature review 8
1.9.2 Modelling and simulation 10
1.9.3 Documentation method 10
1.10 Conclusion 11
CHAPTER TWO 12
LITERATURE REVIEW 12
2.1 Introduction 12
2.2 Background 12
2.3 The wind farm 14
2.4 The wind farm coupling point 15
2.5 Protection overview in wind farms 15
2.5.1 Electrical faults in wind power plants: an overview 15
2.5.2 Protection challenges within wind power plants 15
2.6 Wind farm point of common coupling protection 17
2.6.1 Overview 17
2.6.2 Adaptive protection scheme 19
2.6.3 Distance protection 20
2.6.4 Directional overcurrent protection 21
2.6.5 Differential overcurrent protection 22
2.7 Wind power plant protection challenges and solutions - review 22
2.7.1 Traditional methods 23
2.7.2 Numerical and IEC 61850 standard-based methods 30
2.7.3 Strictly numerical point of common coupling protection 34
2.8 Remarks and observations 36
2.9 The proposed method 38
2.10 Conclusions 38
CHAPTER THREE 39
THEORETICAL FRAMEWORK 39

3.1 Introduction 39
3.2 Power system protection 39
3.2.1 Digital relays 39
3.2.2 Protection schemes for coupling stations 40
3.2.3 Busbar protection 40
3.2.4 Busbar protection requirements 41
3.2.5 Busbar differential protection 41
3.2.6 External and internal fault conditions 43
3.2.7 The practical operation of a differential protection scheme 44
3.2.8 Effects of the wind power plant on the differential protection scheme 46
3.3 Types of wind power plants 47
3.4 Voltage stability 48
3.4.1 Voltage stability concepts 48
3.4.2 Voltage stability analysis 49
3.4.3 Modelling requirements 50
3.5 Prevention of voltage collapse 50
3.5.1 System design measures 50
3.5.2 System-operating measures 50
3.6 Substation automation system 51
3.6.1 IEC 61850 standard 51
3.6.2 IEC 61850 standard protocols 52
3.6.3 Object model 54
3.6.4 Timestamps and quality 55
3.6.5 Communication 55
3.6.6 IEC 61850 standard's benefits 56
3.6.7 Substation Configuration Language (SCL) 58
CHAPTER FOUR 59
MODELLING AND SIMULATION OF THE POWER SYSTEM NETWORK ON RSCAD . 59
4.1 Introduction 59
4.2 The power system network model 59
4.3 Design of logic diagrams for control and monitoring of network quantities .. 61
4.3.1 Monitoring and calculation logics for generator quantities 62
4.3.2 Monitoring and calculation logics for busbars 65
4.3.3 Control, monitoring and calculation logics for dynamic load quantities . 67
4.4 Load flow analysis 69
4.5 The steady-state power flow analysis on RSCAD runtime module 70
4.5.1 Generators or station monitoring 70
4.5.2 Monitoring on load busbars and loads 71
4.5.3 The simplified network system 72
4.6 Load demand increase contingency 73
4.6.1 Overload contingency logic 73

4.6.2 System overloading contingency 74
4.7 Discussion of results 80
4.8 Conclusion 81
CHAPTER FIVE 82
MODELLING OF THE WIND POWER PLANT FOR POWER GRID INTEGRATION ON RSCAD 82
5.1 Introduction 82
5.2 The wind power plant model 82
5.2.1 Wind turbine model 82
5.2.2 Induction generator modelling 89
5.2.3 WTGSUT and medium to high-voltage transformer selection 95
5.2.4 Wind power plant high-voltage transmission line modelling 95
5.2.5 The wind power plant reactive power support device 96
5.3 The wind power plant steady-state load flow simulation 99
5.4 Wind power plant islanded mode of operation 100
5.4.1 Load model under test control modelling 101
5.4.2 Wind power plant power loading 102
5.5 Discussion of results 104
5.6 Conclusion 104
CHAPTER SIX 106
DEVELOPMENT OF THE PROTECTION SCHEME FOR THE INTERCONNECTED SYSTEM 106
6.1 Introduction 106
6.2 The hardware requirements of the designed protection scheme test 106
6.2.1 Analog amplifiers 106
6.2.2 The SEL-487B Protection Automation Control 106
6.3 Modelling of the signalling devices for the scheme on RSCAD 114
6.3.1 Current transformer selection, modelling and configuration 114
6.3.2 Capacitor voltage transformer selection, modelling, and configuration 118
6.3.3 GTAO cards modelling and configuration 120
6.3.4 Configuration of the low-voltage digital interface and its control logic . 123
6.3.5 Modelling and configuration of the fault logics for Bus 2 125
6.4 The interconnected network system with controls components 128
6.5 Device configuration 132
6.5.1 Renaming (aliasing) terminals and bus zones 132
6.5.2 Assigning input contacts 132
6.5.3 Instrument transformer configuration 133
6.5.4 Differential, directional and definite overcurrent elements configuration 135
6.6 Hard-wired protection scheme test 143
6.6.1 315 MW loading 144
6.6.2 420 MW loading 150

6.7 Summary of results 157
6.8 Conclusion 158
CHAPTER SEVEN 159
THE IMPLEMENTATION OF THE IEC 61850 STANDARD-BASED COMMUNICATION 159
7.1 Introduction 159
7.2 Hardware-in-loop test setup for an IEC 61850 standard-based protection scheme 160
7.2.1 Engineering configuration of GOOSE messages for SEL-487B device .. 161
7.2.2 Configuration of the RTDS GTnet GSE for GOOSE status event 173
7.3 IEC 61850 standard-based protection scheme test 179
7.3.1 315 MW loading 179
7.3.2 420 MW loading 185
7.4 Summary of results 191
7.5 Conclusion 192
CHAPTER EIGHT 193
DELIVERABLES, CONCLUSIONS AND RECOMMENDATIONS 193
8.1 Introduction 193
8.2 Thesis deliverables 194
8.2.1 Literature review 194
8.2.2 Theoretical framework 194
8.2.3 Modelling and simulation of the IEEE Nine-bus system on RSCAD 194
8.2.4 Modelling and simulation of the wind power plant on RSCAD 194
8.2.5 Modelling and simulation of coupled WPP into the IEEE Nine-bus system 194
8.3 Conclusions 195
8.3.1 The development of a protection scheme for the coupled system 195
8.3.2 Advancement of the developed protection scheme 195
8.3.3 Testing of the developed protection scheme 196
8.4 Academic and industrial application 196
8.5 Future work 196
8.6 Publication 197
BIBLIOGRAPHY 198
APPENDICES 203
APPENDIX A 203
THE IEEE NINE-BUS SYSTEM PARAMETERS 203
A.1 System data 203
A.2 Forceful data 204
A.3 Synchronous generator excitation and propelling model 205
APPENDIX B 207
THE SYSTEM LOAD SCHEDULER 207
B.1 Dynamic Load 1 (DLoad1) Typical settings 207
APPENDIX C 211
THE WIND POWER PLANT DATA 211
C.1 Vestas wind turbine operating data and rotor data 211

C.2 Wind turbine generator data 212
APPENDIX D 213
SEL-487B ALIAS AND INPUT CONTACT SETTING PARAMETERS 213
D.1 Assign input contacts. (Typical Example for all terminals) 213
APPENDIX E 214
EVENT REPORTS FOR FAULTS AT BUS 2 DUE TO HARD-WIRED TRIP SIGNAL 214
E.1 Events extracted at 315 MW loading 214
E.1.1 Red phase to ground fault 214
E.1.2 Three-phase fault 215
E.2 Events extracted at 420 MW loading 216
E.2.1 Red phase to ground fault 216
E.2.2 Three-phase fault 217
APPENDIX F 219
EVENT REPORTS FOR FAULTS AT BUS 2 DUE TO GOOSE TRIP SIGNAL 219
F.1 Events extracted at 315 MW 219
F.1.1 Red phase to ground fault 219
F.1.2 Three-phase fault 220
F.2 Events extracted at 420 MW 221
F.2.1 Red phase to ground fault 221
F.2.2 Three-phase fault 222
APPENDIX G 224
THE HARDWARE-IN-LOOP (HIL) TEST BENCH SET-UP 224

LIST OF FIGURES

Figure 2.1: The global wind energy installation capacity with effect from 1996 to 2011 (Nahhas, 2013) 12
Figure 2.2: Wind farm with possible coupling points (Gupta, 2018) 14
Figure 2.3: Wind turbine generator fault ride-through capability (Gashi et al., 2012) ... 16
Figure 2.4: Wind farm collector circuit (Jones & Bennett, 2012) 18
Figure 2.5: 500 kV system (Sun et al., 2018) 25
Figure 2.6: Wind farm model showing the collector circuit of 35 kV/110 kV voltage (Zhang et al., 2013) 27
Figure 2.7: Protective relaying system with the FRT capability characteristic curve (Han et al., 2010) 28
Figure 2.8: Wind power plant with DC transmission system to the grid (Yang et al., 2010) 29
Figure 2.9: Panama wind power plant with a double collector circuit zig-zag grounded (Alcázar et al., 2016) 30
Figure 2.10: Communication architecture for smart wind power plants (Ahmed & Kim, 2014) 33
Figure 2.11: Numerical busbar protection scheme (Tart et al., 2010) 35
Figure 2.12: The protection logic for a bus differential protection with an advance zone selection (Guzmán et al., 2005) 36

Figure 3.1: Simple differential protection scheme with parallel feeders monitored by parallel current transformers (Behrendt et al., 2010). 42
Figure 3.2: External or through fault conditions (Andrichak & Cardenas, 1995) 44
Figure 3.3: Internal fault conditions (Andrichak & Cardenas, 1995) 44
Figure 3.4: Current transformer exposed to saturation under external fault for a percentage restrained differential relay (Andrichak & Cardenas, 1995) 45
Figure 3.5: Interface model of a substation automation system (IEC, 2003) 52
Figure 3.6: An IEC 61850 standard object model (Brand, 2005) 54
Figure 3.7: The communication stack for message services (Samitier, 2017) 55
Figure 3.8: Conventional connection between the process and the bay level 57
Figure 3.9: IEC 61850 standard-based connection between the process and the bay level 57

Figure 4.1: IEEE Nine-Bus system 59
Figure 4.2: Sectionalized IEEE Nine-Bus system with new busbar labels 60
Figure 4.3: Area 1 of the IEEE Nine-Bus system in Subsystem 1 (Rack 1) 60
Figure 4.4: Area 2 of the IEEE Nine-Bus system in Subsystem 2 (Rack 2) 61

Figure 4.5: Calculation and monitoring logics for Gen1 63
Figure 4.6: Generator1 P and Q signals to be monitored 64
Figure 4.7: Generator1 and its governor modelled in Subsystem 1 65
Figure 4.8: Bus 1 monitoring and calculation logics 66
Figure 4.9: Reactive power, power factor, apparent power and active power calculation logic for Bus 2 67
Figure 4.10: Power factor, apparent power, RMS voltage, per-unit voltage and RMS current calculation logic for DLoad1 68
Figure 4.11: The RSCAD draft load flow simulation results 69
Figure 4.12: Simplified power system network under steady-state conditions 72
Figure 4.13: RSCAD dynamic load, control logic for automatic power scheduling 73
Figure 4.14: Bus 1 per-unit voltage waveform 74
Figure 4.15: Bus 2 per-unit voltage waveform 75
Figure 4.16: Bus 3 per-unit voltage waveform 76
Figure 4.17: Bus 4 per-unit voltage waveform 76
Figure 4.18: Bus 5 per-unit voltage waveform 77
Figure 4.19: Bus 6 per-unit voltage waveform 78
Figure 4.20: Active power demand by DLoad1 from Bus 2 and active power demanded by Bus 2 from the system 79
Figure 4.21: Reactive power demand by DLoad1 from Bus 2 and active power demanded by Bus 2 from the system 79

Figure 5.1: RSCAD wind turbine model 83
Figure 5.2: Power coefficient of the wind turbine (Cp) 84
Figure 5.3: Rotor radius and gearbox ratio settings 86
Figure 5.4: Generator rated complex power in MVA, rated frequency as well as the generator speed in rpm 87
Figure 5.5: Turbine blades pitch angle and wind speed adjustment and calculation logics 87
Figure 5.6: Induction generator model with the exciter component 89
Figure 5.7: Induction generator mechanical parameters 90
Figure 5.8: Logic for wind turbine generator per-unit speed control 93
Figure 5.9: Excitation circuit control, monitoring and calculation logics 94
Figure 5.10: Wind power plant transmission line system data parameter settings 95
Figure 5.11: WPP terminal reactive power compensator device model settings parameters 97
Figure 5.12: WPP terminal reactive power compensator phase current monitoring settings 97

Figure 5.13: Calculation logic for reactive power injection using the RMS voltage and current 98
Figure 5.14: Frequency and the per-unit voltage monitoring and calculation logic 99
Figure 5.15: Logic for switching between the active and reactive component of the load 101

Figure 6.1: Differential element logic for an SEL-487B Relay 109
Figure 6.2: Filtered differential element logic 109
Figure 6.3: A differential characteristic curve with two slopes 110
Figure 6.4: Directional overcurrent logic for a red-phase 111
Figure 6.5: Directional element characteristic curve 111
Figure 6.6: Fault detection logic – external or internal fault 112
Figure 6.7: Differential protection output element logic 112
Figure 6.8: Main data parameter settings for CT1 116
Figure 6.9: Secondary winding series resistance and the primary winding turns ratio settings for CT1 117
Figure 6.10: Settings for burden resistance of the CT 117
Figure 6.11: Voltage signal names monitored on Bus 2 118
Figure 6.12: Default settings for CVT1 Ferro-resonance filter 119
Figure 6.13: Default settings for CVT data 119
Figure 6.14: Default settings for CVT secondary windings burden parameters 119
Figure 6.15: Default settings for CVT main data 120
Figure 6.16: GTAO1 card in Subsystem 1 for CT1, CT2 and CVT1 secondary voltages and currents 121
Figure 6.17: GTAO1 scaling settings 122
Figure 6.18: GTAO2 card in Subsystem 3 for CT3 and CT4 secondary currents 122
Figure 6.19: Analog current signal scaling for GTAO2 123
Figure 6.20: BRKOne settings – signal named to control breaker 124
Figure 6.21: GTFPI model and circuit breaker control logic 124
Figure 6.22: Settings to define the fault control signals 125
Figure 6.23: Fault logic to control a single-phase-to-ground fault 126
Figure 6.24: Settings to define the fault control signals 127
Figure 6.25: Fault logic to control a three-phase fault 127
Figure 6.26: Area 2 of the modified power system network model in Subsystem 2 (Rack 2) 128
Figure 6.27: Area1 of the modified power system network model in Subsystem 1 (Rack1) 130
Figure 6.28: The coupled system – WPP Group 1 Area 3 Subsystem 3 (Rack 3) 131

Figure 6.29: The coupled system – WPP Group 2 area 4 Subsystem 4 (Rack 4) 131
Figure 6.30: The coupled system – WPP Group 3 area 5 Subsystem 5 (Rack 5) 131
Figure 6.31: SEL-487B relay Group 1 instrument transformer settings 134
Figure 6.32: SEL-487B relay Group 1 TAPs calculated by the AcSELerator Quickset software 134
Figure 6.33: HMI fundamental metering using Group 1 settings under 315 MW load demand 135
Figure 6.34: HMI fundamental metering using Group 1 settings under 420 MW load demand 136
Figure 6.35: HMI differential and restraint currents monitoring at 315 MW load demand 137
Figure 6.36: HMI differential and restraint currents monitoring at 420 MW load demand 137
Figure 6.37: Group 1 filtered differential and phase direction overcurrent element settings 138
Figure 6.38: Group 2 filtered differential and phase direction overcurrent element settings 139
Figure 6.39: SEL-487B relay Group 1 and Group 2 selection logic 140
Figure 6.40: Settings group control word bits 140
Figure 6.41: Phase definite time overcurrent pickup settings entered under Group 1 Settings..... 142
Figure 6.42: Filtered differential element trip condition for Group 1 settings 142
Figure 6.43: Filtered differential element trip bits for all group settings..... 143
Figure 6.44: Branch currents and Bus 2 voltage for R-G fault at Bus 2 under 315 MW 145
Figure 6.45: WPP receiving-end voltage for R-G fault at Bus 2 under 315 MW 146
Figure 6.46: CB-received hard-wired trip command for R-G fault at Bus 2 under 315 MW 147
Figure 6.47: Branch currents and Bus 2 voltage for 3Ph fault at Bus 2 under 315 MW 148
Figure 6.48: WPP receiving-end voltage for 3Ph fault at Bus 2 under 315 MW 149
Figure 6.49: CB-received hard-wired trip command for 3Ph fault at Bus 2 under 315 MW 150
Figure 6.50: Branch currents and Bus 2 voltage for R-G fault at Bus 2 under 420 MW 152
Figure 6.51: WPP receiving-end voltage for R-G fault at Bus 2 under 420 MW 153
Figure 6.52: CB-received hard-wired trip command for R-G fault at Bus 2 under 420 MW 154

Figure 6.53: Branch currents and Bus 2 voltage for 3Ph fault at Bus 2 under 420 MW 155
Figure 6.54: WPP receiving-end voltage for 3Ph fault at Bus 2 under 420 MW 156
Figure 6.55: CB-received hard-wired trip command for 3Ph fault at Bus 2 under 420 MW 157

Figure 7.1: IEC 61850 standard-based HIL interface of the IED and RTDS 160
Figure 7.2: AcSELerator Architect main menu 162
Figure 7.3: AcSELerator Architect – IED 163
Figure 7.4: IED selection 163
Figure 7.5: Renaming project 164
Figure 7.6: Renamed project 165
Figure 7.7: Defined IED properties 166
Figure 7.8: Definition of datasets 166
Figure 7.9: Existing data attributes 167
Figure 7.10: Addition of specific data attributes 167
Figure 7.11: GOOSE transmit definition and settings 168
Figure 7.12: Mapping for transportation of data sets over GOOSE transmit 169
Figure 7.13: Complete transport of the logical node 169
Figure 7.14: Device communication test – device responding 170
Figure 7.15: Sending of the CID file to the physical IED 170
Figure 7.16: Publishing IED network settings confirmation 171
Figure 7.17: CID file sending information 171
Figure 7.18: GOOSE message datasets 172
Figure 7.19: Detailed GOOSE message updates 173
Figure 7.20: GTnet placement 174
Figure 7.21: GTnet placement – modelling of the IEC 61850 SCD file 175
Figure 7.22: Mapping of the IED datasets for GOOSE transmission by the GTnet IED 176
Figure 7.23: Definition of GTnet input signals 177
Figure 7.24: GTnet to word-to-bit converter interface 178
Figure 7.25: Circuit breaker control logic 178
Figure 7.26: Branch currents and Bus 2 voltage for R-G fault at Bus 2 under 315 MW 180
Figure 7.27: WPP receiving-end voltage for R-G fault at Bus 2 under 315 MW 181
Figure 7.28: CB-received GOOSE trip command for R-G fault at Bus 2 under 315 MW 182

Figure 7.29: Branch currents and Bus 2 voltage for 3Ph fault at Bus 2 under 315 MW 183
Figure 7.30: WPP receiving-end voltage for 3Ph fault at Bus 2 under 315 MW 184
Figure 7.31: CB-received GOOSE trip command for 3Ph fault at Bus 2 under 315 MW 184
Figure 7.32: Branch currents and Bus 2 voltage for R-G fault at Bus 2 under 420 MW 186
Figure 7.33: WPP receiving-end voltage for R-G fault at Bus 2 under 420 MW 187
Figure 7.34: CB-received GOOSE trip command for R-G fault at Bus 2 under 420 MW 188
Figure 7.35: Branch currents and Bus 2 voltage for 3Ph fault at Bus 2 under 420 MW 189
Figure 7.36: WPP receiving-end voltage for 3Ph fault at Bus 2 under 420 MW 190
Figure 7.37: CB-received GOOSE trip command for 3Ph fault at Bus 2 under 420 MW 191

Figure A.1: Synchronous generator exciter model 205
Figure A.2: synchronous machine governor or propeller model..... 205

Figure B.1: Dynamic Load 1 scheduler configuration settings..... 207
Figure B.2: Dynamic Load 1 (1-10) schedule (time and values) configuration settings 208
Figure B.3: Dynamic Load 1 (10-20) schedule (time and values) configuration settings 209
Figure B.4: Dynamic Load 1 (20-30) schedule (time and values) configuration settings 210

Figure D.1: Terminal 1 to bus-zone connections..... 213

Figure E.1: Event for Red-phase-to-ground fault at Bus 2 – analogs and digitals..... 214
Figure E.2: Event for Red-phase-to-ground fault at Bus 2 – group 1 settings operated 215
Figure E.3: Event for three-phase fault at Bus 2 – analogs and digitals 215
Figure E.4: Event for three-phase fault at Bus 2 – group 1 settings operated 216
Figure E.5: Event for Red-phase-to-ground fault at Bus 2 – analogs and digital..... 216
Figure E.6: Event for Red-phase-to-ground fault at Bus 2 – group 2 settings operated 217
Figure E.7: Event for three-phase fault at Bus 2 – analogs and digitals 217
Figure E.8: Event for three-phase fault at Bus 2 – group 2 settings operated 218

Figure F.1: Event for Red-phase-to-ground fault at Bus 2 – analogs and digitals 219
Figure F.2: Event for Red-phase-to-ground fault at Bus 2 – group 1 settings operated 220
Figure F.3: Event for three-phase fault at Bus 2 – analogs and digitals 220
Figure F.4: Event for three-phase fault at Bus 2 – group 1 settings operated..... 221
Figure F.5: Event for Red-phase-to-ground fault at Bus 2 – group 2 settings operated 221
Figure F.6: Event for Red-phase-to-ground fault at Bus 2 – group 2 settings operated 222
Figure F.7: Event for three-phase fault at Bus 2 – analogs and digitals 222
Figure F.8: Event for three-phase fault at Bus 2 – group 2 settings operated..... 223

Figure G.1: The HIL test bench setup for the developed protection scheme test in Chapter 6 224

LIST OF TABLES

Table 2.1: Zones of protection with their types of protection (Cardenas et al., 2010) .. 20

Table 3.1: SA Renewable Energy Grid Code Categories (Sewchurran & Davidson, 2017) 47

Table 4.1: Quantities to set and model for monitoring 62
Table 4.2: RSCAD draft load flow results 70
Table 4.3: Quantities monitored at Station 1 to 3 under steady-state power flow 70
Table 4.4: Busbars, 2, 3 and 5 Dload1, DLoad2 and DLoad3 monitored values at the steady-state power flow 71
Table 4.5: Currents monitored from the branches associated with the most significant busbars 72
Table 4.6: Bus 2 and DLoad1 quantities under a step-by-step load increase in the system 80

Table 5.1: Speed of the wind and the angular speed of the rotor 88
Table 5.2: Cp values at different pitch angle adjustments 89
Table 5.3: Steady-state simulation – aerodynamic and mechanical quantities for a WTGU 100
Table 5.4: Steady-state simulation - electrical quantities for WTGU 100
Table 5.5: Steady-state simulation - Wind power plant voltage and frequency 100
Table 5.6: Active and reactive load demand and current from the wind power plant. 102
Table 5.7: WPP active and reactive power values due to active power loading..... 103
Table 5.8: WPP terminal voltage and frequency monitored under active power loading 103
Table 5.9: Active and reactive load demand and current from the wind power plant. 103
Table 5.10: WPP active and reactive power values due to active power loading..... 104
Table 5.11: WPP terminal voltage and frequency monitored under active power loading 104

Table 6.1: Currents monitored during the absence and presence of the wind power plant with no contribution at 315 MW loading 115
Table 6.2: Currents monitored during the presence and contribution of the wind power plant at 420 MW system loading 115
Table 6.3: Terminals to zone configuration for the developed scheme using SEL-487B 133
Table 6.4: Determination of the value of the phase definite time overcurrent pickup for the condition of the load demand transition from 315 MW to 420 MW..... 141

Table 6.5: Protection scheme test procedure under 315 MW loading 144
Table 6.6: Protection scheme test procedure under 420 MW loading 151
Table 6.7: Fault event summary 157

Table 7.1: List of relay word bits and protection logical nodes for SEL-487B device 161
Table 7.2: Fault event summary 191

Table A.1: Initial power flow data 203
Table A.2: Transmission line data 203
Table A.3: Transformer data 204
Table A.4: Generator data 204
Table A.5: Generator data 204
Table A.6: Exciter data 206
Table A.7: Exciter data 206
Table A.8: Governor data 206

Table C.1: Wind turbine operating data 211
Table C.2: Wind turbine operating data 211
Table C.3: Squirrel-cage induction generator parameters (B. Wu, Y. Lang, N. Zargari, 2011) 212

GLOSSARY

Voltage stability: The condition in power systems, where the power system network can maintain its standard node (substation) voltages at the acceptable continuous operating range during its normal operation, even after it has been subjected to power system disturbances.

Voltage collapse: The condition in power systems, where the voltage can no longer recover after it has been fallen below or above the accepted operating range due to power system disturbances, namely faults and sudden increase or decrease in load demand.

Wind Power Plant: A group of wind turbine generators (WTGs) installed in the same area for power generation.

Wind Turbine Generators: A combination of wind turbines (WTs) and electrical generators. Sometimes referred to as Wind Turbine Generator Units (WTGUs). They form a primary stage of energy production in a wind power plant by converting the power extracted from the wind to electrical power.

Wind power plant coupling point: The point at which the wind power plant connects to the grid.

Adaptive protection scheme: The protection scheme that adapts to the conditions of the system and operates well regardless of the changing power system network parameters.

IED: A generic name given to various protection, control, metering and monitoring devices that are implemented from the microprocessor-based technology.

GSE: A communication protocol in the IEC 61850 standard. It is for high-speed control of messaging between IEDs.

GSSE: A control model in GSE protocol, which transports fixed structure binary events and bit pairs between IEDs.

GOOSE: A control model in GSE protocol, which transports any type of data between IEDs.

Interoperability: The ability of two or more IEDs, regardless of the vendor, to exchange data and use it for various functions, namely control, monitoring, protection and metering.

Busbar: A common connection point in a power system network substation.

Numerical relay: A relay capable of acquiring instantaneous samples of voltages and or currents and perform mathematical algorithms for control, monitoring, protection and metering.

Logical Device: It contains the information produced and consumed by a group of domain-specific application functions, that are defined as Logical Nodes.

Logical Node: A functional grouping of data and represents the smallest function, which may be implemented independently in the Logical Device.

ABBREVIATIONS/ACRONYMS

WPP	:	Wind Power Plant
SCIG	:	Squirrel-Cage Induction Generator
WTG	:	Wind Turbine Generator
WTGSU	:	Wind Turbine Generator Substation Unit
CT	:	Current Transformer
IEC	:	International Electrotechnical Commission
IED	:	Intelligent Electronic Device
SAS	:	Substation Automation System
LAN	:	Local Area Network
CVT	:	Capacitor Voltage Transformer
GSE	:	Generic Substation Event
GSSE	:	Generic Substation Status Event
GOOSE	:	Generic Object-Oriented Substation Event
PoCC	:	Point of Common Coupling

CHAPTER ONE
INTRODUCTION

1.1 Introduction

The electrical power system is the combination of electrical components arranged to supply, transfer and consume electric power. It consists of three distinct levels, namely the generation, transmission, and distribution levels. The generation level consists of three-phase synchronous generators that generate electric power at the nominal voltage of about 11 kV to 25 kV, depending on the utility standards. The power generated by these synchronous generators is then transmitted in a form of bulk power over the transmission lines by stepping up the generated medium voltage to high-level voltages for minimization of power losses along the transmission lines (Ray, 2007).

Power system disturbances occur and the load demand keeps changing over time. This may cause maloperation of protective devices and the out-of-range voltage fluctuation in the substations and may violate some of the power system requirements, namely security, and stability. When these challenges are left unattended, they cascade and eventually cause maloperation in the whole system.

The power system requires protection schemes to safeguard its components under the conditions of system disturbances like short-circuit faults. One of the principles of power system protection schemes is that not all of them must operate in the system when the fault occurs, only ones dedicated to that particular fault should operate. This is known as selectivity and is one of the most required features of the power system protection, as it ensures security.

When additional power sources are integrated onto the grid, protection schemes of high standards need to be developed. Various protection schemes are used at this level, mostly distance protection schemes for medium and long transmission lines, and differential current protection schemes for busbar units, short transmission lines, and high-voltage power transformers. In the case of the differential protection schemes, their security feature makes sure that they distinguish between external and internal faults. This guarantees a continuous supply of power to the unaffected areas of power systems while the affected areas are isolated.

Normally, power system faults are temporary and the load increase disturbance is usually long. When short-circuit faults occur, they leave certain areas or generators of

power systems isolated and this causes stress to the generators that are left connected, due to the power demanded by the remaining circuits to supply the loads.

The thesis looks at the security of protection for the point of common coupling between the wind power plant and the power grid. The developed protection scheme complies with the requirements of the electrical protection standard and satisfies the requirements of operational speed, reliability, security, and stability of power systems.

In this chapter, the awareness of the problem, problem statements, research aims and objectives, hypothesis, delimitation of research, the motivation of the study, assumptions as well as the methods used to conduct the study are discussed.

1.2 Awareness of the problem

Power is generated and transmitted over long distances using transmission lines. Long transmission lines, when heavily loaded, are rich in the reactive (magnetic) component which absorbs a large amount of reactive power along the run. This causes an effective difference between the reactive power at the receiving end and at the sending end terminals of the transmission lines, which in turn leads to a reduced voltage at the receiving end of the transmission line system (Ray, 2007). The same applies when the load connected to the substation demands the reactive power, the substation voltage will drop. Therefore, the lack of reactive power at the substation reduces the voltage at the terminal or substation.

The rapid growth in the generation of wind power, as well as the easy control of reactive power produced by wind power plants, plays a significant role in solving the voltage stability challenges. In addition, apart from the clean cheap energy wind power plants produce, they serve as emergency power sources to supply individual loads in an islanded mode of operation.

One of the goals of wind power plants is to inject power into the grid when the load demand increases. The output power characteristics of these units depend on the input power, that if the input power is not constant, the output power will follow the same characteristic.

A wind power plant only contributes to the power system when the wind speed is within the limits. If the wind speed falls below or beyond the limits, under or over voltage conditions will exist on the system, leading to a group of turbines tripping while others remain in operation; especially if the wind turbine generators are not of variable-speed

type. The transmission system the wind power plants are connected to will experience this continuously changing power, leading to the unreliability of the protection system (Pradhan & Joós, 2007).

To keep the reliability of supply to the end-users, protection requirements listed and defined below need to be kept in power system protection schemes.

- **Selectivity**: to sense and isolate only the faulty section.
- **Speed**: to isolate or clear the fault as quickly as possible.
- **Sensitivity**: to sense even the smallest value of the fault current.
- **Stability**: to isolate a faulty circuit and leave the healthy paths operating, supplying power to the customers.
- **Adaptability**: to be flexible to the system conditions and remain operating well.

According to the current research, it is believed that the varying wind speed received by the wind turbine generator units in wind power plants, as well as the changing load demand, contribute to the power variation in the power system. While the study considers the wind power plant integration as one of the possible solutions to the voltage stability challenges, an adaptive protection scheme is developed and covers some of the protection requirements.

Application of the IEC 61850 standard advances protection schemes through its control models to ensure the fulfillment of the power system protection requirements.

1.3 Problem statement

One of the wind power plants benefits is that they generate power closer to the customer. There are two modes in which these power plants can be operated, namely grid-connected and as a standalone mode, depending on the grid stability requirements. In grid-connected mode, wind power plants support the increase in energy demand. The standalone mode of operation is mainly for the cases of grid inadequacy, namely emergency supply for individual loads. There are additional services for a grid-connected mode; these services include frequency and voltage adjustments, harmonic compensation, power backup, network stability, additional reserve, and clearing of load peaks. (Rekik et al., 2015).

The integration of wind power plants in power systems has some negative impacts on protection systems. To ensure the positive effect of the integration of wind power plants, attention is paid to the type of protection schemes to be used.

Researchers have done various studies regarding the protection schemes of grid networks with wind power plant integration. Their focus is mostly based on the protection of the generating units and of the collector busbar which couples each unit to the wind power plant. It is relatively rare to find a study focusing on the protection of the point of common coupling (PoCC) at the transmission level. It has been emphasized from the existing literature that the changing power on the wind power plant side affects the transmission system into which the wind power plants connect. The changing power requires a protection scheme of high-standards. For this reason, it became of great significance to do a study focusing on the transmission-level substation.

Transmission level substations are very critical since they are the major hearts of power systems. As already mentioned, the power at these substations keeps changing, and therefore, protection schemes of high-standards are in high demand at this level.

An adaptive protection scheme is defined as a scheme that adapts to the conditions of the system and operates well regardless of the changing power system network parameters. However, for communication, devices that form such a protection scheme must have the capability of subscribing to the information from other devices located at other points within the system. IEC 61850 standard, a universal language for protective devices, makes it possible to make use of the information among protective devices for decision making by any device, while at the same time adding possibilities in advancing the protection system used to overcome protection issues.

This thesis focuses on two challenges, voltage stability and the design of an adaptive protection scheme to improve conditions of wind power plant integration into the grid.

Research problem statement: To investigate, design and implement methods and algorithms for IEC 61850 standard-based adaptive protection scheme for a common point of coupling between a wind power plant and the grid.

1.4 Research aims and objectives

This study builds on the knowledge that wind power plants are the increasing alternative renewable source of energy, as well as on the information about the integration of such renewable energy sources to the power system grid where power is insufficient.

While the main objective of the study is to develop an adaptive protection scheme for the common point of coupling, a contingency study is done, to investigate the necessity

of wind power plant integration into the power grid. The following is a list of objectives on how the aim is fulfilled:

- A literature review of the existing publications for the design and implementation of the protection schemes of the coupling point of a wind power plant to the power grid.
- Investigation of the existing logical nodes for monitoring and protection of renewable energy sources in the conditions of the smart grid.
- Theory of: Wind power plant and aerodynamic principles. Protection schemes for integration of the distributed energy resources (DERs) to the power grid.
- Development of a model of the considered power system without and with integrated DERs.
- Conduct the load flow analysis, contingency analysis, stability analysis (voltage).
- Development of a protection scheme for the conditions of power grid operation, islanding, and full integration of the DERs to the grid.
- Investigation of the operating behaviour of the protection scheme in the conditions of various disturbances (loss of synchronization, faults, overload, etc.).
- Development of a testbed for implementation of the developed protection schemes, Hardware In the Loop real-time simulation, and investigations of the system behaviour.

1.5 Hypothesis

The wind power plant point of common coupling is one of the significant parts of the transmission system. Some of the grid code specified requirements are referred to this point. Apart from ensuring the wind power plant conforms to the grid compliance test, the protection scheme designed for this point must be of a high standard. Hence the adaptive protection scheme becomes one of the most significant applications at the point.

Application of the IEC 61850 standard within the protection of the coupling point between the wind power plant and the power grid provides possibilities for controlling and monitoring all the changes within the system. With IEC 61850 standard-based protection scheme, all protection requirements are met at a low cost, as well as at maximum reliability (A. Ahmed & Kim, 2017). Additionally, the standard provides possibilities for the application of devices from any vendor, instead of looking for specific ones.

1.6 Delimitation of research

This research deals with an in-depth analysis of the integration of DERs (which in this case are referred to as a complete wind power plant). It focuses on the coupling point between the wind power plant and the transmission network of 230 kV and its IEC 61850 standard-based protection scheme.

Since the IEC 61850 standard increases the adaptability of the protection scheme, the scheme does not only offer protection and control but monitoring as well. The proposed protection scheme is modelled and tested using the Real-time Simulator Computer-Aided Design (RSCAD). Additional software platforms are used, in application to the protective devices. The International IEEE Nine-bus transmission network is used, and its simulations focus on the load flow, contingency analysis, and stability analysis (in terms of voltage). Simulation cases are computed using the Real-Time Digital Simulator (RTDS) devices.

The operating behaviour of the protection schemes is based on various disturbances, namely the load increase and internal busbar faults.

1.7 The motivation of the research problem

Wind power plants are the most vital types of renewable energy sources increasingly employed in smart grids for generating power mostly as a distributed generation system (Emmanuel Olufemi et al., 2017). They are driven by wind, and it is a natural effect that the wind is varying, so the output of the generating units varies with regards to the changing wind throughout the day. This effect causes nonlinearity in the system to which the wind power plant sends power. The widespread of this effect may lead to damage of equipment, the grid may no longer be guaranteed safe, and the system may shut down where the distributed generation is no longer contributing to the grid system at all.

The distributed energy resources aim to increase the reliability of the system and improve the ability of the grid to withstand natural disturbances (Han et al., 2010), namely the load demand increase. Due to the support wind power plants give to the power grid, it is of great interest to pay more attention to their protection, control, and monitoring, to fulfil the end-user's needs from the power grid, as well as to improve the reliability of the grid system.

IEC 61850 standard is a worldwide standard for the communication of intelligent electronic devices. In addition, the development of new technologies for protection has led the protective device vendors to the great achievement of developing new

protective devices suitable for the application of the IEC 61850 standard (Mnguni, 2014).

Findings from the existing literature are that there are very few protection schemes implemented and tested for wind power plant coupling into the transmission system. Even for the few implemented schemes, it is very rare to find a study covering both the voltage stability and security at the same time, as these go hand-in-hand. For this reason, the study is initiated about the grid insufficiency through the application of the load demand, the coupling of the modelled wind power plant, as well as the development of the IEC 61850 standard-based protection of the common point of coupling at the transmission level has been taken.

The RTDS provides real-time simulation cases that are a replica of the physical power system. In addition, these real-time simulations provide a means to test physical devices by interfacing them with the RTDS. The type of testing used guarantees full implementation and validation of results, as it involves the testing of the physical protective devices.

1.8 Assumptions

Till now, research has been done, and findings have led to the following assumptions:

- The selected power system network model meets the requirements of the power system studies, namely stability and security.
- The applied contingencies form the precise method of calculating the grid capabilities to fulfil the load demand.
- The modelled wind power plant meets the grid code requirements and passes the compliance test before it even fulfils the power system grid load requirements.
- The combination of the power system network and the wind power plant model creates the conditions leading to the need for an adaptive protection scheme.
- The testbed developed in the laboratory successfully matches the power system grid network and its distributed generation.
- The physical protective devices used for the laboratory test setup comply with the IEC 61850 standard.
- Most importantly, because the test involves the physical protective device interface, therefore it completely matches the real-world implementation of the protection scheme.

1.9 Research design and methodology

This research aims to design and implement methods and algorithms for adaptive protection schemes that improve the integration of distributed generation into the power grid. It first looks at the grid capabilities by looking at the load demand requirements. While wind power plant modelling is not part of the scope, but it is considered for this research. However, more attention is paid to the control and monitoring of the combined wind power plant and the transmission grid network for the condition of operation at the common point of coupling.

The existing technologies make it possible to meet the aforementioned objectives. The study aim is achieved through research methods, namely literature review, theoretical framework, modelling and simulations, and documentation method.

1.9.1 Literature review

The literature exists about wind power plants and their protection schemes. The literature related to these wind power plants is collected by reading recently published journals and books, and information from the internet, accompanied by discussions with experts in this field.

1.9.1.1 Distributed energy resources (DERs)

The study of these special types of renewable sources (wind power plants in this case) is done with the support of the existing literature.

The widespread application of the IEDs, as well as the building-up of the wind power plants, integrated into the existing power system networks, have triggered a lot of interest to go further with the investigation in advancing the protection schemes that are suitable for systems of such.

1.9.1.2 Protection and monitoring methods

Due to the complexity of the system integrated with wind power plants, the functions of monitoring and protection need to be considered. To carry out these functions, different protection schemes and their features are studied and understood well. These protection schemes are achieved by using one or more protective devices. The selection of the protection scheme to be used depends on the voltage level of the system as well as the type of equipment to be protected. Selectively, among all other protection schemes, distance protection is more suitable for the transmission system and it is achieved by using a distance (impedance) protection relay. According to the existing literature, distance protection relays are commonly used as main or backup for

line protection for the following reasons: they improve the overall reliability index of the protection scheme and they can handle high fault resistance with ground faults when a quadrilateral characteristic is set (Pradhan & Joós, 2007).

However, the study looks at the point where the wind power plant is coupled, and the only point a wind power plant can be coupled is at the bus or node, which requires a unit-type of protection known as the bus differential protection, for its importance. Due to the advantage that the technology has improved, the numerical forms of differential protection relays are available which have multiple built-in protection logics in a single package of the device that covers multiple conditions of the protected system.

With the IEC 61850 communication standard, the protection scheme includes IEDs that communicate with each other, covering all the possible protection aspects that comply with the principles of the SAS. The intelligence of these devices accommodates the communication methods that are offered by the IEC 61850 standard. The communication standard helps to increase the ability of system monitoring. The methods used in approaching the development of the protection schemes are provided with more detailed information in the remaining chapters.

1.9.2 Modelling and simulation

This study makes use of the IEEE Nine-bus power system transmission network to which the wind power plant integration is implemented. The transmission network and the wind power plant used are modelled on the RSCAD software. In the implemented protection scheme(s), protective relay devices are used and their configuration setting is completed through the application of each device's software.

The simulation cases are calculated by the RTDS devices. These simulation cases are based on the load flow of the power transmission network without and with the integration of the wind power plant and it is achieved by using the runtime of the RSCAD software, where results are observed and recorded. When the wind power plant is integrated into the transmission system, the study of an adaptive protection scheme is considered.

One of the requirements of the study is the contingency analysis, and at least out of many, the system overloading is considered. The overload contingency, as viewed at the transmission voltage level, requires the wind power plant that produces the same level voltage. The wind power plants from the found literature do not meet the requirements of this study. For this reason, it has been found of great significance to model a wind power plant model from scratch by using the existing turbine parameters from the wind turbine manufacturers and the generator parameters from the literature material.

Challenges are experienced during the wind power plant modelling because of the controllers that need to be developed to tune the wind turbine generators in the case of making them adaptive to the input wind. Literature is found, where the wind turbine generator controllers are explained and designed, but because of the limited time of the study, none of those controllers are implemented within the study. Therefore they are out of the scope and the designed model of a wind power plant is tuned manually.

A Hardware-In-the-Loop (HIL) test is completed in the laboratory through the support of a specially built test bench. The test bench includes the physical protective device(s) interfaced with the RTDS devices for testing the proposed protection scheme.

1.9.3 Documentation method

The thesis document is divided into eight chapters and appendices as listed and described in the following bullets.

- **Chapter 1**: The introduction of the study, a description of the problem, and hypothesis.
- **Chapter 2**: The literature review of the existing publications about the wind power plant common point of coupling protection schemes.
- **Chapter 3**: Theory of power system voltage stability, wind power plant benefits for voltage stability improvement method, power system protection, substation automation systems (introducing communication standard).
- **Chapter 4**: Simulation and modelling studies for the investigation of power system voltage stability challenges.
- **Chapter 5**: Wind power plant modelling for the conditions of power grid integration.
- **Chapter 6**: Development of the protection scheme for the conditions of the grid system without and with the wind power plant contribution.
- **Chapter 7**: Implementation of the IEC 61850 standard-based protection scheme for the conditions of the grid system without and with the wind power plant contribution.
- **Chapter 8**: Deliverables, conclusions and recommendations.
- **Appendices**: Significant attachments, namely figures missing from the body of the thesis documents, modelling parameters, and some results.

1.10 Conclusion

The background of the study is done in this chapter through the description of the key items, namely the awareness of the problem, problem statement, research aims and objectives, hypothesis, delimitation of research, the motivation of the research problem, assumptions, and lastly, the research design and methodology.

The next chapter discusses the literature found from different journals, conference papers as well as books about the wind power plant common point of coupling protection schemes.

CHAPTER TWO
LITERATURE REVIEW

2.1 Introduction

The objective of the power systems is to ensure continuous supply to the end-users at all times. Disturbances occur in power systems, some for a short period and others for a longer duration, depending on the nature of the cause. Longer duration disturbances include voltage sags that are experienced in substations, which usually occur when the load demand increases.

There are certain voltage levels under which the power system is not allowed to operate. If attention is not paid to such a condition, the whole system may shut down. There are various solutions to this phenomenon, each with advantages over the other.

There are some challenges experienced by the power grid when it comes to the integration of wind power plants for load demand support. This chapter focuses on the power system protection-related challenges introduced by wind power plant integration into the grid. The literature review will focus more on protection challenges at the point of common coupling for wind power plants.

2.2 Background

It is believed that the traditional fossil fuel primary energy resources will be depleted in the next coming years. This will lead to a complete transition to renewable energy resources.

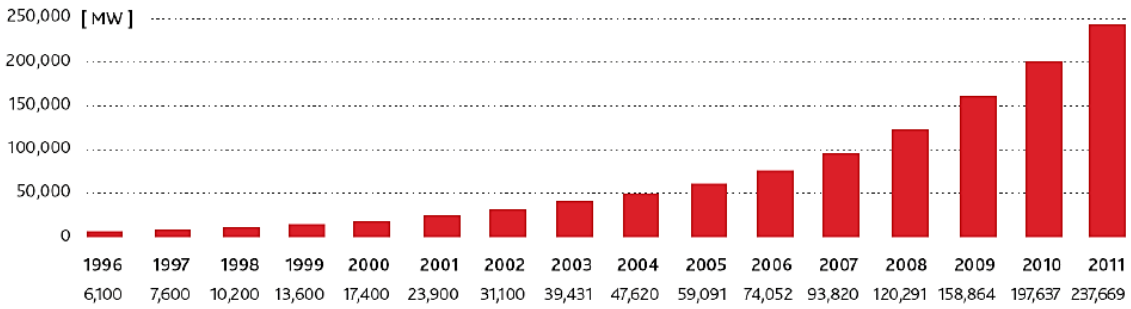

Figure 2.1: The global wind energy installation capacity with effect from 1996 to 2011 (Nahhas, 2013)

Wind energy has been leading in installations have been increasing as seen in the worldwide megawatt installation capacity from 1996 to 2011 shown in Figure 2.1. At

the end of 2014, the world's estimated installed total capacity of wind power was 370 GW (Mahmoud & Oyedeji, 2017).

Depending on the grid stability requirements, there are two modes in which WPPs can be operated, namely grid-connected and standalone modes. In the grid-connected mode, WPPs contribute additional power when the load demand increases in the power system grid. In standalone (islanded) mode, they serve as an emergency supply for individual loads when the power supplied by the power system grid is insufficient.

There are additional services for the conditions in a grid-connected mode, namely frequency and voltage adjustments, harmonic compensation, power backup network stability, additional reserve, and clearing of load peaks (Rekik et al., 2015).

One of the power system requirements is to keep the power grid supply system stable at all times. There are control techniques used on the mechanical side of the traditional generating units that ensure the stability of the system in the conditions of power system disturbances, but their operation is limited when severe disturbances like sudden increase or decrease in load demand occur in the system. In the case of an increase in load demand, additional power sources are required for the recovery of the power system grid, and wind power plants in grid-connected mode are used for this reason.

Like any other source of power, wind energy has challenges, especially when it comes to integration into the existing grid. For instance, the protection system at the common point of coupling may experience some challenges.

The wind energy industry is still growing linearly. For this reason, there is a need to look at the possibilities of advancement of protection schemes for the common point of coupling, especially during the era of smart protection technology.

2.3 The wind farm

A wind farm is defined as a group of wind turbine generators (sometimes referred to as generating units) installed in the same area for power generation. These generators are coupled together to generate enough power to be added to the power system grid and delivered to the consumers. The generating units, a primary stage of energy production in wind farms, are coupled through various circuits in a form of substations. These substations have switchgear and protection equipment. Substations located in each generating unit consist of metal-clad transformers.

Figure 2.2 below shows a single-line representation of a wind farm layout with possible connection points (Gupta, 2018).

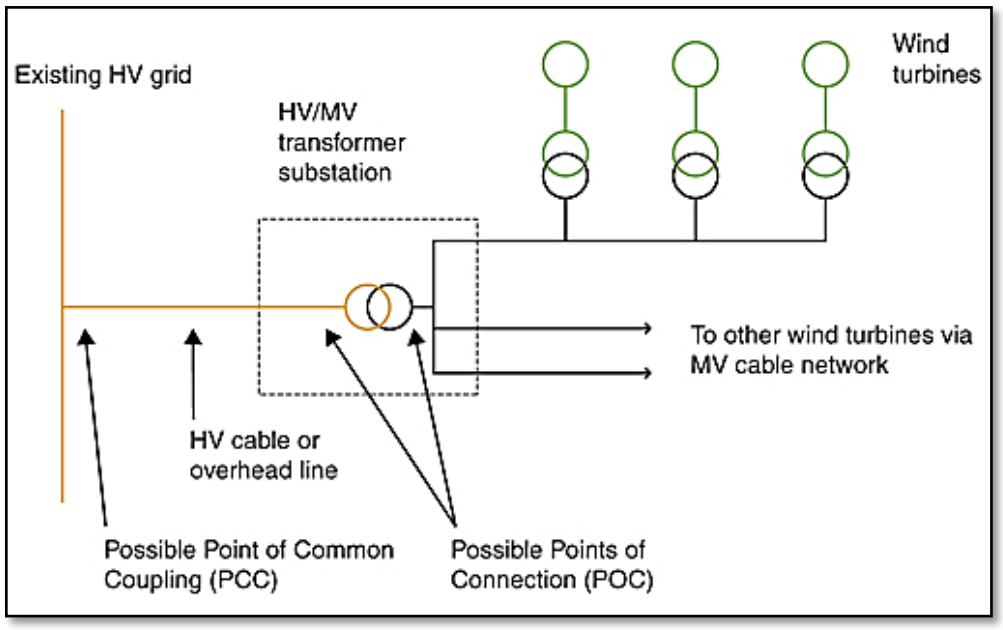

Figure 2.2: **Wind farm with possible coupling points (Gupta, 2018)**

Generating units with their step-up transformers are joined together with a busbar and another step-up transformer couples the wind farm onto the high voltage busbar, the intake to the power system grid.

The design of a wind farm has to follow the standards that are set regarding their integration into the power system grid. Those standards are set to minimize challenges the utility will experience during the operation of wind farms while integrated into the grid. If those standards are not met, the owner of the wind farm will not be allowed to integrate their wind farm into the grid (Davidson, 2017).

2.4 The wind farm coupling point

The coupling point of a wind farm is generally defined as the point at which the wind farm connects to the power grid. The purpose of wind farms is to contribute with energy to minimize energy cost by generating power at the distribution level, when necessary, feed continuously into the grid (Emmanuel Olufemi et al., 2017; Siniscalchi-Minna et al., 2019). The integration of wind farms into the power system grid adds several advantages. To mention a few, reduced transmission, increased reliability, and improved power quality.

2.5 Protection overview in wind farms

One of the most significant reasons to do power system protection studies in wind power plants is to ensure continuous power to the loads. The protection study looks at reliability, stability, security, etcetera. When these issues are paid attention to, the overall grid operation becomes successful (Kawady et al., 2008; Emmanuel Olufemi et al., 2017).

2.5.1 Electrical faults in wind power plants: an overview

Firstly, an electrical fault is any disturbance in an electrical power network that may cause the system to operate abnormally. This disturbance can cascade if not stopped and lead to further equipment damage as well as danger to personnel. Like in any other power system network, all types of electrical faults are possible. The types of electrical faults that usually occur in the power system networks are listed below:

- The line to line fault,
- The line to neutral or to the ground or earth fault,
- Three-phase fault, etc.

These types of faults do occur in wind power plants, though there are other types of faults which include the mechanical faults within the turbine generators and the power electronics components that are used in the wind turbine generator.

2.5.2 Protection challenges within wind power plants

Wind power plants need proper grounding for the protection of the plant equipment from the voltage transients that occur on the healthy phases during ground faults. Wind turbine generators (WTGs) and their step-up (low-voltage to medium voltage) transformers are ungrounded. This requires grounding to be done at the medium voltage to a high-voltage substation. If the WTG remains in operation while the collector circuit has tripped for a ground fault, the system remains operational in an islanded mode conducting with the ground phase. Therefore the phase-to-ground voltage of the

healthy phases may end up reaching the value of the phase-to-phase rated voltage, or even more (Alcázar et al., 2016).

The fault ride-through (FRT) in the wind farm operation allows generating units to continue operating for several seconds even if a fault occurs. If the generating unit is set to operate in this mode, under the fault, the generator will continue supplying the grid, causing overvoltage challenges. The fault current fed to the grid will affect the fault characteristics of the grid, especially when the wind farm is integrated on a large scale. Besides, the power system protection schemes on the grid, characteristic settings, and coordination which were set according to the fault characteristics of the grid parameters will be damaged, and no longer guarantee the safe operation of the grid (Han et al., 2010).

The wind turbine generators with FRT capabilities require an FRT protection scheme with a voltage versus time characteristic setting as shown in Figure 2.3 below. This protection scheme keeps the wind turbine generator synchronized to the wind power generating station connecting to the grid.

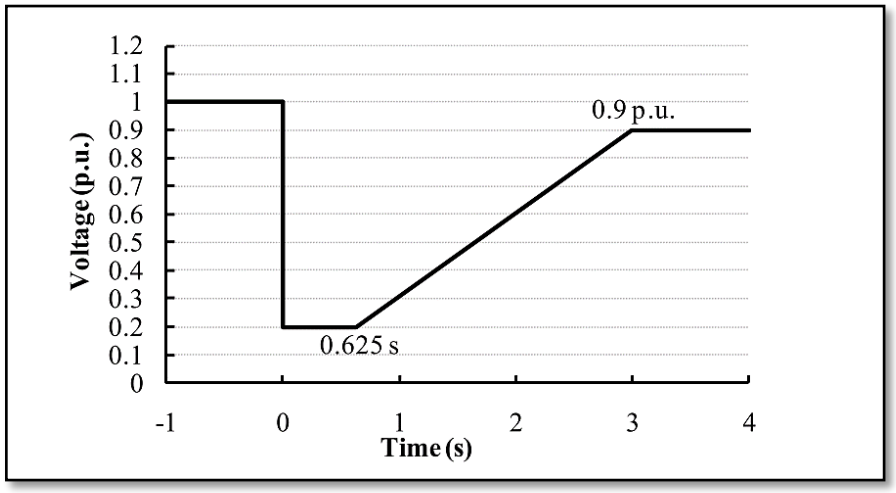

Figure 2.3: **Wind turbine generator fault ride-through capability (Gashi et al., 2012)**

When additional sources are integrated into the power system network, the flow of current becomes bidirectional, especially during fault conditions. In the wind power plant collector circuit, the burden on the collector relay is increased to protect the main trunk and the small conductors, and when the detection of the fault is necessary on the primary side of the generator step-up transformer, the sensitivity of the collector relay is compulsory. Therefore directional overcurrent element is required, to provide security for the generator output, as well as sensitivity for all the collector faults (Jones & Bennett, 2012).

2.6 Wind farm point of common coupling protection

The point of common coupling (PoCC) is the point where the wind farm meets the power grid. This point can be viewed from two sides based on the voltage level. The first is the medium-voltage side, before the medium-voltage to a high-voltage step-up transformer, and the other is viewed from the high-voltage side. The high-voltage side PoCC is considered the most important, for the switchgear on the transmission voltage level is the most expensive equipment.

Electrical protection has come a long way and it has been advancing with regards to the evolution of technology and different protection techniques have been applied in the safeguarding of the coupling substation to the power grid. Therefore, this section looks at the evolution of protection techniques for the PoCC as well as the challenges faced by each protection technique.

2.6.1 Overview

Protection deals with safeguarding the power system and its components to avoid further damages during system disturbances. Distributed generation provides backup power to improve the reliability of the power system supply network (Niwas et al., 2009).

Wind generators should be kept continuously supplying to the grid to maintain and improve power quality. It is due to the effect of wind speed variation that the voltage and frequency will change on the system. However, it is a requirement that a unit should be disconnected from the system once its voltage exceeds or goes below the rated stator voltage by 10% (Han et al., 2010).

Difficulties have been experienced in protected systems where the integration of wind farms takes place after the configuration has been done, that the protective devices, when traditionally configured, see this variation as a fault since the current will also rise above the predetermined setting values. It is a requirement to have a protection scheme that adapts or withstands such conditions, to maintain system reliability. Such a system includes a protection scheme which may be a combination of a group of protective devices. To mention a few: high voltage line protection, collector line protection, wind power system protection, step-up transformer protection, etc. (Ma et al., 2018).

The new generation of IEDs works with the IEC 61850 standard, which makes it easier to form a communication path between all the protection devices within the system,

with additional advantages of sharing information among them for decision making and complete monitoring and control at any point.

Each zone of protection has its special type of protection scheme. It mostly depends on the cost of equipment that a special type of protection is dedicated to.

Wind farm collector circuits consist of underground distribution cables connecting generating units to the collector bus through step-up distribution transformers. These transformers are protected by built-in fuses and low voltage circuit breakers. Underground cables connecting these units are protected by a simple feeder protection relay with the directional function (Jones & Bennett, 2012).

An example of a circuit with such a protection scheme is shown in Figure 2.4 below (Jones & Bennett, 2012) where MCM (million cubic meters) represents the unit of measurement for the area of the conductor.

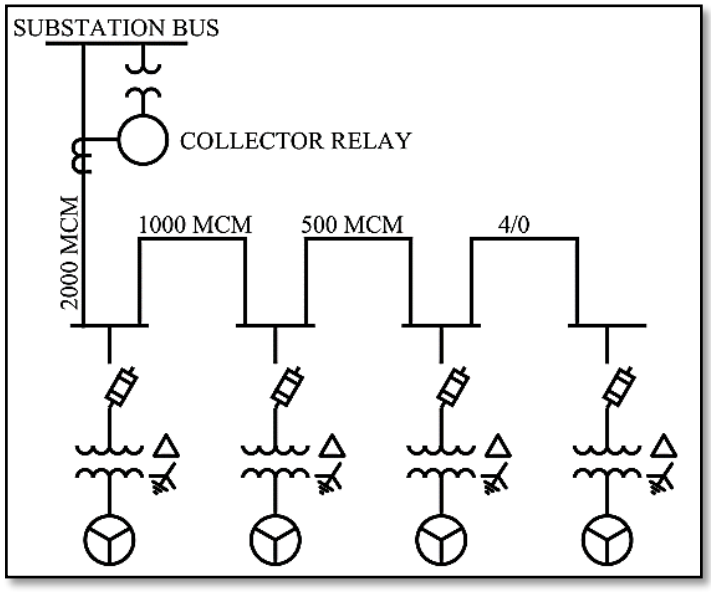

Figure 2.4: Wind farm collector circuit (Jones & Bennett, 2012)

The collector relay connected from the SUBSTATION BUS subscribes for both voltages and currents, therefore, able to measure the combined quantities (voltages, currents, and power) from the four generating units of the wind farm. Since the collector relay subscribes to both voltages and currents, it also monitors the power quality of the system.

The objective is to design and advance a protection scheme that will be adaptable to the network parameters before and after the wind farm has been coupled to the power system network.

2.6.2 Adaptive protection scheme

Due to the increased penetration of distributed energy resources to distribution networks, protection becomes more challenging. The bidirectional flow of power, the contribution of fault current from the distributed generation, as well as the grid code fault-ride-through requirements (Kauhaniemi et al., 2014), lead to the requirement of a protection scheme that will adapt to the conditions of the system. The main objective of adaptive protection is to change the settings of the relay to match the power system conditions.

The wide application of this technology exists because it has automatic settings. Based on its function and the information used, the technique of protection is divided into two parts, adaptive protection devices and adaptive protection systems (Chandraratne et al., 2019).

Generating units are grouped to supply power to the grid. The point of common coupling is exposed to a continuously changing environment. An adaptive protection scheme uses an outside variable to change the operating characteristic. A true form of adaptive protection combines advanced protection algorithms and communications with the sharing of information. Adaptability eliminates the impact of remote information on the relay's operation (Moxley & Becker, 2018).

The protection scheme on the transmission system sees the changing environment as a fault. In the case of the overcurrent protection schemes, relays will trip, isolating the wind farm from the grid (Pradhan & Joós, 2007). The adaptive distance protection scheme is suitable for such disturbances. Its digital version provides features like monitoring and communication, and it adapts to the system changes without performing unnecessary operations (Pradhan & Joós, 2007). Monitoring of the system state leads to an advanced definition of the loads and generation. Two possible forms of protection exist, which adapt to the system conditions, distance protection, and directional protection (Kauhaniemi et al., 2014).

A complete adaptive protection scheme covers all the protection zones of the system. Possibly, there are six zones of protection on a wind farm. Each zone has various forms of protection, depending on the equipment to be protected.

Table 2.1 below shows the zones of protection with possible protection schemes for each zone (Cardenas et al., 2010).

Table 2.1: Zones of protection with their types of protection (Cardenas et al., 2010)

Zones	Wind generator zone	Collector feeder	Collector bus	High voltage transformer	Transmission line	Capacitor bank
Types of protection	Instantaneous phase overcurrent for LV phase faults	Phase and neutral overcurrent	Bus differential	Transformer differential	Distance or current differential protection	Phase overcurrent
	Inverse time overcurrent for generator overload protection	Under-voltage	Breaker failure	Restricted ground fault	Pilot schemes	Unbalanced current
	Instantaneous neutral overcurrent for LV ground fault protection	Overvoltage	Backup overcurrent	Sudden gas pressure	Backup phase and neutral overcurrent	
	Inverse time negative sequence overcurrent for unbalance protection	Under frequency			Breaker failure	
	Generator under-voltage	Over frequency				
	Generator over-voltage	Anti-islanding				
	Generator under frequency	Synchronization				
	Generator over frequency					
	Transformer short circuit protection using MV fuses					
	Transformer differential for large transformers (>1 MW)					
	Transformer backup phase overcurrent					
	Synchronization					

Overcurrent, distance, and differential protection are necessary for a complete protection scheme (Chandraratne et al., 2019).

2.6.3 Distance protection

High or extra high voltage transmission lines are protected using distance protection (Z. Y. Xu et al., 2010). Distance protection is the best suitable scheme especially for a

transmission system integrating the wind farm to the grid. They protect all types of faults within their reach. This type of protection identifies the fault type and the location and estimates the resulting impedance by using the current and the voltage from the fault point until the relay's location (Pradhan & Joós, 2007; Kauhaniemi et al., 2014). This calculation is easily done using Ohm's Law principle. Simply

$$Z = \frac{V}{I} \tag{2.1}$$

where Z is the impedance in Ohms, V, the voltage at the relay's location in Volts, and I, the measured line current in Amps (Kauhaniemi et al., 2014).

Distance protection relays can be used as the main or backup protection (Sun et al., 2018). Distance relays, unlike overcurrent relays, are not impacted by the magnitude of the source impedance but are limited by the load impedance (Moxley & Becker, 2018). To have a successful adaptive setting method for distance protection schemes, it is a requirement to subscribe to a distance protection relay located on the transmission line to the information on the wind farm. This allows remote monitoring of the behaviour of the generating unit through the device located on the transmission system.

One of the reasons for advancing protection schemes is to increase their adaptability to the changing system conditions. Distance protection relays for transmission lines were developed to replace the overcurrent protection relays. This was in response to the requirement to accommodate the rapidly varying generation connections which would determine the disturbances beyond the operating point which initiates false tripping (Moxley & Becker, 2018).

2.6.4 Directional overcurrent protection

The connection of distributed generation to a distribution network makes it no longer a radial network since the fault current is coming from all sources joined to the power system network during the fault conditions. This is the main reason why the fault level is so unique when compared with the radial structure (Chandraratne et al., 2019).

High generator output, different cable sizes, the inrush current of the wind turbine generator step-up transformer, as well as wind turbine generator technologies cause complications in the protection of the wind farm collector circuits.

The requirement of fault detection on the low voltage side of the wind turbine generator step-up transformer increases the requirement of sensitivity for collector faults. Directional overcurrent relays are necessary for a balance between security for the generator output and sensitivity for all collector faults.

Traditional overcurrent protection does not guarantee sensitivity in detecting remote faults and backup protection for wind turbine transformers (Jones & Bennett, 2012). Application of directional overcurrent relays is necessary when the flow of current is bidirectional through the location of the relay. To identify the current direction, both voltage and current measurements are required (Kauhaniemi et al., 2014).

2.6.5 Differential overcurrent protection

Differential protection is a unit type of protection for a specific zone or a piece of equipment. It is the most reliable protection scheme, which therefore suits the protection of the most important power system components like busbars, transmission lines, power generators, and power transformers.

This type of protection is widely used for these aforementioned components. The differential overcurrent protection fits well within the common point of coupling between the wind power plants and the transmission grid. This protection technique operates with Kirchhoff's Law principle, it compares the currents from the current transformers that are located at each end of the protected unit and isolates that unit from the circuit if the differential current (operating current) exceeds the amount of the restraining current. It is mainly used as the internal protection of the equipment where the differential current is greater than zero (Saad et al., 2015; Chandraratne et al., 2019).

Power transformers, busbars, and transmission lines are some of the most important elements in a power system network, as a result, they require continuous monitoring and quick protection. Overcurrent faults in transformers and busbars lead to severe disturbances in transmission networks (Medeiros et al., 2016).

2.7 Wind power plant protection challenges and solutions - review

Various challenges pertinent to wind power plant protection and their solutions have been addressed. There is still a need to look at wind power plant protection as a whole. Some protection challenges originate from the wind turbine generator tower, while some originate from the overall system electrical circuits.

2.7.1 Traditional methods

A study was done in 2001 by the authors, (Ledesma & Usaola, 2001). These authors looked at the transient performance of the grid with a doubly-fed induction generator after the occurrence of system disturbances. They proposed a protection scheme that disconnects the generator during the fall of voltage. Their scheme had the auto-reclosing function to connect the generator after a few seconds if the voltage rise occurs. The auto-reclosing function helps to maintain power quality after system faults.

(Pradhan & Joós, 2007) did the study of an adaptive setting of a distance protection relay by looking at the effects the fluctuation input wind to the wind turbine generators has on the transmission system. The authors applied the adaptive settings with the protection of a transmission system connecting to the wind farm. They dealt with the settings of the wind farm side relay, where they used the ratio of the local voltage and current, and information about the number of participating generators on the wind farm. The quadrilateral characteristic is the chosen setting, for its ability to handle high fault resistances with ground faults. The results analyzed are from a 400 kV, 60 Hz power system network. The impedance is varied from 0 Ω to 50 Ω. Several case studies are done based on the varying voltage level, varying source impedance of the wind farm, and varying system frequency. To handle the changing wind farm conditions, the author proposed an adaptive setting method for the distance relay.

(Liu & Dawalibi, 2010) put their focus on the wind farm's possible types of faults. They did a thorough study of the extensive fault simulations looking at different points of the fault to determine adequately the grounding system performance for the substation and wind turbines. They used the unspecified tools of computation for their analysis. So, they proposed a grounding system that was based on the safety criteria by the IEEE Standard 80-2000 (standard for safety in AC substation grounding). Their simulation design and technique were accurate and realistic, and they can be used in the design of a larger wind farm.

(Ma et al., 2010) did the study of different faults in a distribution network, and proposed an adaptive distance protection scheme for a distribution system with distributed generation. The authors simulated the proposed technique on a 10 kV distribution network. The proposed technique can clear the fault with high sensitivity and selectivity.

(Zheng et al., 2011) proposed a relay that uses the magnitude of the positive sequence component in the fault current to detect a fault on a parallel wind turbine generator. The positive sequence current magnitude is used to decide either on the instantaneous or

delayed operation. This method can minimize the outage section, and the undesirable disconnection of the whole large wind farm on some healthy wind turbine generators can be avoided.

(Wang et al., 2011) looked at the prominent impact the large scale wind farms have on the operation of the grid. The authors analyzed the behaviour of the wind farm in case of ground related faults. They established a real wind farm model on the PSCAD/EMTDC to look at the aforementioned phenomenon. They discovered that there is a requirement for a special type of protection.

(Khoddam & Karegar, 2011) focused on the analysis of the performance of the distance relay on the doubly-fed induction generator integrated system. The authors have dealt with the simulation on the MATLAB. They have discovered from the results that the distance protection relay is not suitable for protection lines connected to wind farms when its settings are set fixed.

(Wenhao et al., 2011) looked at the effect of the changing wind input to the wind farm, and proposed an adaptive relaying algorithm. Their model is done on MATLAB. One of the advantages of the proposed algorithms is that the setting value of the protective system can adapt to the disconnecting and connecting changes of the wind farm by calculating the impedance of the system using both the measured voltage and currents.

(Li et al., 2011) conducted a study where they improved the sensitivity of the protection of a distribution network with branching short lines. They did their simulation on the PSCAD/EMTDC. Their technique improved the sensitivity of the protection.

(Cai & Su, 2011) did the study of the fault analysis on the large-scale wind power system. They did the fault current comparison between power system networks with two types of distributed sources, the doubly-fed induction generator, and the hydropower plant. Their analysis is based on the fault amplitude. (Richter & Lepa, 2012) did the study about protection in wind power plants. They proposed the overvoltage protection scheme, where they concluded with findings that further investigation should be done. They saw a need for the development and testing of new protective devices.

(Jones & Bennett, 2012) studied the protection of a wind farm collector feeder using the directional overcurrent relay element. They aimed to increase the sensitivity of the overcurrent protection towards the faults. The setting approach is done, where the collector feeder protection is secured by considering the relay's load encroachment

function. Under this setting, the relay can block overcurrent elements from operating for the load. In their study, it is stated that the relay monitors the positive sequence impedance. Their study has focussed on the collector circuits, where they only considered the point of generating units until the collector bus bar.

The application of the load encroachment has increased the security of the security over the entire range of the generating current angles while detecting faults on the collector feeders. From their study, it is found that the directional overcurrent element guarantees a balance between security for generator output and sensitivity for all collector feeder faults.

(Sun et al., 2018) looked at the effects large doubly-fed induction generator (DFIG)-based wind farms have on the power system grid. The authors have discovered that the generator distance backup protection potentially experiences some difficulties during its operation. Their study was conducted on the transmission system where the wind farm is integrated at the 500 kV bus. They have stated that the DFIG-based wind farms appear as STATCOMS at the nearby generators. Due to this, the generator distance protection experiences the under-reach, over-reach, or time delays during the operation when these types of wind farms are coupled to the system. In an attempt of solving the aforementioned issues, the authors did an in-depth assessment of the performance of the generator distance protection for a system where the DFIG-based wind farm is integrated.

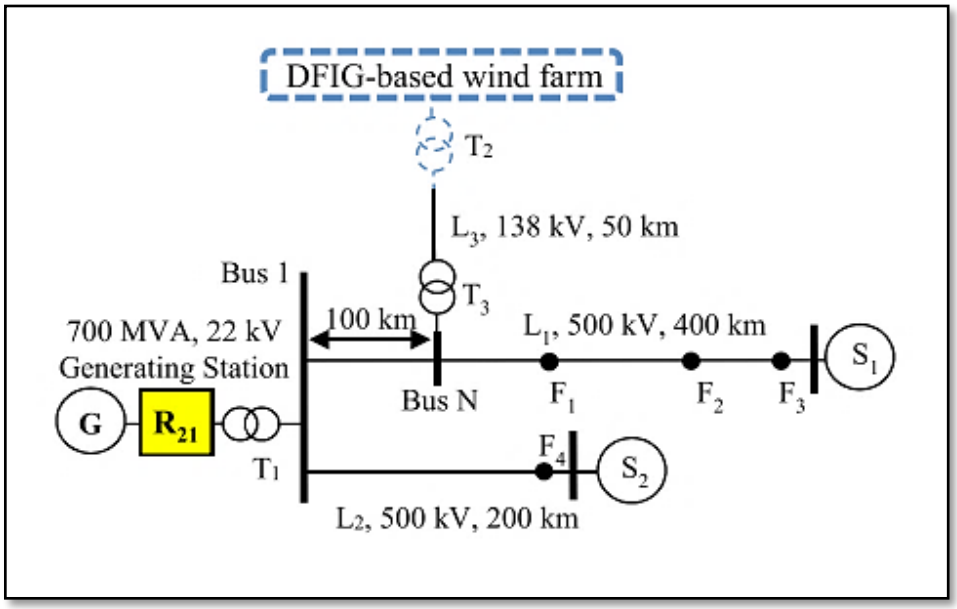

Figure 2.5: 500 kV system (Sun et al., 2018)

Their simulations were done on the EMTP/RV platform, and their model is mathematically based. The 500 kV system is shown in Figure 2.5 above on the previous page. In the figure above, R_{21} is a generator distance protection relay. G, S1, and S2 are generators. However, G is the generator considered for their study. F1 up to F4 are fault locations and, the dotted circuit represents the wind power plant.

(Ma et al., 2018) did a study on the protection of the collector circuits for a doubly-fed induction generator (DFIG)-based wind farm. The authors looked at the sensitivity and selectivity issues when it comes to the protection of the collector circuits of such wind power plants. (Ma et al., 2018) first did the analysis of the protection schemes for a wind farm up to the collector circuit and did the calculations of the voltage drop from the protection relay's location u to the location of the fault and calculated the adaptive setting coefficient.

Having that mentioned, it can be seen that the authors aimed to make the protection scheme adaptive to DFIG behaviour. Nevertheless, they did their study and the protection scheme was done and tested in the real-time digital simulation (RTDS) platform, where the different types of faults were located and tested. Since the authors' study uses the distance protection scheme, they have selected the quadrilateral characteristic because it makes the distance relay more adaptive to the system conditions. Their results are compared between the traditional protection method and the adaptive one they have developed.

(Wu & Yu, 2018) discovered an issue of large DC components-caring short circuits in wind farms that have weak feed characteristics. The authors mentioned that the DC components in the short circuit currents cause the current transformer saturation. Their study was based on the current transformer saturation when longitudinal (line) differential protection is applied to the transmission line of the wind farm. They believe that it is the current transformer saturation that causes line differential protection maloperation in the system. Therefore they came with the algorithm known as the three-sample value product and applied it to the line differential protection scheme in a form of a microcomputer protection algorithm to solve the delayed operation. Their study was conducted on PSCAD. However, the current transformer saturation test was done in Matlab/Simulation.

(Zhang et al., 2013) discovered that the amplitude of the single-line-to-ground fault becomes extremely small in collector circuits due to the control circuits that the wind farms use, as well as the short length of the collector cables. The authors believed that

the numerical relays sometimes fail to detect fault currents of such amplitudes. Therefore they developed the technique called a single-phase-to-ground fault detector that works with the numerical protective device to improve the sensitivity for detecting even the smallest amount of fault currents.

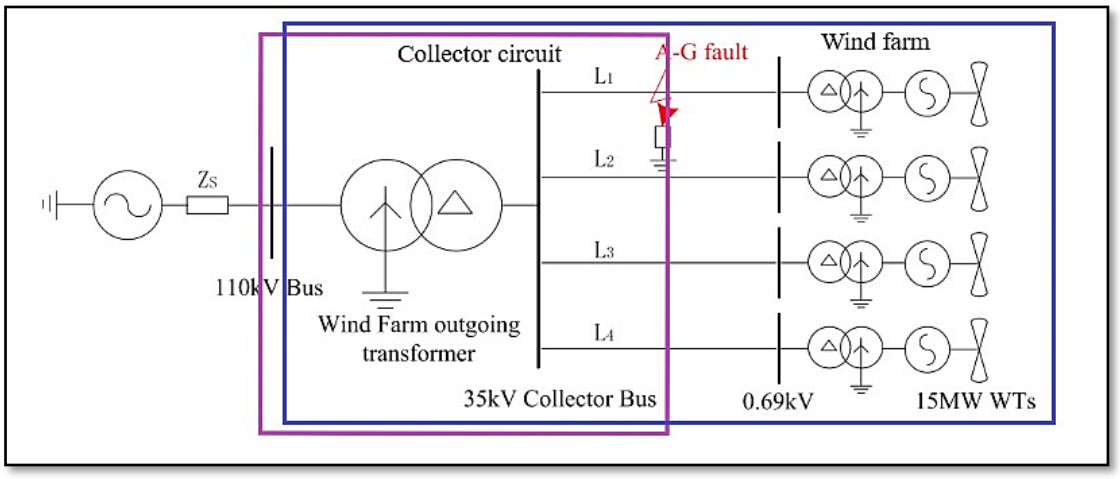

Figure 2.6: **Wind farm model showing the collector circuit of 35 kV/110 kV voltage (Zhang et al., 2013)**

The algorithm they have developed is for the medium voltage collector bus. (Zhang et al., 2013) proved their study using PSCAD/EMTDC and Matlab software platforms using the actual wind farm shown in Figure 2.6 above.

The wind farm consists of a doubly-fed induction generator (DFIG) and permanent magnet induction generator (PMIG) units. The collector circuit on this wind farm is made up of an overhead line. To test their study, different cases were considered based on the fault location as well as different types of wind turbine generator units. The first test is done when the wind farm consists of a DFIG type with four wind turbine generator units for a 1 km line length from each unit. The second case is when the PMIG units are used, and the lengths are different for all the collector lines. The last case is when a mix of wind turbine generator types are used, with different line lengths. Their study has proven the validity of the algorithm for both theoretical and simulation test analysis.

According to (Song et al., 2012), doubly-fed induction generators are one of the conventional wind turbine generator unit types. These types of generators have the capability of adjusting the frequency, amplitude, and phase of the rotor voltage through the rotor-side converter with four quadrants to control the DFIG's operating conditions. Therefore these generators are declared the most efficient wind turbine generators since they can produce power at multiple ranges of wind speeds. The authors believe that the reactive power is not compensated very well in power system networks where

the DFIG-based wind farms are integrated due to the low-voltage-ride-through (LVRT) capabilities of these units have, which makes the fault last for a long time on the system.

These authors even mentioned the challenges that occurred in these other wind power plants on the 24th of February 2011 in Jiuquan Wind Power, where the insulation breakdown occurred in a 35 kV switchgear cable, where 598 wind turbines in 10 wind farms tripped. In addition, another incident occurred on the 17th of April 2011, where the box-type transformer was broken on the high-voltage side. Again, another 702 wind turbines were tripped on a wind farm. The aforementioned incidents are a clear indication of how protection schemes need to be advanced in these systems to avoid the lack of reliability and to improve the power quality in the system. This is why the authors applied the static VAr compensator (SVC) to improve the voltage compensation in the system. Their method forms part of the protection method within a wind farm, where the overvoltage or undervoltage issues are avoided within a period of 100 ms.

Other authors who emphasized the importance of the doubly-fed induction generator are (Han et al., 2010). However, they discovered a challenge when it comes to the AC-DC-AC power converter used to excite the machine. The issue with it is that it makes the fault characteristics differ from the synchronous generator's thereby causing difficulties to the traditional protection in the grid, especially now that the DFIG units have the fault ride-through (FRT) capabilities, for the generator unit will remain connected to the system for a certain period even under fault conditions.

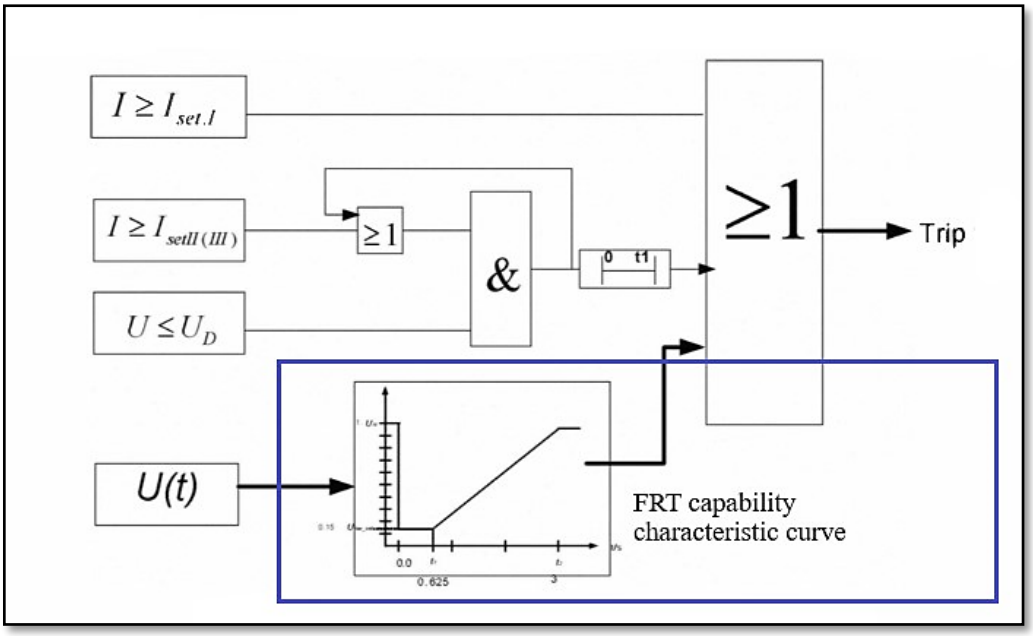

Figure 2.7: **Protective relaying system with the FRT capability characteristic curve (Han et al., 2010)**

These authors developed an adaptive protection scheme that encounters the FRT duration during the fault before the trip decision is sent to the point of common coupling (PoCC) breaker. Figure 2.7 above on the previous page shows the block logic of the relaying scheme they have used for their study. The method of protection the authors have developed does not only protect the system but ensures that the fault ride-through of the generating units are encountered during the protection decisions.

Wind power plants can be located thousands of meters away from the grid. This makes the transmission of power more significant. In other countries, or for some utility needs, direct current (DC) systems are used to avoid or reduce power losses in long-distance power transmission. For wind farms whose transmission lines need extremely long transmission lengths to reach the transmission grid stations, DC systems are used, where the alternating current (AC) power is converted to DC for transmission to the stations located far away from the wind power plants.

The DC transmission system is shown in Figure 2.8 below, where the power is transmitted from a wind power plant to the grid.

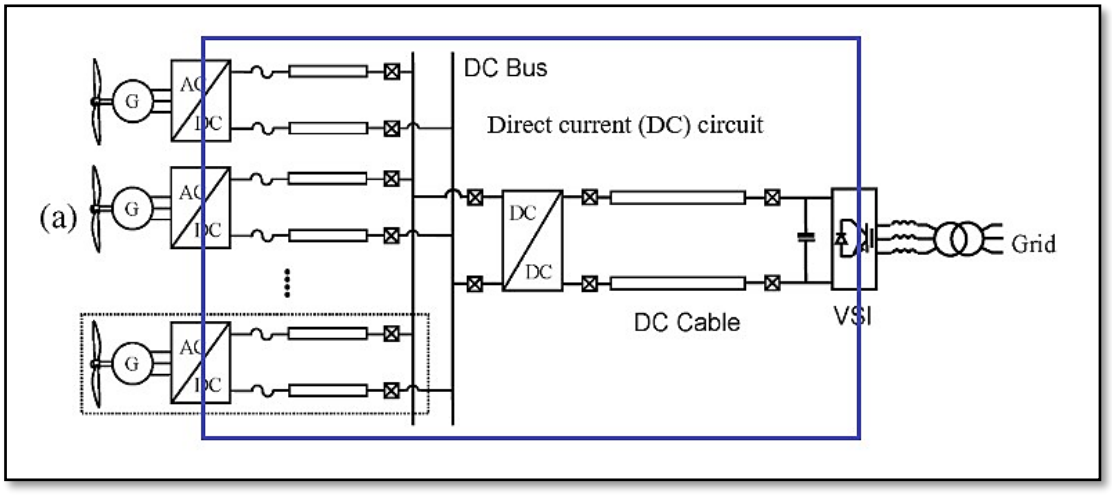

Figure 2.8: **Wind power plant with DC transmission system to the grid (Yang et al., 2010)**

According to (Yang et al., 2010), DC systems are most popular for offshore wind power plants. These authors mentioned that the high voltage DC systems are robust to electrical faults, due to their regulated currents with a filtering reactance connected in series with cables. This is why DC systems do not suffer that much in short-circuit faults, hence overcurrent relays are not that important for these systems. The voltage change detection is one of the protection methods used in DC transmission systems. The authors did the study of the short circuit faults occurring in DC transmission

systems where they did a thorough study in fault analysis and proposed a method of protection without switchgear. The simulation studies are conducted on the PSCAD/EMTDC simulation platform.

2.7.2 Numerical and IEC 61850 standard-based methods

The advancement of technology has led to the application of communication networks in the power industry, where digital protective devices started to use a common communication language.

Another study was done by (Alcázar et al., 2016) who looked at the challenges experienced by wind farm collector circuits. They looked at the effects mainly in the protection scheme. One of the most significant challenges they have spotted is that, if the collector protection scheme operates for a ground or earth fault and the wind turbine generators remain in operation, the system will remain an islanded ground system in operation with a grounded phase. The challenge with that is, the phase-to-ground voltage of the healthy phases adopts the phase-to-phase rated voltage or even more.

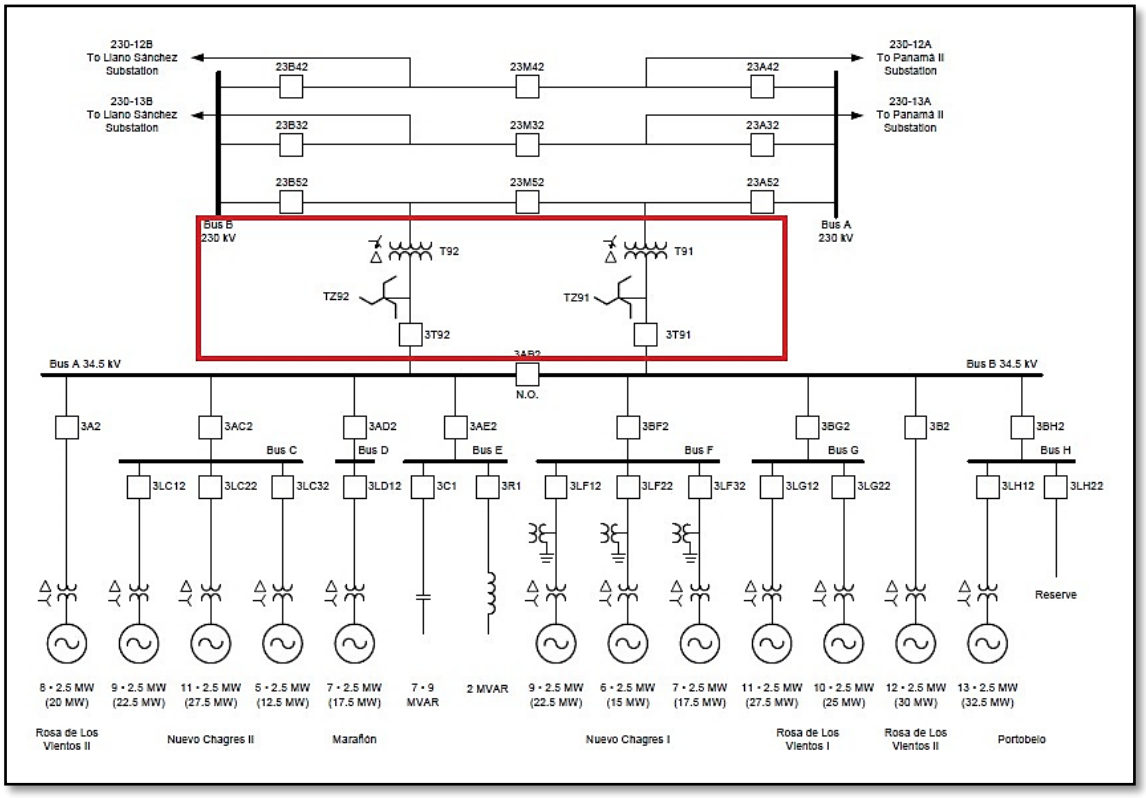

Figure 2.9: **Panama wind power plant with a double collector circuit zig-zag grounded (Alcázar et al., 2016)**

The new design of wind turbine generators has voltage ride-through capabilities, where the generators continue to feed an islanded collector circuit for several seconds, and due to this, the system may be vulnerable to over-voltage challenges. The authors

believed that the proper grounding of the collector circuits is essential in the wind farm. The solution they had to this challenge is to introduce a proper grounding for the collector circuit, and for that, they emphasized the zig-zag grounding method of the collector circuit, as shown in Figure 2.9 above on the previous page. The red surrounded area shows the collector circuit with a zig-zag grounding system.

Since their study was based on the 230 kV transmission system, various protection schemes were introduced.

The authors studied the short-circuit and protection coordination. The transmission system they considered was protected as follows:

Transmission line:

Two multifunctional relays provide primary and backup protection for a transmission line. Each relay provides the following functions:

- Line differential (87L) protection that uses phase (87LP), negative sequence (87LQ), and zero-sequence (87LG) differential elements to provide phase and ground fault protection,
- Directional-comparison permissive underreaching transfer trip (PUTT) scheme that uses 21 and 21N elements for directional discrimination,
- Distance protection that uses 21 mho elements polarized with memorized positive-sequence voltage and 21N quadrilateral elements,
- Ground directional overcurrent protection that uses a current-polarized zero-sequence directional element, and negative- and zero-sequence voltage-polarized directional elements that measure impedance.Automatic reclosing with synchronism checking (25) and undervoltage (27) supervision.
- Each multifunction relay provides 87L and directional-comparison protection, therefore each line has dual 87L and dual directional-comparison protection. These relays communicate over two fibre-optic channels using optical power ground wire cables mounted on each transmission line. Each multifunction relay has two serial ports for 87L communication and two serial ports that support a proprietary peer-to-peer communications protocol. The relays can monitor communications channels. A bay controller provides the following functions:
- Breaker-failure protection,
- Local/remote switchgear control, interlocking, and circuit breaker supervision,
- Data collection from the substation switchyard and data forwarding to the supervisory control and data acquisition (SCADA) gateway.

Transformer protection:

Two multifunction relays provide redundant primary and backup transformer protection. Each relay provides the following functions:

- Differential (87) protection,
- Overcurrent (51) protection. However for a high-voltage side, 51/51N elements are used, and for the low-voltage side, 51/51N and 51G,
- Restricted earth fault protection on the high-voltage side, and
- Supervision of the sudden-pressure relay (63).

A bay controller provides the following functions:

- Breaker-failure protection,
- Local/remote switchgear control, interlocking, and circuit breaker supervision, and
- Data collection from the substation switchyard and data forwarding to the SCADA gateway.

Zig-zag grounding transformer protection:

The protection for this transformer uses a multifunction relay that provides overcurrent (51) protection.

Distribution system protection:

Another multifunctional relay exists on the 34.5 kV collector circuit, that provides the following functions:

- Phase and ground overcurrent protection (50/51, 50N/51N),
- Ground directional overcurrent protection when required that uses a current-polarized zero-sequence directional element, and negative- and zero-sequence voltage-polarized directional elements that measure impedance,

The relay automatically selects the best directional element for each fault,

- Under frequency (81) alarming, and
- Over- and undervoltage (59/27) alarming.

The protection and control system by (Alcázar et al., 2016) is done based on the current technology of protection and the protection coordination is considered. Therefore, the main solution to the challenge is the introduction of the zig-zag grounding method on the collector circuit as well as the strong coordination of the protection schemes for the system.

The availability of communication standards between field electronic and digital devices leads to more studies. The authors (Ahmed & Kim, 2014) developed the algorithm of communication in a wind power plant for monitoring. They used the IEC 61400-25 (communications for monitoring and control of wind power plants) to provide the

information interchange for a wind power plant. Using the standard, they were able to advance the wind power plant monitoring and control functions. For instance, the communication architecture (see Figure 2.10 below) they have used allowed the measurement for analog, status information interchange, control, and protection information among field protection devices.

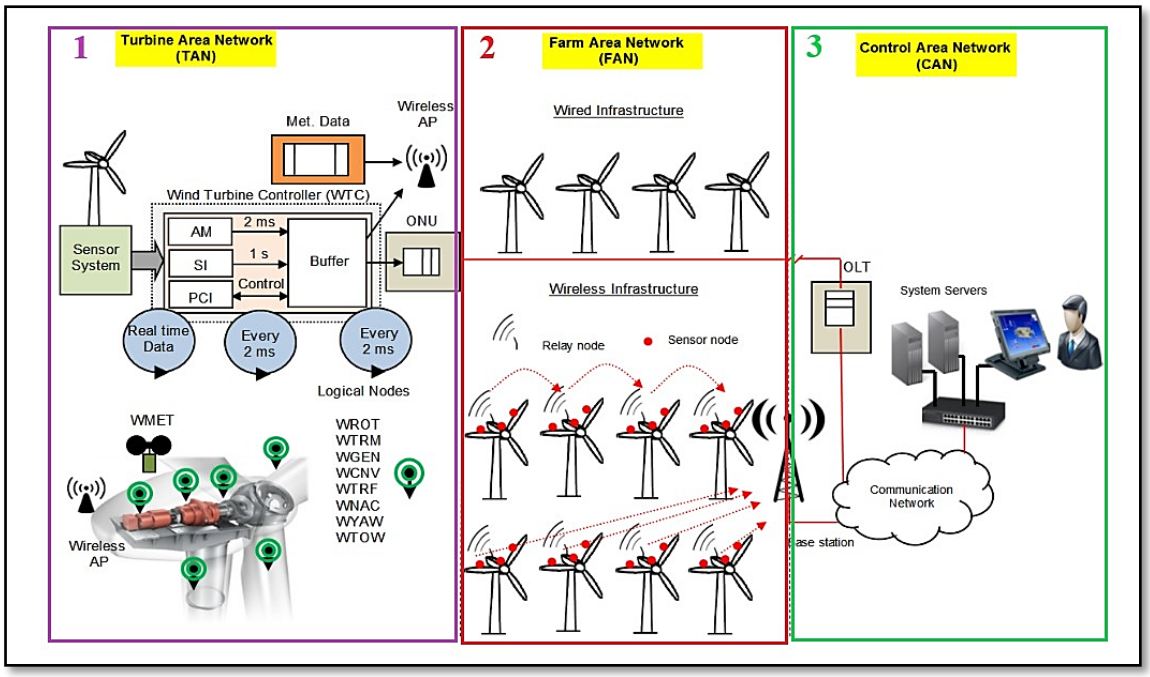

Figure 2.10: **Communication architecture for smart wind power plants (Ahmed & Kim, 2014)**

The communication network architecture in Figure 2.10 above has three parts. The first part shows the wind turbine area network, the second part is a wind farm area network and the third part is the control area network.

The first part deals with the advanced monitoring of each turbine unit. With the presence of the logical nodes for wind turbine sensors, information can be sent to the control center for control of each unit. This process applies to the whole wind farm area shown in Zone 2 of Figure 2.10.

In 2010, the authors, (Cardenas et al., 2010), looked at the issues of the design of the protection of wind farms. The authors' concern was the design, construction, and maintenance decisions that need to be made for a wind farm, namely the location of relays and the way copper wiring is arranged between measurement sources and protective devices, as well as realistic and affordable maintenance. The issue is when the relays are located at each turbine, it becomes difficult when wind farms are located offshore. They lead to the high cost of installation and maintenance.

The authors here propose a protection and control approach based on the IEC 61850-9-2 (process bus). This technique uses merging units (MUs) and central relaying units (CRUs), and it reduces the cost. In the future, this approach will help to replace the fuses that are used in the protection of wind farm integrated networks, since the capacity of the generating units is increasing.

2.7.3 Strictly numerical point of common coupling protection

The development of the numerical protection techniques and how they can be implemented in busbar protection offers many advantages. The conventional busbar differential protection schemes are more like a unit zone of protection because of a single current input that they subscribe from, where all the currents from all the current transformers in branches of the network are summed up to make a single input current to the relay. The current busbar protection techniques can easily select the zone to be protected based on the information they carry about the design of the network they are protecting (Apostolov, 2014).

The challenges experienced by the utilities have called out for the busbar protection schemes to have a minimum of two separate differential elements within a single unit, and both of these elements must be able to trip within a period of no later than 30 ms. Since these designs are made of a single unit that may be responsible for the protection of the entire substation, they must include a set of distributed bay units connected to the CTs for each feeder or line. This is how numerical busbar protection schemes are formed (Tart et al., 2010).

Since the numerical busbar protection techniques include distributed bay units that measure the analog signals from the power system, the connection between these units and the central unit is achieved through Ethernet communication. A communication network exists, which transports the information from these units to the central unit. Therefore, in the modern protection techniques, from the principles of the substation automation systems, a single unit controls all the functions of the power system through the calculation algorithms using the information it receives from the analog subscribers (bay units) from all the branches of the network. Figure 2.11 below on the next page shows the example of the numerical busbar protection scheme. The solid lines in the figure are the inputs from the power system to the bay units, and the dotted lines represent the communication (usually fibre optics) between the central unit and the bay units (Tart et al., 2010).

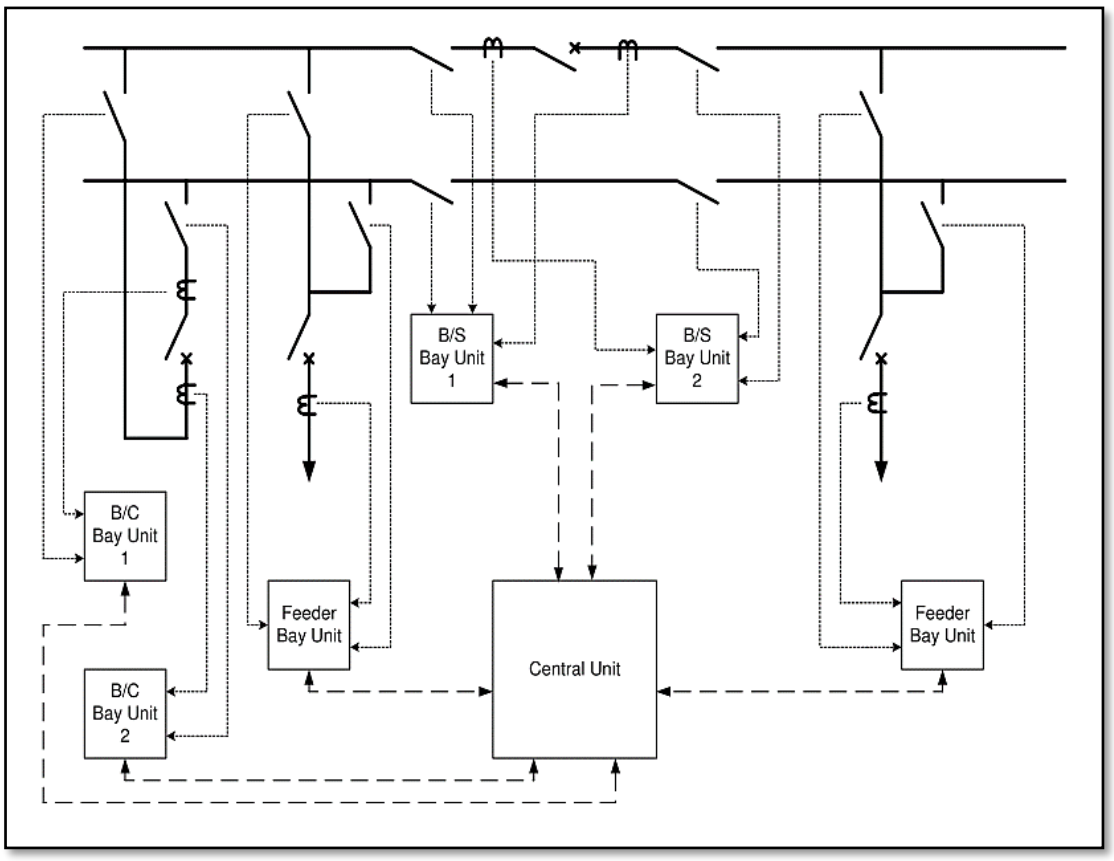

Figure 2.11: **Numerical busbar protection scheme (Tart et al., 2010)**

The authors (Hughes, 2005; Mohan & Chatterjee, 2010) described the benefits of numerical busbar protection techniques for electrical substations. In their studies, they put more emphasis on network stability and security. They went on and described the performance constraints of the protection system, namely safety, availability, and reliability.

Authors (L. Xu et al., 2010) looked at the numerical busbar protection requirements, i.e, fast operating times for all internal busbar faults, security for external faults where heavy CT saturation occurs, as well as the minimum delay for evolving faults. In their study, they have managed to develop a protection algorithm that meets the aforementioned requirements. For instance, their protection scheme was able to do the current phase comparison, and through this capability, the reliability of the busbar protection scheme is achieved. The results in their study show that the phase current comparison mostly improves the reliability of the busbar protection. The second advantage of the developed algorithm is that when comparing with other CT saturation detector techniques, it takes no delays to unblock the busbar biased differential protection when the external fault occurs.

The authors (Guzmán et al., 2005) proposed one of the most reliable busbar protection schemes with an advanced zone selection. The protection method they have developed covers all the busbar protection requirements. As a result, their technique was later implemented in digital protection relays, especially the ones from Schweitzer Engineering Laboratories (SEL). However even today, the numerical busbar protection relays operate in this logic. Figure 2.12 below shows the block diagram of the calculation logic they have developed.

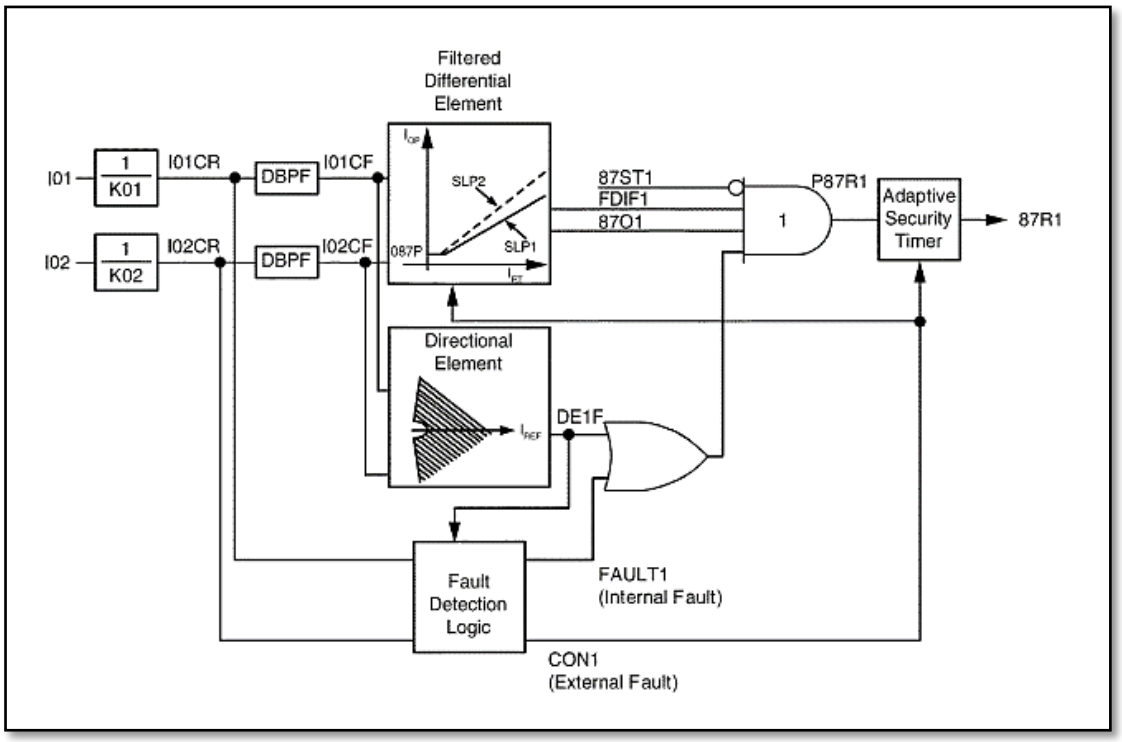

Figure 2.12: **The protection logic for a bus differential protection with an advance zone selection (Guzmán et al., 2005)**

The logic in the figure is made for unit zone protection. In this case, the zone is referred to as the phase. For a protected node, there can be more than one branch (incoming or outgoing three-phase lines). Therefore in a numerical relay, each protection logic is responsible for the calculation algorithm of each phase, and the calculation is done in consideration of all the branches for a single node.

The next section presents the remarks and observations made from the studies reviewed in the first up to the third parts of the section.

2.8 Remarks and observations

Studies have been done in the past regarding wind power plants (WPPs). Some focused on the impacts wind power plants have on the grid, while others focused on the protection of wind power plants, as well as the protection of the power system where

wind farms are integrated to. During the literature review, the following observations were made:

The impact wind power plants have on the utility grid has been discussed. Different protection algorithms were proposed for the wind farm point of coupling. The algorithms proposed in the current literature focus on different points of the power system grid. Most of the proposed algorithms are limited only to the calculation-based type of protection. There are very few algorithms where the communication standard was applied. For instance, one of the protection studies with communication was proposed by the author (Cardenas et al., 2010), with the application of the IEC 61850-9-2 (Process bus) for a wind power plant.

In addition, the unfortunate part about these protection algorithms is that very few of them were implemented in the form of a real-time simulation (RTDS) platform, as it stands to be the best simulation tool for testing the physical devices interface within the simulation case running on the computer. Besides, it is very rare to find a study with the point of common coupling (PoCC) protection scheme, even the few that are found, none of them considered the IEC 61850 standard compliant physical protective device test. Therefore, it is not easy to conclude that these algorithms are well implemented and tested properly. Hence the proposed study deals with the design and implementation of protection methods in real-time simulation, where the physical devices will be included.

There is literature covered regarding protection techniques of the power system grid where wind farms are integrated. However, even though the IEC 61850 standard is applied to these techniques, there are very few or no papers published regarding real-time testing and implementation.

The current technology of busbar protection relays offers the protection function based on this logic shown in Figure 2.12 of the previous section. However, it is just the technology of communication that is becoming more advanced, depending on the requirements to automate the protected system. Hence the proposed study focuses on the full application of the protection algorithm based on the protection technique developed by (Guzmán et al., 2005), and utilizes the protective device to its desired capacity.

2.9 The proposed method

The proposed technique makes use of the IEC 61850 standard-based microprocessor-based protection devices to implement adaptive protection functions for the power system grid, where a wind power plant is integrated. The applied communication technique (IEC 61850 standard) provides a high-speed communication mechanism between IEDs. The use of the existing IEC 61850 standard control model GOOSE, in support of logical nodes (LNs), makes it possible to reduce the rate of hardwiring within the protection scheme while offering the high-speed communication network between the IEDs. The mutual existence of the LNs among the applied protection IEDs of different vendors makes the availability of the communication between those devices.

The proposed technique uses the Real-time digital simulator (RTDS) devices with their software Real-time Simulator Computer-Aided design (RSCAD) software.

2.10 Conclusions

The literature was reviewed in this chapter for different methods of protection used in a power system where wind power plants integration takes place. It first defines the point of common coupling (PoCC), follows by describing the impacts of wind farms on the power grid, where it states the grid code requirements, power quality challenges, power system transients, and voltage sags. The overview of the protection in wind power plants is described. The definition of the point of common coupling is done.

Most importantly, the review of the wind power plant protection challenges and solutions is done, looking at traditional and numerical methods.

The remarks based on the observations made out of the literature findings are done, and the proposed method has been discussed and complimented based on the existing techniques of protection due to wind power plants integration.

CHAPTER THREE
THEORETICAL FRAMEWORK

3.1 Introduction

For power system studies, it is always essential to understand the factors contributing to the problem, as finding a solution to the problem is easier than understanding the problem. Challenges faced by power system protection and control schemes at the point of common coupling, as well as the methods used to advance them to ensure the guaranteed stability in the system, and most importantly the modelling and simulation tool is covered in this chapter.

3.2 Power system protection

Power system protection refers to the branch of electrical power engineering that deals mainly with the safeguarding of electrical power system components from faults. It is done by disconnecting the faulty parts from the entire network. Safeguarding of the electrical network and its components can be achieved through electrical protection schemes. Various protection schemes exist in power systems and are applied depending on the equipment protected, or the voltage level at the location of the protected equipment. The protection schemes contribute to power system stability by isolating only the faulty components and leave the healthy network operating normally, and this is achieved through the application of protective devices.

3.2.1 Digital relays

Digital relays or microprocessor-based relays are sometimes called numerical relays. They are a result of the advancement of the integrated circuits (ICs) which has made it possible for the emergence of microprocessors. Or else, these relays can be defined as the reduced version of the central processing unit (CPU) of a computer and they are made of very fast and low-cost microprocessors. Microprocessor-based relays do not work as simple as comparators, however, they are based on the numerical calculation carried on data obtained from the protected or monitored system. The data they process is in discrete form. These relays are programmable and this makes them flexible and accurate in operation (Ray, 2007). Digital relays in combination with the existing communication standard, advance the functions of the current generation of relays by increasing features of the substation automation system (SAS).

However, since the proposed system of study looks at the coupling of the wind power plant at the transmission level, therefore this part discusses the protection schemes necessary for the coupling station connecting the wind power plant to the transmission

system, namely current differential busbar protection and the high-voltage transformer current differential protection.

Besides, the protection schemes provided have to ensure maximum protection to improve the stability of the power system, therefore the communication standard is introduced and is discussed further in the later sections.

3.2.2 Protection schemes for coupling stations

The wind power plant has the main step-up transformer which steps up the medium voltage to the level suitable for transmission. The step-up transformer has the incoming and the outgoing busbar. The outgoing busbar couples the whole wind power plant to the transmission system, therefore, called a coupling busbar. The medium-voltage busbar, high voltage step-up transformer, and the outgoing busbar make a complete substation, therefore the combination of the two can be called the coupling station. Since the outgoing bus is at the transmission system, some power quantities of the transmission are measured through the same bus. These quantities are power factor, per-unit bus voltage, fault level, etc. The protection scheme that needs to be developed for this point is the protection that has three functions, namely protection, monitoring, and control which will maintain the system stability, as required from the busbar protection aspects.

3.2.3 Busbar protection

The protection scheme for any power system network should protect the whole system under any type of fault. The unlimited line protection schemes, namely distance and overcurrent systems meet this requirement, but the busbar faults get cleared after some time delay. When these protection schemes are applied as unit protection, the busbars are left unprotected. Busbars have been left unprotected for some reasons as follow:

- There has been a belief that the busbars are always safe because of their high degree of reliability.
- It was feared that the maloperation of a busbar protection scheme might cause the widespread dislocation of the power system, which if not cleared very quickly, would cause more loss than would the very infrequent actual bus faults.
- It was hoped that the back-up protection would provide sufficient bus protection when needed.

At the distribution level, the busbars are enclosed in metal-clads. The risk of faults occurring in metal-clads is very small, however, like any faults, dangerous if ignored, because of the increasing concentration of the short-circuit MVA, which indeed may result in the complete loss of the substation due to fire. This effect may even lead to

the prolonged interruption of power from the substation. In the case of sectionalized busbar systems, where each section has its protection system, the fault occurring in one section does not affect the other section, since the initiated trip will only be meant for that particular section. This means that the important loads can still be supplied from the healthy sections, therefore do not suffer the power outages.

Busbar protection is a requirement when the system protection does not cover busbars, and when power system stability is a requirement. The unit busbar protection provides this, with the additional advantage that, if the busbars are sectionalized, only the faulted section will be disconnected in cases of fault. Therefore, the unit busbar protection scheme does the best when the busbars are sectionalized.

3.2.4 Busbar protection requirements

It is the most common power system protection practice to ensure that the reliability, selectivity, speed, and sensitivity of the protection are always kept. The four fundamental requirements are discussed in the parts below (Altuve et al., 2017).

- **Reliability**: Reliability is the ability of the protection system to trip when required, and not trip when not required. When the protection system trips while required, it is said to be dependable and secured when it does not trip when it is not required. Whether it is the transmission line, or a transformer, or bus bar protection, reliability of protection is very important (Lin et al., 2006).
- **Selectivity**: Selectivity is when the protection can discriminate between the faulty and healthy sections, and trip only for the faulty ones, leaving the healthy sections operating normally. This feature increases the stability of the protected power system network.
- **Speed**: The protection system must be as quick as possible, such that it prevents extended damages to the equipment. When the fault occurs, the current may rise and eventually damages the power system components if not cleared.
- **Sensitivity**: This is the ability of the protection system to detect even the smallest amount of faults and respond.

3.2.5 Busbar differential protection

The busbar differential protection scheme is necessary for high-speed protection of the system to avoid further damages to the equipment. It maintains system stability and ensures the continuous supply of power to the load. Some types of protection schemes are commonly applied in the protection of the bus bars, namely low impedance differential protection schemes, high impedance differential protection schemes, and biased percentage differential protection schemes (Guzmán et al., 2005).

The high impedance differential protection scheme is used to overcome the current leakage during the current transformer saturation when a high-current external fault occurs. This scheme requires careful attention in current transformer selection, for it only requires a special type of current transformers, whereas the low impedance approach does not need dedicated current transformers. Therefore, it is clear that the high impedance differential approach is more expensive than the low impedance.

Security is one of the most significant requirements in the protection scheme, and to achieve it, another special type of protection is used, having the directional protection principle. With this principle, the protective device can distinguish between the external and the internal faults. In this case, the external faults are called the through faults. The scheme works in a way that when the current flows away from the bus, it is taken as through fault and no trip commands are issued by the device, however, if the currents are flowing to the bus bar, it is taken as the internal fault, therefore trip command must be issued by the device, isolating the bus bar (Chothani & Bhalja, 2011).

Current transformers (CTs) are used to monitor and scale the currents entering and leaving the busbar and transform it into small quantities easy to be handled by the protective relaying devices. A simple differential protection scheme is shown in Figure 3.1 below with current transformers monitoring the currents in parallel feeders (Behrendt et al., 2010).

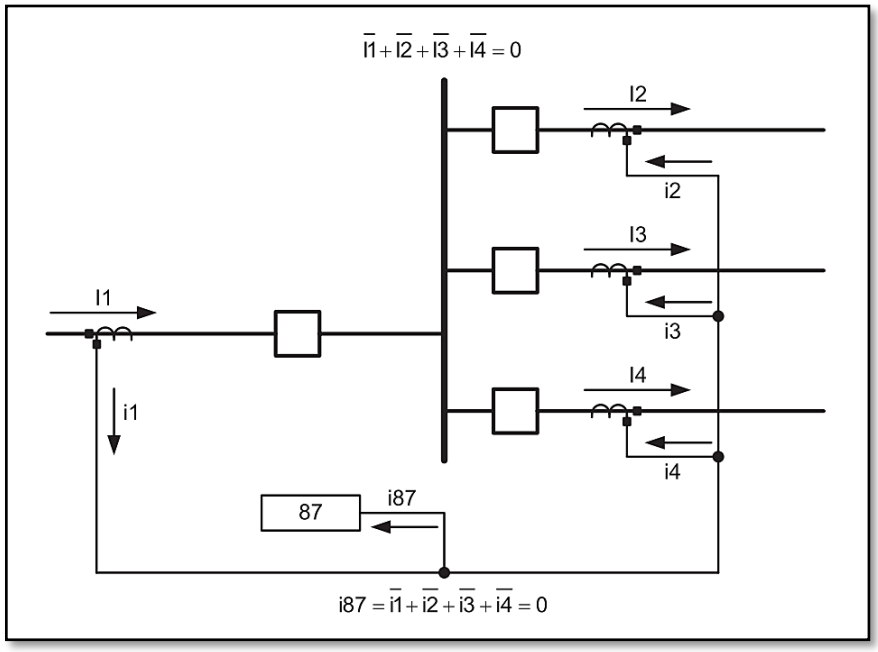

Figure 3.1: **Simple differential protection scheme with parallel feeders monitored by parallel current transformers (Behrendt et al., 2010).**

The protective device processes the secondary currents from the current transformers and calculates whether a differential current exists, and trip the circuit breakers by using the differential element, which will be activated only when the differential currents are calculated non-zero, and only if that non-zero differential current exceeds the threshold value set on the differential element of the protective device. All the secondary currents are compared on the same base as the primary currents, this is why the ratios of the parallel feeder CTs must be made equal.

The protective relay must be able to distinguish between the external (through) faults and the internal faults. Differential relays can block the differential element from operating for a short period after detecting the through fault. This approach is not appropriate, because the relay delays trip commands even for internal faults. To overcome this issue, differential relays with directional current detection are used. These relays can identify the direction of the current. One of the advantages of these relays is that even during the heavy current transformer saturation, the phase angle of the currents can still be determined (Behrendt et al., 2010; Guzmán et al., 2005).

3.2.6 External and internal fault conditions

The total currents entering the node are the same as currents leaving the node. Therefore, summing these currents will lead to a total of zero, which would be the same under normal load conditions. Under the internal fault condition, the sum of all the currents entering the node is not equal to zero, however equal to a value (differential). The ideal bus differential current protection relaying system uses the fact that the sum of all the currents will be zero for through faults. Practically, some challenges cannot be avoided, which makes the ideal operation of the differential protection scheme not valid. However, steps are taken to overcome these challenges even under non-ideal situations (Andrichak & Cardenas, 1995).

The condition of the external fault is shown in Figure 3.2 below on the next page. It can be seen in the figure that all the current flows from other branches (feeders) to the faulty branch. Though by the look it seems that the currents have changed the direction, this does not mean that the fault is internal to the busbar. This, therefore, means that the sum of all the branches (I1 + I2 + I3 + I4 + I5) connected to the bus will be equal to the fault current (I6 = If). In the figure, IF represents the fault current, the same as I6.

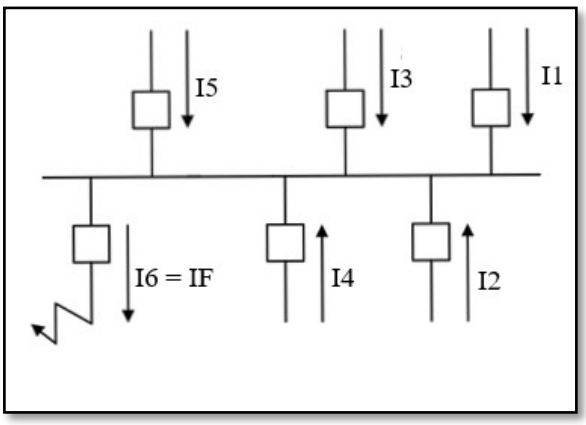

Figure 3.2: External or through fault conditions (Andrichak & Cardenas, 1995)

The internal fault condition is illustrated in Figure 3.3 below. In addition, it can be seen in the figure that all the branch currents flow to the fault path, the busbar or node itself on this point. Since the faulty path is the busbar, the currents will sum up, making the total of the fault current (I1 + I2 + I3 + I4 + I5 + I6 = If) flowing right through the busbar. Under this condition, the busbar needs to be isolated because thousands of amperes are flowing through it, and such values of currents can cause severe damages to the busbar and equipment close to it.

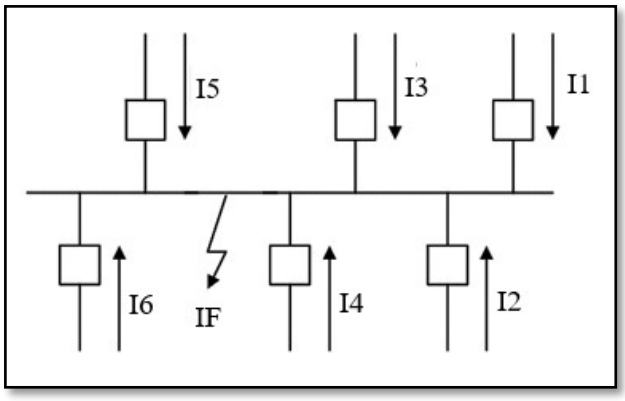

Figure 3.3: Internal fault conditions (Andrichak & Cardenas, 1995)

3.2.7 The practical operation of a differential protection scheme

A general assumption is that the saturation level differs for each CT. In the case of a through or external fault, the CT closer to the fault position will always be the one vulnerable to saturation. For instance, in Figure 3.4 below on the next page, the CT circled red is closer to the fault.

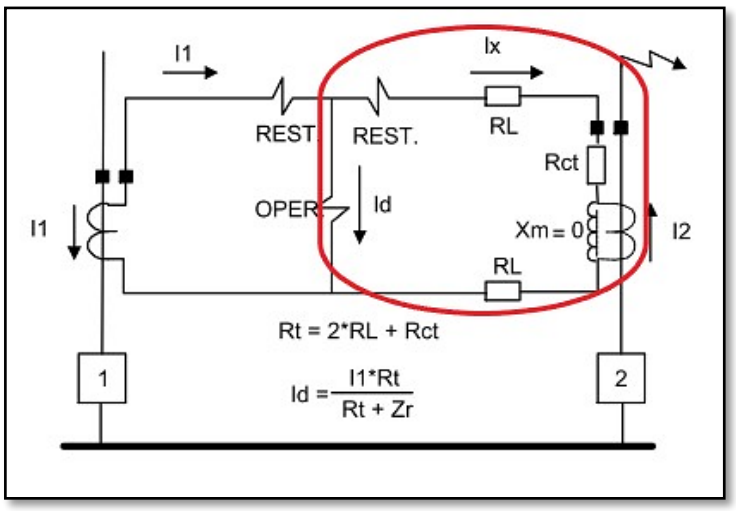

Figure 3.4: **Current transformer exposed to saturation under external fault for a percentage restrained differential relay (Andrichak & Cardenas, 1995)**

During the external fault at feeder 2, overcurrent will exist on the feeder because it is the only path the currents flowing to the faulty path would flow through, regardless of the presence of any other feeders or branches connected on the same busbar. Due to the overcurrent flow on this branch, the CT primary side will experience a large current, leading to the saturation of the transformer core. When this happens, the secondary current is no longer proportional to the primary currents and is distorted and this is considered an error. Distorted waveforms may have extremely high amplitudes, causing the imbalance of currents comparison between the two comparing CTs, leading to a differential element operation.

To view the effects of the CT saturation on differential protection relays under external faults, the percentage restrained differential relay is used. The operating principle of the percentage restrained differential protection relay states that the relay operates only when the operating or differential is greater than the product of the percentage slope and the restrained current.

Under normal load conditions, the restraining current is always greater than the differential current. In the differential relay, the restrained current is the sum of the absolute values of the currents measured from the CT secondary terminals whilst the differential current is the absolute sum. In the case of the transformer saturation, as indicated in Figure 3.4 above, the CT on the right-hand side is located on the faulty branch, therefore exposed to high-currents, leading to errors in the secondary currents. Though the CTs have the same turns ratio, the secondary current produced is no longer equal due to the distorted waveforms of the left-hand side CT, which may be high or lower than the secondary currents of the other CT. The imbalance between the two

CTs leads to the flow of current on the differential element (Andrichak & Cardenas, 1995)

Besides the effects of current transformer saturation, additional network branches affect the differential protection scheme. The differential relaying system is configured based on the flow of current on the protected branch. Say the substation or busbar has two branches, where the current comparison is done between two CTs; the currents entering and leaving the branch according to Kirchhoff's are considered. When another branch is added to the system while the relaying circuits like CTs and are not changed, the whole differential relaying scheme can no longer do a precise comparison of the current flow through the busbar.

There can be more than one case where a differential protection scheme would need to be reconfigured. The new technology of protective devices allows protection engineers to configure multiple sets of settings using different groups. Nevertheless, the study takes into consideration the addition of the wind power plant, in compensation for the power required due to the system load increase.

3.2.8 Effects of the wind power plant on the differential protection scheme

Besides Kirchhoff's current law principle, the busbar differential protection scheme looks at the changing impedance and admittance of the system to distinguish between the internal and the external faults (Hughes, 2005).

Additional circuits lead to the change in impedance and admittance of the power system network. A change in network configuration requires a change in differential protection configuration. However, adaptive protection schemes exist, that compensate for power system network changes up to a certain level.

The addition of power sources constitutes the change in network parameters. There are two methods by which generators can be added to the system. One is by connecting a generator through the step-up transformer on the busbar side, and the other is by connecting a generator direct on the busbar. A wind power plant connects to the system through a step-up transformer, and such a connection is considered an indirect coupling.

Depending on the wind power plant scale (large or small scale), network parameters vary. There is usually a huge impact on the system parameters when a wind power plant of a large scale is coupled than a small scale. Taken into consideration is the wind

power plant category, for instance, category C of the renewable power plants are those that can generate a power of more than 20 MW.

3.3 Types of wind power plants

There are two modes in which wind power plants can be operated, i.e. grid-connected and as a standalone mode, depending on the grid stability requirements. In grid-connected mode, wind power plants support the increase in energy demand. The standalone mode of operation is mainly for the conditions of grid insufficiency, namely emergency supply for individual loads. There are additional services for a grid-connected mode, these services include frequency and voltage adjustments, harmonic compensation, power backup, network stability, additional reserve, and clearing of load peaks (Rekik et al., 2015).

One of the grid requirements is to keep the system stable, and this is mostly achieved by having additional power sources connecting to the grid system. In addition to the specified grid code requirements, renewable energy sources are categorized into five categories, known as A1, A2, A3, B, and C (Sewchurran & Davidson, 2017). Each renewable power plant category has a specified minimum volt-ampere (VA) capacity it has to produce and the voltage level for a system to which it can be connected. Table 3.1 below lists the renewable power plant categories and specifies the voltage levels at which they can be connected.

Table 3.1: SA Renewable Energy Grid Code Categories (Sewchurran & Davidson, 2017)

Category	Minimum size (kVA)	Maximum size (kVA)	Connection level voltage
A1	0	13.8	LV
A2	13.8	100	LV
A3	100	1 000	LV
B	0	20 000	MV
C	>20 000	-	MV/HV

Based on the requirement stated by the South African Renewable Energy Grid Code (SAREGC) requirements, wind power plants are required to supply or absorb the reactive power to support the network voltage. In addition, they must play the role of controlling the power factor of the system within the specified point and respond to the new setpoint. This is to say that wind power plants (WPPs) may have great support in power system reactive power.

The coupling of the wind power plant in any grid system changes the configuration of the grid and this leads to a different flow of power. This is one of the wind power plant integration issues into the grid and its effect on protection schemes is mitigated by ensuring a proper design of the protection scheme.

3.4 Voltage stability

Voltage stability is the condition where the system can maintain its standard node voltages at the acceptable continuous operating range during its normal operation, even after the power system disturbances. The power system voltage is said to be unstable if one or more node voltages fall out of the acceptable continuous operating range.

The lack of reactive power in the system is the main cause of voltage instability. More reactive power demand from the node causes a voltage decrease in the node, and vice versa for reactive power injection into the node (Reis et al., 2009; Kundur, 1993).

3.4.1 Voltage stability concepts

Voltage control and stability challenges were once primarily associated with weak systems and long lines, but now are associated with heavily stressed systems (Kundur, 1993). In addition, generator reactive power is declared a principal factor in voltage collapse.

3.4.1.1 Transmission system characteristics

Transmission lines are rich in magnetic (reactive) components, which causes a larger amount of reactive power absorption along the transmission line when heavily loaded, and reactive power supply when lightly loaded, especially in long transmission lines. This causes a huge difference between the sending end and the receiving end reactive power, which affects the voltage at the receiving end terminal (Ray, 2007).

3.4.1.2 Reactive power compensating device characteristics

Reactive power cannot be transported over several kilometers of a transmission line because it requires significant voltage drops that are not allowed for the system. To supply reactive power, compensators or over-excited generators are introduced in the system near the loads where it is required (Vasantharathna, 2016). There are several types of configurations into which these compensators are operated, namely shunt capacitors, regulated shunt compensators, and series capacitors.

3.4.2 Voltage stability analysis

The voltage stability analysis of a power system network involves the examination of two aspects, namely the proximity to voltage instability and the mechanism of voltage instability.

- **Proximity to voltage instability**: This aspect is based on the investigation of how close the system is to voltage instability. Physical quantities, namely load level, active power flow through the critical interface, and reactive power reserve are used to measure the distance to instability. Planning and operating decisions depend on the appropriate measures of the given situations of the system. Possible contingencies, namely line outages, loss of generating unit, or a reactive power source, system overloading, etcetera are considered (Kundur, 1993).
- **Mechanism of voltage instability**: For this aspect, time-domain simulations are included with appropriate modelling where the events that are leading to instability are captured in chronological order. These simulations are time-consuming and do not provide sensitive information and a degree of stability. The system dynamics behind the voltage stability are usually slow and therefore, can be effectively analyzed by static methods that examine the viability of the point of equilibrium presented by specific power system operating conditions. The analysis by using the static methods allows examination of a wide range of system conditions and provides much insight into the cause of the problem and the identification of the major contributing factors. Dynamic analysis is useful for a detailed study of specific voltage collapse situations, protection and controls coordination, and the testing of remedial measures. Dynamic simulations examine whether and how the steady-state equilibrium point will be reached (Kundur, 1993).

Voltage stability is divided into two types, static and dynamic voltage stability. The static voltage stability requires the analysis through the use of algebraic equations, while the dynamic requires the modelling of the precise replica of the voltage instability (Marison et al., 1993). Simulation-based models are essential for dynamic voltage stability analysis. Therefore, appropriate power system network models must be used, with simulation cases and various contingencies for predicting the voltage collapse point to accomplish the statistical analysis of the system voltage stability challenges.

The determination of how close the system is to voltage instability condition is determined by increasing the system load in a predefined manner which represents the stress of the system based on the historical and forecast data. However, it is important to consider the load pattern that results in the smallest stability margin (Kundur, 1993).

3.4.3 Modelling requirements

Planning studies are performed normally for minimum and maximum load conditions. Under minimum load conditions, the possibility of high voltages is examined, and under maximum load conditions, the possibility of low voltages and instability are examined. There are some other forms of investigations in power system engineering, namely circuit analysis and load or power flow analysis. In the circuit analysis, the parameters of the impedance, voltage, and current sources are specified, all nodal voltages and branch currents can just be calculated using the simple expression where the relationship between the voltage and current is linear. In the load or power flow analysis, loads and sources are defined in terms of powers, not in impedances or ideal voltage or current generators. All power system network branches, transformers, and overhead or underground cables are defined in terms of impedance, where the relationship between power, voltage, and impedances is non-linear (Vasantharathna, 2016). This requires the use of appropriate methods when these circuits are to be used.

3.5 Prevention of voltage collapse

There are design and operating measures that can be taken for the prevention of voltage collapse in power systems (Marison et al., 1993; Kundur, 1993; Vasantharathna, 2016).

3.5.1 System design measures

- Reactive power compensating device application
- Network voltage and generator reactive power control
- Protection or control schemes coordination
- Transformer tap-changer control
- Under-voltage load shedding schemes

3.5.2 System-operating measures

- Stability margin
- Spinning reserves
- Operator’s action

Reactive power compensation by capacitors is limited. When the voltage sags occur in the system, only a small amount of reactive power will be produced by the capacitor bank. An alternative method is opted for, the wind power plant source, and can be coupled locally at the point of voltage collapse. The wind power plant supplies both the active and the reactive power to the system and therefore guarantees a great improvement in terms of load demand fulfilments. How wind power plants assist the grid is further discussed in the next section.

3.6 Substation automation system

Substation Automation Systems (SASs) were introduced in the 1980s and are used for control, protection, monitoring, communication, etcetera in substations for improvement of the reliability of power systems (Kaneda et al., 2008; Koshiishi et al., 2012; MacKiewicz, 2006). The Electrical Power Research Institute (EPRI) and the Institute of Electrical and Electronics Engineers (IEEE) started to define a Utility Communications Architecture (UCA) in the early 1990s, where the reliability of the SAS was then improved by the addition of the IT-based solutions, namely Ethernet Local Area Network (LAN) (Koshiishi et al., 2012). About four years later around 1994, these institutes formed a Substation Control and Protection Interface (SCPI) group and began to work on UCA 2.0 (simply called UCA2) for field devices. They combined efforts with IEC Technical Committee 57 (TC57) and drafted proposals for international standardization of communication (IEC 60870-5-103) for substation automation systems in 1997. Between 2003 and 2005, the SCPI group work resulted in a widely used IEC 61850 standard with its main purpose ensuring interoperability between the field devices (Kaneda et al., 2008; Brunner, 2005).

3.6.1 IEC 61850 standard

IEC 61850 is a standard made for substation automation systems. It describes the communication between the IEDs in the substation and supports power system protection, monitoring, and control (Song et al., 2017). IEC 61850 consists of at least two communication protocols, i.e client/server and Generic Substation Event (GSE). GSE communication protocol within IEC 61850 is for high-speed control of messaging. It automatically broadcasts messages containing status, control, and measured values onto the network for use by subscribers. Its objects quickly and conveniently transfer status, controls, and measured values between peers on an IEC 61850 network. This is done through the concept of Logical Nodes (LNs) mapping.

There are three communication levels involved in the substation automation system: process level, bay level, and station level. The application of IEC 61850 GSE control within the substation automation has been trending. However, the protocol does not imply the full application of the IEC 61850, it minimizes hard wiring in the substation by increasing the capability of the digital relays to share the status messages via Ethernet Local Area Network (LAN). In this case, instrument transformers and sensors are connected directly to the protective equipment at the bay level. The conversion of analog to a discrete signal is performed by the IEDs. Figure 3.5 below shows the

substation automation communication levels (International Electrotechnical Commission, 2004).

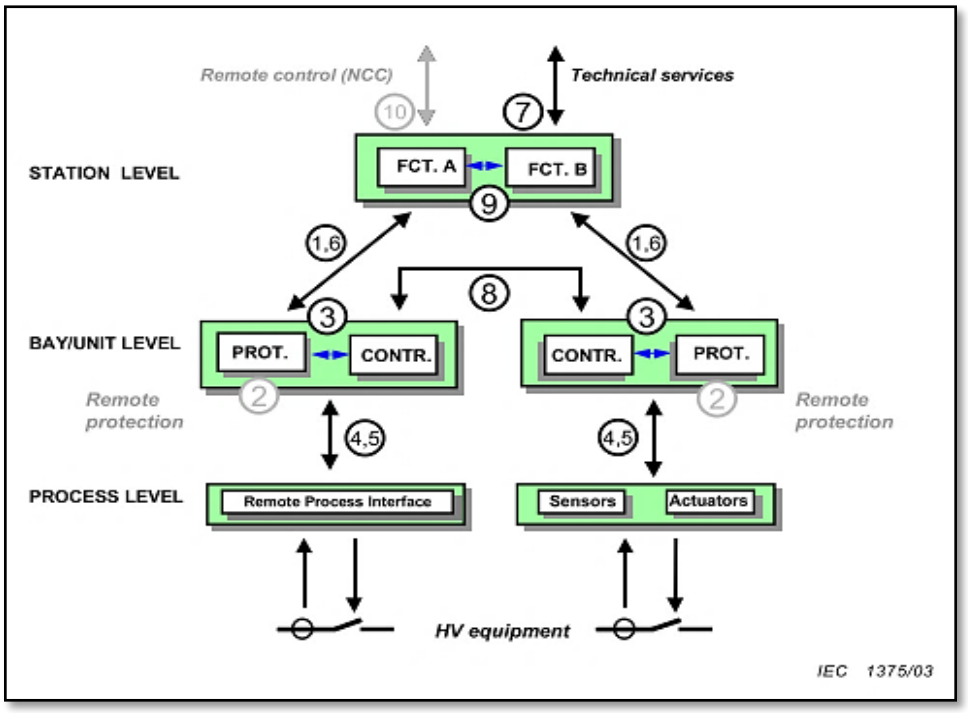

Figure 3.5: **Interface model of a substation automation system (IEC, 2003)**

Copper wires connected from the sensors and instrument transformers have effects during the long runs. The sensor output signal is low power and the distribution of this signal is impossible in the hardwire way (Bajanek, 2014).

Current carrying wires can induce an unnecessary magnetic field which may interfere with the communication processes. In addition, copper is expensive (Kanabar & Sidhu, 2011), and it is difficult to fault find in the network of many wires.

Merging Units (MUs) and conventional instrument transformers (based on the IEC 61850-9-2) are designed for the replacement of analog signal-carrying conductors. They convert analog signals to digital, ready to be sent through Ethernet LAN (based on IEC 8802-3) to the bay level where protection IEDs are located. This option allows the easy replacement of copper wiring by fibre-optic wires from the process level to the upstream of the communication network.

3.6.2 IEC 61850 standard protocols

Generic Substation Event (GSE), has two control models, Generic Object-Oriented Substation Event (GOOSE) and Generic Substation Status Event (GSSE). These

control models deal with different types of substation data, differentiated as follows (Mekkanen et al., 2014; Fernandes et al., 2014):

- **GOOSE**: It deals with any data format, it can be the status or value, grouped into a set of data that is transmitted in a form of Ethernet data packets within a period of 3 ms to 4 ms and works on the publisher to subscriber mechanism on multicast or broadcast mode.
  Examples of data formats are analogue data, binary data, integer values, etc.
- **GSSE**: As defined in the Utility Communications Architecture 2 (UCA2.0), it can only share the status data and uses the strings of bits rather than a group of binary data. Same as in GOOSE, GSSE data are grouped in a set of data that is transmitted in a form of Ethernet data packets within a period of 3 ms to 4 ms. In addition, it works on the publisher to subscriber mechanism on multicast or broadcast mode.
  Examples of GSSE data formats are status change into an event, fixed structure binary event, and bit pairs.

GSSE is an old control model, therefore simpler than the GOOSE data but in some other devices, it handles data faster. The GSE uses the multicast/broadcast service, that enables the distribution of an event message to more than one IED, which can be achieved by using plenty of copper wires in a traditional substation.

The advancement of technology has led to field devices that perform a variety of functions in a single box, which makes the availability of various analog and digital connection points on the device. The IEC 61850 standard contains a variety of application methods for substation and field device functions through the application of logical nodes and communication services both defined as Abstract Communication Service Interface (ACSI) to escape from the physical wiring of the output terminals from the devices that carry a variety of functions (Koshiishi et al., 2012).

The application of an abstract communication service interface allows the sharing of information through the LAN among the field devices by the defined logical nodes which carry many functions from each device pertinent to the status of the power system network. The function carried by these devices may be for monitoring, control, recording of events, and protection (Kaneda et al., 2008). The following is an overview of the substation automation functions:

- **Monitoring**: Monitoring of switchgear status, tap changing position and status of the transformer and tap changer, the status of protection and control equipment, monitoring of electrical quantities, e.g. current, voltage, frequency, power, and reactive power, etc.

- **Control**: Control of switchgear and transformer tap, synchronization check and interlocking, voltage regulating control and voltage reactive power control, etc.
- **Recording**: Recording the monitoring data and manipulation/control of facility/device, fault record of facility and device disturbance record, etc.
- **Protection**: Protection of a transmission line, transformer, feeder, busbar, generator, shunt reactors, shunt capacitors, etc.

These functions may vary from project to project and they are carried out by logical nodes that are transported through the LAN, and for that, it is necessary to discuss an object model for an IEC 61850 standard-based substation automation system.

3.6.3 Object model

Depending on the IEC 61850 standard scope, the object model is related to the domain substation. All the functions, including the data images about the devices available at the process level, are divided into the smallest realistic functional blocks which may communicate together, which may be implemented separately in devices whose functions are dedicated. These functional blocks are objects and are called Logical Nodes (LNs). Logical nodes deal with the functional grouping of data for a specific function. The functions in a logical node can be compulsory, optional, or conditional.

Examples of logical nodes include the data of a circuit breaker contained in a logical node XCBR or all data of a timed overcurrent protection element contained in logical node PTOC. All logical nodes have data and data have attributes (Brand, 2005; Brand et al., 2005). Figure 3.6 below on the next page is the illustration of an object model.

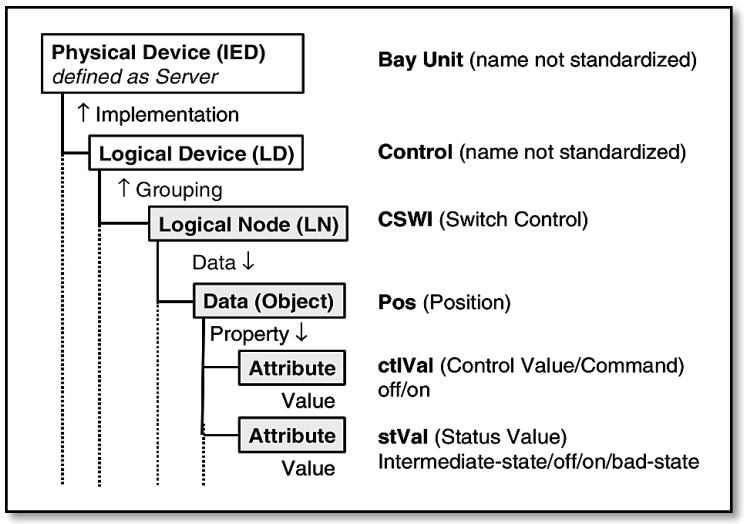

Figure 3.6: An IEC 61850 standard object model (Brand, 2005)

3.6.4 Timestamps and quality

IEC 61850-7-2 describes the GOOSE service model which provides the possibility for fast and reliable system-wide distribution of input and output data values, in which a retransmission scheme is specifically used to achieve the appropriate level of reliability.

When a SendGOOSEMessage request is generated by the GOOSE server, the current data values are encoded in a GOOSE message and transmitted on the multicast association. The event causes the server to invoke a SendGOOSE service as a local application issue as defined in IEC 61850-7-2. When this happens, a message is generated for each update. Additional reliability is achieved by retransmitting the same data with gradually increasing SqNum and retransmission time.

3.6.5 Communication

The communication network makes use of normal communication models, namely the International Organization of Standardization (ISO) or Open System Interconnection (OSI). These models make the communication stack which consists of the Ethernet layer (layer 1 and layer 2), and the Transmission Control Protocol (TCP) or Internet Protocol (IP) (layer 3 and layer 4), and Manufacturing Message Specification (MMS) (layer 5 to layer 7) (Brand, 2005).

Figure 3.7 below on the next page shows the communication stack for massage services in IEC 61850 communication network.

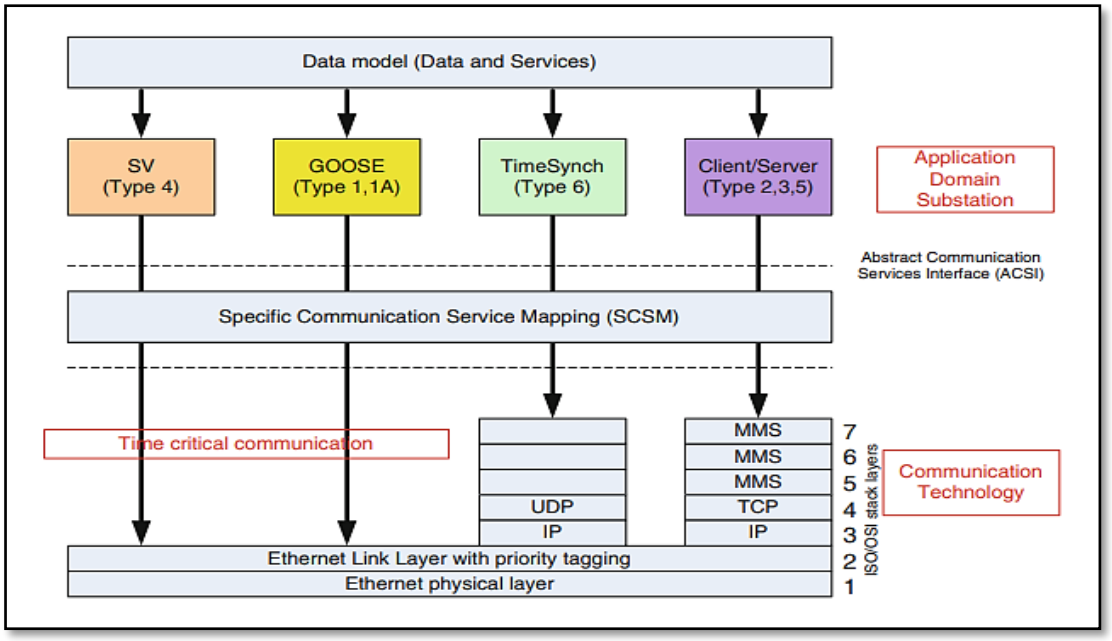

Figure 3.7: The communication stack for message services (Samitier, 2017)

The object model and its services are mapped to the seventh layer. The messages whose time is critical are not delayed, they are mapped directly to the second layer. Such types of messages are Sampled Analog Values (SAVs), Generic Object-Oriented Substation Event (GOOSE) containing status messages like indications, blocking, and tripping signals (Brand, 2005; Brunner, 2005).

3.6.6 IEC 61850 standard's benefits

IEC 61850 standard is a requirement for intelligent applications. It has features that show its power to introduce new intelligent applications. The standard applications are complex and efficient for power system management, system stability and quality management (Brand, 2005). IEC 61850 connects various types of intelligent electronic devices from different vendors. It aims to facilitate interoperability and enable the logical configuration of the substation automation system.

An IEC 61850 standard-based substation automation system is done through an Ethernet LAN (Kaneda et al., 2008). Apart from that, the IEC 61850 standard has the following features:

- The substation is modelled as a complete object that is standardized to control and process the data from the process devices like switchgear, instrument transformers and other sensors, power transformers, and other protection functions mapped in the same model.
- The substation configuration language (SCL), is used for the exchange of the configured data between different configuration tools that are used to identify or specify the substation, to configure the substation automation system and to configure individual IEDs
- Lastly, the IEC 61850 (as has already been mentioned in the previous parts) reduces the substation wiring by replacing the analog and digital signal copper wires with a single Ethernet LAN link from the process devices to the protection, control and monitoring devices found at the bay level. This moves the analog to digital conversion from the bay level to the process level.

Figure 3.8 and Figure 3.9 below and on the next page show the conventional versus the IEC 61850 standard-based connection between the process station and the bay station (Brunner, 2005). In Figure 3.8, it is shown that the analogue signals from the process level reach the bay control station, and in Figure 3.9, analogue signals end in the process station.

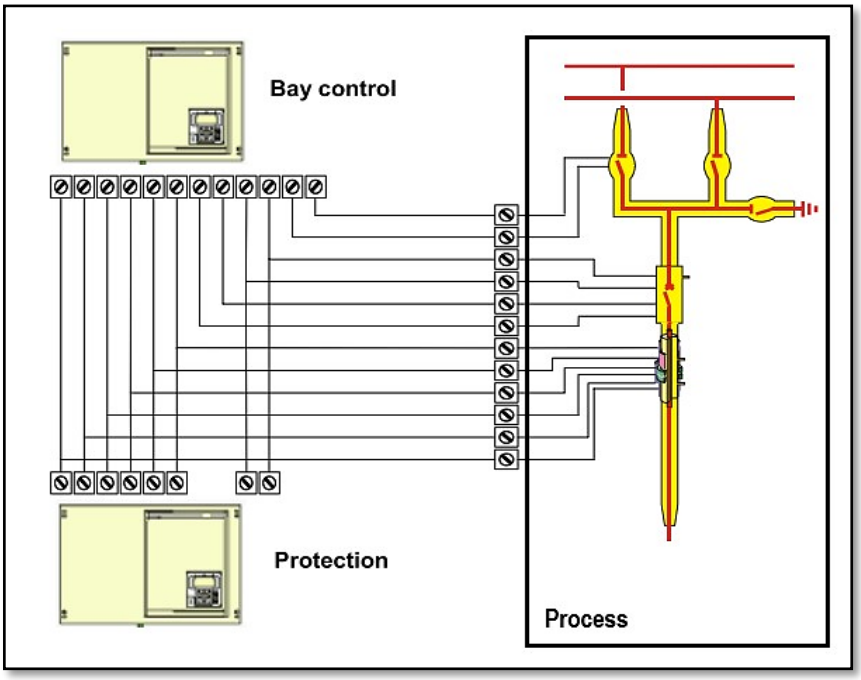

Figure 3.8: Conventional connection between the process and the bay level

It is through the application of IEC 61850-9-2 that the analog can only end in the process station. To achieve this, merging units (MUs) are used and they convert the analogue signals to digital signals that can be mapped through fibre-optic cables or Ethernet cables to the bay station, where decisions and commands are carried out by protective devices.

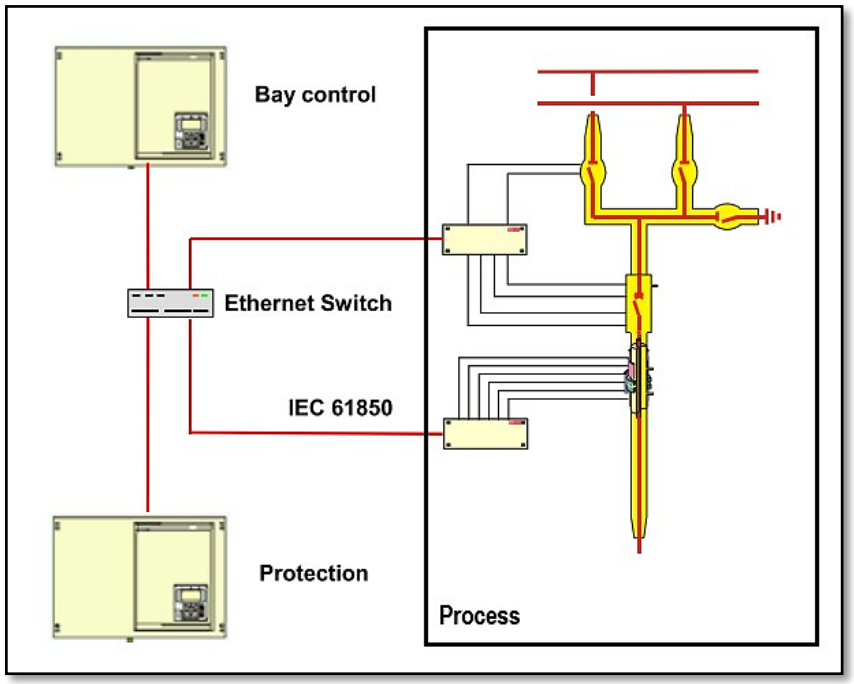

Figure 3.9: IEC 61850 standard-based connection between the process and the bay level

The design of the substation automation systems deals with the sequence of steps starting from the design specifications up to the commissioning of a project-specific system. In addition, because the IEC 61850 standard uses the file services as one of its protocols to share data over the Ethernet network for processes by other devices compliant with the standard, the following section looks at the Substation Configuration Language (SCL).

3.6.7 Substation Configuration Language (SCL)

The Substation Configuration Language (SCL) is defined as the Extensible Mark-up Language (XML)-based configuration language that is used in the support of the database configuration data exchange between different tools that sometimes come from different vendors. To ensure the formal description of the Substation Automation (SA), the SCL consists of four different files listed as follows (SEL, 2018):

- **IED Capability Description (ICD) file**: As the name says “capability description”, it describes the features or capabilities of an IED, including the information contained by the logical node and the support of GSE.
- **System Specification Description (SSD) file**: This type of file describes a single-line representation of the substation and its required logical nodes.
- **Substation Configuration Description (SCD) file**: It contains the information pertinent to all IEDs, communication network configuration data as well as the description of the substation as a whole.
- **Configured IED Description (CID) file**: (Usually many for a single IED), describe a single IED within the created project and include the location or address information.

3.7 Conclusion

For validation of results and clear conclusions to be drawn, it is necessary to perform various case studies for calculations and investigations of power system challenges before working on the interconnected system.

In this chapter, the theory about voltage stability, wind power plants, their benefits and the challenges they introduce into the grid system, protection schemes pertinent to the common point of coupling, substation automation systems, as well as the simulation tools suitable were discussed.

The next chapter uses RTDS and RSCAD for the modelling and simulation study of the considered power system network for the investigations of the power system voltage stability challenges.

CHAPTER FOUR
MODELLING AND SIMULATION OF THE POWER SYSTEM NETWORK ON RSCAD

4.1 Introduction

Various simulation tools are used in power systems, for modelling and simulation studies. These tools form modern methods of solving mathematical algorithms in a faster way than conventional methods. For this chapter, the power system network model is built on Real-time Simulator Computer-Aided Design (RSCAD) software and is used as the foundation of investigations for voltage stability challenges and later for protection studies. The contingencies (in terms of the load demand increase) are applied and the statistical analysis of the active power versus voltage (PV) and the voltage over reactive power (QV) is done.

4.2 The power system network model

One of the requirements in power system engineering studies is the accuracy of results and clear conclusions. The IEEE Nine-bus system as shown in Figure 4.1 below was used for this study.

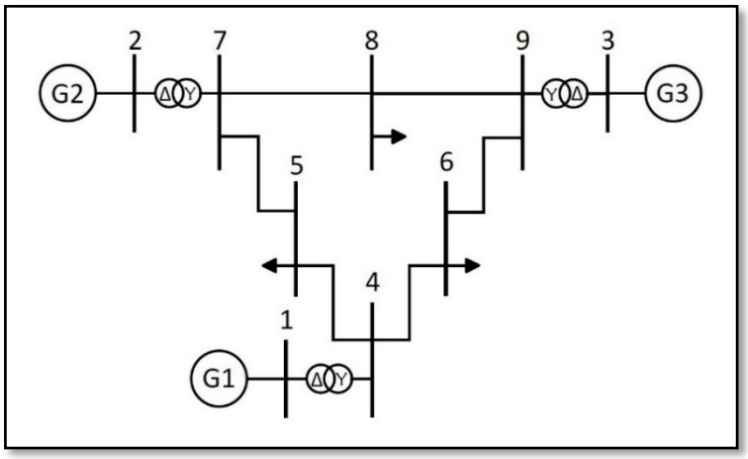

Figure 4.1: IEEE Nine-Bus system

The network system was divided into two areas, namely; Area 1 and Area 2 due to its size. Figure 4.2 below on the next page shows the sectionalized IEEE Nine-Bus system with revised busbar identities. Its parameters are presented in Appendix A of this document.

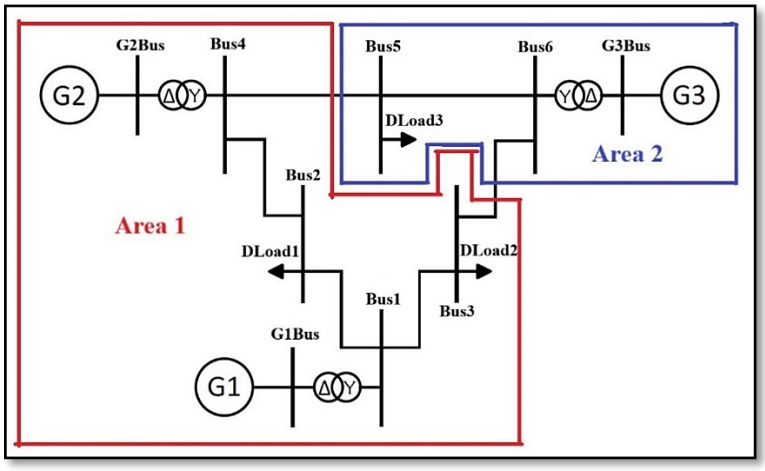

Figure 4.2: Sectionalized IEEE Nine-Bus system with new busbar labels

Figure 4.3 below shows Area 1 is modelled in Subsystem 1 (Rack 1) and Figure 4.4 shows Area 2 modelled on Subsystem 2 (Rack 2) of the Real-Time Digital Simulator (RTDS).

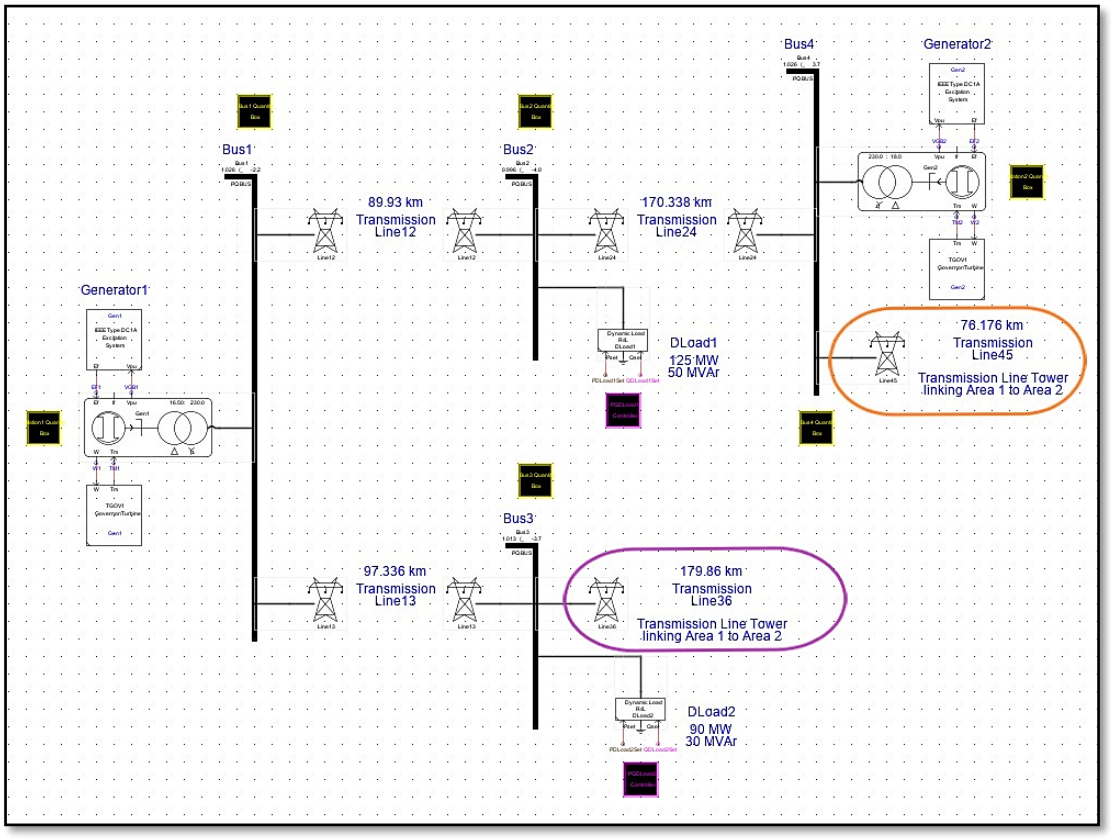

Figure 4.3: Area 1 of the IEEE Nine-Bus system in Subsystem 1 (Rack 1)

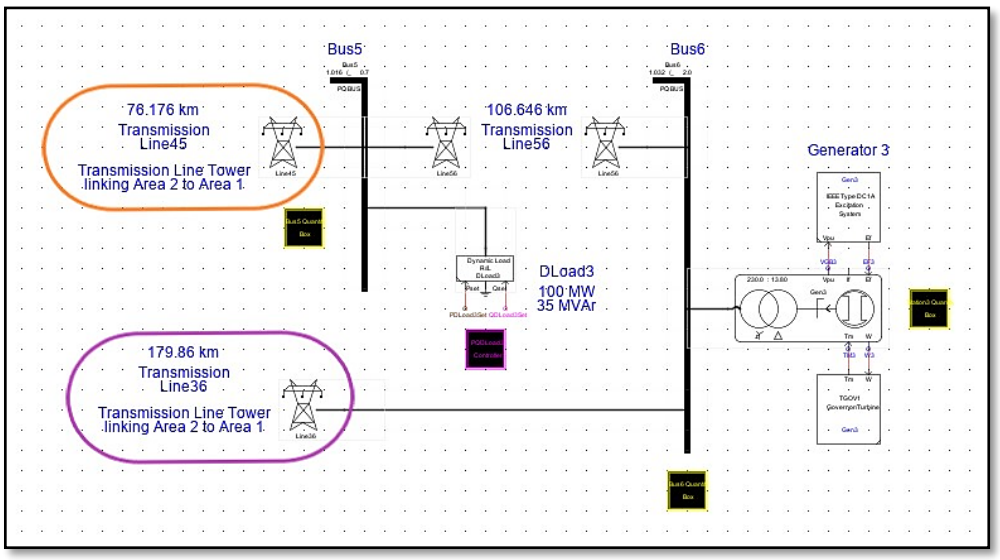

Figure 4.4: Area 2 of the IEEE Nine-Bus system in Subsystem 2 (Rack 2)

4.3 Design of logic diagrams for control and monitoring of network quantities

In the case where active power losses and reactive power absorption in the system are required for monitoring, the user needs to design additional logic to calculate the difference between the sending-end or generated and receiving/consumed power. This is based on the principle that the active or reactive power lost or absorbed on the transmission is the difference between the active or reactive power generated and the active or reactive power consumed by the load.

For the network in figures, 4.3 and 4.4, modelling and settings for monitoring are done based on the order presented in Table 4.1 below on the next page, where the monitored quantities are indicated “Yes”, and “Space” for non-monitored.

Table 4.1: Quantities to set and model for monitoring

Component	Generators			Busbars						Dynamic loads		
Parameters number	**1**	**2**	**3**	**1**	**2**	**3**	**4**	**5**	**6**	**1**	**2**	**3**
Frequency	Y	Y	Y									
Angular speed	Y	Y	Y									
Torque	Y	Y	Y									
Voltage (PU)	Y	Y	Y	Y	Y	Y	Y	Y	Y	Y	Y	Y
Reactive Power	Y	Y	Y		Y	Y		Y		Y	Y	Y
Power factor	Y	Y	Y		Y	Y		Y		Y	Y	Y
Voltage (RMS)	Y	Y	Y	Y	Y	Y	Y	Y	Y	Y	Y	Y
Apparent Power	Y	Y	Y		Y	Y		Y		Y	Y	Y
Active Power	Y	Y	Y		Y	Y		Y		Y	Y	Y
Current (RMS)	Y	Y	Y	Y	Y	Y	Y	Y	Y	Y	Y	Y
	Yes = Y, No = Space											

4.3.1 Monitoring and calculation logics for generator quantities

Generating stations consist of synchronous machines whose mechanical shafts are driven by prime movers. There are two principal parameters in a prime mover, the angular velocity and the torque. The operation of the synchronous generators, therefore, depends on these parameters.

There are two operating modes generators can be operated, on lock and free mode. On the lock mode, the generators produce power based on the rotational speed of the prime mover. In the free mode, the operation of the generator is based on the mechanical torque input to the generator.

The frequency in the generators can be monitored by using the angular velocity of the generator which varies with regards to the time when the generators are loaded. The value of the frequency on the mechanical side of the generator can be calculated using the expression

$$f = \frac{\omega}{2\pi} \tag{4.1}$$

In this expression, ω is the rotational speed of the generator in units of radian per second (rad/sec).

To monitor the frequency for Gen1 the divider junction is used as shown in Figure 4.5 below. In the figure, the signal named *W1* is the angular rotational speed measured in rad/sec monitored from Gen1. The signal named *fGen1* is the calculated frequency and 2π is a constant in radians of measure.

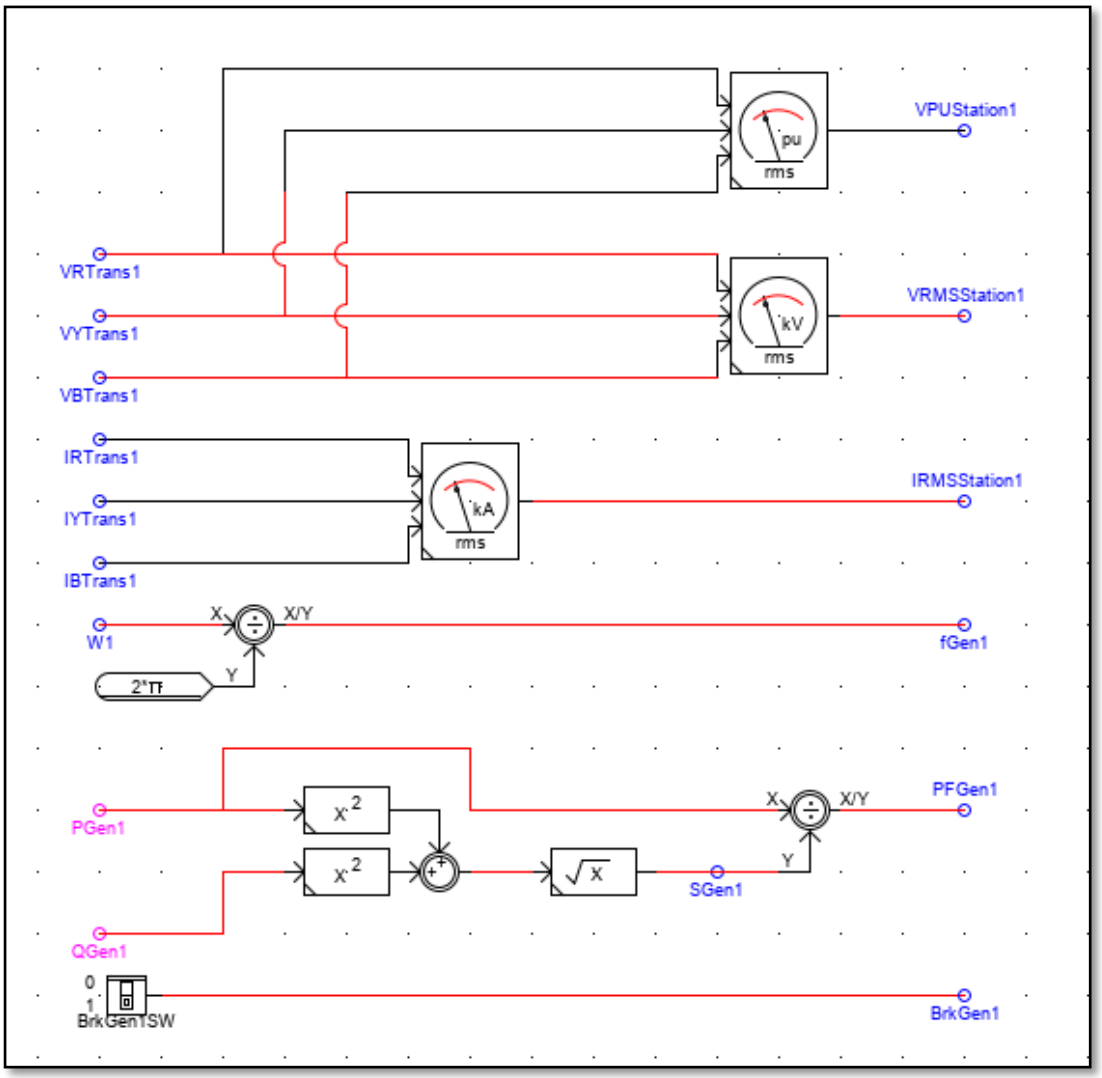

Figure 4.5: **Calculation and monitoring logics for Gen1**

In addition to the above figure, the logic is shown, for calculating the RMS current fed to Bus1 by Gen1. The RMS meter produces the current with signal named *IRMSStation1* from the current signal names *IRTrans1, IYTrans1* and *IBTrans1* signal names monitored from the high voltage side of the transformer in Station 1. Another logic is shown in the above figure, for per-unit and RMS voltage calculation, wherein the figure, signal names *VPUStation1* and *VRMSStation1* are per-unit and RMS voltage signals output from the per-unit and RMS meters calculated from the actual voltage

signals (*VRTrans1, VYTrans1* and *VBTrans1*) from the high voltage side of Transformer1 in Station 1. In addition, the logic diagram in the above figure measures the active and reactive power from Gen1 to calculate power factor and apparent power using the power triangle principle. The signal names for these quantities are labelled and shown as *PFGen1* and *SGen1* in the same figure.

The input signal names *PGen1* and *QGen1* on the presented calculation logic are active and reactive power signal names made available for monitoring in Gen1 as shown in Figure 4.6 below.

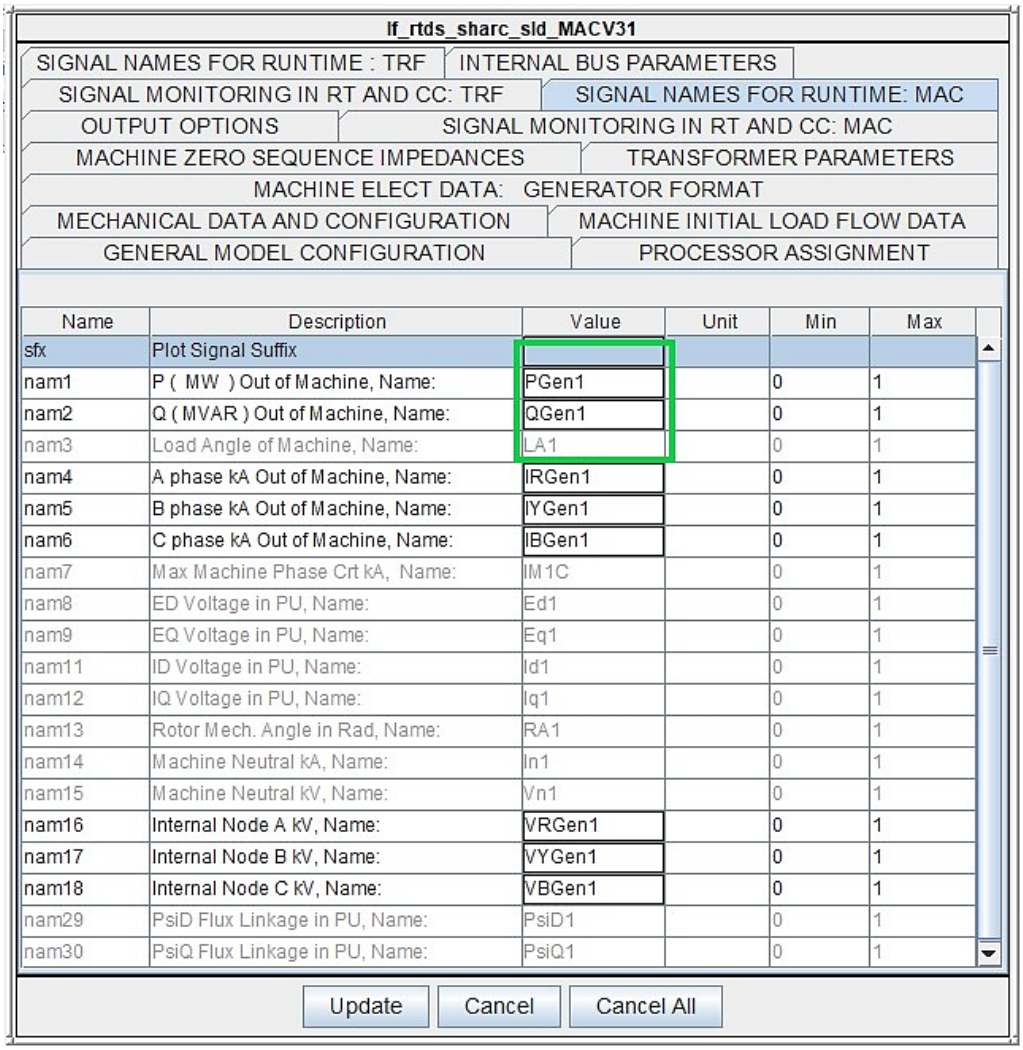

Figure 4.6: **Generator1 P and Q signals to be monitored**

The voltage and current produced by Gen1 are set available for monitoring. Because the simulation cases in this section are based on the high voltage transmission side of the network model, the two signals are not monitored. The same components and logic are done for the rest of the station generators Gen2 and Gen3 respectively.

In Figure 4.7 below, the generator is shown with its governor/turbine. The angular speed signal named *W1* is monitored from the generator and is input to the governor/turbine. *TM1* is the signal named for the governor/mechanical torque, which makes an input to the synchronous generator.

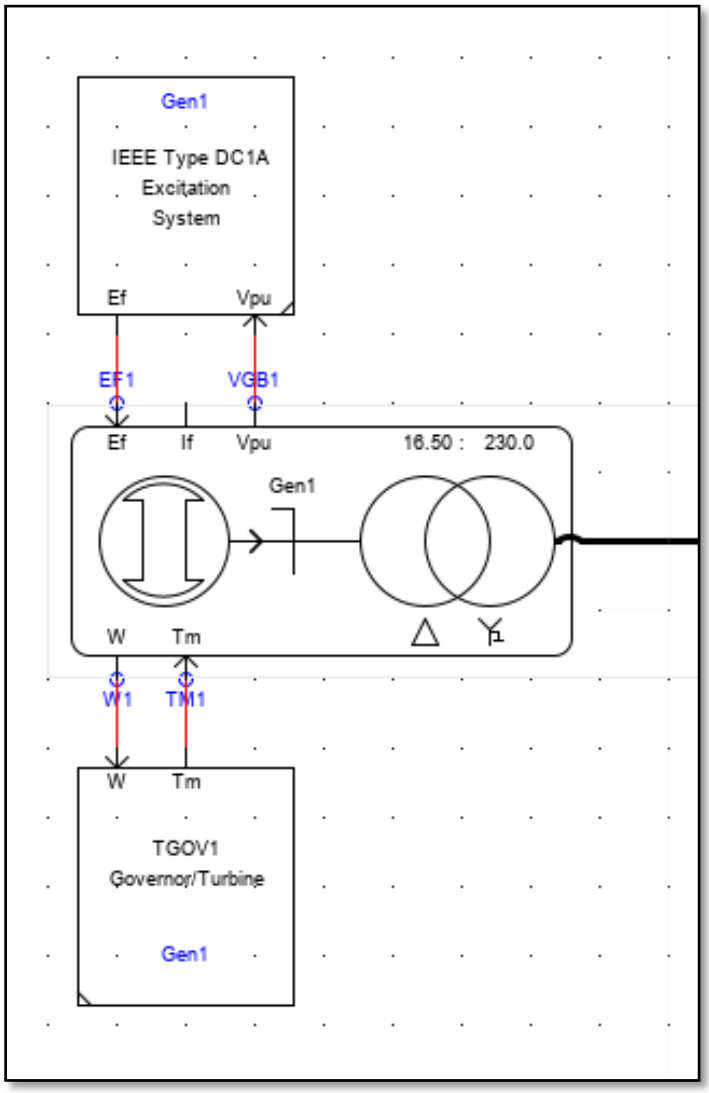

Figure 4.7: **Generator1 and its governor modelled in Subsystem 1**

All the generators in the Nine-bus network have the same setup. Therefore, monitoring signal names are completed in a similar manner.

4.3.2 Monitoring and calculation logics for busbars

The power system model used for this study was reduced to six busbars. The busbars with loads are usually more vulnerable to voltage instability. Therefore, out of the six busbars, three busbars are only limited to monitoring of three signals, the PU and RMS voltage for Bus1, Bus4 and Bus6. The PU voltage, reactive power, power factor, RMS voltage, apparent power, active power and RMS current are monitored for the rest of the busbars.

The monitoring of the per-unit voltage, RMS voltage and current for Bus1 is brought to RSCAD runtime by modelling the logic shown in Figure 4.8 below. In the figure, Zone calculation logic for PU and RMS voltage is shown with output signal names *VPUBus1* and *VRMSBus1* calculated from the voltage monitored from the busbar, whose signal names are *VRBus1, VYBus1* and *VBBus1*.

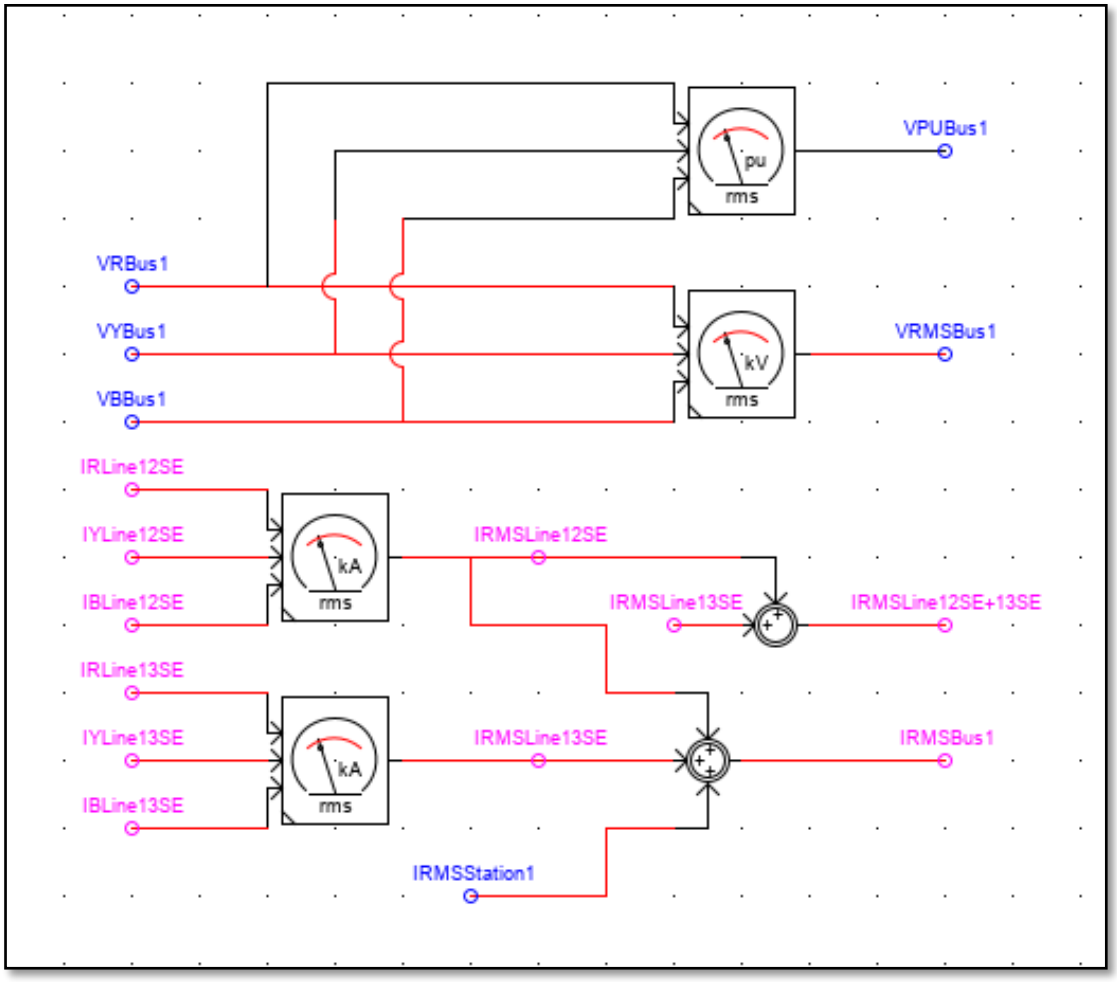

Figure 4.8: **Bus 1 monitoring and calculation logics**

To monitor the RMS value of the current in this busbar, RMS values of the currents from the three branches are summed together. Two RMS meters are shown in the same figure (Figure 4.8 above). They are used to calculate the RMS currents from the two branching transmission lines labelled Line12SE and Line13SE in the network presented in figures, 4.3 and 4.4 of Section 4.2, and these RMS output currents are added together with that of the current delivered by Staion1 to this busbar.

In addition, in the above figure, signal names, *IRMSLine12SE*, *IRMSLine13SE* and *IRMSStation1*, are the RMS current signal names calculated and monitored from the first sending transmission line branch, the second sending end transmission line branch

and the Station1 feeder. Signal named *IRMS12SE+13SE* is the sum of the RMS currents from the two sending end branching transmission lines from Bus1.

The reactive power, power factor, apparent power and active power are monitored for Bus 2, Bus 3, and Bus5 since they are loaded. To monitor these quantities, additional logic is modelled for these busbars as shown in Figure 4.9 below. The signal names *PBus2*, *QBus2*, *SBus2* and *PFBus2* are the active power, reactive power, apparent power and the power factor monitored in Bus 2.

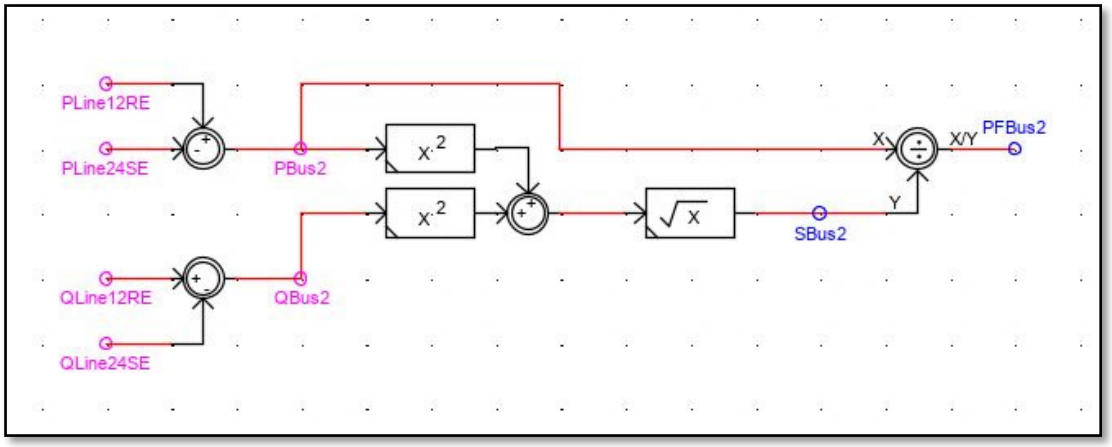

Figure 4.9: **Reactive power, power factor, apparent power and active power calculation logic for Bus 2**

The power is delivered by the transmission lines on each busbar, and Bus 2 is fed from two transmission lines, Line12 and Line24. The link to these busbars is through the receiving end and sending the end of Line12 and Line24. Both these receiving and sending ends of the two lines have the option to monitor the active and reactive power.

The same settings are done for the sending end of Line24, and the signal names for this line are labelled *PLine24SE* and *QLine24SE* as can be seen on the input of the power factor calculation logic in Figure 4.9 above. In addition, the signal names for the monitored power on each busbar will end with the busbar number, and the signal names for the currents added depend on the signal names of the currents of the transmission lines connected to that busbar.

4.3.3 Control, monitoring and calculation logics for dynamic load quantities

The power system network model understudy has three dynamic loads whose input power can be made variable depending on the investigations conducted per simulation cases. Initially, the investigations are based on the initial loading of the system, and, the control of these loads is done using the sliders. Therefore, no control logic is designed for loads. The power generated from the stations is delivered to the loads

connected to busbars, Bus 2, Bus 3 and Bus 5. In addition, the current is drawn from the busbar by each load.

To monitor these quantities on the RSCAD runtime, the logic shown in Figure 4.10 below is developed.

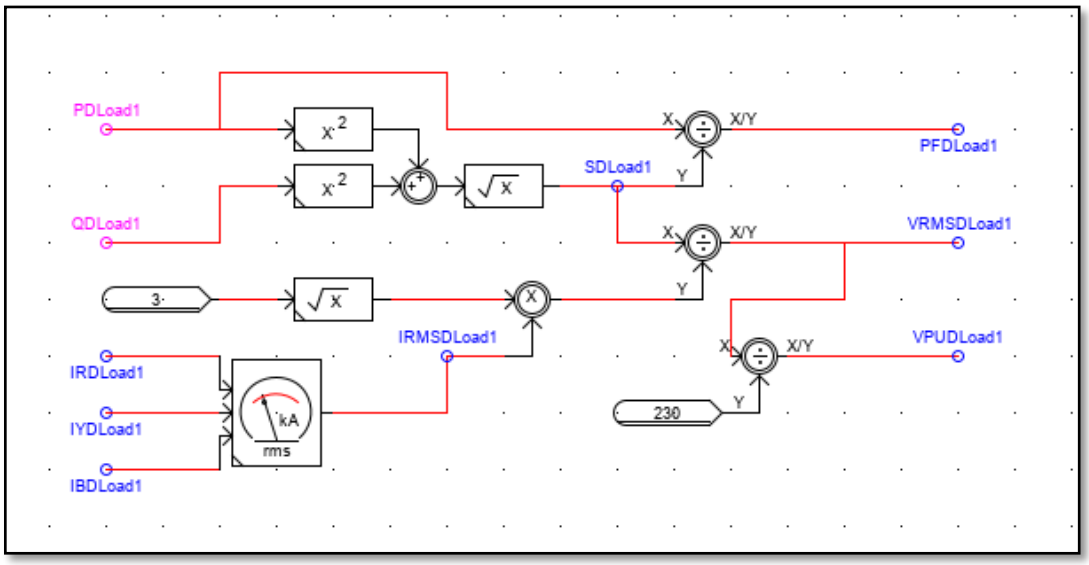

Figure 4.10: **Power factor, apparent power, RMS voltage, per-unit voltage and RMS current calculation logic for DLoad1**

There are five input signals to the logic, labelled *PDload1*, *QDLoad1*, *IRDLoad1*, *IYDLoad1* and *IBDLoad1*. These signals are active, reactive power and line currents monitored from DLoad1 and are made available for monitoring on RSCAD Runtime The active and reactive power signals are used for the calculation of power factor and apparent power with signal names *PFDLoad1* and *SDLoad1* using the power angle triangle technique. The line currents monitored are used for calculating the RMS currents drawn by the load from Bus 2 and the output is given the signal name *IRMSDLoad1*. The signal names *VRMSDLoad1* and *VPUDLoad1* in Figure 4.10 above are the signal names for monitoring the RMS and per-unit voltage measured on the load. The per-unit voltage is simply calculated by taking the ratio of the actual measured RMS voltage signal over the rated voltage of 230 kV as shown in the above figure. The RMS voltage signal is calculated from the three-phase voltage calculation expression

$$\text{VRMSDLoad1} = \frac{\text{SDLoad1}}{\sqrt{3}\ \text{IRMSDLoad1}} \qquad (4.2)$$

Where *SDLoad1* and *IRMSDLoad1* are the apparent power and RMS current calculated for DLoad1. These settings are the same for all the other loads in the system,

except for signal names. The signals to be monitored are set while the calculation logics are modelled.

All these signals are now available on the RSCAD runtime for monitoring the network during the simulation cases.

4.4 Load flow analysis

One of the basic tasks in investigating the power system network challenges is that of verifying the stability of the busbar or node voltages. The load flow was simulated and the results are as shown in Figure 4.11 below.

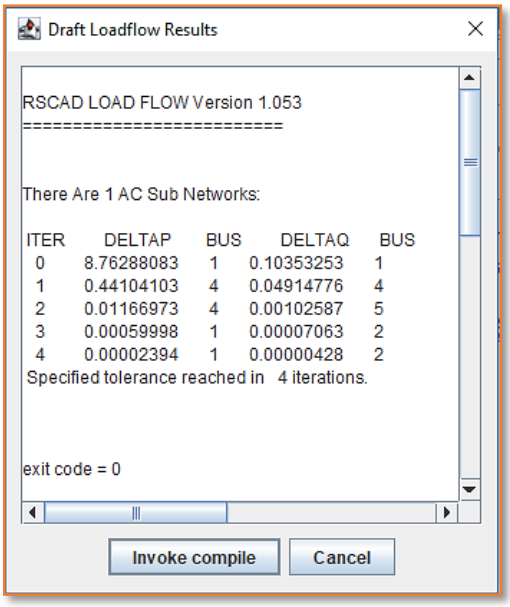

Figure 4.11: **The RSCAD draft load flow simulation results**

When the draft load flow simulation is invoked, the busbar voltages, generated and consumed real and reactive power can be read on the draft network modelled in subsystems, 1 and 2.

The results are recorded in Table 4.2 below, where P_G and Q_G represents the active and reactive power generated during the draft load flow in megawatts (MW) and megavars (MVARs), and P_L and Q_L represents the active and reactive power demanded by the loads during the draft load flow in megawatts (MW) and megavars (MVARs). In addition, the per-unit busbar voltage magnitudes and their phase-shifts are recorded after the RSCAD draft load flow calculation has been compiled.

Table 4.2: RSCAD draft load flow results

Bus	Bus type	Voltage (pu)	P_G (MW)	Q_G (MVAr)	P_L (MW)	Q_L (MVAr)
Gen1Bus	Slack	1.04∠0°	71.779751	36.267457	-	-
Gen2Bus	PV	1.025000∠ 8.363888°	163.000000	11.23	-	-
Gen3Bus	PV	1.025000∠4.022079°	85.000000	-3.720376	-	-
Bus1	PQ	1.020690∠27.767750°	-	-	-	-
Bus2	PQ	0.992780∠26.324740°	-	-	125.0	50.0
Bus3	PQ	1.006400∠26.565460°	-	-	90.0	30.0
Bus4	PQ	1.022990∠32.788440°	-	-	-	-
Bus5	PQ	1.012840∠30.292890°	-	-	100.0	35.0
Bus6	PQ	1.028280∠31.313340°	-	-	-	-
Total			319.779751	47.497453	315.0	115.0

4.5 The steady-state power flow analysis on RSCAD runtime module

A variety of monitoring options are available on the runtime module, namely RMS meters and plots. For instance, during the steady-state analysis of the power flow in the system, RMS meters can be used. For disturbance (or transient) analysis, the plots are used.

4.5.1 Generators or station monitoring

It is the awareness that, even though the concern of the study is based on the busbars or substations that suffer the most in voltage stability issues, the initial simulations are based on all the busbars of the system for verification purposes. This is the reason why this part shows the monitoring results even for the busbars that are least significant for the investigation.

Table 4.3 below shows the meters for the initial runtime simulation results of the system under steady-state conditions for the three generating stations of the network.

Table 4.3: Quantities monitored at Station 1 to 3 under steady-state power flow

Quant.	Freq. (Hz)	Ang. Spd. (rad/sec)	PU Torque	RMS V (kV)	PU V.	P (MW)	Q (MVAr)	PF	S (MVA)
Station 1	50	314.2	0.7218	234.8	1.021	71.81	36.26	0.8927	80.44
Station 2	50	314.2	1.634	235.3	1.023	163.0	11.24	0.9976	163.4
Station 3	50	314.2	0.854	236.6	1.029	85.03	-3.708	0.9991	85.11

The results recorded in the above table were monitored while the system generators were on lock mode.

Two variables can be used to conclude whether the system is operating on a steady-state; these are frequency and angular speed. The frequency is at 50 Hz and the angular speed is at 314.2 rad/sec. These variables usually change when the system experiences some disturbances. In simulation studies, these variables change when the contingencies are applied.

4.5.2 Monitoring on load busbars and loads

The loaded busbars tend to respond with unstable characteristics when the system is exposed to disturbances. The voltages usually drop when the load demand increases, while the current increases. Under steady-state load flow simulations, monitoring is focussed on loaded busbars and loads. The voltage stability studies require precise monitoring of the node voltages. Table 4.4 below shows the results recorded from the meters for busbars, 2, 3 and 5 where dynamic loads, DLoad1, DLoad2 and DLoad3 are connected.

Table 4.4: Busbars, 2, 3 and 5 Dload1, DLoad2 and DLoad3 monitored values at the steady-state power flow

Quantities	Per unit voltage	RMS voltage (kV)	RMS currents (kA)	Active power (MW)	Reactive power (MVAr)	Power factor	Apparent power (MVA)
Bus 2	0.9928	228.3	0.6995	125	50	0.9285	134.6
DLoad1			0.3404	125	50	0.9285	134.6
Bus 3	1.006	231.5	0.4765	90	30	0.9487	94.87
DLoad2			0.2366	90	30	0.9487	94.87
Bus 5	1.013	232.9	0.5368	100	35	0.9439	105.9
DLoad3			0.2626	100	35	0.9439	105.9

The initial active power demanded by the dynamic loads, DLoad1, DLoad2 and DLoad3 from the busbars, 2, 3 and 5 is 125 MW, 90 MW and 100 MW respectively. In addition to the above table, the recorded voltage measurements are within the accepted continuous operating range.

The currents that flow through the branches associated with busbars, 2, 3 and 5 were monitored and recorded in Table 4.5 below on the next page.

Table 4.5: Currents monitored from the branches associated with the most significant busbars

Busbar connected to	Branches	RMS current (kA)	Total RMS current (kA)
Bus 2	Line12RE	0.1209	0.3403
	Line24SE	0.2194	
Bus 3	Line13RE	0.0772	0.2359
	Line36SE	0.1587	
Bus 5	Line45RE	0.1873	0.2580
	Line56SE	0.0707	

The total RMS current recorded in the above table is equal to the current flow to each dynamic load. This is why the right-hand side column of this table contains the same values as those of the total RMS values in the fourth column of Table 4.4.

Another part of steady-state power flow calculations is that of verifying the amount of power consumed by the loads and the one that is lost or absorbed during transmission to the one that is generated by the system generators. From this analysis, conclusions can be drawn about the initial conditions of the system that it operates well. Part 4.5.3 provides a single line representation of the simplified system under study.

4.5.3 The simplified network system

Under normal system operating conditions, the active power loss and the reactive power absorbed during the transmission must be equal to the difference between the generated and consumed active and reactive power. This is proven by the results shown in Figure 4.12 below which presents the simplified power system network of the interconnected system used.

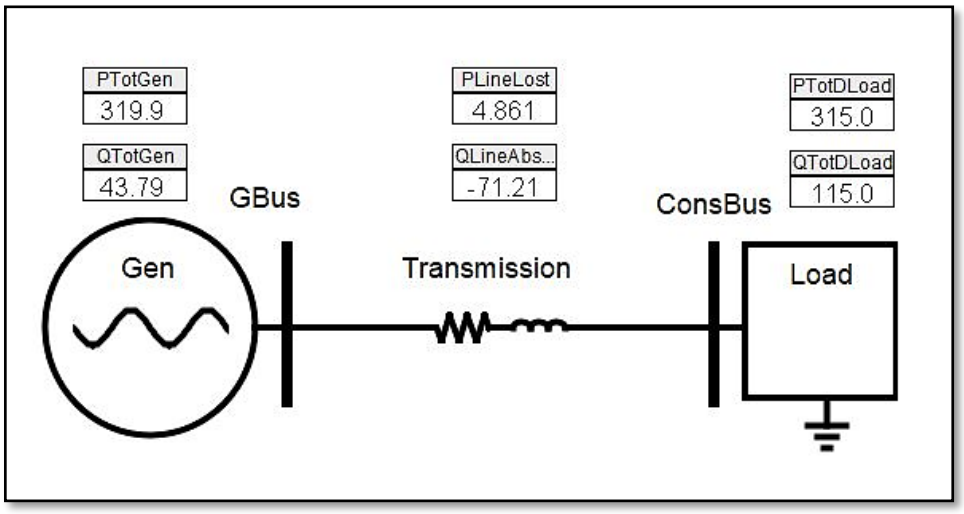

Figure 4.12: Simplified power system network under steady-state conditions

The measurements shown in the above figure match the characteristics for normal operating conditions of power systems in that, the power generated is equal to the sum of the power losses and the demand active power. The same applies to the reactive power, it is still balanced, as the reactive power supplied by the transmission line makes the difference between the generated and consumed reactive power by the generators and the load respectively.

4.6 Load demand increase contingency

A contingency study is performed in this section, to investigate the effect of the load demand increase on the busbar voltages. To perform the load demand increase in RSCAD, the load scheduler component is used for the logic to perform this function as described in Part 4.6.1. In addition in this section, the overload contingency case study is presented in Part 4.6.2.

4.6.1 Overload contingency logic

RSCAD power system dynamic loads can be tuned externally using the control logic, where P and Q setting inputs are fully made available for the external logic for tuning. Figure 4.13 below shows the dynamic load control logic.

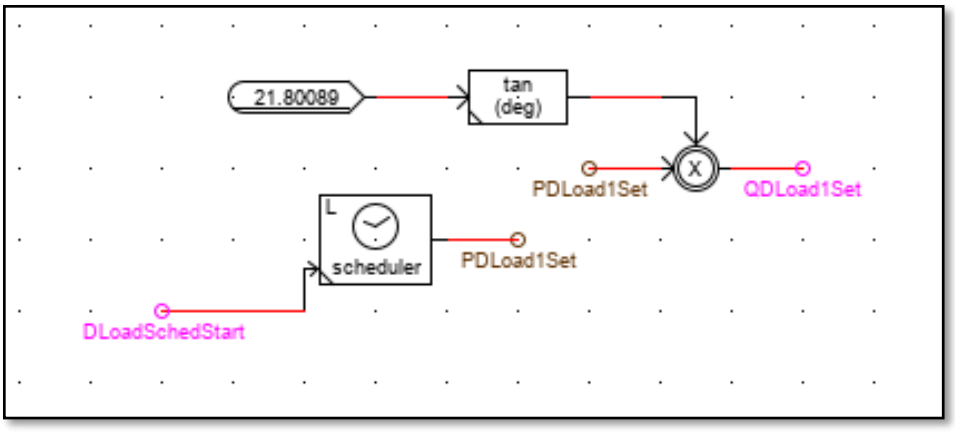

Figure 4.13: RSCAD dynamic load, control logic for automatic power scheduling

In the above figure, the signal names *PDLoad1Set* and *QDLoad1Set* are to control DLoad1. The signal named *DLoadSchedStart* is for controlling the state (*ON/OFF*) of the scheduler component and is an output from a binary switch. The component labelled “scheduler” plays the role of increasing the load demand by multiplying the given multiplier with the initial values of power. Settings for this component are by default at the initial rated power of the dynamic loads. The load scheduling settings and multiplier values are shown in Appendix B at the end of this document. The “tan(deg) component is the multiplier of the active power input signal to the dynamic load. The output signal *QDload1Set* is the reactive power to the load based on the simultaneous

increase between the variables P and Q, to keep the power factor of the load constant. The power demand will remain in the initial state until the load scheduler switch is put on the on position on the runtime.

4.6.2 System overloading contingency

To assess the loading contingency the load is instantly increased by 5 MW in each load after every 0.1 seconds until the voltage collapse point is reached. The voltage is monitored for both the least significant and most significant.

4.6.2.1 Bus 1 to 6 per-unit voltages

When the instant load increase is simulated, the voltage sags were experienced in the system, especially in the busbars with loads connected. The results shown in the figures below show the per unit voltage waveforms under this event.

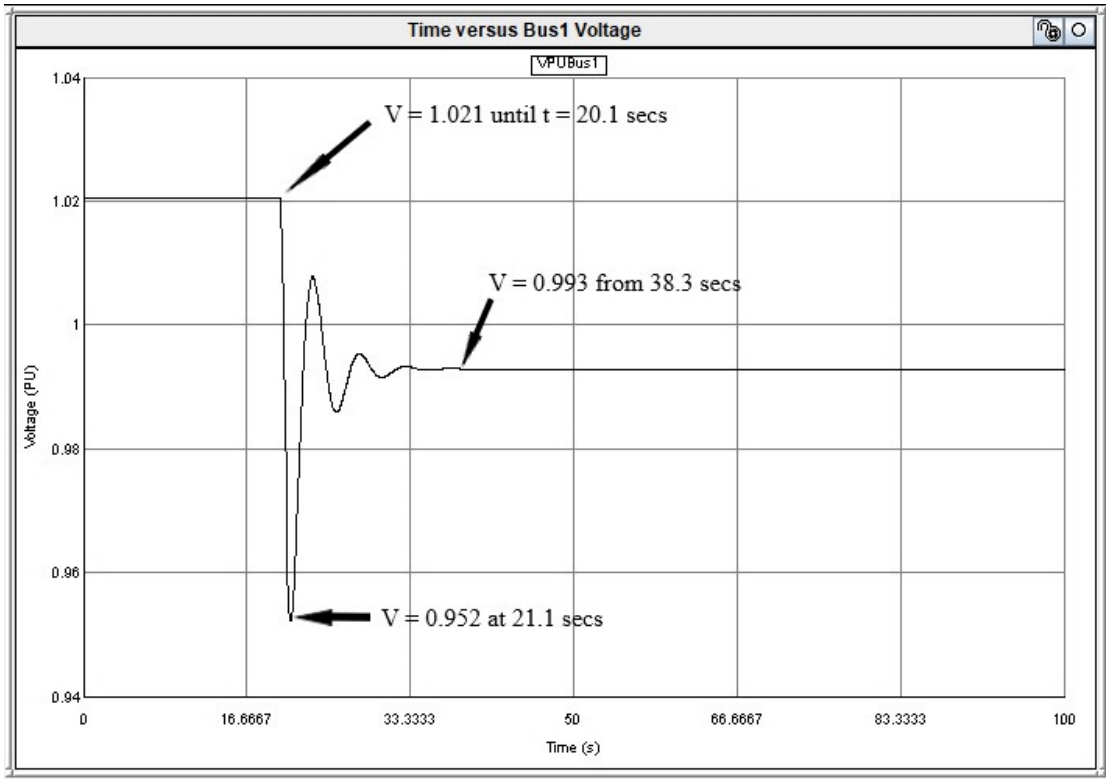

Figure 4.14: Bus 1 per-unit voltage waveform

In Figure 4.14 above, the initial voltage is 1.021 PU and this is when the initial loading is 315 MW. An instant load increase began at 20.1 seconds and a voltage decrease was experienced in Bus 1. At 21.1 seconds, the busbar voltage was at 0.952 PU for a very short period and suddenly recovered for 0.993 PU at 38.3 seconds. According to the specified continuous operating range of the node voltages, these values are still accepted. Based on these observations, Bus 1 is healthy.

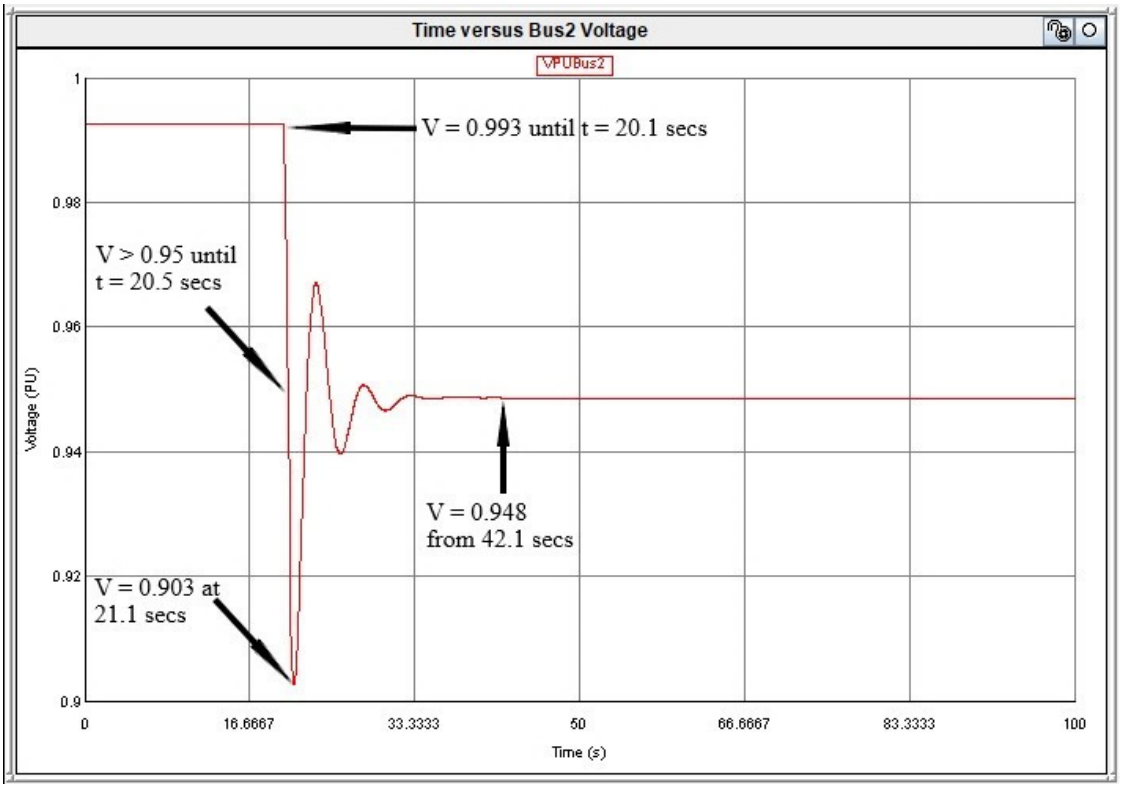

Figure 4.15: **Bus 2 per-unit voltage waveform**

In Figure 4.15 above, the initial voltage is 0.993 PU until 20.1 seconds. An instant increase in load demand begins until 20.1 seconds. It shows that the busbar voltage went below the minimum operating range of 0.95 PU starting from 20.5 seconds until 21.1 seconds. The voltage tries to recover between 21.1 seconds and 42.1 seconds but it does not get back to the accepted continuous range, therefore is unstable.

In Figure 4.16 below on the next page, the initial voltage is 1.006 PU. The voltage is at the accepted range until the time of 20.7 seconds elapses. After this time, it is when the busbar voltage begins to collapse. When the duration of the event expires at 21.1 seconds, the voltage goes back to stability after 50.4 seconds.

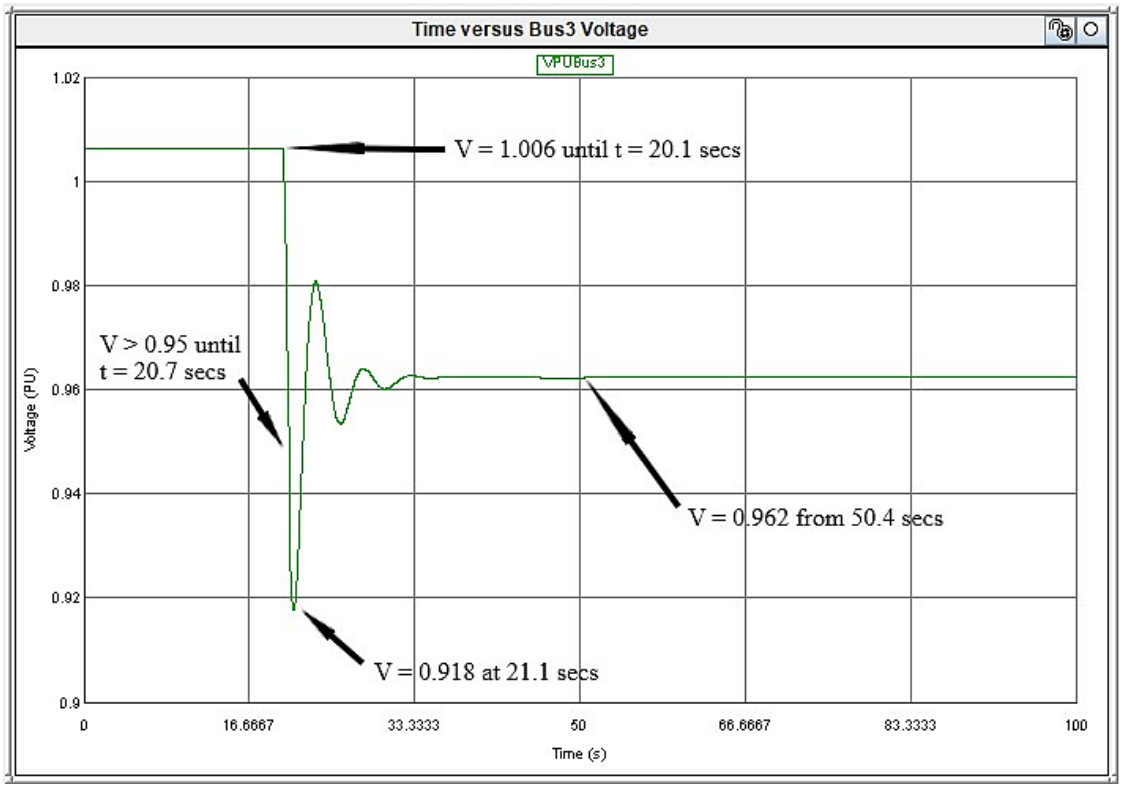

Figure 4.16: Bus 3 per-unit voltage waveform

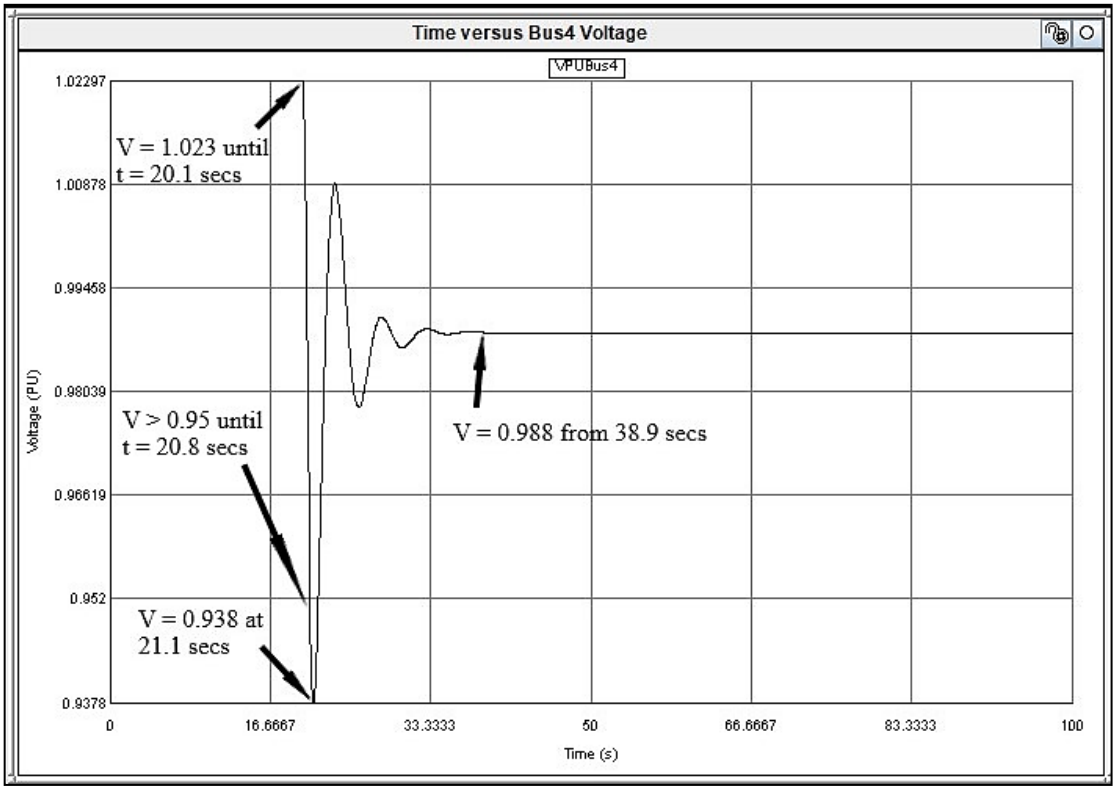

Figure 4.17: Bus 4 per-unit voltage waveform

In Figure 4.17 above, the initial value of the voltage was 1.023 per-unit. When an instant increase in load demand began, a decrease in busbar voltage was experienced. The minimum operating voltage of 0.95 per-unit was experienced before 20.8 seconds. It

was found that the voltage has reached the instability level of 0.938 per-unit at 21.1 seconds. The voltage recovery was experienced after the event.

In Figure 4.18 below, the initial busbar voltage was at 1.013 PU until 20.1 seconds. After this time when the load continued to increase instantly, the voltage decreased and began to collapse after 20.7 seconds. However, it went back to stability.

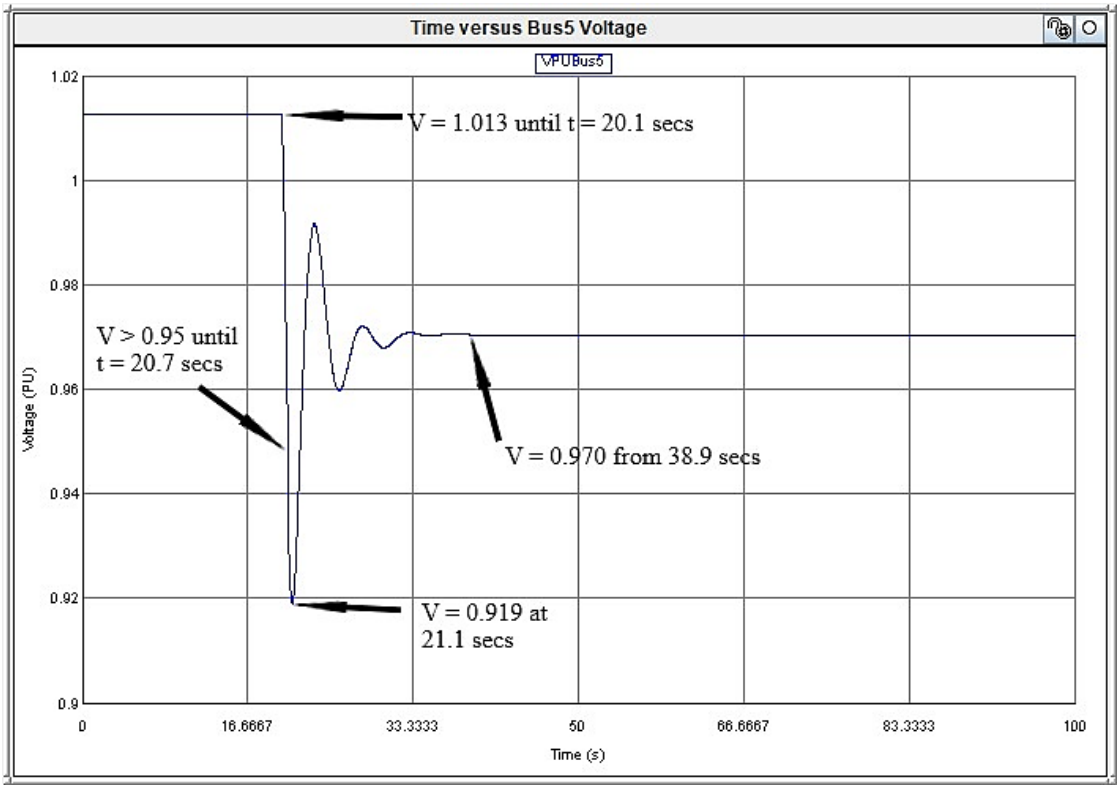

Figure 4.18: **Bus 5 per-unit voltage waveform**

In Figure 4.19 below on the next page, the initial busbar voltage was at 1.028 PU until 20.1 seconds. After this time when the load continued to increase instantly, the voltage decreased and began to collapse after 20.9 seconds. It was found that the voltage was 0.946 PU at 21.1 seconds during the last 15 MW increase in the system. However, at 51.2 seconds, the voltage went back to stability.

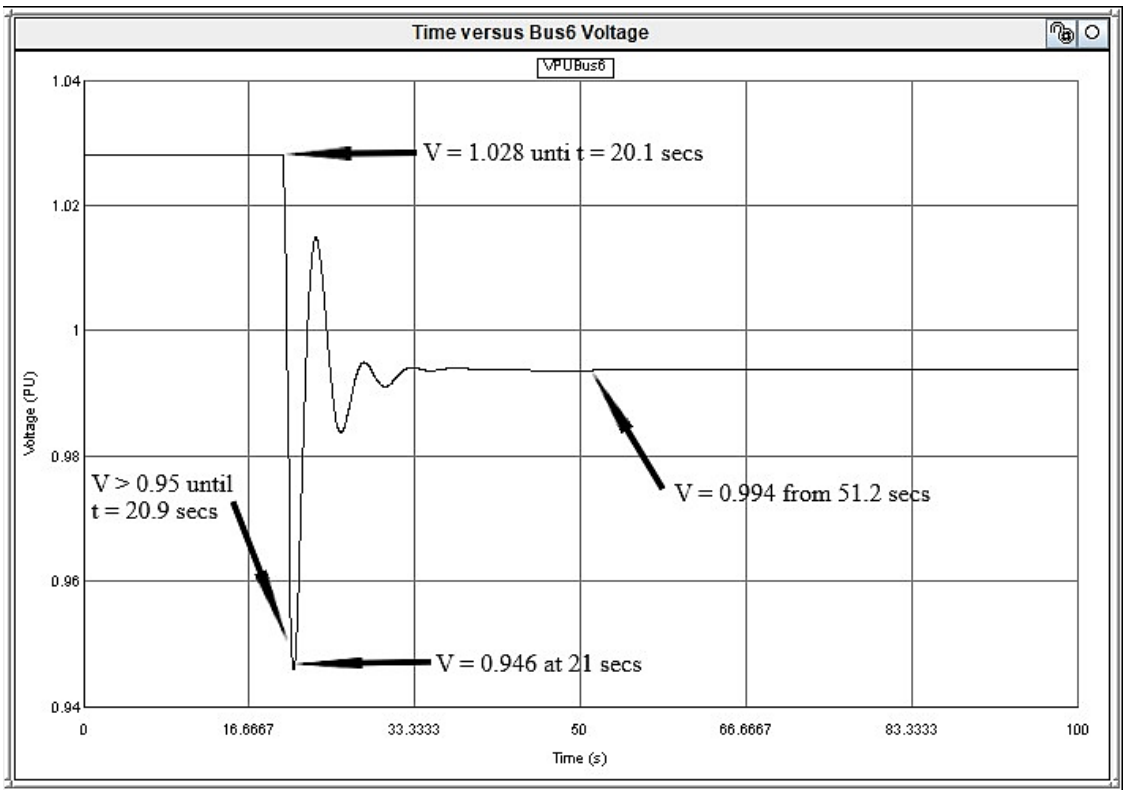

Figure 4.19: Bus 6 per-unit voltage waveform

The results shown in figures, 4.14 to 4.19 above show that the voltage instability is experienced in Bus 2. For this reason, only Bus 2 active, reactive and apparent power plots are discussed in Part 4.6.2.2. While the instant increase in load demand was applied to the entire system, the waveforms displaying the amount of power consumption during the event were recorded. This is in support of the PV and QV curves as was discussed in the theory section of Chapter 3.

The waveform plots provided in the part below show the power demand by the load and the power demanded by Bus 2 from the grid due to the load connected to it.

4.6.2.2 Active, reactive and apparent power demand by DLoad1 at Bus 2

The observations were made on the power demand value at the point where the voltage at Bus 2 was 0.95 PU. It can be seen in Figure 4.20 that the active power (P) demand at that instance (20.5 seconds) was 145 MW. Beyond this value, the busbar voltage began to fall below the accepted continuous operating range and never recovered. In this case, the active power demand by the load is the same as the active power at the busbar. This means that the power demanded from the busbar is the same as the power demanded by the busbar from the system generators.

Figure 4.20 and 4.21 below on the next page show the Bus 2 and DLoad1 active and reactive power demand corresponding values during the event.

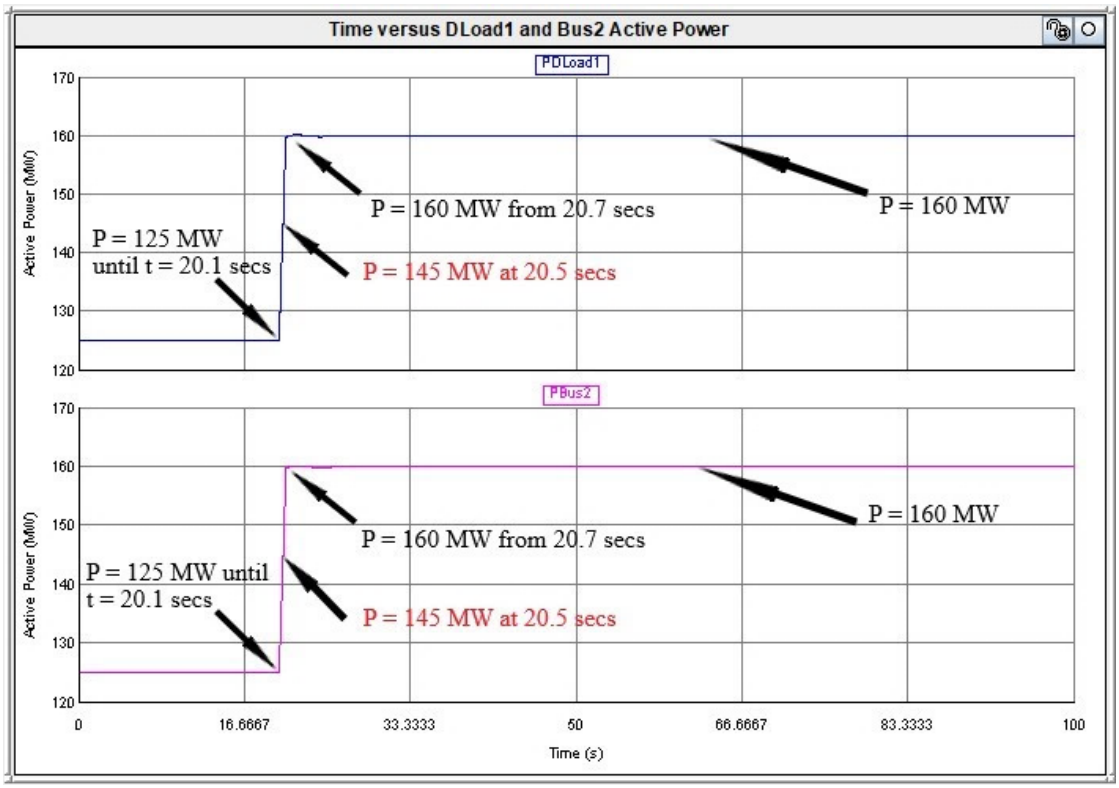

Figure 4.20: Active power demand by DLoad1 from Bus 2 and active power demanded by Bus 2 from the system

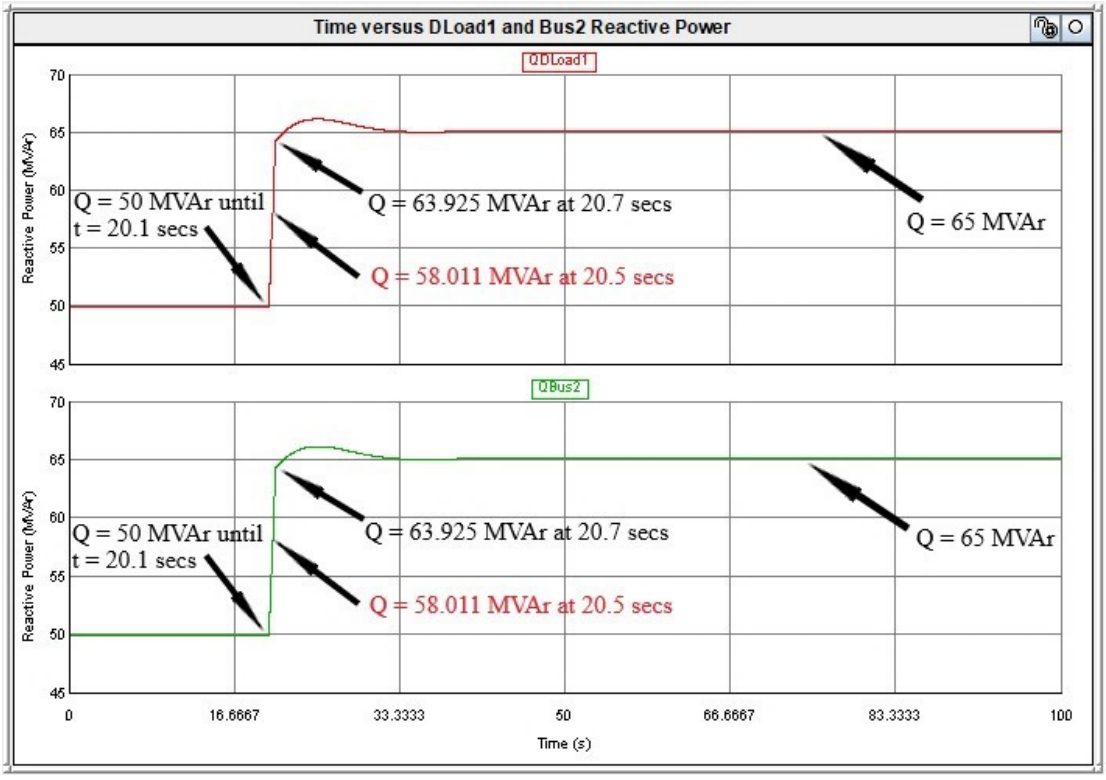

Figure 4.21: Reactive power demand by DLoad1 from Bus 2 and active power demanded by Bus 2 from the system

As can be seen in Figure 4.21 above, the reactive power demanded by the load and the reactive power demanded by Bus 2 from the grid is 58.011 MVAr, and this occurred

at 20.5 seconds at the minimum acceptable continuous operating voltage of 0.95 per-unit.

The power measured on the busbar is the actual power the substation draws from the system to fulfil the load demand requirements. This discrimination of power monitoring helps in the analysis of power contributed by the system generators when additional power sources are available, whose contribution to the load requirements reduces the dependency of the loads to the system generators.

4.7 Discussion of results

When the system overloading was implemented, the voltage at Bus 2 did not recover. The results obtained during this contingency were recorded as shown in Table 4.6 below for per-unit voltage, active, reactive and apparent power viewed from both the load and the busbar.

Table 4.6: Bus 2 and DLoad1 quantities under a step-by-step load increase in the system

Duration	VBus2	PBus2	QBus2	SBus2	PFBus2
Seconds	Per Unit	Watt	Var	VA	N/A
20.1	0.9928	125 000 000	50 000 000	134 629 120	0.928477
20.2	0.984	130 000 000	51 827 956	139 950 481	0.9289
20.3	0.974	135 000 000	53 709 677	145 291 877	0.929164
20.4	0.964	140 000 000	56 129 032	150 832 583	0.928181
20.5	0.950	145 000 000	58 010 753	156 173 773	0.928453
21.1	0.903	160 000 000	63 925 000	172 297 000	0.928627
42.1	0.948	160 000 000	63 925 000	172 297 000	0.928627
Duration		**PDLoad1**	**QDLoad1**	**SDLoad1**	**PFDLoad1**
Seconds		Watt	Var	VA	N/A
20.1		125 000 000	50 000 000	134 629 120	0.928477
20.2		130 000 000	51 827 956	139 950 481	0.9289
20.3		135 000 000	53 709 677	145 291 877	0.929164
20.4		140 000 000	56 129 032	150 832 583	0.928181
20.5		145 000 000	58 010 753	156 173 773	0.928453
21.1		160 000 000	63 925 000	172 297 000	0.928627
42.1		160 000 000	63 925 000	172 297 000	0.928627

The overall initial load demand in the system was 315 MW (125 MW + 90 MW + 100 MW). However, the results in the above table are analyzed locally for a seven-iteration overall load increment of 5 MW after every 0.1 seconds up to 21.1 seconds.

Initially, the load demand of 125 MW was experienced at Bus 2 and the voltage was 0.9928 per-unit. When the instant increase of load by 5 MW per 0.1 seconds was affected, the voltage at Bus 2 fell below 0.95 per-unit after the fifth iteration at 20.5 seconds and never recovered up to the seventh iteration where the maximum power demand was 160 MW.

4.8 Conclusion

The IEEE Nine-bus system was selected and modelled in this chapter, for the investigations of voltage stability issues. Power flow simulations were done for both steady-state and abnormal conditions. The steady-state power flow simulations were done for the verification of system parameters. The abnormal load simulations were used for the calculation of the voltage collapse point. While the abnormal load conditions were simulated in the system, the relationship between the voltage and power demand was evaluated. Above 145 MW to 160 MW load demand, the voltage collapse was declared because it fell out of the range specified for transmission systems. The most vulnerable busbar was Bus 2, in Area 1 of the system. For this reason, the additional power source is added to this busbar, to contribute with power when the load demand increases so that the system can remain stable even at 160 MW load demand at Bus 2.

The most effective method of solving the voltage instability conditions in power systems is by adding additional power sources. For this study, the wind power plant is used as an additional source due to one of its advantage, namely reactive power support.

The wind power plant is modelled and simulated in the next chapter. In the following chapter, the wind power plant operation as a standalone is evaluated. This assists in ensuring the ability of the power source to contribute to the grid as integrated into the grid in Chapter 6.

CHAPTER FIVE
MODELLING OF THE WIND POWER PLANT FOR POWER GRID INTEGRATION ON RSCAD

5.1 Introduction

The load demand increase in the grid causes the voltage decrease in substations. One of the best solutions to solve this is by integrating the additional power sources into the grid. The wind power plant was selected in the previous chapter due to its reactive power contribution to the grid. It is modelled in this chapter, for the conditions of power grid integration to solve the voltage stability issues of the power system network.

5.2 The wind power plant model

The wind turbine generator considered is a V117-4.2 MW from Vestas. This wind turbine drives a 4 MW squirrel-cage induction generator (SCIG) whose parameters were adopted from the published literature. Wind turbine generator units (WTGUs) are modelled, six in each subsystem. This makes a wind power plant (WPP) of eighteen WTGUs. The total capacity has added up to a 75.6 MW wind power plant, considered a large-scale wind power plant.

5.2.1 Wind turbine model

The wind turbine generator requires a mechanical prime-mover to produce electrical power. The selected prime mover is a V117-4.2 MW wind turbine and its RSCAD model is shown in Figure 5.1 below on the next page.

The wind turbine model in the figure has three input signals written pitch (deg), wind speed (km/hr) and speed (pu). To get this wind turbine model working, there are parameters required to be set and the mapping of control and calculation logics for these input signals is required.

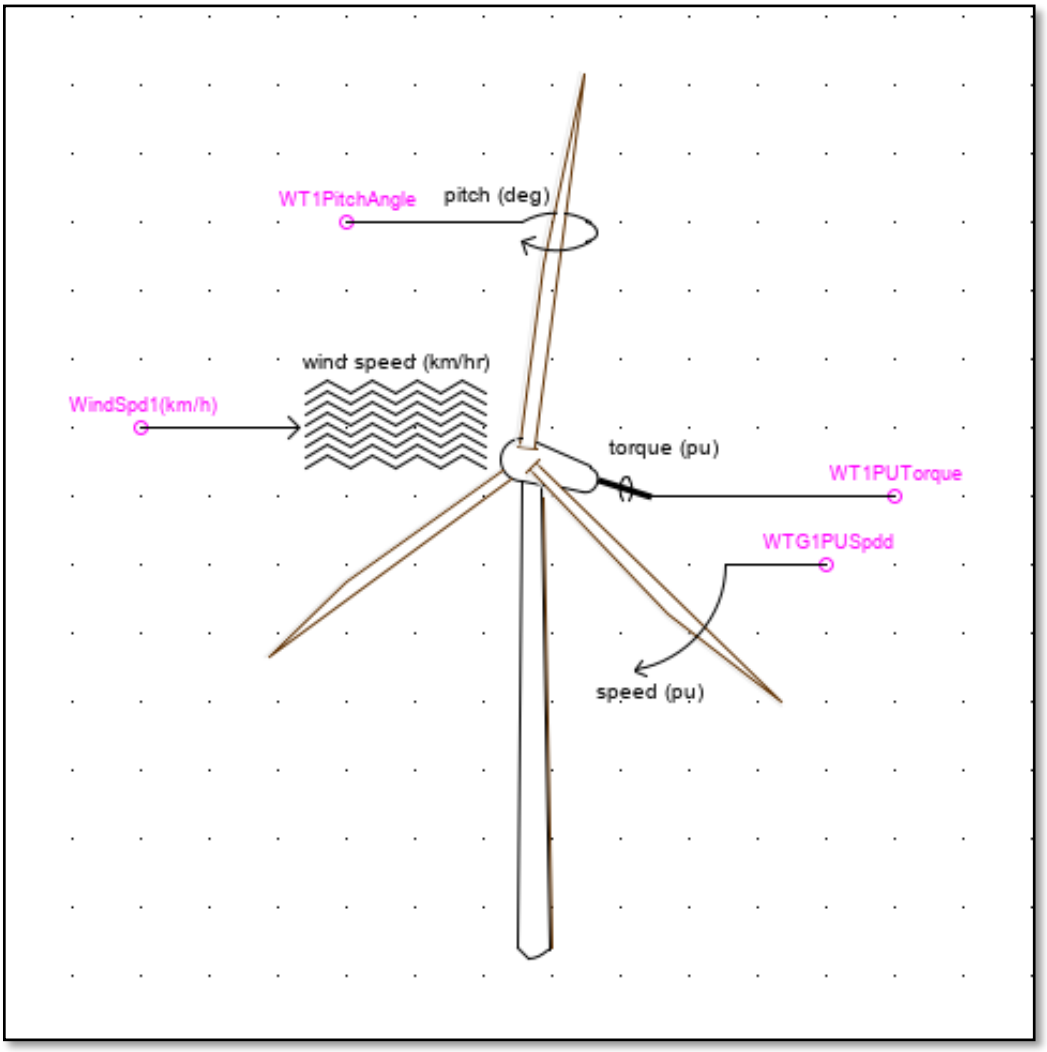

Figure 5.1: RSCAD wind turbine model

This part deals with the settings parameters of the wind turbine model and the modelling of control and calculation logic. Once these control and calculation logics are modelled, an output signal with the name torque (pu) is then coupled to a generator for the conversion of mechanical power to electrical power.

5.2.1.1 Wind turbine modelling

The first step in modelling a wind turbine model is that of defining the input signals to control the wind turbine. The three inputs and one output, pitch (deg), wind speed (km/hr) and speed (pu) and torque (pu) have been discussed. These input signals are defined with signal names as can be seen in Figure 5.1 above. The signal names *WindSpd1(km/h)* and *WT1PitchAngle* are input signals from the wind speed and pitch angle adjustment. *WTG1PUSpdd* is the feedback per unit speed signal from the driven generator. The signal named *WT1PUTorque* is the output per unit torque of the wind turbine.

Wind turbine generators convert about 40% up to 48% of the power produced by the moving wind. These percentage values represent the efficiency of the wind turbine, referred to as the turbine's power coefficient (C_p). Figure 5.2 below shows the C_p constant values, k_1, k_2 k_3 and k_4 used when modelling the wind turbine.

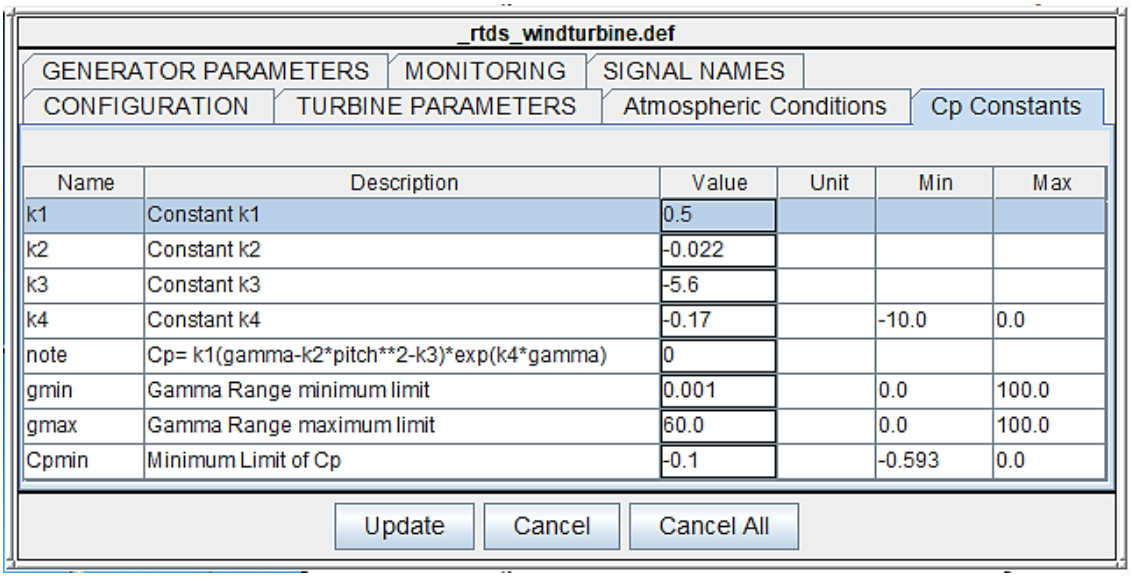

Name	Description	Value	Unit	Min	Max
k1	Constant k1	0.5			
k2	Constant k2	-0.022			
k3	Constant k3	-5.6			
k4	Constant k4	-0.17		-10.0	0.0
note	Cp= k1(gamma-k2*pitch**2-k3)*exp(k4*gamma)	0			
gmin	Gamma Range minimum limit	0.001		0.0	100.0
gmax	Gamma Range maximum limit	60.0		0.0	100.0
Cpmin	Minimum Limit of Cp	-0.1		-0.593	0.0

Figure 5.2: **Power coefficient of the wind turbine (Cp)**

Various equations exist for the power coefficient. For the availability of constants, k_1, k_2 k_3 and k_4 on the RSCAD wind turbine model, the expression below is used

$$C_p = k_1(\lambda + k_2\beta^2 + k_3)e^{k_4\lambda} \tag{5.1}$$

Where; β and λ are the pitch angle adjustment of the wind turbine blades and the tip speed ratio of the wind turbine. The tip speed ratio (λ) is given by the expression

$$\lambda = \frac{v_W}{\omega_{TR}} \tag{5.2}$$

Where, v_W and ω_{TR} are the velocity of wind in meters per second (m/s) and rotational velocity of the turbine rotor in radians per second (rad/sec) respectively.
The constants in expression (5.1) have the values, $k_1 = +0.5$, $k_2 = -0.022$, $k_3 = -5.6$ and $k_4 = -0.17$.

The wind turbine generator model used has the turbine rotor nominal rotational speed of 9.9 rpm. To transform the speed produced by the wind turbine rotor, wind turbine generators are built with gearboxes to perform this function. Therefore, a gearbox ratio is calculated and set.

To calculate a gearbox ratio, we use the nominal values. At a nominal wind speed of 14 m/s, the wind turbine rotor rotational speed is 9.9 rpm while the rated rotor speed of the induction generator is 1510.5 rpm. For this generator to produce the rated power, at least a rotational speed of 1510.5 rpm must be received from the propeller (turbine shaft), which will be on the secondary side of the gearbox in this case. The gearbox ratio is determined from the expression

$$\omega_{\mathbf{GR}} = \mathrm{G}\omega_{\mathbf{TR}} \tag{5.3}$$

Where G is the gearbox ratio, $\omega_{\mathbf{GR}}$ and $\omega_{\mathbf{TR}}$ are the rated angular rotor speed of the generator's rotor and the wind turbine.

To calculate the value of the gearbox ratio, $\mathbf{G}$ was made the subject of the above expression as follows:

$$\mathrm{G} = \frac{\omega_{\mathbf{GR}}}{\omega_{\mathbf{TR}}} \tag{5.4}$$

The nominal speed values for both the wind turbine rotor and the induction generator are substituted as follow:

$$\mathrm{G} = \frac{1\,510.5\ \mathrm{rpm}}{9.9\ \mathrm{rpm}}$$

$$\mathrm{G} = \frac{50.35\pi\ \mathrm{rad/s}}{1.036705\ \mathrm{rad/sec}}$$

$$\mathrm{G} = 152.5757576$$

Another method is used for calculating the gearbox ratio by looking at the amount of torque required by the machine, in comparison with the one produced by the turbine. For this calculation, the mechanical torque expression of the wind turbine is considered and is written as

$$\mathrm{T_T} = \frac{\mathrm{P_T}}{\omega_{\mathrm{TR}}} \tag{5.5}$$

Where, $\mathrm{T_T}$ and $\mathrm{P_T}$ are the mechanical torque (in Newton-meters (N.m)) and power (in Megawatts (MW)) produced by the wind turbine.

The amount of torque required by the generator to produce the nominal power of 4 MW is 25.671 kN.m and the torque produced by the wind turbine is calculated as

$$\mathrm{T_T} = \frac{4\ \mathrm{MW}}{1.036705\ \mathrm{rad/sec}}$$

$$T_T = 3.858378\ \text{MN.m}$$

The mechanical torque required to drive the wind turbine generator is transferred through the gearbox of the wind turbine using the principle defined by the expression

$$T_G = \frac{T_T}{G} \tag{5.6}$$

In the above expression, T_G is the generator torque. In addition, G is made the subject of the formula and the following expression is obtained

$$G = \frac{T_T}{T_G} \tag{5.7}$$

The values, 3.858378 MN.m and 25.671 kN.m are then substituted in the variables, T_T and T_G as follows

$$G = \frac{3.858378\ \text{MN.m}}{25.671\ \text{kN.m}}$$

$$G = 152.5757576$$

Figure 5.3 below shows the gearbox ratio and the turbine rotor radius parameter settings.

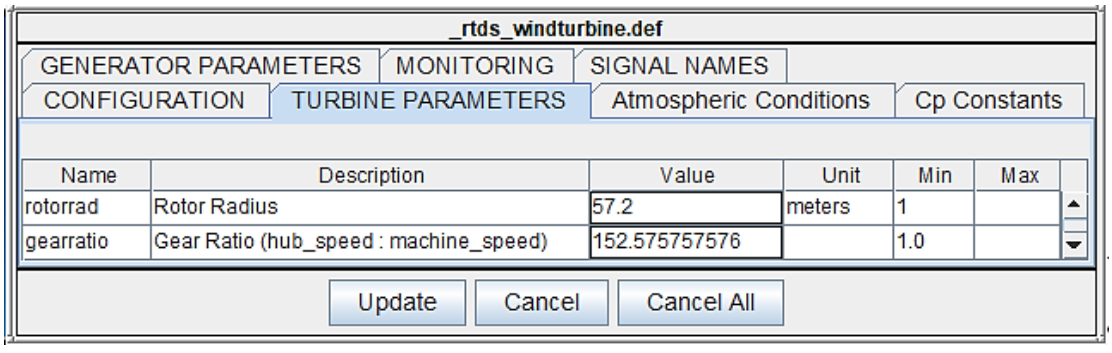

Figure 5.3: Rotor radius and gearbox ratio settings

Another setting parameter involved in the wind turbine generator model is the rated MVA, rated frequency, as well as the rated rpm of the generator to be coupled.
These settings are shown in Figure 5.4. The setting values shown in the above figure can be found in Appendix C.

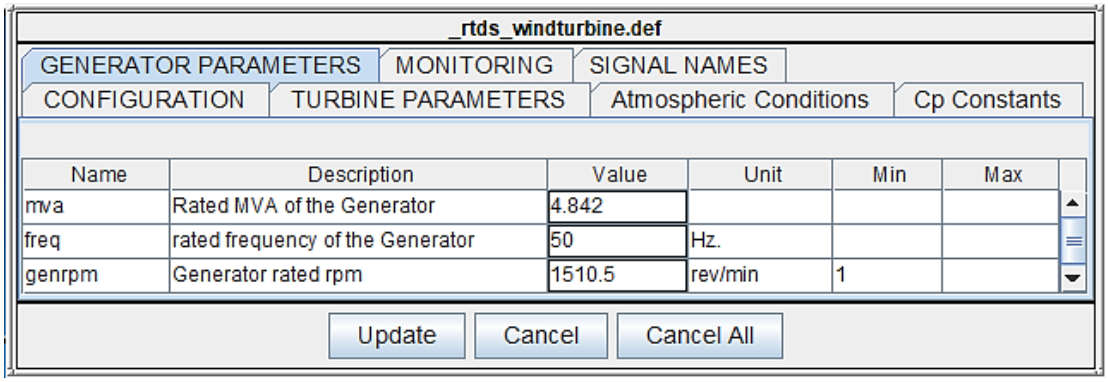

Figure 5.4: **Generator rated complex power in MVA, rated frequency as well as the generator speed in rpm**

Part of the given specifications for a wind turbine model under study is the standard operating temperature range, specified as -20 ^{O}C to 45 ^{O}C. A decision is made on the default temperature value of 25 ^{O}C, where the wind turbine is assumed to be producing the nominal power of 4/4.2 MW under this temperature.

5.2.1.2 Design of wind turbine control and calculation logics

The wind turbine model produces the output per unit roque or high-speed rotation based on the two principal input signals, the pitch angle control adjustment and wind speed.

The control logic for these inputs is shown in Figure 5.5 below.

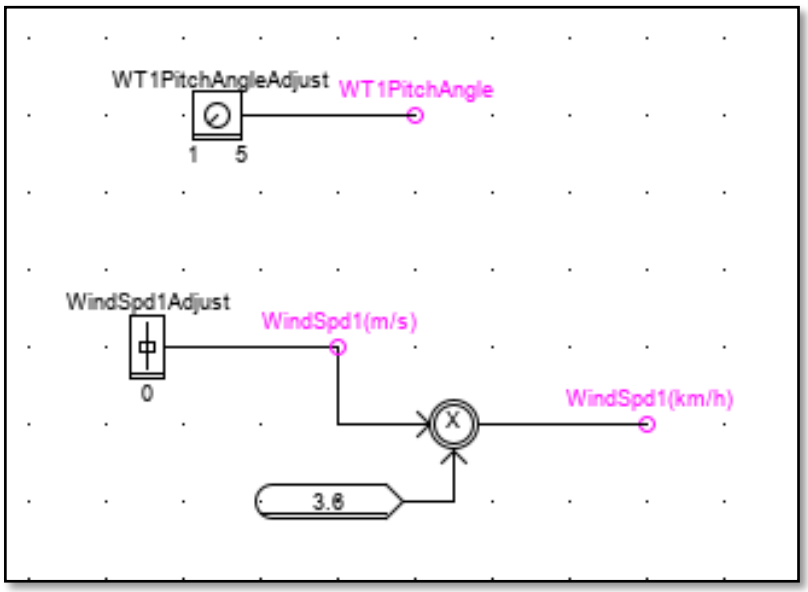

Figure 5.5: **Turbine blades pitch angle and wind speed adjustment and calculation logics**

The wind speed range specified in the given wind turbine specifications is in meters per second (m/s) and the wind speed input signal to the turbine model provided is

required in kilometres per hour (km/h). It is more precise to monitor and tune the wind speed in meters per second, therefore the logic to control and inject the wind speed to the wind turbine provided is designed such that its adjustments are in m/s while the output is in units required by the wind turbine. The equation is derived for this function and its mathematical expression is as

$$x = 3.6(v_w) \tag{5.8}$$

Where, x represents the wind speed in km/h and v_w is the wind speed in m/s. In the above figure, the component with **X** is the multiplier, and the component by the name WindSpd1Adjust is the slider for tuning the wind speed range. The output signal *WindSpd1(m/s)* exists from the slider, it multiplies with the constant number 3.6. The output labelled *WindSpd1(km/h)* is the wind speed input on the wind turbine model.

The dial selector switch with output signal named *WT1PitchAngle* is shown in the above figure. It is for use for the selection of the wind turbine blades' pitch angle.

The wind speed operating range of the Vestas V117-4.2 MW wind turbine is specified from 3 m/s to 25 m/s. In addition, the rotational (angular) speed of the turbine rotor is specified in correspondence to the wind speed range and the data is shown in Table 5.1 below.

Table 5.1: Speed of the wind and the angular speed of the rotor

Wind speed (m/s)	The angular speed of the turbine rotor (rpm)	The angular speed of the turbine rotor (rad/sec)
3	2.1	0.219911
14	9.9	1.036705
23	-	-
25	17.6	1.843068

Two parameters influence the turbine efficiency (*Cp*), β and λ. The *Cp* values are determined for each tip speed ratio with different pitch angle adjustments and the results are shown in Table 5.2 below on the next page.

Table 5.2: Cp values at different pitch angle adjustments

V_w	Cp	Wh	λ	β
3	0.405892	0.219911	13	0
14	0.375725	1.036705	13	5
25	0.285222	1.843068	13	10
36	-0.07679	2.666666	13	20
47	-0.82978	3.48	13	32

The value of the tip speed ratio (λ) is constant because the relationship between the increase in wind speed is directly proportional to the increase in the angular speed of the turbine rotor.

5.2.2 Induction generator modelling

The power measured from the output of the wind turbine is the mechanical power and is transferred in the form of a per-unit mechanical torque to the generator it is coupled with. The generator selected is a squirrel-cage induction generator for its simplicity and low-costs. Figure 5.6 below shows the induction generator model.

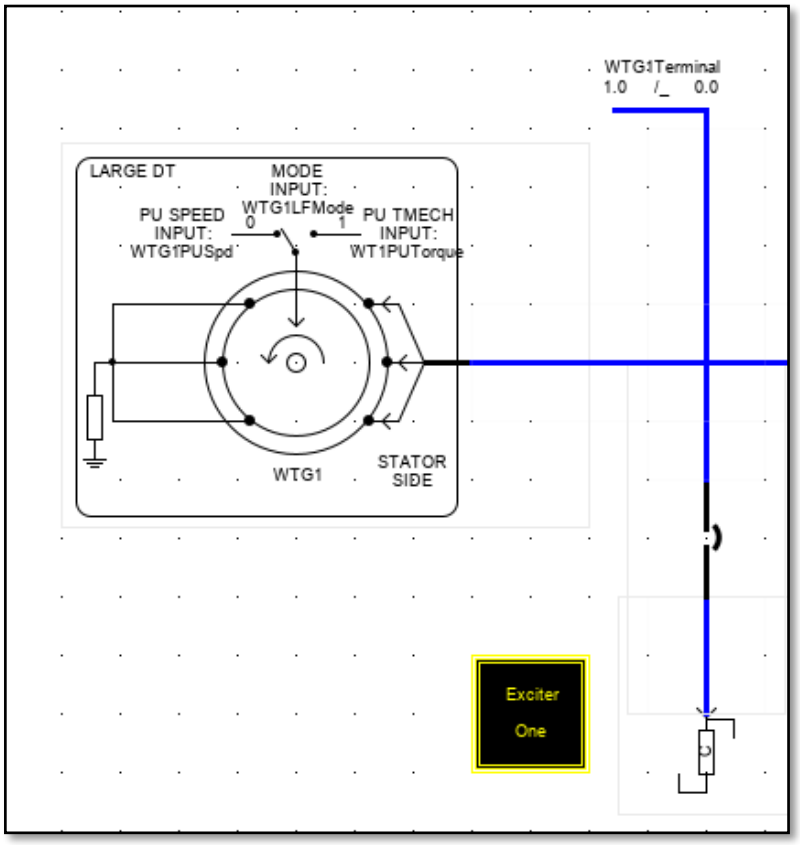

Figure 5.6: Induction generator model with the exciter component

The induction generator model shown in the above figure has three input signals written as *PU SPEED INPUT*, *MODE INPUT* and *PU TMECH INPUT*. Between *PU SPEED INPUT* and *PU TMECH INPUT* signals, one is used, depending on the selected *MODE INPUT* input signal which defines the mode at which the generator is driven. In addition to the above figure, the component with symbol "*c*" is the induction generator excitation circuit for stator terminal voltage build-up.

The electrical parameters for the induction machine can be found in Appendix C.

The stator, rotor and core resistance and reactance parameters of this machine are entered in per-unit values. These values are calculated from the base values specified by the guide for RSCAD induction generator modelling. The following are base values specified for calculating the per-unit values of the machine:

- Base voltage (V_B): Rated line-to-neutral stator voltage of the generator as the base value for the voltage
- Power: Rated MVA of the machine is used as the base value for the power
- Base current (I_B): Rated stator current of the machine is used as the base value for the current
- Base impedance (Z_B): The rato of the base voltage (V_B) over the base current (I_B) is used as the base value for the base impedance

Another setting is that of the generator's inertia constant. As specified from its units, MWs/MVA, is calculated from the values provided in the generator specifications and the value is set in the mechanical parameters as shown in Figure 5.7 below of the induction generator parameter settings below.

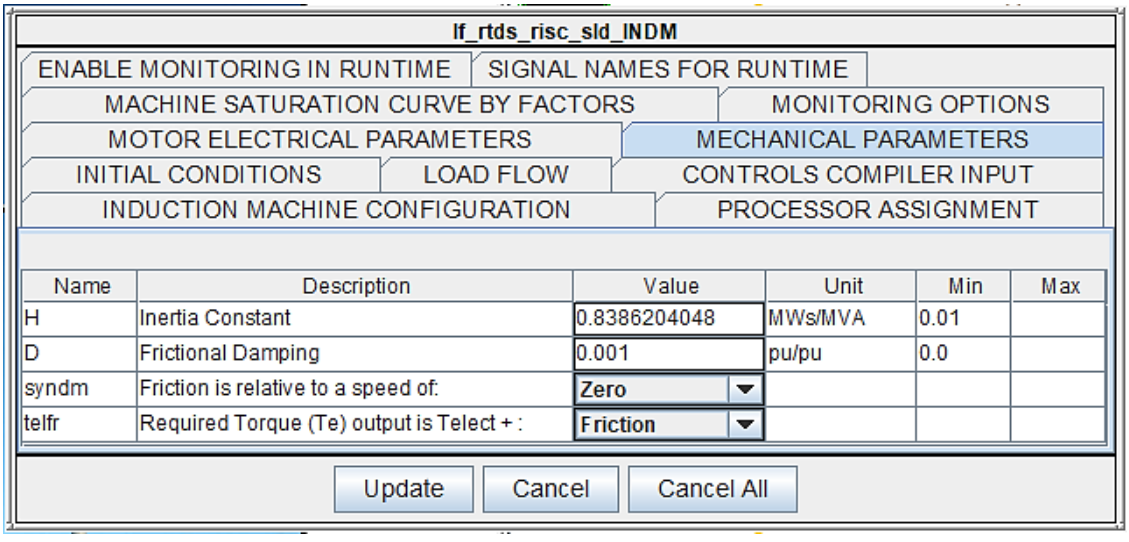

Figure 5.7: **Induction generator mechanical parameters**

The induction generator produces electric power by converting the mechanical power input to its shaft. The voltage at the generator's stator terminal will never build-up even the torque from the prime mover is enough. For a voltage build-up on the stator terminals of the induction generator, an exciting circuit is required. the external circuitry is required, which produces the voltage from the small amount of current available at the stator terminals during the rotation of the machine's rotor. Therefore, the excitation circuit is designed in the part below, and its parameters are calculated from the available electrical parameters of the induction generator.

5.2.2.1 Modelling for induction generator excitation circuit

The first step is to determine the apparent power (S) from the given electrical parameters of the induction generator.

$$\mathrm{S} = \sqrt{3}\mathrm{IV} \tag{5.9}$$

$$\mathrm{S} = \sqrt{3}\ (0.69888\mathrm{A})(4\ \mathrm{kV})$$

$$\mathrm{S} = 4.84198\ \mathrm{MVA}$$

Induction machines are known as machines that draw a lagging current from the circuit, and their power factor is always assumed to be 0.8 lagging. Therefore,

$$\mathrm{P} = 4.84198\ \mathrm{MVA}\ (0.8)$$

$$\mathrm{P} = 3.99999\ \mathrm{MW}$$

$$\mathrm{Q_T} = \sqrt{\mathrm{S^2} - \mathrm{P^2}} \tag{5.10}$$

where Q_T is the total reactive power of the excitation circuit.

$$\mathrm{Q_T} = \sqrt{(4.84198\ \mathrm{MVA})^2 - (3.99999\ \mathrm{MW})^2}$$

$$\mathrm{Q_T} = 2.72853\ \mathrm{MVAr}$$

The value calculated here is the minimum reactive power required to excite the induction machine to produce a voltage at the stator terminals. For low-cost, the combination of the capacitors to produce Q_T is usually connected in delta or mesh connection. Therefore, per-phase reactive power is three times less than the total reactive power.

$$\mathrm{Q_P} = 0.909510\ \mathrm{MVAr}$$

where Q_P is the per-phase reactive power.

From this, we calculate the current that will flow through each capacitor can be calculated as follows:

$$I_Q = \frac{Q_P}{V_{Phase}} \tag{5.11}$$

where I_Q and V_{Phase} are the current flow in the reactive component and the per-phase voltage, is equal to the line-to-line voltage because of the connection method of the reactive component.

$$I_Q = \frac{0.90951\ \text{MVAr}}{4\ \text{kV}}$$

$$I_Q = 0.22738\ \text{kA}$$

In addition, the capacitive reactance of the per-phase capacitor is determined as follows:

$$X_C = \frac{V}{I_Q} \tag{5.12}$$

$$X_C = \frac{4\ \text{kV}}{0.22738\ \text{kA}}$$

$$X_C = 17.59169\ \Omega$$

The capacitance required for each capacitor is obtained as follows:

$$C_P = \frac{1}{2\pi f X_C}$$

where f is the rated frequency of the generator, and X_C is the capacitive reactance for each capacitor.

$$C_P = \frac{1}{2\pi(50)(17.591697)}$$

$$C_P = 180.94325\ \mu\text{F}$$

In a wind power plant, inductions generators are connected in parallel and the excitation capacitor banks connected to each terminal of a generator make parallel circuits. The capacitor banks, when connected in parallel increase the capacitance in the system.

Therefore, the value of the capacitance calculated above may vary, depending on the number of wind turbine generators connected to complete the wind power plant.

The induction generator consists of two types of quantities, mechanical and electrical quantities and some need to be monitored for analysis purposes. In addition, the input signals that drive the induction generator depends on the control, monitoring and calculation components from the wind turbine model, and some of these components required special modelling. The part below presents the modelling of the control components for both the induction generator and its excitation circuit.

5.2.2.2 Modelling for induction generator and excitation circuit control, monitoring and calculation logics

There is a relationship between wind speed and turbine rotor speed. The rotor speed increases as the wind speed increases. Because of this relationship and the per-unit speed control input to the driven generator, a logic is designed (see Figure 5.8), that calculates the per-unit speed from the speed of the wind.

The nominal speed of the wind is 14 m/s, and the wind turbine is expected to be producing the nominal power of 4 MW at this speed. At 14 m/s of wind speed, the per-unit speed input to the generator is expected to be at 1. The diagram in Figure 5.8 below makes use of the calculated per-unit speed of the wind and applies it to the generator.

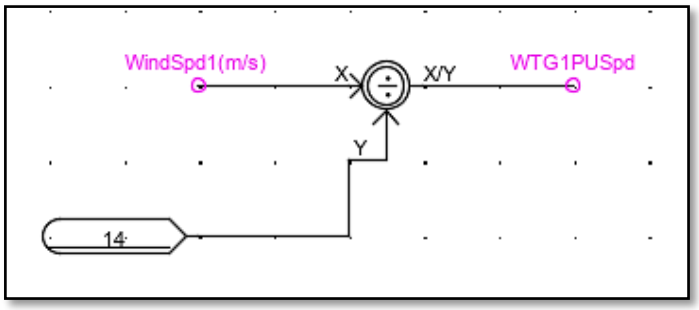

Figure 5.8: Logic for wind turbine generator per-unit speed control

In Figure 5.8 above, constant 14 is the rated wind speed in meters per second (m/s) and is used as the base value for obtaining the per-unit output signal. The signal *WindSped1(m/s)* is the output from the wind input speed adjusting slider for the wind turbine. The *WTG1PUSpd* signal is connected to the generator as part of the control signals.

The excitation circuit of the induction generator model is modelled as shown in Figure 5.9 below, to fulfil the requirements of control, monitoring and calculation logic of the induction generator electrical quantities.

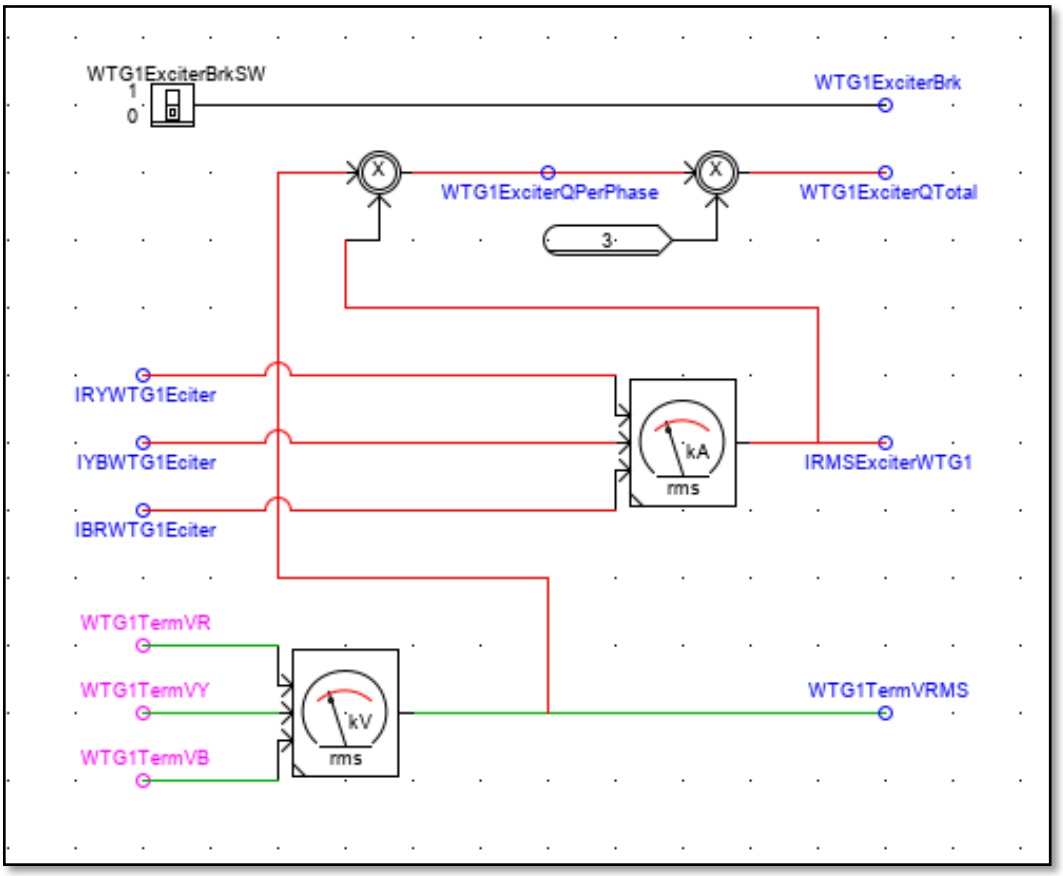

Figure 5.9: **Excitation circuit control, monitoring and calculation logics**

The binary switch with the name WTG1ExciterBrkSW in the figure is for controlling (*ON/OFF*) the circuit breaker for the excitation circuit. the calculation logic for the reactive power produced by the excitation circuit is shown with the output signal names *WTG1ExciterQPerPhase* and *WTG1ExciterQTotal* for per-phase and total reactive power produced. This logic uses the product of the RMS voltage and current seen by the circuit. The signal names *IRYWTG1Eciter*, *IYBWTG1Eciter* and *IBRWTG1Eciter* are the phase currents monitored from the capacitor bank modelled as the excitation circuit for the induction generator. Another meter is shown in the figure, for calculating the RMS voltage of the induction generator stator terminals.

It is just the small amount of voltage and current that makes a voltage build-up in the capacitor bank when the prime-mover is turning the shaft of the induction generator.

5.2.3 WTGSUT and medium to high-voltage transformer selection

There are eighteen wind turbine generator substation units (WTGUSs) modelled for this wind power plant, whose selected individual step-up transformers can handle 5 MVA apparent power at full load. That being said, from the collector exists a 24 kV to 230 kV step-up transformer required to deliver eighteen times 5 MVA (equals to 90 MVA) to the transmission system through the transmission lines. Therefore, a minimum of 90 MVA transformer is selected.

5.2.4 Wind power plant high-voltage transmission line modelling

RTDS offers two models of transmission lines, the travelling wave transmission lines and PI section models.

The travelling wave transmission line model is generally preferred only for line models whose length is 15 km and above. Otherwise, the PI section model is used.

To accomplish the interconnection of the wind turbine groups across each subsystem, and later to the power grid, the travelling wave transmission line model is modelled and it guarantees accuracy. Figure 5.10 below shows the transmission line parameter settings.

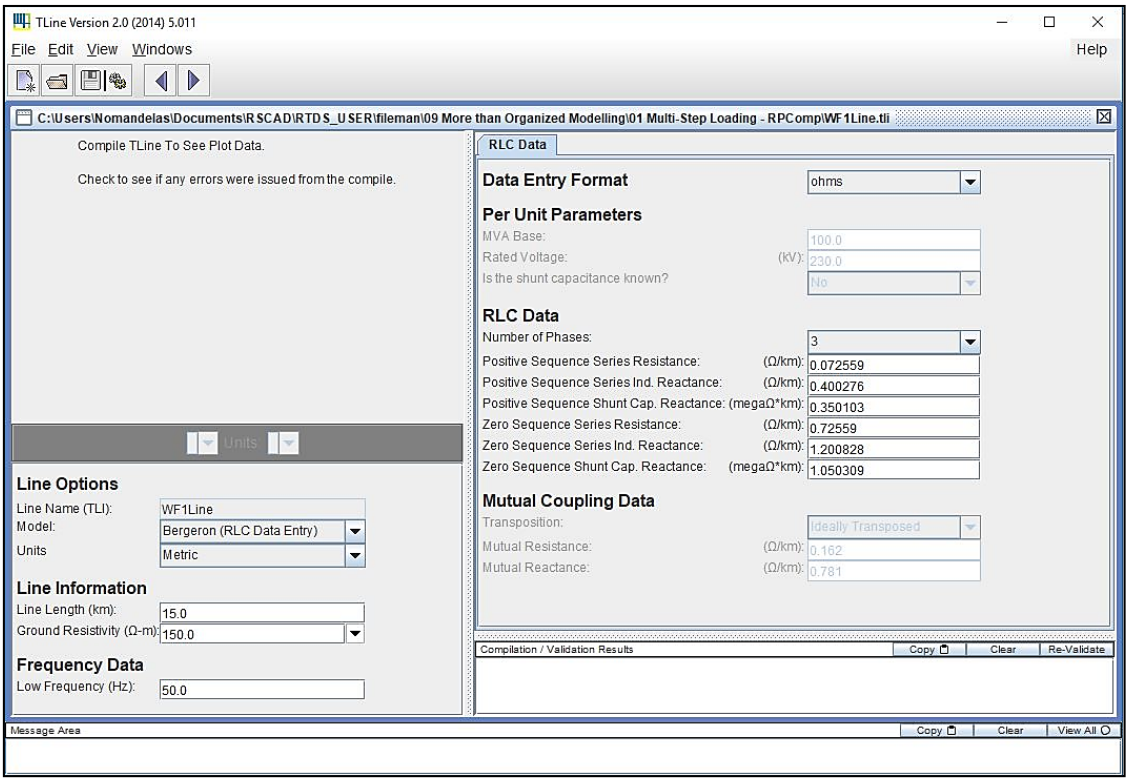

Figure 5.10: Wind power plant transmission line system data parameter settings

5.2.5 The wind power plant reactive power support device

Transmission lines are rich in reactance than resistance, therefore, the amount of active power lost along transmission is usually far lesser than the reactive power absorbed. Reactive power compensators are usually installed at the receiving end of the transmission lines to compensate for the reactive power absorbed through transmission lines. The modelling of the reactive power support device is completed in this part, where the 15 MW load increment is considered and used as the reference from the power system presented in the previous chapter, where the system was only one iteration left before it reached the point of voltage collapse. The corresponding reactive power for this amount of active power is calculated based on the grid code specified power factor of 0.95 and is 4.930261578 MVAr. This value is used as the minimum reactive power the reactive power support device should produce. For this model, the capacitor bank is used and its capacitance is calculated using the expression

$$C_P = \frac{I_Q}{2\pi f V_P} \tag{5.13}$$

In the above expression, I_Q and V_{Phase} are the current flow in the reactive component and the per-phase voltage, is equal to the line-to-line voltage because of the connection method of the reactive component. The value of I_Q can be found by using the expression

$$I_Q = \frac{Q_P}{V_{Phase}} \tag{5.14}$$

$$I_Q = \frac{1.643420526\ \text{MVAr}}{0.9(230\ k\text{V})}$$

$$I_Q = 0.07939229594\ \text{kA}$$

Therefore,

$$C_P = \frac{0.07939229594\ \text{kA}}{2\pi(50)(0.9\ \text{PU}(230\ \text{kV}))}$$

$$C_P = 0.1220838294\ \mu\text{F}$$

Capacitor banks cause a lot of transient currents in the power system, which might affect other power system components. For this model, the transients were reduced by using sequential switching, where the capacitor banks are divided into multiple units.

For the capacitor bank presented above, only fourteen units were modelled due to a limited number of RTDS processor cards. Therefore, each unit is fourteen times less than $0.1220838294\ \mu F$, connected in parallel with each other, which then gives $0.00872035286\ \mu F$ capacitor bank. The settings parameter for each capacitor bank is shown in Figure 5.11 below. Only one setting for one unit is shown in this part, though all other units have the same settings window, with different labelling of signals.

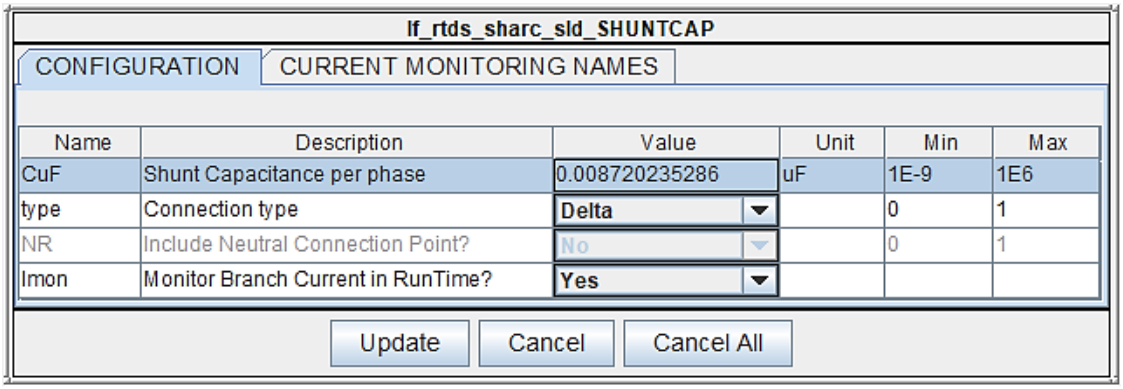

Figure 5.11: **WPP terminal reactive power compensator device model settings parameters**

Part of the capacitor bank parameter settings includes monitoring of currents at each phase of the capacitor bank as shown in Figure 5.12 below.

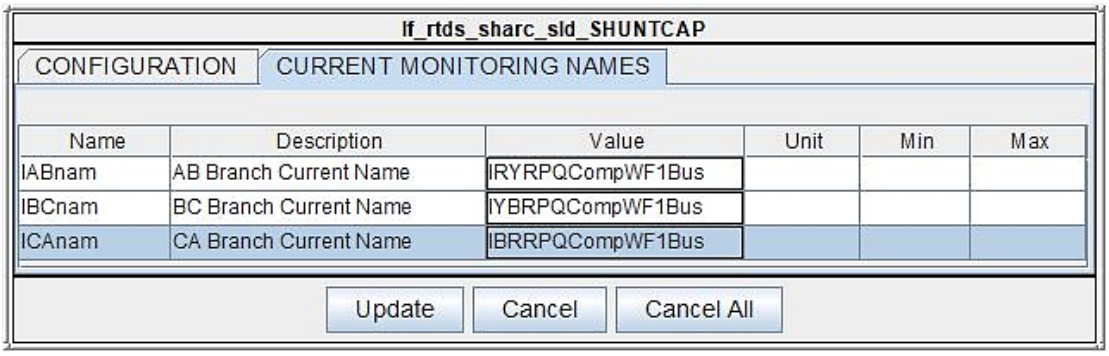

Figure 5.12: **WPP terminal reactive power compensator phase current monitoring settings**

By using the relation between the voltage and current on the reactive power production by capacitor banks, the logic for monitoring the reactive power produced by the reactive power support device model is developed as shown in Figure 5.13 below on the next page.

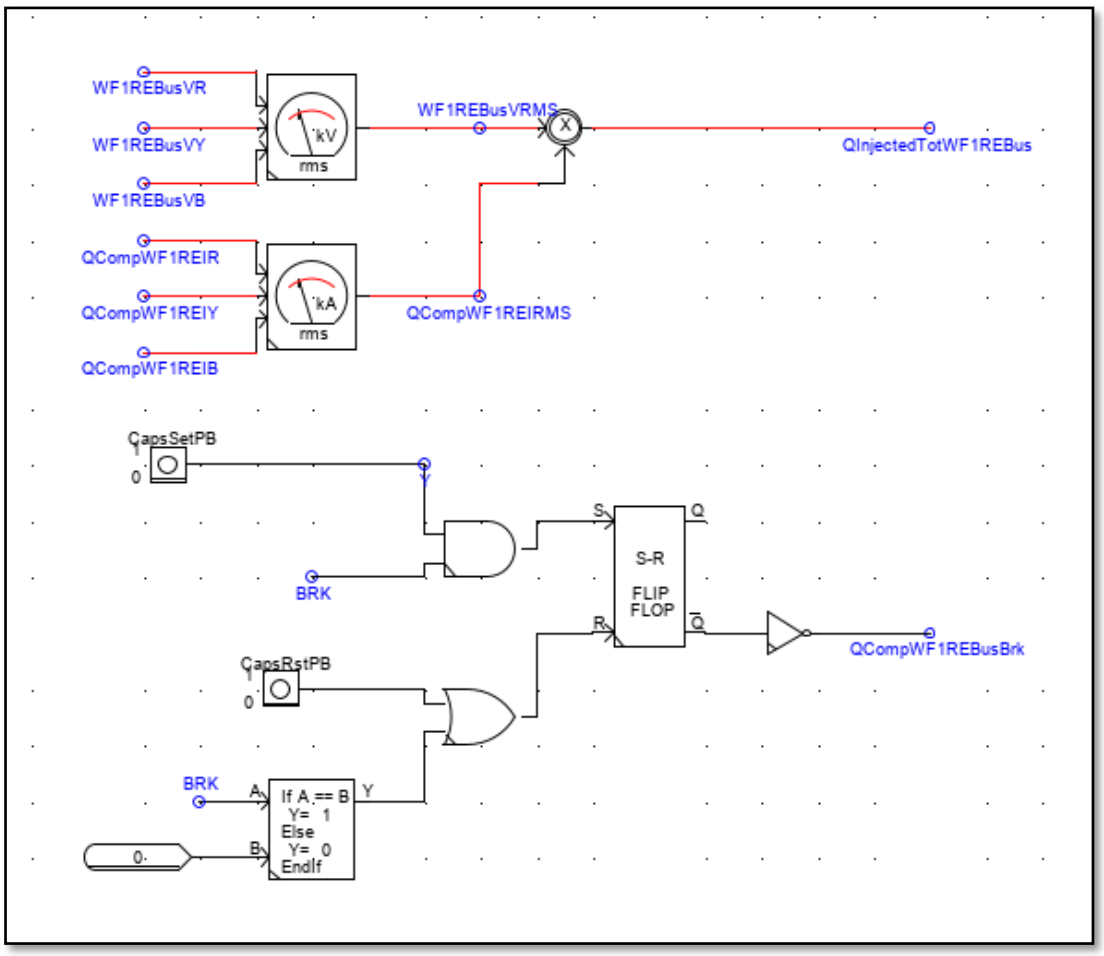

Figure 5.13: **Calculation logic for reactive power injection using the RMS voltage and current**

In the same figure above is the logic for controlling the reactive power compensation and it is designed in a way that there will be no reactive power compensation unless the load is at a certain value of demand.

Another logic diagram is developed as shown in Figure 5.14 below on the next page, for monitoring at the sending end side of the wind power plant.

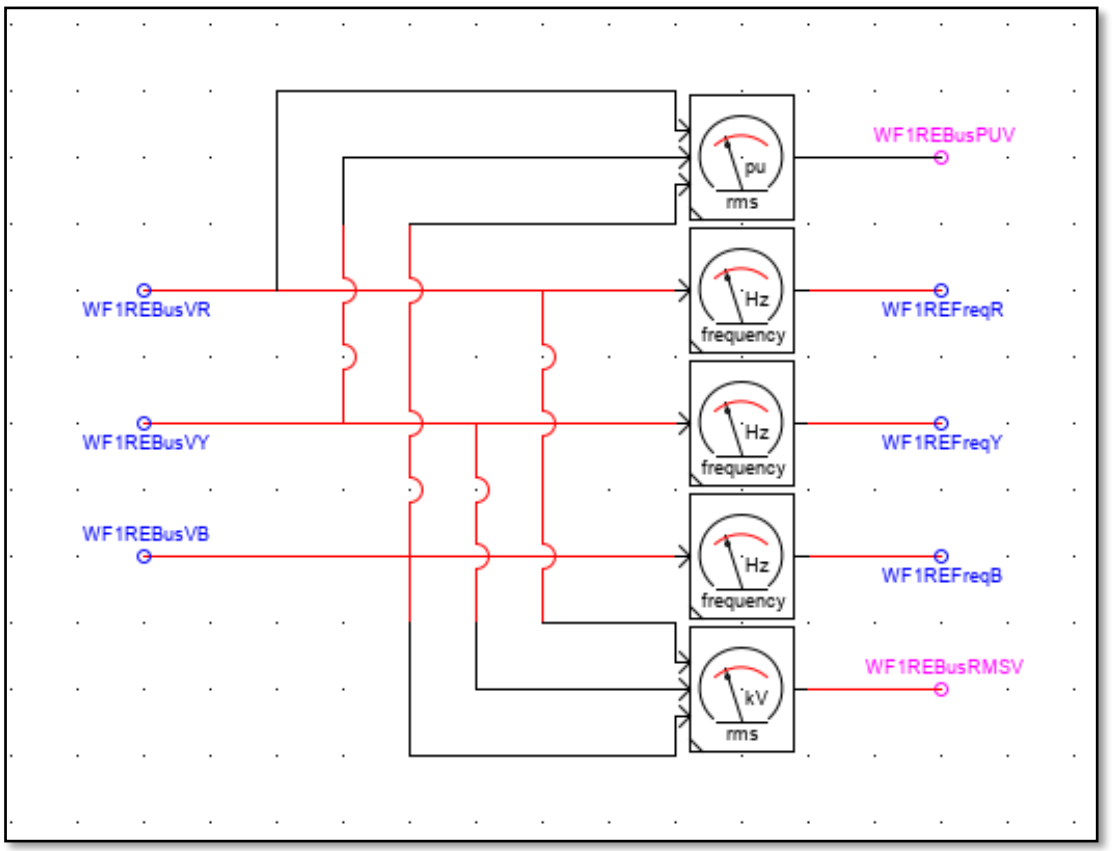

Figure 5.14: **Frequency and the per-unit voltage monitoring and calculation logic**

The logic diagram shown above is for calculating the receiving-end per-unit and RMS voltage, and frequency. The logic shown in the above figure is used to calculate the aforementioned quantities based on the output terminal voltage of the wind power plant. The same calculation logic is modelled for the sending-end terminal of the wind power plant.

5.3 The wind power plant steady-state load flow simulation

The wind power plant steady-state load flow simulation test is completed in this section. At least one wind turbine generator is monitored for aerodynamic and mechanical quantities. This simulation was done at $25^{o}C$ with an air density (ρ) of 1.654 kg/m^3, the humidity of 30%, air pressure of 1415 mbar and a wind speed of 14 m/s. Tables, 5.3 and 5.4 below on the next page show the values monitored for aerodynamic, mechanical and electrical quantities for one of the wind turbine generators from the wind power plant.

Table 5.3: Steady-state simulation – aerodynamic and mechanical quantities for a WTGU

Air density (kg/m^3)	Wind speed (m/s)	Wind power (MW)	WT Cp	Wind turbine power (MW)	Wind turbine rotor speed (rad/sec)	Wind turbine rotor speed (PU)	Wind turbine torque (PU)
1.652	14	23.31	0.1718	4.003	1.037	1.000	0.9921

Table 5.4: Steady-state simulation - electrical quantities for WTGU

WTGSU currents (kA)		WTG terminal current (kA)	WTG terminal voltage (kV)	WTG terminal voltage (PU)	WTG electrical torque (PU)	WTG exciter reactive power (MVAr)	WTG terminal active power (MW)	WTG terminal reactive power (MVAr)	WTGG exciter current (kA)
Primary	Secondary								
0.01563	0.001302	0.268	4.332	1.083	0.00986	2.122	0.02404	-2.010	0.1633

The electrical quantities were monitored on the output terminal of the wind power plant and the results are recorded in Table 5.5 below for voltage and frequency.

Table 5.5: Steady-state simulation - Wind power plant voltage and frequency

WPP output voltage (PU)		WPP output frequency (Hz)	
Sending	Receiving	Sending	Receiving
1.086	1.083	50	50

The grid codes specify the continuous operating per-unit voltage level for Category C renewable power plants as 0.9 (minimum) to 1.0985 (maximum). As can be seen in the above table, under normal load flow conditions, the voltage measured on the high-voltage busbar of the wind power plant is at 1.083 per-unit, therefore acceptable.

Another quantity specified in grid codes is the operating frequency of a renewable power plant. It is stated that the renewable power plant can be allowed to run continuously at the frequency range between 49 Hz to 51 Hz. The receiving-end terminal frequency for this wind power plant does not violate any of these ranges as it is at 50 Hz as shown in the above table.

5.4 Wind power plant islanded mode of operation

In this section, the load is connected at the wind power plant receiving end terminal, where the power demand is increased until the voltage at the wind power plant terminal collapses. This simulation forms part of the wind power plant compliance test.

The section is organized as follows: Part 5.4.1 presents the modelling of the controller for the load model under test. Part 5.4.2 presents the two case studies, the first when the wind power plant supplies the purely resistive load and the other when both resistive and reactive parts of the load are active.

5.4.1 Load model under test control modelling

At least a load of 15 MW of a lagging power factor of 0.95 is supplied in this test. The test is completed for two conditions, when the load is made resistive only and when both the resistive and reactive are included.

To perform the function of switching these two features of the load, the logic is designed, which allows the switching *ON/OFF* the reactive component of the load as shown in Figure 5.15 below.

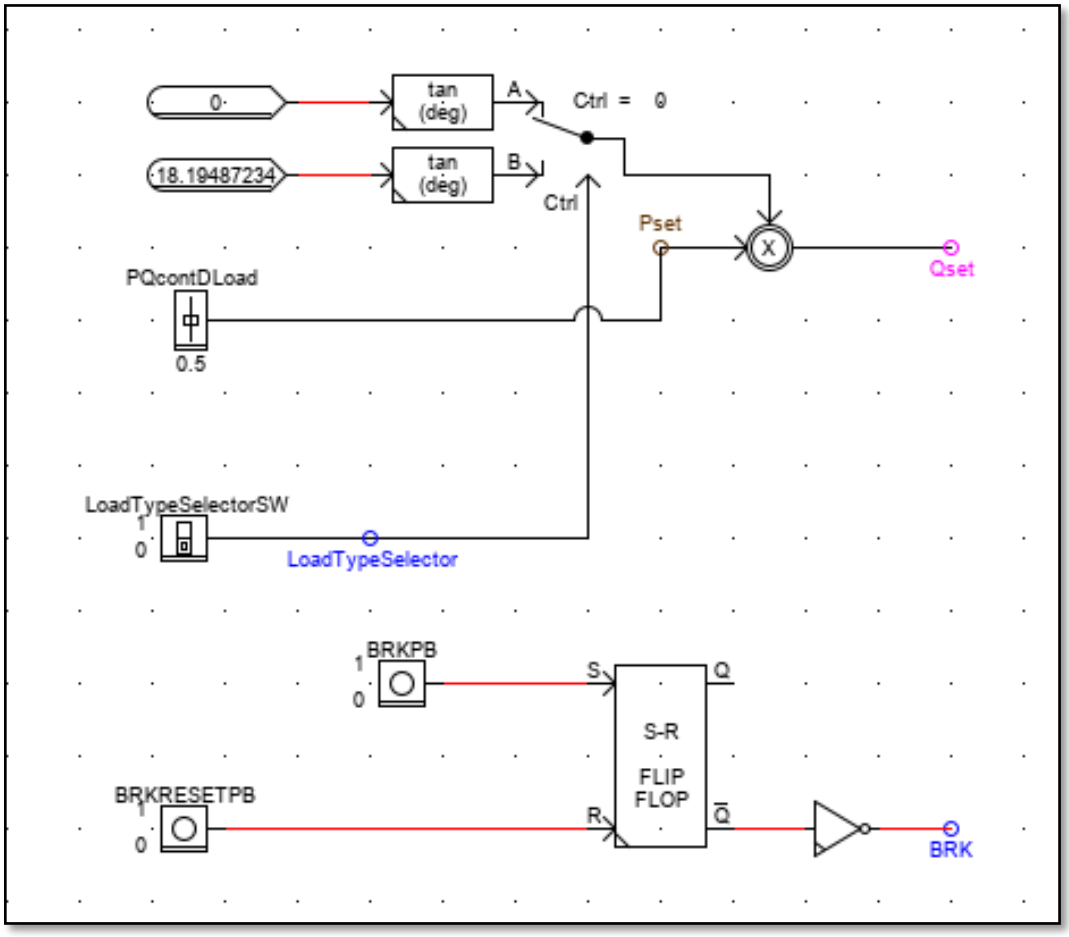

Figure 5.15: **Logic for switching between the active and reactive component of the load**

In the figure, the logic for activating and deactivating the reactive component of the load is controlled by the switch with the name LoadTypeSelectorSW whose output signal name is *LoadTypeSelector*. In addition to the above figure, the component tan(deg) depends on the output signal *LoadTypeSelector*. When the switch is ON, its output triggers the position of the *Ctrl* to the *B* position, activating the *tan(deg) B* which makes

the reactive power demand non-zero in the load by multiplying angle the tan of angle 18.1948723 degrees (which correspond to a load of 0.95 power factor) by the active power P to get the reactive power Q.

The aim is to assure the wind power plant's capability to supply the required amount of active and reactive power as required at Bus 2 of the transmission system studied in Chapter 4.

5.4.2 Wind power plant power loading

This section aims to confirm the wind power plant capabilities to supply an individual load by testing the amount of active power and reactive power demand it can withstand without experiencing any voltage collapse, while at the same time complying with the minimum and maximum accepted continuous voltage operation.

5.4.2.1 Active power loading

For this test, power demand is increased while at the same time the reactive power compensation is increased, to prevent the system from collapsing while a 15 MW load is not yet fulfilled. In this case, all reactive power compensator capacitor bank units are not switched on. Table 5.6 below shows the values recorded from the meters for monitoring the power drawn by the load from the wind power plant.

Table 5.6: Active and reactive load demand and current from the wind power plant

Load characteristic		Power demand		Current drawn (kA)
Active (x)	Reactive (x)	Active (MW)	Reactive (MVAr)	
x		15	0.1641	0.03987

The results in the above table show the reactive power demand at 0.1641 MVAr while the reactive power characteristic is not yet activated in the load. This is because of the minimum value that the RSCAD dynamic load setting allows, is a must to define at a value not equal to zero.

While the load demand is set to 15 MW, the sending and receiving-end active and reactive power, as well as the receiving-end reactive power of the compensating device was monitored and recorded as shown in Table 5.7 below on the next page.

Table 5.7: WPP active and reactive power values due to active power loading

WPP active power output (MW)		WPP reactive power output (MVAr)		WPP receiving-end reactive power compensation (MVAr)
Sending	Receiving	Sending	Receiving	
15.01	15.00	-1.827	0.1641	0

The sending and the receiving-end terminal the actual voltage (kV), per-unit voltage and frequency were monitored and are recorded in Table 5.8 below.

Table 5.8: WPP terminal voltage and frequency monitored under active power loading

WPP output voltage (kV)		WPP output voltage (PU)		WPP output frequency (Hz)	
Sending	Receiving	Sending	Receiving	Sending	Receiving
217.3	217.3	0.9448	0.9448	49.92	49.92

5.4.2.2 Active and reactive power loading

For this test, power demand is increased while at the same time the reactive power compensation is increased, to prevent the system from collapsing while a 15 MW + j4.925 MVAr load is not yet fulfilled. As a result, all reactive power compensator capacitor banks step-by-step switching was initiated. Table 5.9 below shows the active and reactive power demand by the load, and the last column of the table is the current drawn by the load under this condition.

Table 5.9: Active and reactive load demand and current from the wind power plant

Load characteristic		Power demand		Current drawn (kA)
Active (x)	Reactive (x)	Active (MW)	Reactive (MVAr)	
x	x	15	4.925	0.03815

While the load demand is set to 15 MW + j4.925 MVAr, the sending and receiving-end active and reactive power, as well as the receiving-end reactive power of the compensating device was monitored and recorded as shown in Table 5.10 below on the next page.

Table 5.10: WPP active and reactive power values due to active power loading

WPP active power output (MW)		WPP reactive power output (MVAr)		WPP receiving-end reactive power compensation (MVAr)
Sending	Receiving	Sending	Receiving	
15.01	15.00	-4.056	2.7384	2.187

The sending and the receiving-end terminal the actual voltage (kV), per-unit voltage and frequency were monitored and are recorded in Table 5.11 below.

Table 5.11: WPP terminal voltage and frequency monitored under active power loading

WPP output voltage (kV)		WPP output voltage (PU)		WPP output frequency (Hz)	
Sending	Receiving	Sending	Receiving	Sending	Receiving
239	239	1.039	1.039	49.94	49.94

The results in Table 5.11 show an effective improvement in wind power plant terminal voltages and this is because of the reactive power compensation installed at the receiving-end terminal of the wind power plant.

5.5 Discussion of results

The 15 MW load demand was fulfilled without the contribution of the reactive power compensator. The terminal voltage of 1.039 per-unit was experienced at the wind power plant receiving end terminal, is satisfactory according to the terminal voltage requirements specified by the grid codes.

When the reactive component of the load was introduced, the reactive power compensator units were switched on to contribute to reactive power demand by the load. In addition, the voltage measured at the terminals of the wind power plant was still satisfactory based on the requirements specified by the grid codes.

5.6 Conclusion

The load demand changes over time and may decrease or increase. Both these changes need to be dealt with by keeping the generation side in control concerning load changes. When the load demand increases up to a level where system generators can no longer afford to supply the required amount of power, power system instability may be experienced. One of the solutions to this challenge is the integration of additional power sources. For this reason, the wind power plant was modelled in this chapter and tested in the islanded mode of operation where the load was connected

and supplied. The aim was to check if the wind power plant meets the standards as specified by the grid code requirements.

CHAPTER SIX
DEVELOPMENT OF THE PROTECTION SCHEME FOR THE INTERCONNECTED SYSTEM

6.1 Introduction

The wind power plant model from the previous chapter is interconnected with the power system network used in the study. The resultant interconnected system is operated in two load conditions, the initial and the increased load demand. When operated in these conditions, the manner in which the current flows changes and this change requires a suitable protection scheme to safeguard the system for both conditions. For this reason, the Point of Common Coupling protection scheme is developed in this chapter, to protect the power systems even when the wind power plant contribution takes place.

The protection scheme developed in this chapter is tested in the form of a Hardware-In-Loop.

6.2 The hardware requirements of the designed protection scheme test

To complete the Hardware-In-Loop (HIL) test, the SEL-487B Protection Automation Control device was interfaced with the Real-Time Digital Simulators (RTDS) through three Omicron analog amplifiers, CMS 356 and two CMS 156. Since the designed protection scheme needs to suit two different conditions of the integrated power system network, two different protection scheme settings are used in the SEL-487B relay.

6.2.1 Analog amplifiers

The RTDS devices use twelve 16-bit gigabit transceiver analog output (GTAO) cards to produce a voltage of +/-10 Volts. The analogue outputs from the GTAOs are sampled every micro-second and the card's output channels are updated synchronously. The GTAO card is available on the RSCAD draft components. The analog amplifiers amplify +/-10 Volts signals to instrument transformer secondary sampled value ranges for voltages and currents for use by the external hardware measurement units or protective devices.

6.2.2 The SEL-487B Protection Automation Control

The SEL-487B is a bus differential current protection relay that offers circuit breaker failure and backup overcurrent protection. It protects busbars under short circuit fault conditions. For buses with less than seven terminals, a single SEL-487B Relay is enough, however for eight up to ten terminals, two SEL-487B Relays are required. For as many as twenty-one bus terminals, three relays are required, where each relay

provides as many as six independent and adaptable protection zones. The SEL-487B used for this study has eighteen analog currents and three analog voltage inputs.

There are various busbar configurations in power system networks, however, this study is based on a simple (single) busbar unit. Because the busbar of this system has four terminals, only one relay is used and it subscribes to three current channels and a single voltage terminal for the advancement of protection functions through directional current elements.

One of the most challenging activities with SEL-487B is the system configuration which includes the following:

- Renaming (Aliasing) terminals and bus zones
- Assigning input contacts to the selected relay logics
- Declaring terminal-to-bus zone connections
- Configuring bus couplers and check zones, and
- Assigning logic to relay outputs.

In total, ten topics were visited to achieve the scheme settings for this device, namely input, logic, and output assigning process, relay differential element composition, current transformer requirements, disconnect requirements, alias names, bus-zone configuration, bus-zone-to-bus-zone connection, zone supervision, trip logic, and output assignment.

The differential scheme settings for the SEL-487B relay are categorized into two, namely the system configuration and scheme configuration. The system configuration involves terminal-to-bus-zone and bus-zone-to-bus zone assignments, zone supervision, and zone-switching supervision settings.

The scheme configuration involves enabling the settings, differential and sensitive differential element settings, directional element settings, and the output assignments. To achieve the differential protection scheme, terminals are assigned to the relevant phase differential zone logic inside the relay. The following part is an overview of the configuration of this relay.

6.2.2.1 The SEL-487B Relay differential protection elements

The philosophy of busbar protection schemes has two-out-of-two trip criteria. The scheme uses two separate measuring elements, where the operation depends on the agreement between these elements. The two-out-of-two trip criteria are achieved by using the dual differential element combination (main zone and check zone) or

differential element and directional element combination (main zone and directional zone).

Directional and differential elements have their advantages and disadvantages. Differential elements/amplitude comparators are exposed to current transformer saturation, which usually occurs in networks with high faults if CT selection is not done properly. Directional elements/phase comparators are exposed to high impedance faults, in networks with impedance grounding. Relay selection is completed during the design of the power system network, however, changes (e.g. extension) in the network influence the network characteristics.

The modern version of the busbar protection solves this challenge by including the protection elements that allow the different network parameters. The protection elements must ensure of the continual, uncompromising relay performance even if the network parameters change.

The general requirements for the busbar protection scheme are a fast operating time for all internal busbar faults, security for load flow (external or through faults) with heavy CT saturation, and minimum delay for evolving faults. SEL-487B Differential Protection Relay meets all these requirements. Each differential element for this relay is responsible for each phase.

The SEL-487B Relay can only protect for two zones, provided that the total number of terminals connected to the protected busbar is less than six. In addition, because the differential protection relay works on a per-phase basis, it has the differential protection element for each phase. The differential element consists of three elements, filtered differential, direction and the fault detection logic element. which assists in the adaptability of the differential protection scheme.

The SEL-487B Relay Red-phase differential element logic is shown in Figure 6.1 below on the next page with terminals, I01 and I02. This element can only protect a single phase of a busbar unit with two branches. But because it is a configurable element, multiple inputs can be assigned to ensure that even the busbar with multiple branches is protected. The logic shown in the above figure consists of the filtered differential element with two output signals named, *FDIF1* and *87O1*.

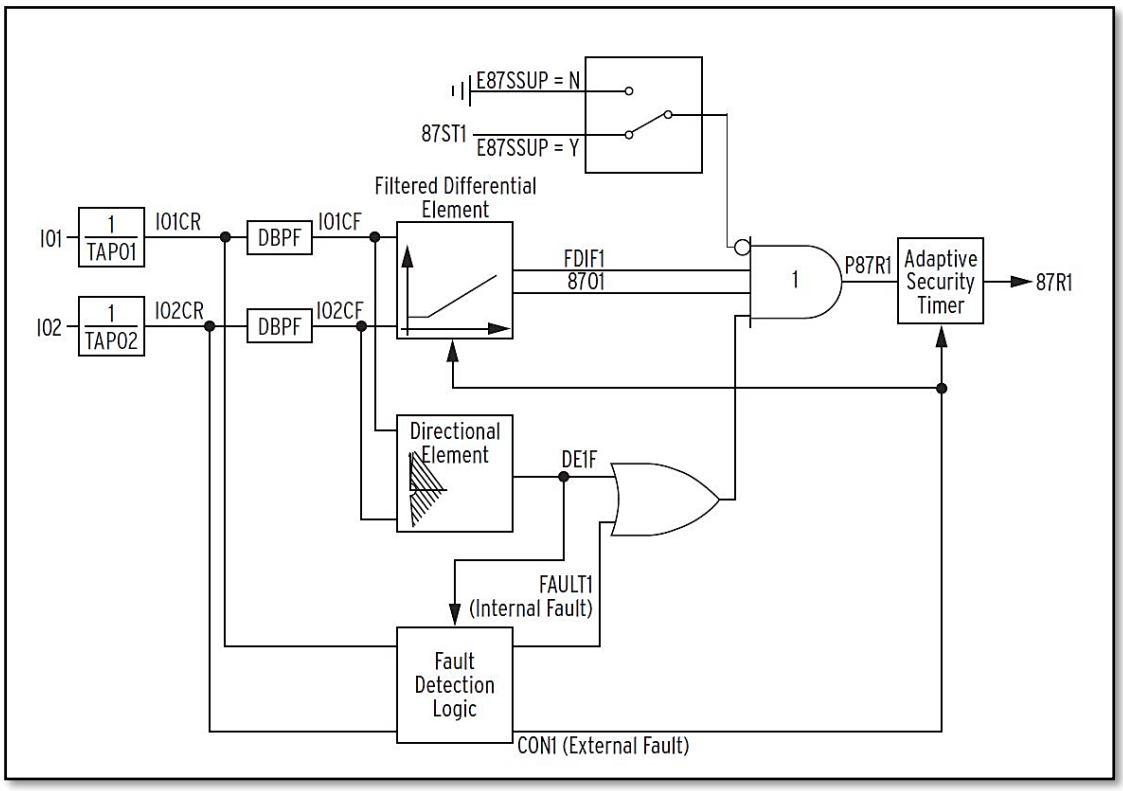

Figure 6.1: **Differential element logic for an SEL-487B Relay**

The complete element logic for a filtered differential element is as shown in Figure 6.2 below.

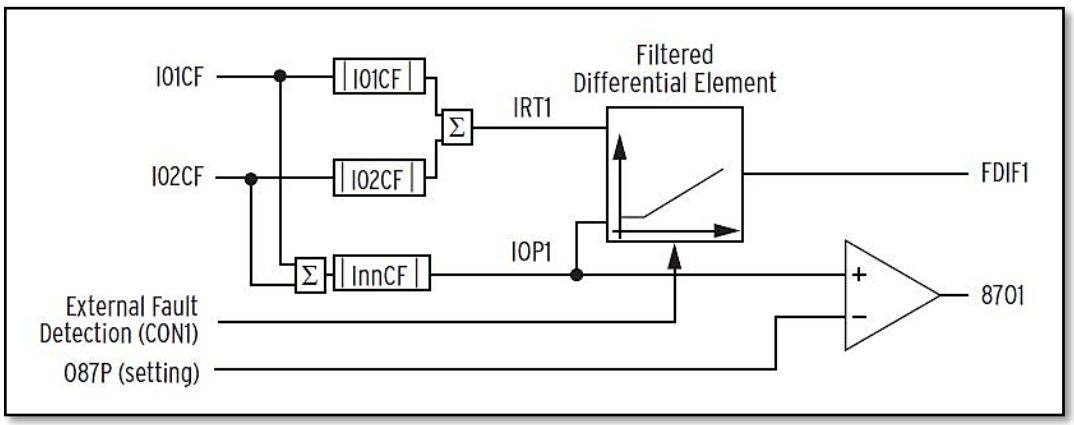

Figure 6.2: **Filtered differential element logic**

The *FDIF1* output of the logic shown in the above figure is activated only when the differential current (operating current) IOP1 is greater than the O87P setting's value and greater than the product of the selected percentage slope and the restrained current value. *87O1* is instantaneous and becomes active when the IOP1 is greater than the value of the O87P setting.

The slope characteristic curve of the filtered differential element logic is shown in Figure 6.3 below. Slope 1 and Slope 2, each responsible for various conditions. Slope 1 applies in the case of internal faults, and for faults that occur externally, Slope 2 operates. Slope 2 is triggered for operation by the fault detection logic and is part of the differential element logic. This slope is considered the securing slope because it blocks the relay from operating when the fault is external.

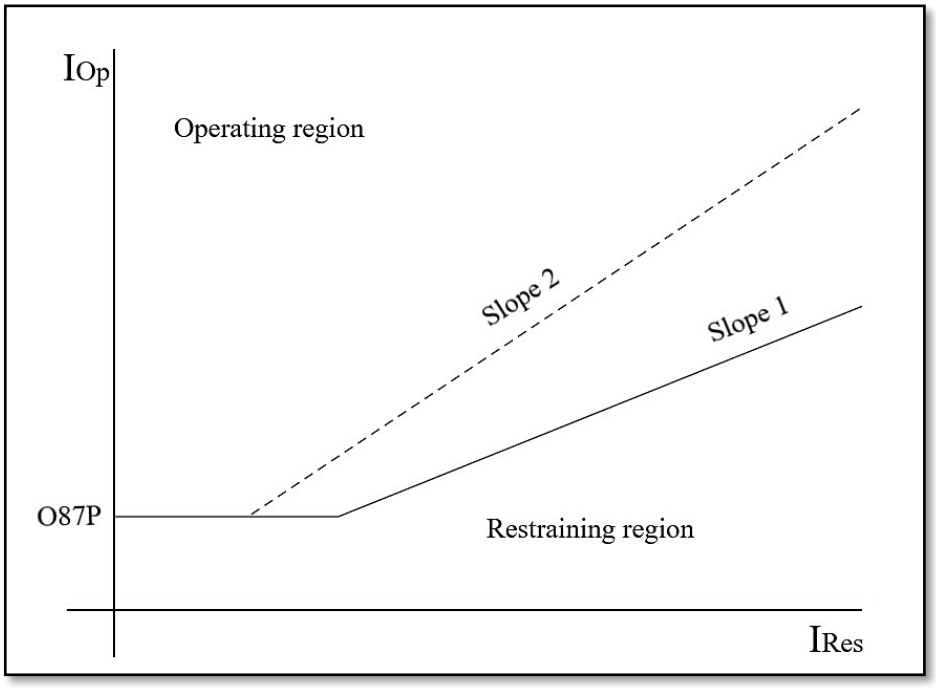

Figure 6.3: **A differential characteristic curve with two slopes**

6.2.2.2 The SEL-487B directional element

Another element included in the differential element is the direction element logic. It provides additional security during the external faults when heavy current transformer saturation occurs.

Same as the differential element, the directional element works on a per-phase basis. This element compares the direction of the current flow at the reference terminal to that of other measuring terminals. Its settings involve the directional element supervision pick-up (50DSP) and are set as the threshold.

The relay selects the first terminal as a reference (IREF) and compares the direction of the current of the two remaining terminals. *DE1F* asserts if the direction of these terminals coincides with the direction of the reference current according to the directional element characteristic shown in the figure (SEL, 2018). The directional element logic is shown in Figure 6.4 below on the next page.

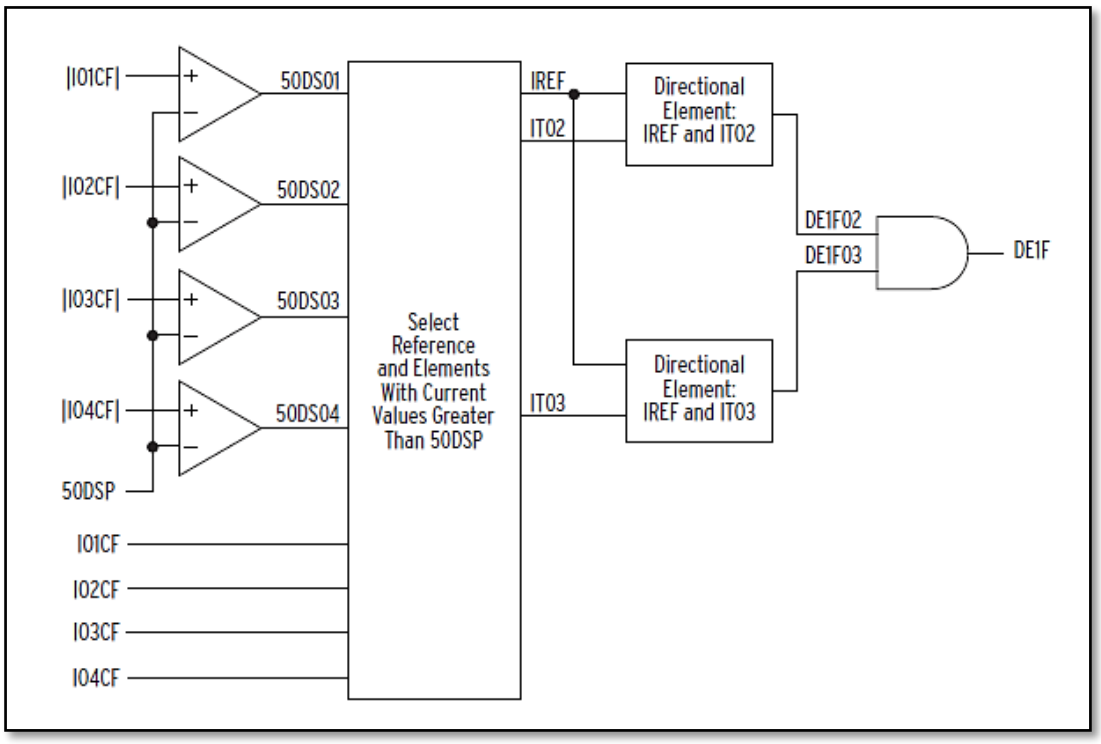

Figure 6.4: Directional overcurrent logic for a red-phase

The directional element monitors the terminal with the phase current magnitude greater than 50DSP and its operation is based on the directional characteristic curve shown in Figure 6.5 below.

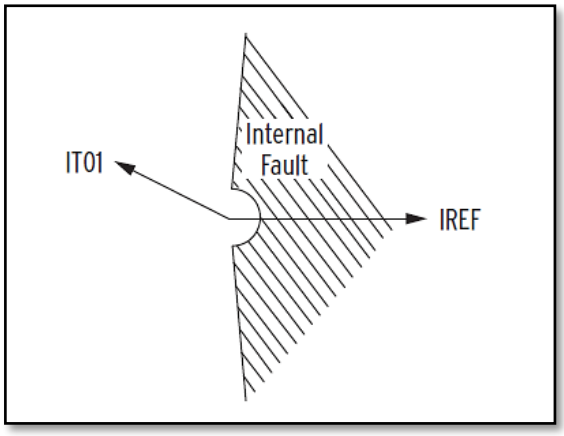

Figure 6.5: Directional element characteristic curve

In addition to the differential element, the fault detection logic exists, to determine whether the fault is external or internal to the protected zone or unit. The logic is shown in Figure 6.6 below on the next page.

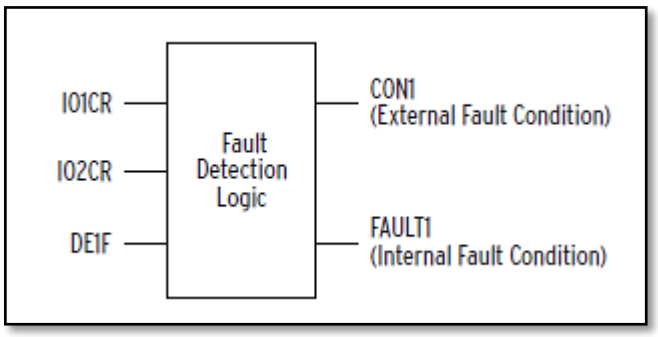

Figure 6.6: Fault detection logic – external or internal fault

The last element of logic involved in the differential calculation algorithm is its output logic and is described in the next part.

6.2.2.3 The differential protection element logic

The final stage of the differential calculation logic in an SEL-487B relay is the assignment of the output relay word bits command to the circuit breaker controls. To access the output relay word bits from the relay, the element logic shown in Figure 6.7 below exists. In the figure, *87R1* is the restrained differential element word bit and is assigned to the differential final stage output which produces binary 1 when all the differential element actions are fulfilled. The 87R1 output is asserted after the instantaneous differential element pick-up (*P87R1*) experiences a time delay in cycles.

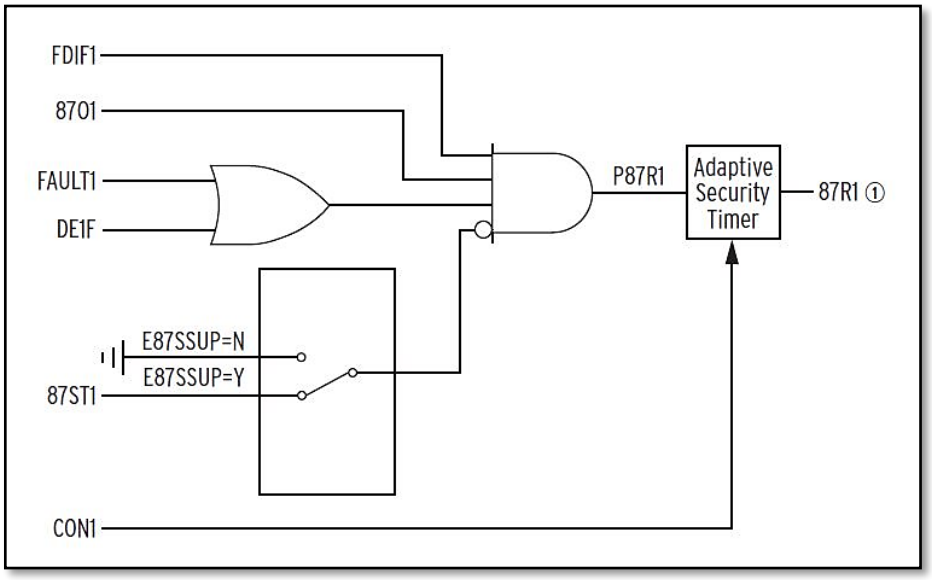

Figure 6.7: Differential protection output element logic

The assertion of the *P87R1* depends on five conditions as listed below, wherein the mentioned elements, the figure “1” represents the phase (zone) protected by the differential zone element.

- ***FDIF1***: The filtered restrained element picked-up bit must be high (1). This means that the filtered per-unit differential current must be greater than the product of the operating slope (in percentage) and the filtered per-unit restraint current, and the product must lie on the operating region of the differential characteristic curve.
- ***87O1***: The restrained element picked-up bit must be high (1). The filtered per-unit differential current must be greater than the restrained differential element threshold setting current.
- ***FAULT1***: The *FAULT1* word bit must be high (1). This can be high only if the zone z element detects an internal fault.
- ***DE1F***: *DE1F* must be high (1). This is high only if the directional overcurrent element supervision has been picked up.
- ***87ST1***: Sensitive differential element supervision must be zero. It can be zero only if the *E87SSUP* is set yes (Y) for the scheme, where the output of the element is declared zero.
- ***CON1***: *CON1* is the relay word bit output from the external fault detection logic, which asserts only when the external fault is detected. When all the previous conditions are met, the *P87R1* word bit becomes true and activates the adaptive security timer. *CON1* sets the security timer, and when it asserts, the relay's operating time delay is increased by 0.4 cycles. The increase in time delay increases the security of the protection element.

When all the four conditions are met, the *P87R1* word bit becomes true (1). This bit operates instantaneously, and cannot be used as a trip command for a circuit breaker where the differential protection scheme is used for security reasons. Therefore, the additional condition needs to be met within the protection scheme, where the external fault detection logic is set.

The digital inputs to the logic come from different calculation logic, for instance, *FDIF1* and *87O1* are binary outputs from the filtered restrained differential element and the restrained differential element. The logic for these binary signals has already been configured and tested. *FAULT1* is a binary output from the internal fault detection logic. This logic does not need to be configured, it is built within the differential relay and only depends on the existing differential calculation values.

DE1F is an output from the directional element logic. For binary output *DE1F*, the directional element operation needs to be explained. The directional element provides additional security during the external faults when heavy current transformer saturation occurs. Same as the differential element, the directional element works on a per-phase

basis. This element deals with the comparison of the current direction at the reference terminal to the direction of the current at all other measuring terminals in each phase. The directional overcurrent element supervision pick-up (50DSP) is set as the threshold.

The various protection elements and the feature of switching over from one group of settings to another by the SEL-487B device made it a suitable device for the protection developed for the system used. Hence it is used in this chapter.

The configuration of the RSCAD instrument transformers and the GTAOs, engineering configuration of SEL-487B Relay for control, monitoring and protection of the power system network used for this study is presented in the next sections for the accomplishment of the protection scheme developed for the interconnected network system.

6.3 Modelling of the signalling devices for the scheme on RSCAD

The protective device used for this study makes use of analog voltages and currents from the Real-time digital simulator devices to perform calculations, decisions and control algorithms. To receive these signals from the RTDS, instrument transformers and the GTAO card models are configured using RSCAD, for sampling the simulated real-time virtual voltages and currents measured on the interconnected system in RTDS devices.

6.3.1 Current transformer selection, modelling and configuration

The differential protection scheme is a unit type of protection scheme that looks at the current entering and leaving the node. To achieve this type of current flow and maintain the precise differential calculations, the selection of current transformers must be done properly.

The primary rating of the CT should be within the range of about 120% to 150% of the full load current. The aim is to make the secondary currents as small as possible to prevent saturation of current transformers by selecting CT transformers with a large number of turns. For this reason, 150% of the full load current of the interconnected network system is used.

$$\mathrm{CT_{PrimaryTurns}} = 150\%\mathrm{I_{FullLoad}} \tag{6.1}$$

Where, $\mathrm{CT_{PrimaryTurns}}$ and $\mathrm{I_{FullLoad}}$ represent the turns ratio of the current transformer and the full load current monitored under normal load conditions of the system.

To obtain the current transformer turns ratio values, the load ampere current values of the system must be known. For this reason, the currents were recorded from the system under both load conditions, and these values are recorded in Table 6.1 and Table 6.2 below. The values recorded in these tables present currents monitored in the branches supplying the protected branch of the system.

Table 6.1: **Currents monitored during the absence and presence of the wind power plant with no contribution at 315 MW loading**

	Standalone transmission power system network	Transmission power system network with wind power plant
Branches	**Primary currents (kA)**	**Primary currents (kA)**
ILine12RE	0.1444	0.1437
ILine24SE	0.2147	0.2146
IDLoad1	0.3404	0.3402
IWF1Line	-	0.001814
Total current	0.6995	0.700314

Table 6.2: **Currents monitored during the presence and contribution of the wind power plant at 420 MW system loading**

Transmission power system network with wind power plant	
Branches	**Primary currents (kA)**
ILine12RE	0.1709
ILine24SE	0.1958
IDLoad1	0.453
IWF1Line	0.1746
Total current	0.9943

Bus 2 consists of three branches, with the names *Line12RE*, *Line24SE*, *LineWF1,* and *DLoad1Feeder*. The value of currents flowing in these branches is not the same.

For differential protection schemes, parallel-connected CTs are configured to be of the same turns ratio and this is a requirement for precise differential calculations within the differential protection device. *DLoad1Feeder* branch current makes the sum of the *Line12RE*, *Line24SE*, and (or) *LineWF1* branch currents.

The CTs are selected based on the highest current, thus when the wind power plant is contributing to the system. Using Expression 6.1, the CT ratio is calculated at maximum as

$$\mathrm{CT_{PrimaryTurns}} = 150\%\mathrm{I_{FullLoadMax}}$$

$$\mathrm{CTLine24SE_{PrimaryTurns}} = 150\%(0.453\ \mathrm{kA})$$

$$\mathrm{CTLine24SE_{PrimaryTurns}} = 679.5\ \mathrm{A}$$

The calculated value is approximately equal to the 700 turns ratio in terms of CT ratio standards. The secondary winding series resistance and burden impedance are selected based on a 240:1 CT found in the IEEE Guide for Selection of Protection CTs, where the series resistance of the CT is 0.61 Ohms and 4 Ohms for burden impedance. The series resistance and the burden impedance were calculated using the 0.61 Ohms and 4 Ohms. The resultant values were 1.77917 and 11.66667 Ohms for the series resistance and burden impedance. The setting values were done and the CTs configured on RSCAD as shown in the consecutive figures, 6.8 to 6.10 below and on the next page.

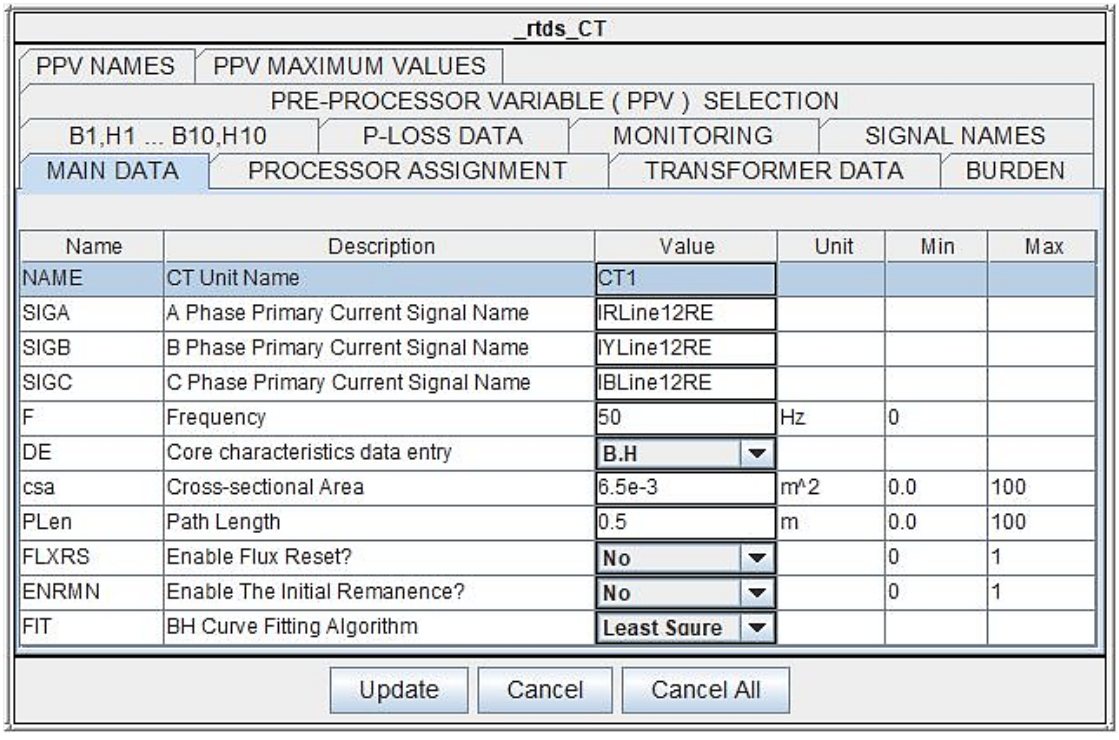

Figure 6.8: **Main data parameter settings for CT1**

In the above figure, the name of the CT, primary current signals of the CT, and most importantly the nominal frequency of the system are entered. The primary current signal names entered are line currents monitored from the branch, Line12RE

transmission line where the current transformer is connected. These line currents were set to be monitored in RSCAD Runtime.

The current transformer data is set and the secondary windings resistance and the primary turns ratio of the CT are set as shown in Figure 6.9 below.

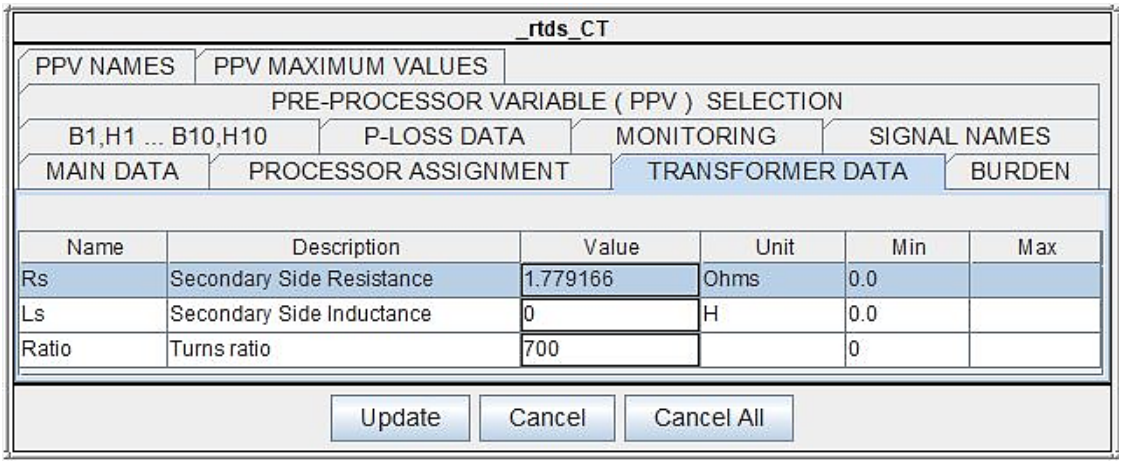

Figure 6.9: **Secondary winding series resistance and the primary winding turns ratio settings for CT1**

The RSCAD CT models have options to set signals for monitoring. the secondary currents from the CT are more significant since the physical device used for the protection scheme uses them for differential calculations and decision making.

The last settings that were done for CT1 are that of the secondary windings terminal burden resistance, calculated based on the 240:1 CT available from the CT standards. This setting takes into account the resistance of leads connected from the secondary terminals of the CT to the input terminals of the protective device, including its internal circuits which in combination with the CT circuits make a loop. The value obtained was 11.6667 Ohms and is set as shown in Figure 6.10 below.

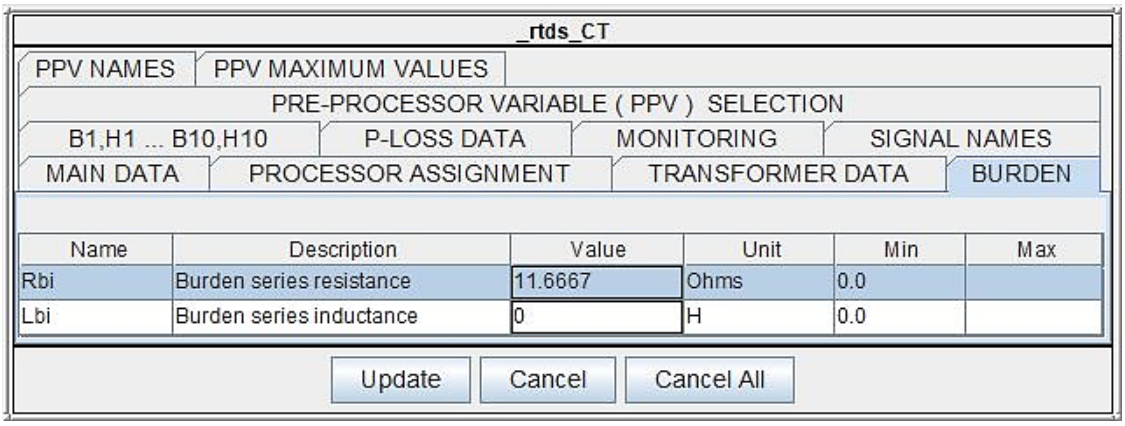

Figure 6.10: **Settings for burden resistance of the CT**

This configuration is the same for the rest of the current transformers, CT2, CT4 (CTWF1), and CT3 for branches *Line24SE*, *LineWF1* transmission line, and *DLoad1Feeder*.

In addition to the analog signals required by the physical device from the RTDS devices, the voltage transformer is required and is configured in the next part.

6.3.2 Capacitor voltage transformer selection, modelling, and configuration

The CVT is suitable for protection and is chosen for economic reasons. It is designed such that the primary voltage is scaled to an intermediate level before applying to the protection or metering device. The scaling in the CVT is completed by the stacked capacitors. The CVT is prepared for Bus 2 voltage monitoring and is mapped to this busbar through voltage signals set for monitoring at the busbar as shown in Figure 6.11 below.

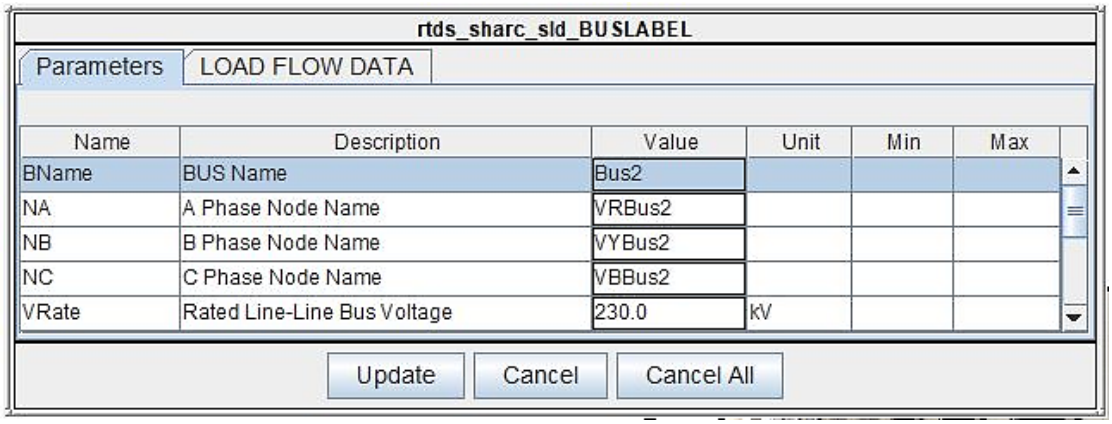

Figure 6.11: Voltage signal names monitored on Bus 2

The signal names for voltages shown in the above figure were used for monitoring in RSCAD Runtime. These voltage signal names are set in the VT primary voltage signals. In addition, the secondary voltages from the CVT are also set for monitoring.

The CVT can be used for a 230 kV system when a required burden voltage required is in the range of 110 to 120 Volts. For protection and monitoring purposes, the required operating range of voltage for secondary devices is of the above-specified range.

The aim is to achieve the secondary voltage that is within the range specified by the instrument transformer standards for protection CVTs. The CVT presented in this part meets the requirements. Some parameters are left on default and this does not affect the secondary output voltage. Figures, 6.12 to 6.15 below show the default settings for the selected CVT.

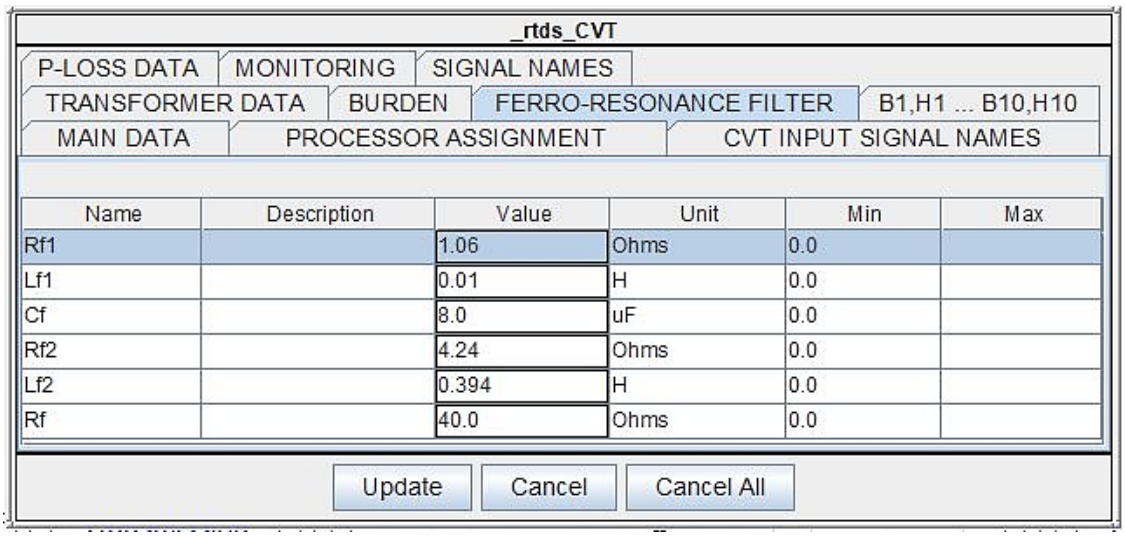

Figure 6.12: Default settings for CVT1 Ferro-resonance filter

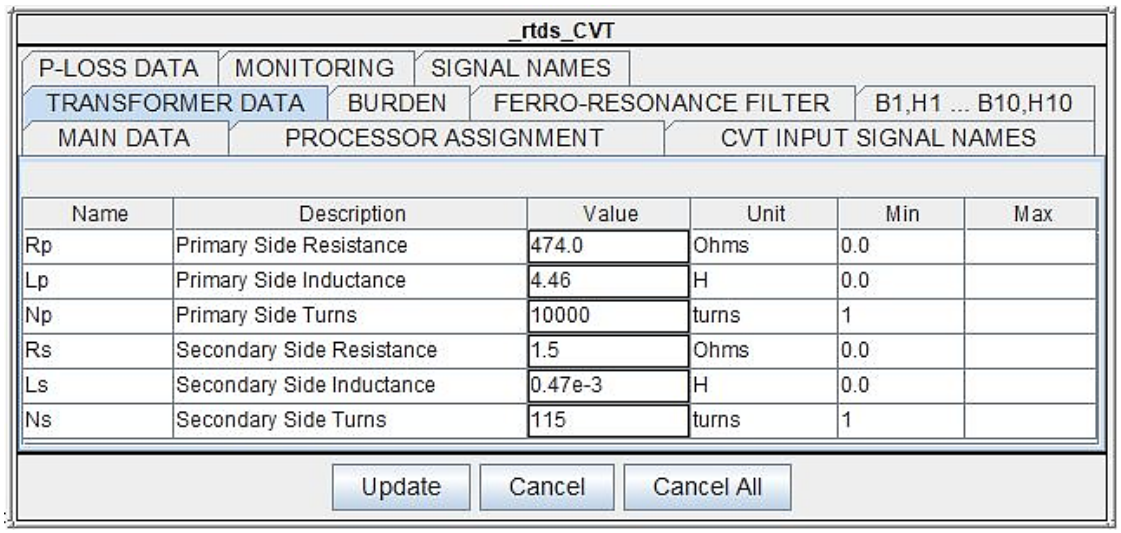

Figure 6.13: Default settings for CVT data

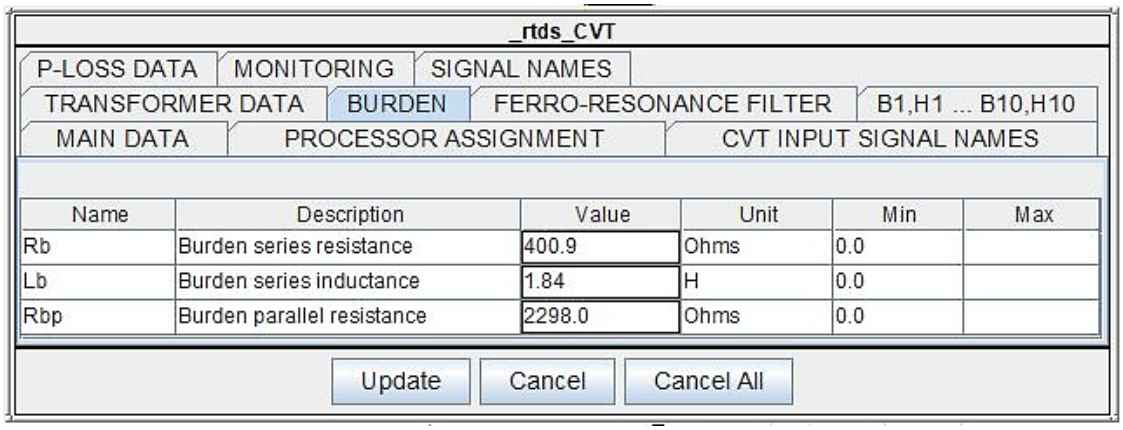

Figure 6.14: Default settings for CVT secondary windings burden parameters

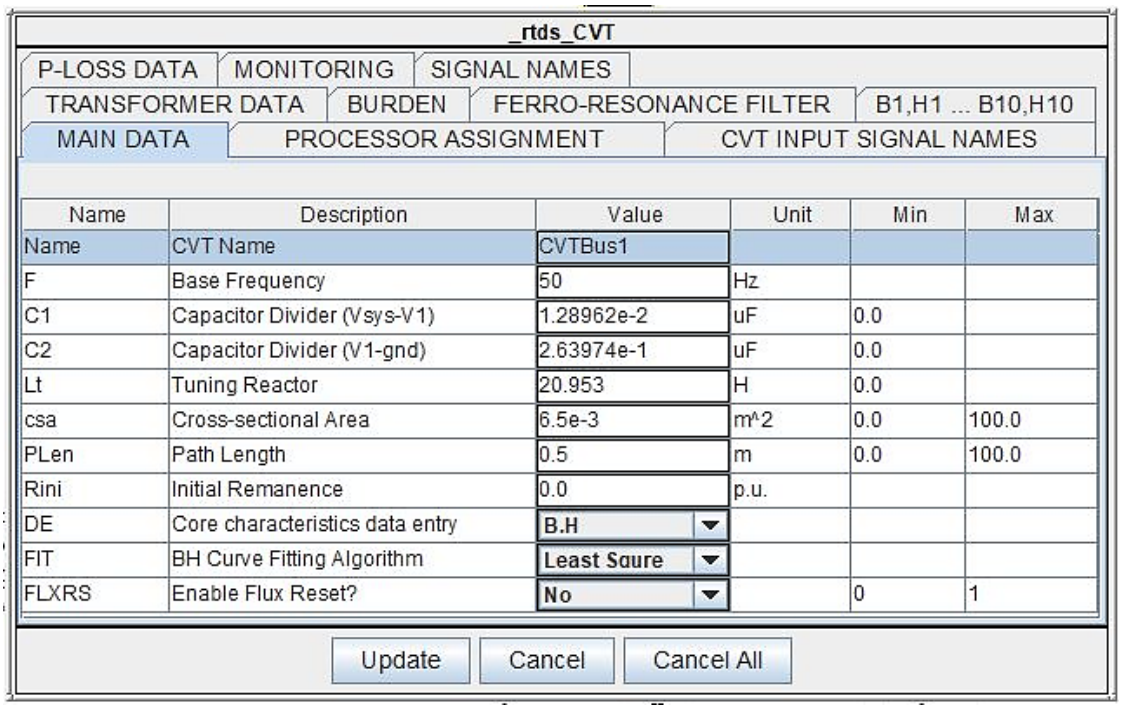

Figure 6.15: **Default settings for CVT main data**

6.3.3 GTAO cards modelling and configuration

To interface the protective device to RTDS simulations for control of the virtual power system network, the digital to analog conversion is completed using the Gigabit Transceiver Analog Output (GTAO) card which makes the actual analog CT secondary currents available to the physical monitoring, control, or protection device.

The GTAO cards are available in the RTDS Rack 1 and Rack 3. The power system network model is, therefore, prepared, with its signals set for exports and imports across Subsystem 1 and Subsystem 3 of the Real-time digital simulators, 1 and 3, for secondary currents signals from *DLoadFeeder* branch CT (CT3) and *LineWF1* CT (CT4) to reach the second GTAO model in Subsystem 3 (Rack 3) as shown in Zones 4 and 5 of Figure 6.16 below.

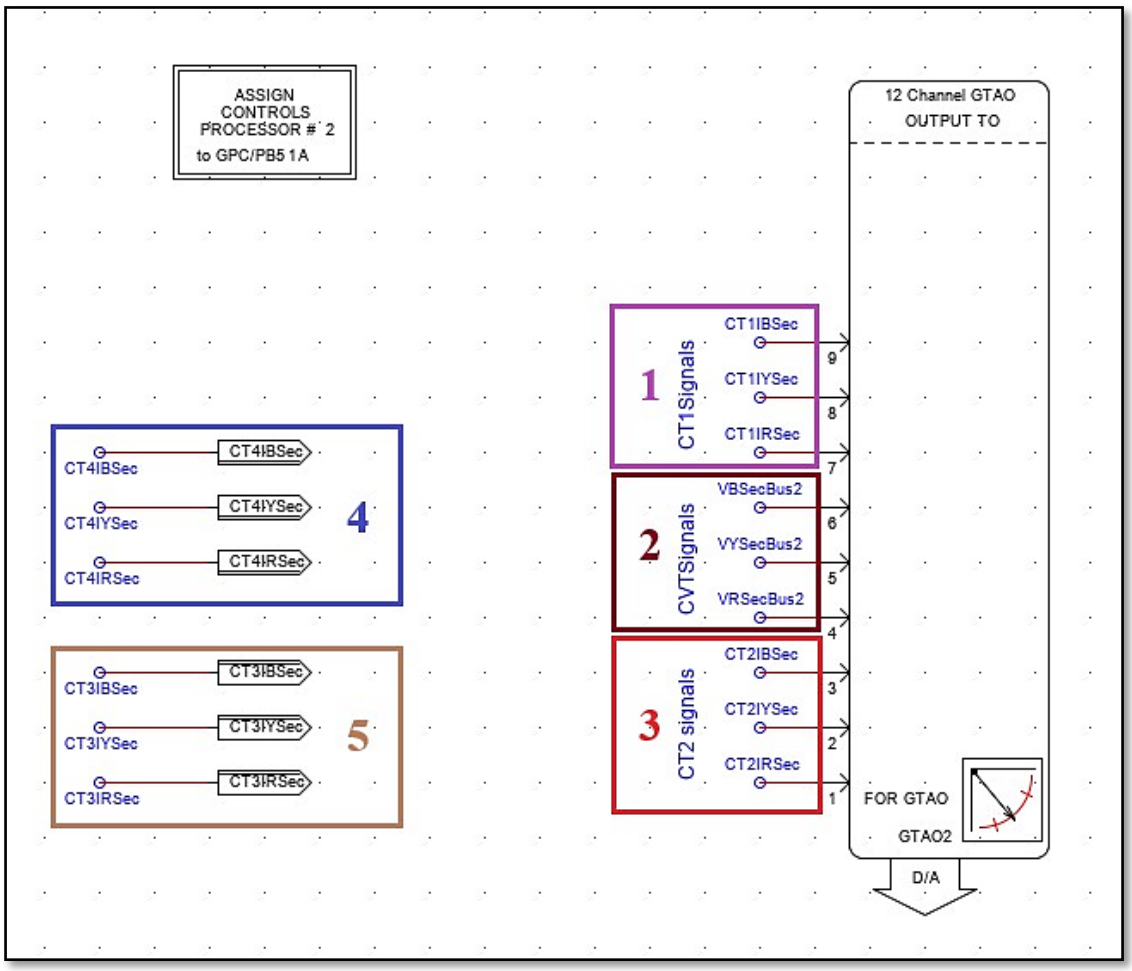

Figure 6.16: **GTAO1 card in Subsystem 1 for CT1, CT2 and CVT1 secondary voltages and currents**

The GTAO shown in Figure 6.16 above is modelled in Subsystem 1 (Rack 1). Zones, 1 to 3 in the figure show the secondary current signals from CT1, secondary voltage signals from CVT1 and secondary current signals from CT2. This GTAO card is set to convert two sets of three-phase currents and a set of three-phase voltage signals only. Therefore channels, 1 To 3 and 7 to 9 are used for currents. Channels, 4-6 are used for voltage signals.

Another part of the GTAO modelling is to ensure the actual output analog voltages and currents as measured from the RSCAD virtual instrument transformers. This goal is achieved by setting GTAO signal scaling as shown in Figure 6.17 below on the next page.

rtds_risc_ctl_GTAOOUT

OVERSAMPLING FACTORS | SIGNAL ALIGNMENT DELAY OPTION

D/A OUTPUT SCALING | PROJECTION ADVANCE FACTORS

CONFIGURATION | ENABLE D/A OUTPUT CHANNELS

Name	Description	Value	Unit	Min	Max
scl1	Chnl 1 Peak value for 5 Volts D/A out:	25	units	-1.0e6	1e6
scl2	Chnl 2 Peak value for 5 Volts D/A out:	25	units	-1.0e6	1e6
scl3	Chnl 3 Peak value for 5 Volts D/A out:	25	units	-1.0e6	1e6
scl4	Chnl 4 Peak value for 5 Volts D/A out:	301	units	-1.0e6	1e6
scl5	Chnl 5 Peak value for 5 Volts D/A out:	301	units	-1.0e6	1e6
scl6	Chnl 6 Peak value for 5 Volts D/A out:	301	units	-1.0e6	1e6
scl7	Chnl 7 Peak value for 5 Volts D/A out:	25	units	-1.0e6	1e6
scl8	Chnl 8 Peak value for 5 Volts D/A out:	25	units	-1.0e6	1e6
scl9	Chnl 9 Peak value for 5 Volts D/A out:	25	units	-1.0e6	1e6

Update | Cancel | Cancel All

Figure 6.17: GTAO1 scaling settings

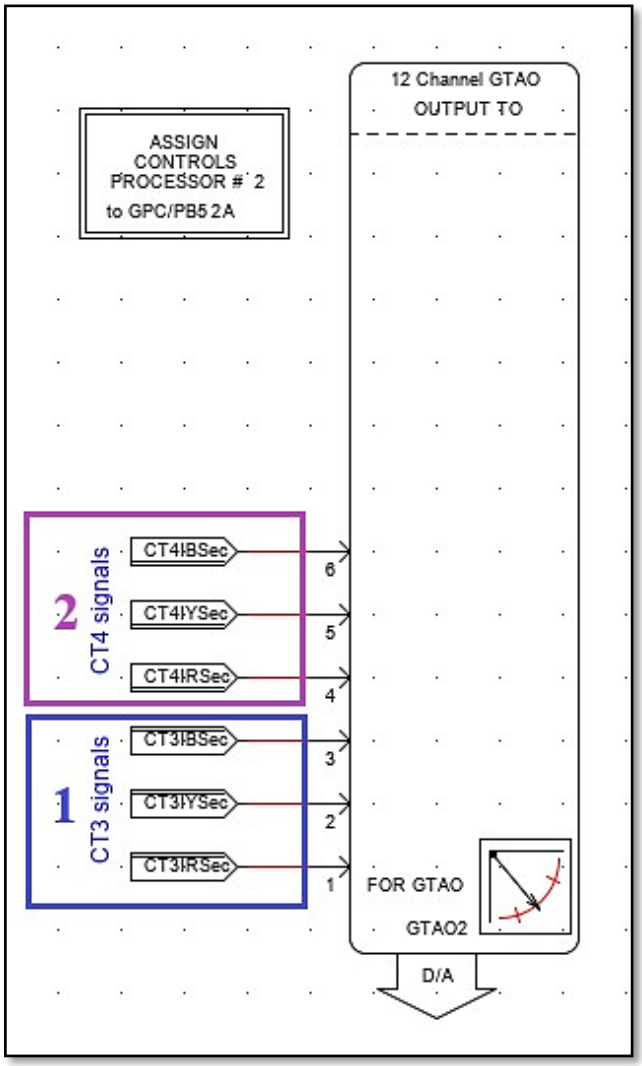

Figure 6.18: GTAO2 card in Subsystem 3 for CT3 and CT4 secondary currents

Figure 6.18 above shows the GTAO2 card modelled in Subsystem3 (Rack 3) of the RTDS device. In the figure, Zone 1 shows the import current signals that were set for export in Subsystem 1 (Rack1). The scaling settings for GTAO2 are shown in Figure 6.19 below for current signals.

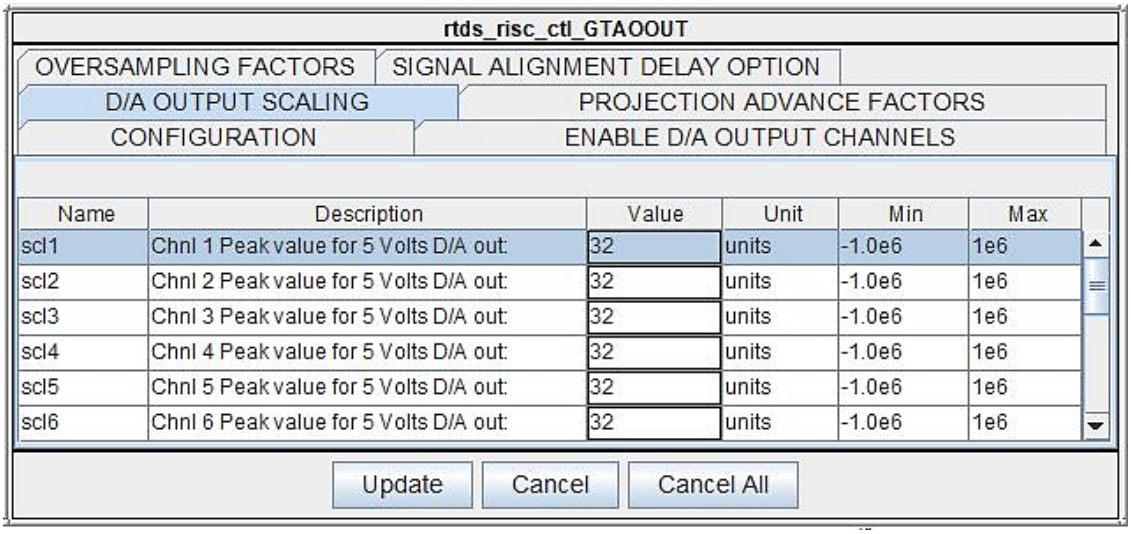

Figure 6.19: **Analog current signal scaling for GTAO2**

Testing of the protection scheme requires the injection of short-circuit faults in the power system network model. This is achieved through the use of the fault control and simulation logics available in the RSCAD component library.

The developed protection scheme makes use of the physical device test on runtime simulations where the control signals from the device are sent back to the RTDS virtual circuit breakers. To accomplish this closed-loop control system, the low-voltage digital interface of the RTDS racks is configured in the part below.

6.3.4 Configuration of the low-voltage digital interface and its control logic

The interconnected system consists of three supply branches connecting to Bus 2. In the case of a fault, the entire busbar section has to be isolated from the system by disconnecting all the supplying branches. Three circuit breakers are modelled to perform this function. These circuit breakers are controlled using signals named *BRKOne*, *BRKTwo* and *BRKThree*. Figure 6.20 below on the next page is an example of circuit breaker settings where the name of the signal to control the breaker is defined. All the phases share the same signal name. The setting is the same for the rest of the circuit breakers but with unique control signal names.

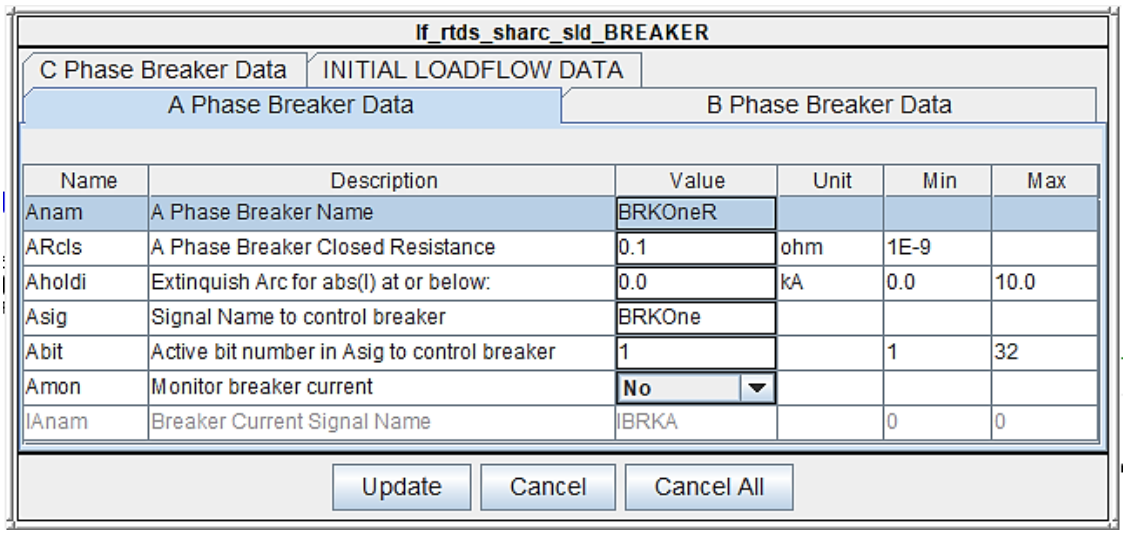

Figure 6.20: BRKOne settings – signal named to control breaker

Time is the most significant factor in protection studies. Practically in power systems, the time delay exists during the circuit breaker operation. Usually, in high-voltage transmission networks, the circuit breaker operation takes from 0.2 to 0.3 seconds (Dhivya & Sakthivel, 2018).

To make the simulation studies realistic, it is advisable to pay attention to the time parameter in protection studies, to validate the conclusions.

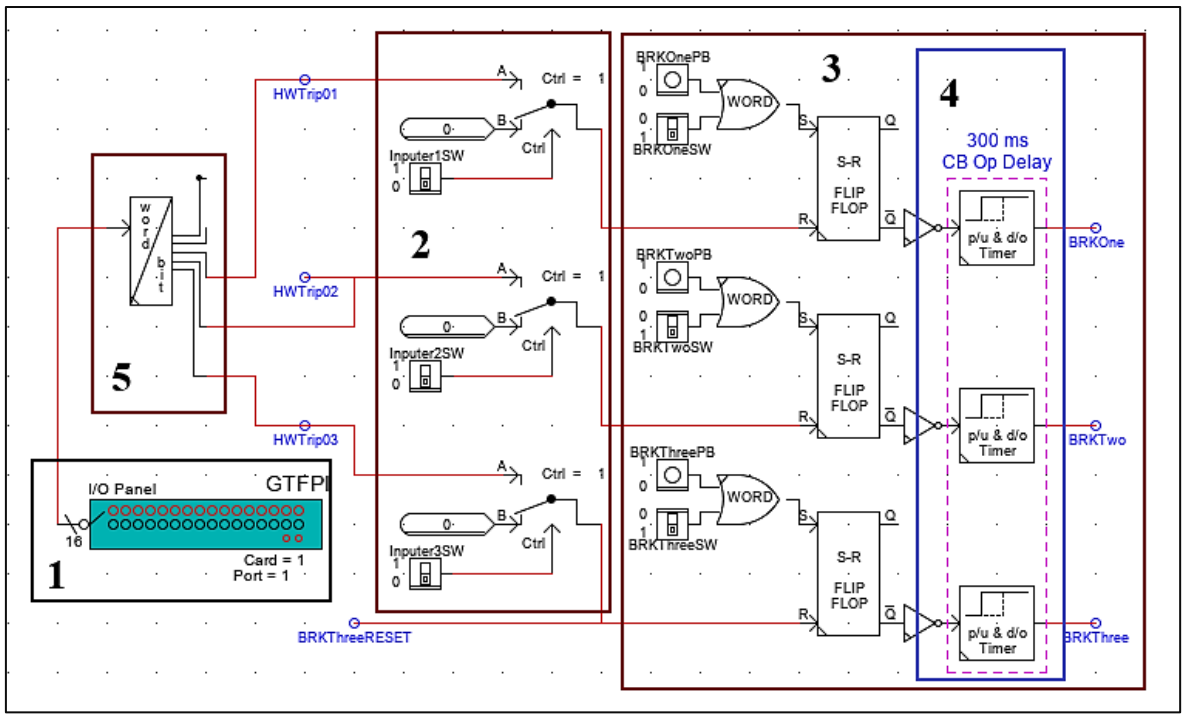

Figure 6.21: GTFPI model and circuit breaker control logic

For this reason, the designed logic used to interface the physical device with the RTDS devices makes use of the timers to accommodate for circuit breaker operation delays. The circuit breaker control logic is shown in Figure 6.21 above on the previous page and is connected from the GTFPI model shown in Zone 1.

The GTFPI model shown in Zone 1 represents the physical RTDS front panel binary input connector from the physical protective device. There are three outputs used from the protective device, therefore three sets of binary input wires from the relay are used for sending binary trip commands to the front panel of RTDS, which on the later stage go to the virtual breaker control logics shown in Zone 3 of the figure. Zone 2 is the logic used to activate and deactivate the trip command from the protective relay.

The developed protection is tested using various types of busbar faults at the coupling point. RSCAD offers the fault locators and their control logics for the simulation of faults. The following part presents the configuration of these fault locators and logics.

6.3.5 Modelling and configuration of the fault logics for Bus 2

Most power system faults are single-line to ground, but for validity of the protection scheme phase elements, additionally to single-line to ground faults, three-phase faults are also simulated.

Fault locators and logic are used to locate and inject, define the type of short-circuit fault (whether line-to-ground, three-phase-to-ground, all-three-phase, line-to-line, etcetera) and its duration (optional in cycles) for fault simulation studies. The fault simulation logics are modelled in this part, accommodating at least single-phase-to-ground and three-phase faults at the busbars of the system.

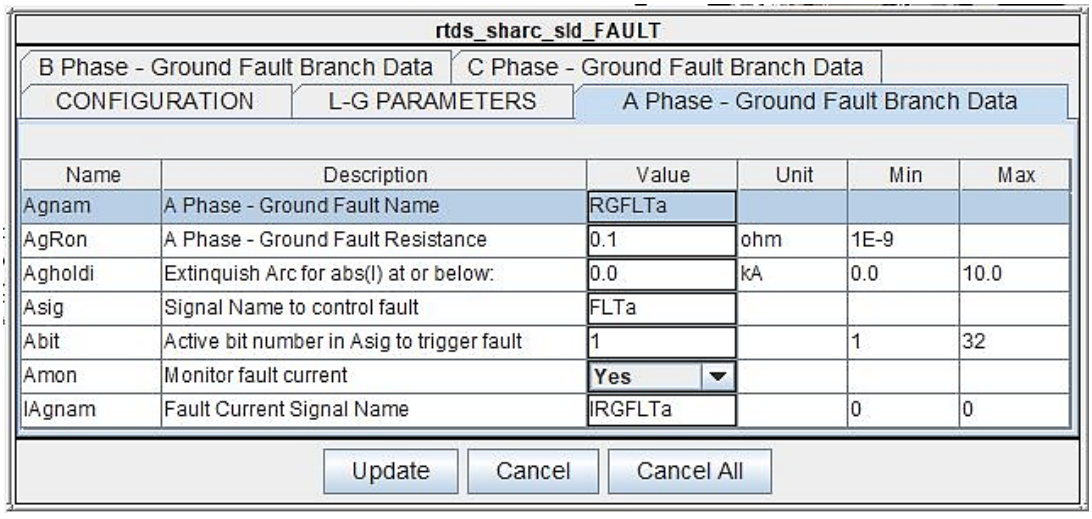

Figure 6.22: Settings to define the fault control signals

Other parameters are entered in the fault locator component settings, to define the phase on which the fault should occur and the fault current that must flow in that phase to the ground. Figure 6.22 above on the previous page shows these settings. In the figure, the signal named to control the fault is *FLTa* and its binary bit to apply the fault trigger is made “1”. In addition, the phase on which the fault must occur is RGFLTa.

These settings are the same, for the rest of the phases, except for Agnam, IAgnam settings. For instance, for a Yellow phase, Agnam is set *YGFLTa* and IAgnam is *IYGFLTa*. The logic to control the fault locator is shown in Figure 6.23 below.

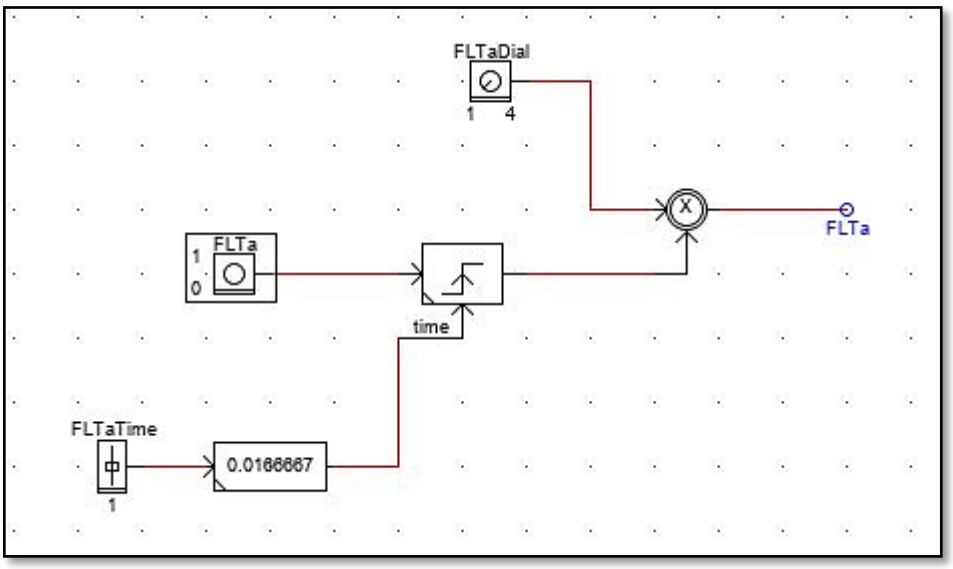

Figure 6.23: **Fault logic to control a single-phase-to-ground fault**

In the above figure, the component with the name FLTaTime is a slider used for adjusting the duration of the applied fault. FLTa is the pushbutton used to apply the fault, FLTaDial is a multiposition dial selector switch used to select the phase at which the fault must occur, and *FLTa* is the signal word bit that is mapped to the fault locator logic and is used to apply the fault trigger to the fault locator. Its output bit is “1” when the FLTa component is pressed while the FLTaDial position is in any position except the first position.

In addition, Figure 6.24 below on the next page shows the settings to define the fault control signals at Bus 2. In the figure, ABnam is set to RYFLTa, ABSig to *FLTa2*, ABbit to 1 and ABnam to *IRYFLa2*. The name RYFLTa is the name of the fault that is occurring between the phases, Red and Yellow. *FLTa2* is the signal named to control the fault, whose output is binary “1” when active. In addition, *IRYFLTa2* is the signal named set to monitor the fault current.

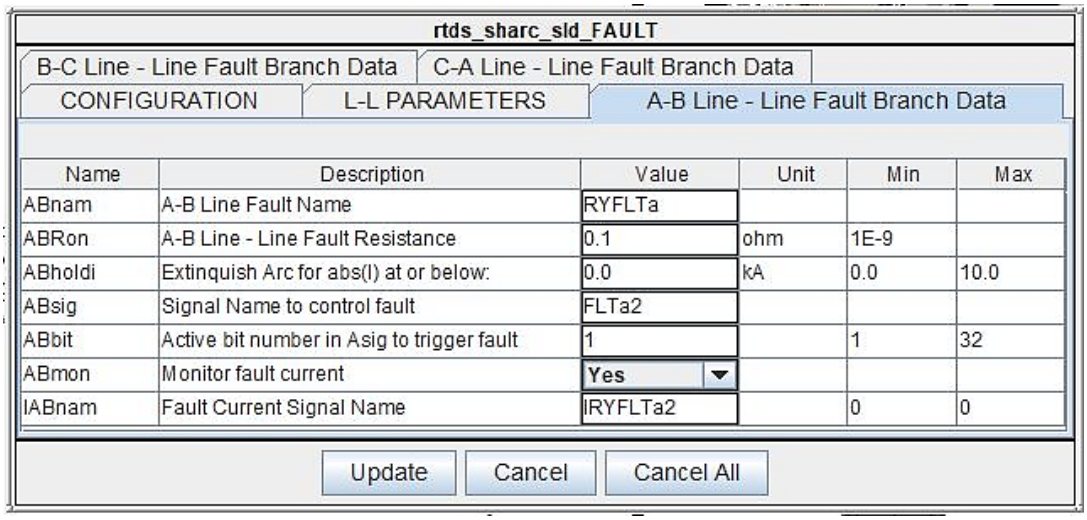

Figure 6.24: Settings to define the fault control signals

Figure 6.25 below is the fault control logic to control a three-phase fault. The signal named to control the fault is the same for all the phases. The components used for logic in Figure 6.25 are the same as those of the logic to control a single-phase-to-ground fault, except for fault dial selector with only two positions, 1 and 2. When put in position 1, there are no faults injected into the system and when 2 is selected, only a three-phase fault is injected and the output bit “1” triggers all the phases for this type of fault.

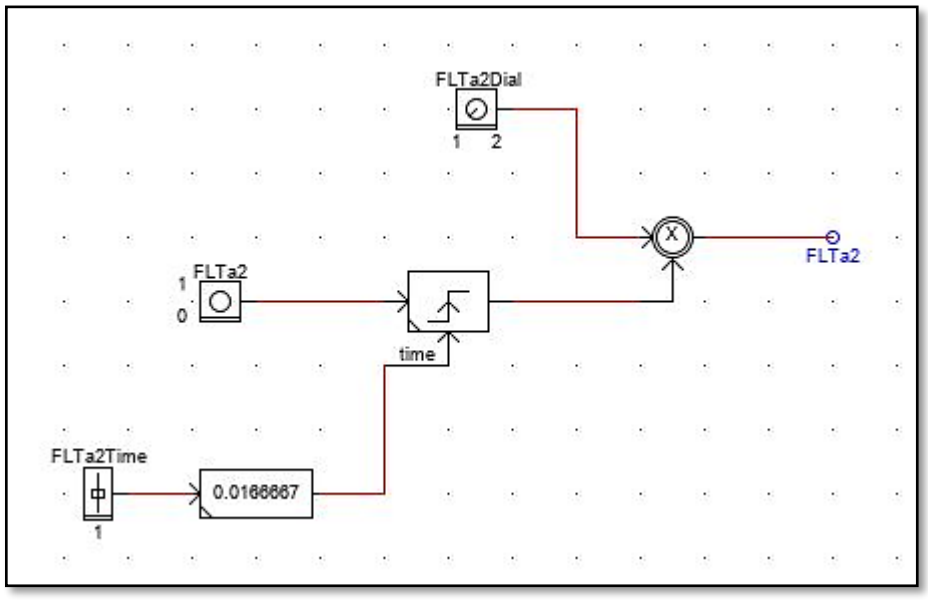

Figure 6.25: Fault logic to control a three-phase fault

The settings presented in this part are the same for the rest of the busbars, Bus 3 and Bus 5, except for component labelling and signal names. After the modelling and

configuration of these components, the power system network model was modified and the control components were located in their positions in the network.

6.4 The interconnected network system with controls components

Figure 6.26 below shows Area 2 as modelled in Subsystem 2 (Rack 2). In the figure, Zone 1 shows the fault locator and its control logics enclosed in two boxes shown in the same zone. These logics are linked to Bus 2 (see Figure 6.27) for busbar fault simulation. The two transmission line towers are circled purple and orange, they connect this subsystem to Area1 of the network in Subsystem 1 (Rack 1).

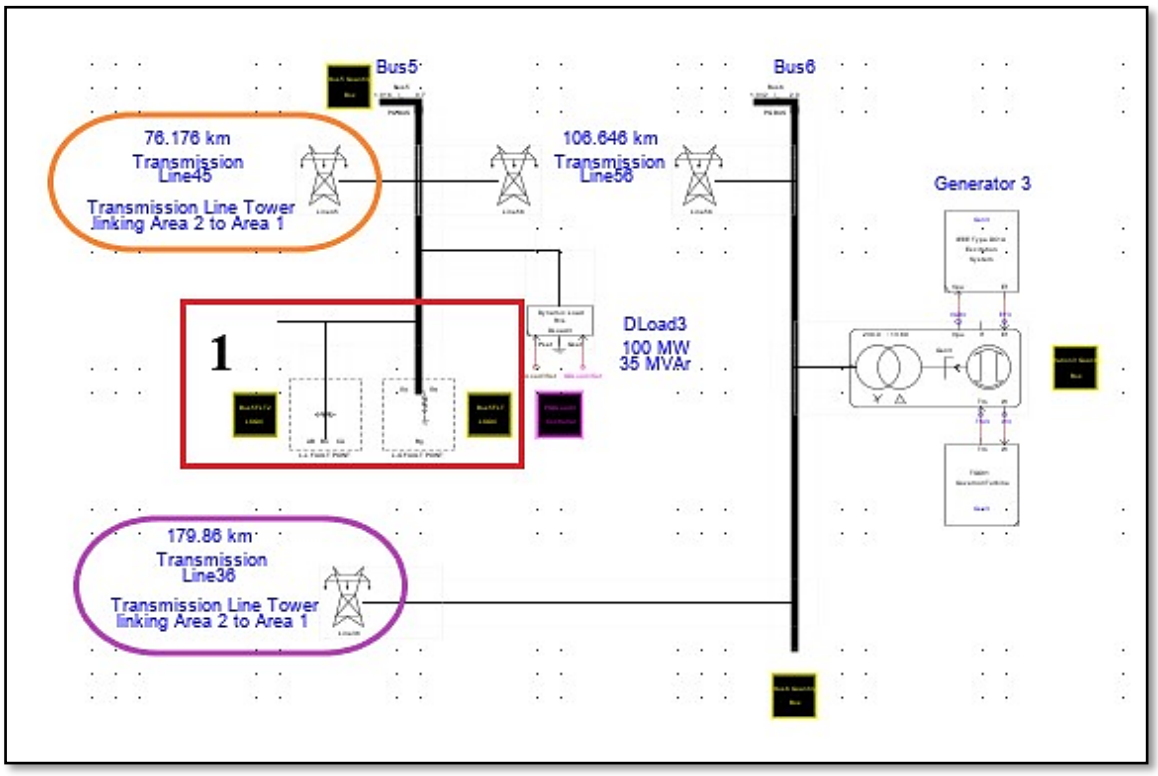

Figure 6.26: **Area 2 of the modified power system network model in Subsystem 2 (Rack 2)**

Another area of the power system network model is modelled in Subsystem 1 (Rack1) as shown in Figure 6.27 below on the next page. In this figure, Zone 1, 5, 6 and 9 are CTs for wind power plant, the transmission line 12, the transmission line 24 and dynamic load 1 feeder branches respectively. Zone 3 is a capacitor voltage transformer for measuring the voltage at Bus 2. Zone 2, 4 and 7 are the circuit breakers used for control of Bus 2 used as the point of common coupling of the system. Zone 12 and 13 are the Bus 3 and Bus 2 fault locators and control logics respectively.

In addition, the orange and purple zones are connection points to Subsystem 2 (Rack 2). Zone 11 represents the bay control station for the system. Zone 14 is the connection

point for all the wind power plant group wind turbine generator units that are modelled in subsystems, 3-5. Each group consists of six wind turbine generator units.

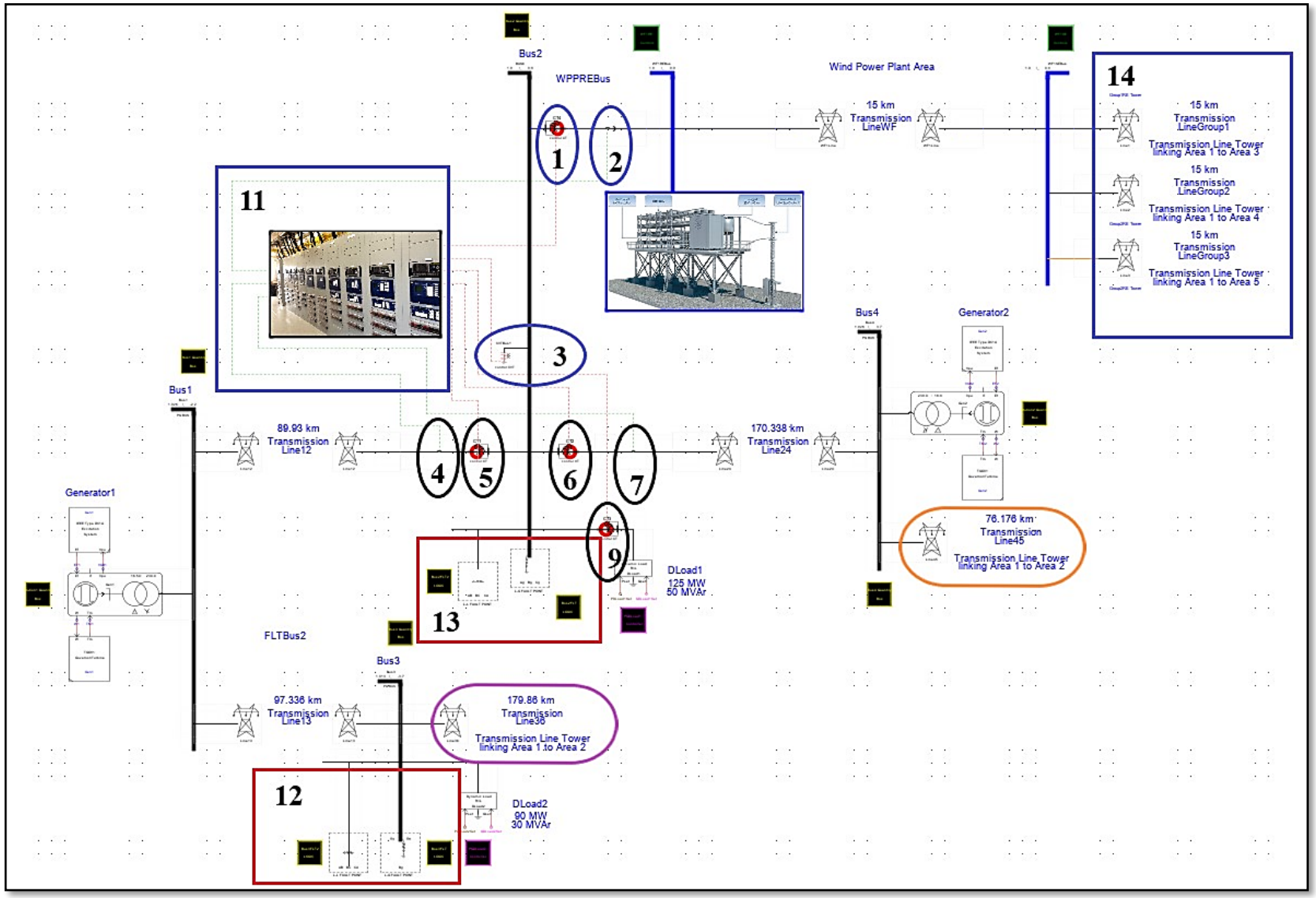

Figure 6.27: Area1 of the modified power system network model in Subsystem 1 (Rack1)

These groups of wind turbine units are shown in figures, 6.28 to 6.30 below.

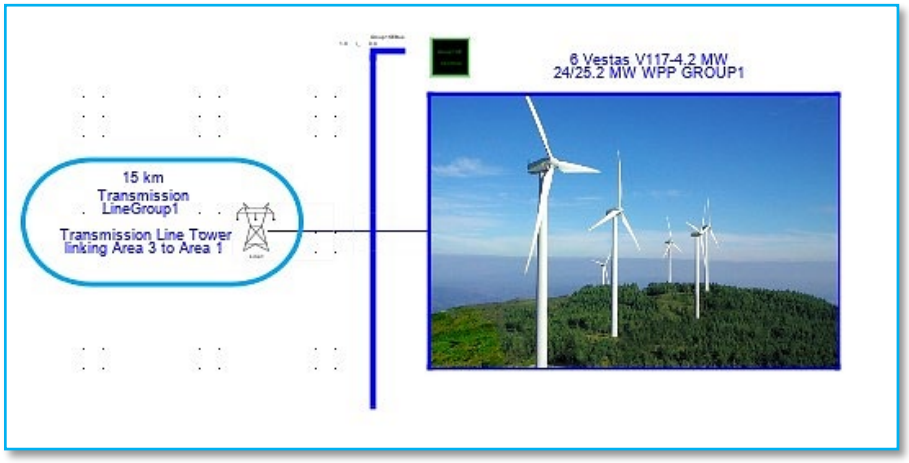

Figure 6.28: The coupled system – WPP Group 1 Area 3 Subsystem 3 (Rack 3)

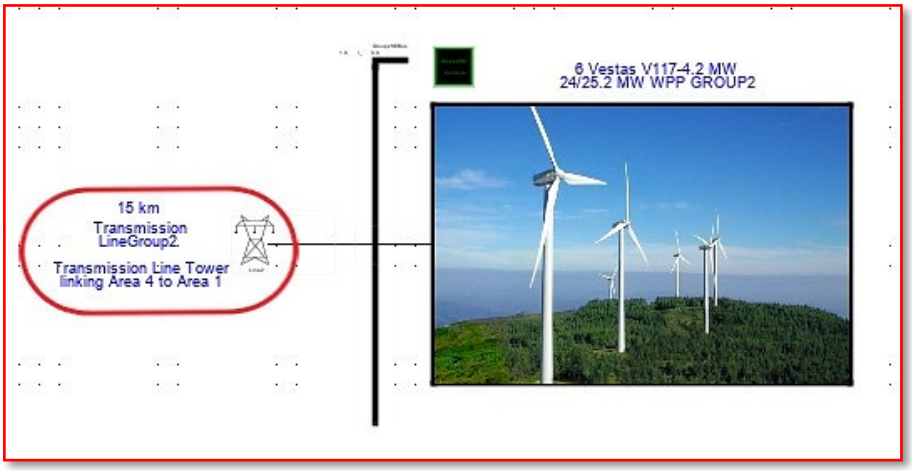

Figure 6.29: The coupled system – WPP Group 2 area 4 Subsystem 4 (Rack 4)

Figure 6.30: The coupled system – WPP Group 3 area 5 Subsystem 5 (Rack 5)

6.5 Device configuration

The configuration of the SEL-487B Protection Automation Control device is completed in this section using the AcSELerator Quickset.

The configuration of this scheme is completed such that both operating conditions of the interconnected resultant system are met. That being said, two settings group are chosen for the device, to suit both conditions, when the load is 315 MW and when it is 420 MW. The following parts present the configuration procedure as described in Part 6.2.2 of this chapter.

6.5.1 Renaming (aliasing) terminals and bus zones

The first task of configuring the SEL-487B is that of renaming (aliasing) the elements or relay word bits the way that suits the protection scheme. The configuration is completed based on the structure of the protected unit. In addition, these settings are independent of the group settings, they apply to all the groups.

6.5.2 Assigning input contacts

The SEL-487B relay has six differential elements and the protected system has four terminals, which requires only three out of six differential elements, namely Bus Zone 1 (Red Zone), Bus Zone 2 (Yellow Zone) and Bus Zone 3 (Blue Zone). The aliasing of these elements has been done and the previous part referred them to Appendix D, where the bus zones, BZ1, BZ2 and BZ3 were renamed to BUSZR, BUSZY and BUSZB.

In this part, the connection between the input line current terminals is mapped (assigned) to the corresponding differential elements for the protected three-branch-fed and one-branch output busbar unit. For simplicity, this mapping is shown in a form of a table. However, the snapshots that show the AcSELerator Quickset configuration for this setting are attached in Appendix D.

In Table 6.3 below on the next page, input I01, I04, I07 and I10 are the red (A) phase and relay terminals and are linked to the differential element which does the differential calculations for this phase. This applies to all the selected remaining inputs, I02, I05, I08 and I11 for yellow (B) phase CTs, and I03, I06, I09 and I12 for blue (C) phase CTs.

Table 6.3: Terminals to zone configuration for the developed scheme using SEL-487B

Relay terminals		Bus zone elements	
Element name	Alias name	Element name	Alias name
I01	IR1	BZ1	BUSZR
I04	IR2		
I07	IR3		
I10	IR4		
I02	IY1	BZ2	BUSZY
I05	IY2		
I08	IY3		
I11	IY4		
I03	IB1	BZ3	BUSZB
I06	IB2		
I09	IB3		
I12	IB4		

The configuration presented in the above table is logically achieved through the configuration done within the AcSELerator software by assigning each terminal to a phase differential protection block. Physical connections are done on the device to link the analog input voltage and current signals to the relays' CTs and CVTs to interface the power system network with the internal logic of the device. The earthing point is compulsory for differential protection relaying system. For this reason, the CTs are connected in Y (star) configuration.

6.5.3 Instrument transformer configuration

The instrument transformer settings are done on this part. The same settings that were entered during the RSCAD modelling and configuration of the signalling devices for the scheme in section 6.3 are used. In addition, these settings are dependent on group settings. They are done for both settings groups, Group 1 and Group 2 to make the adaptability of the protection scheme for both operating conditions of the system. These values are kept the same for both settings group.

The CT turns ratios were selected based on the maximum load condition of 420 MW to accommodate even for minimum load condition of 315 MW. The settings values are configured using the AcSELerator Quickset as shown in Figure 6.31 below on the next page for Group 1 and are the same for Group 2 settings. In addition, the current transformer value-based calculated current normalization factor settings values are done by the AcSELerator Quickset as shown in Figure 6.32 below on the next page for Group 1 settings.

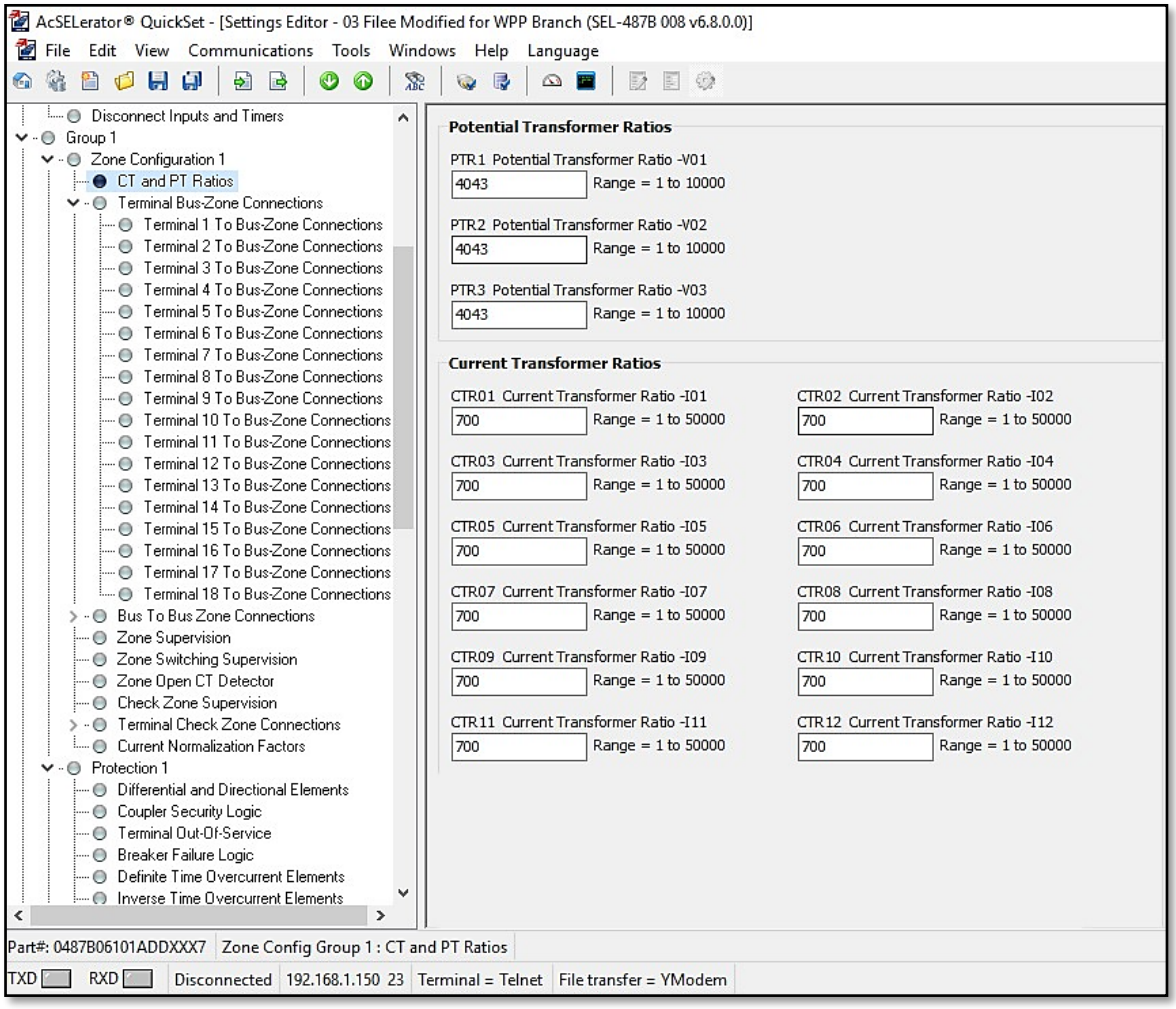

Figure 6.31: SEL-487B relay Group 1 instrument transformer settings

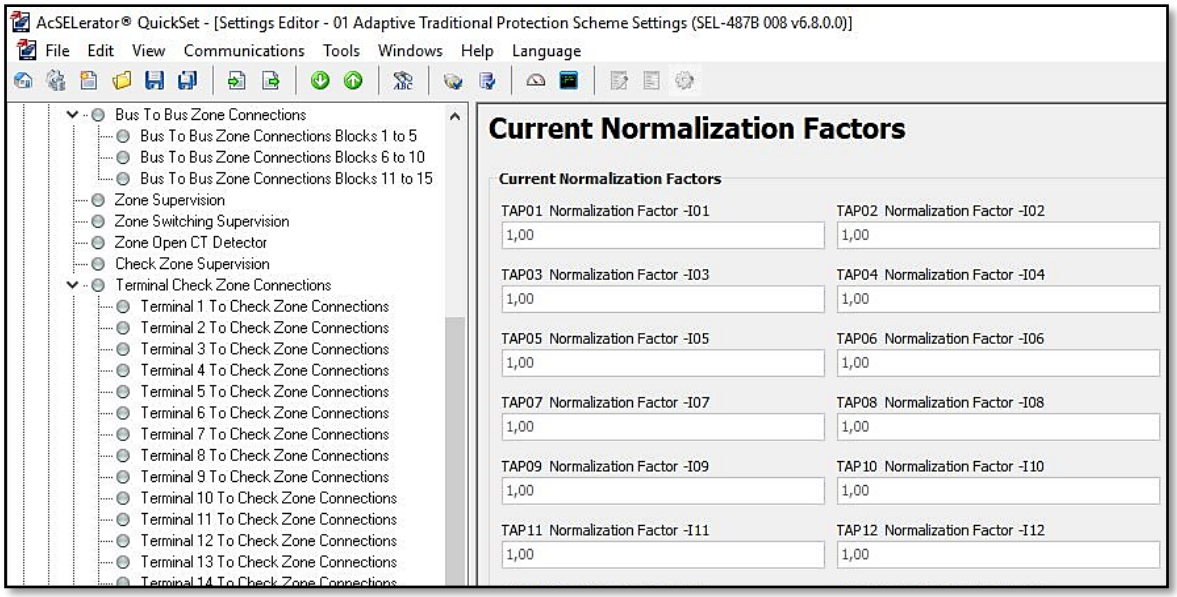

Figure 6.32: SEL-487B relay Group 1 TAPs calculated by the AcSELerator Quickset software

6.5.4 Differential, directional and definite overcurrent elements configuration

The complete differential protection requires the setting of filtered differential and directional element settings. The filtered differential element settings involve the setting of the restrained differential element pickup (O87P) and the restrained slope (SLP1 and SLP2) percentage settings.

The operation of the directional element depends on the directional overcurrent element pickup (50DSP). The value of this setting is obtained by making one of the branches a reference terminal. The per-unit value of the current flowing in this branch is used as a directional element pickup setting. Before the decision was made for 50DSP setting, the load flow was simulated and the differential and restraining currents were calculated based on the primary values of the actual currents viewed from the relay's HMI under normal loading conditions. The AcSELerator Quickset HMI display was used for monitoring these currents in real-time and the results are shown in figures, 6.33 and 6.34 below and on the next page.

Because the current transformers are the same for all the groups, monitoring of currents is done using Group 1 settings for both the minimum and the maximum load of 315 MW and the 420 MW respectively.

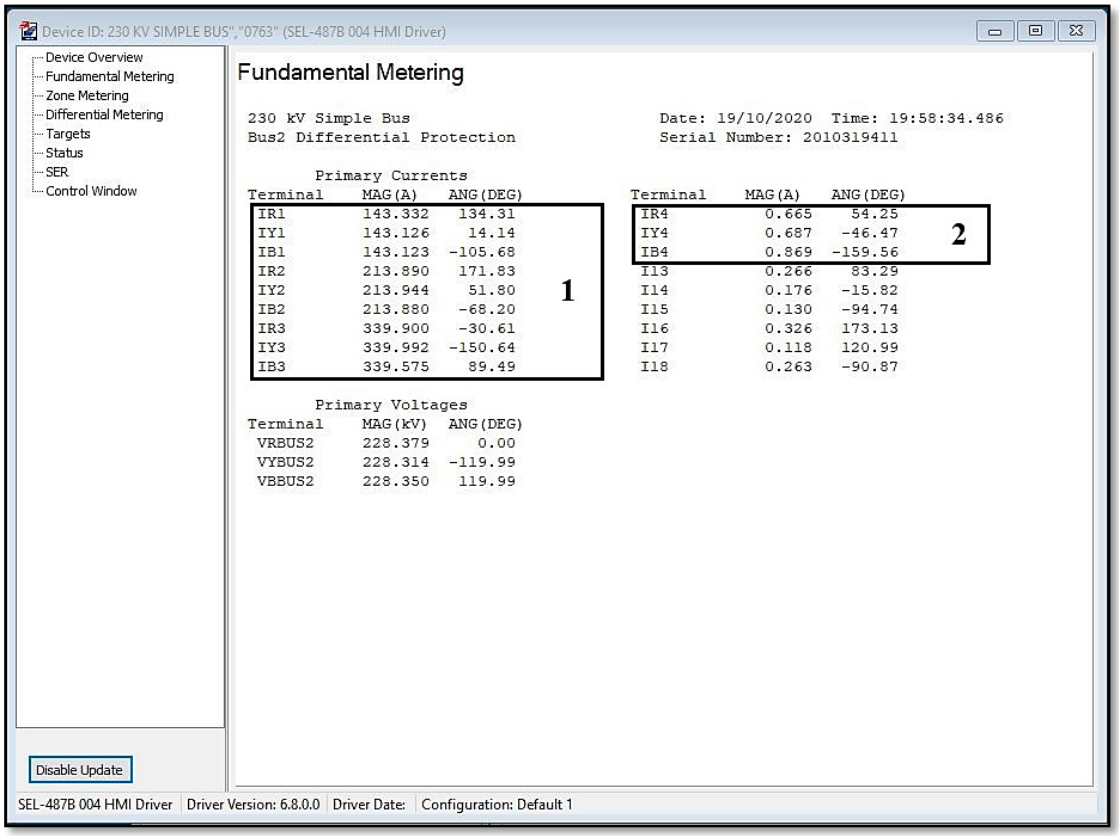

Figure 6.33: HMI fundamental metering using Group 1 settings under 315 MW load demand

Zone 1 and 2 of the above figure show the metering values of the primary currents seen by the relay. The currents in Zone 2 are too small and this is because of the little or no contribution of the wind power plant to the grid system, as the load can still be supplied by the existing system generators.

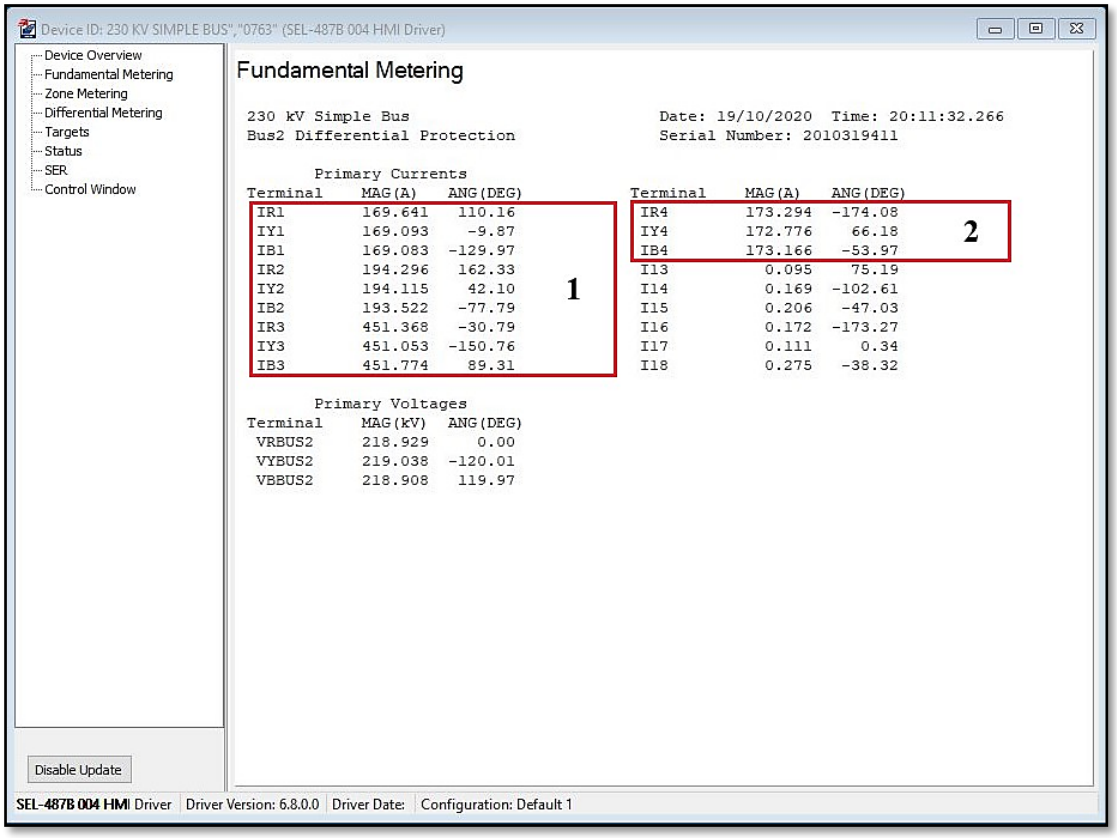

Figure 6.34: **HMI fundamental metering using Group 1 settings under 420 MW load demand**

In addition, in the figure above, Zone 1 and 2 show the metering values of the primary currents seen by the relay. Zone 2 values show larger values of currents. In this case, the wind power plant is contributing to the system because the load demand has increased up to a point where the existing generators can no longer maintain the load requirements.

6.5.4.1 Group 1 and Group 2 differential and direction element settings

The operating principle of the phase differential element is that the trip command is issued when the operating current is greater than the restrained differential element pickup (O87P) and greater than the product of the slope and the restraining current ($I_{Op} > I_{PU} > SLP(I_{Res})$). To decide on the differential pickup current settings for initial and maximum load conditions, the differential and the restraining currents are monitored for both conditions and the results are recorded as shown in Figure 6.35 and Figure 6.36 below on the next page.

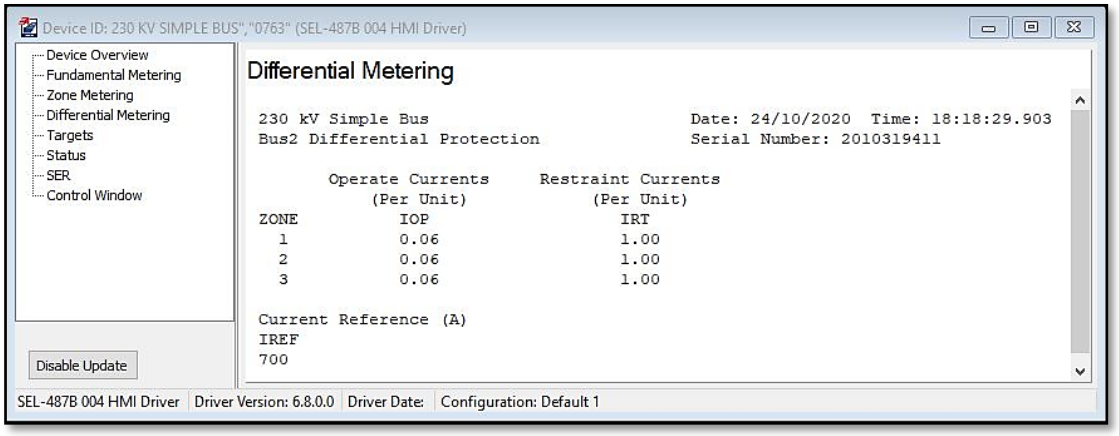

Figure 6.35: **HMI differential and restraint currents monitoring at 315 MW load demand**

In the above figure, the operating current as monitored using Group 1 settings is far less than the restraining current. When the initial load conditions of the system are simulated, the Group 1 settings of the relay are initially active and the results are recorded. When the load increase is implemented from 315 MW to 420 MW, the Group 2 settings take over and the results are as shown below, monitored under the operation of the group.

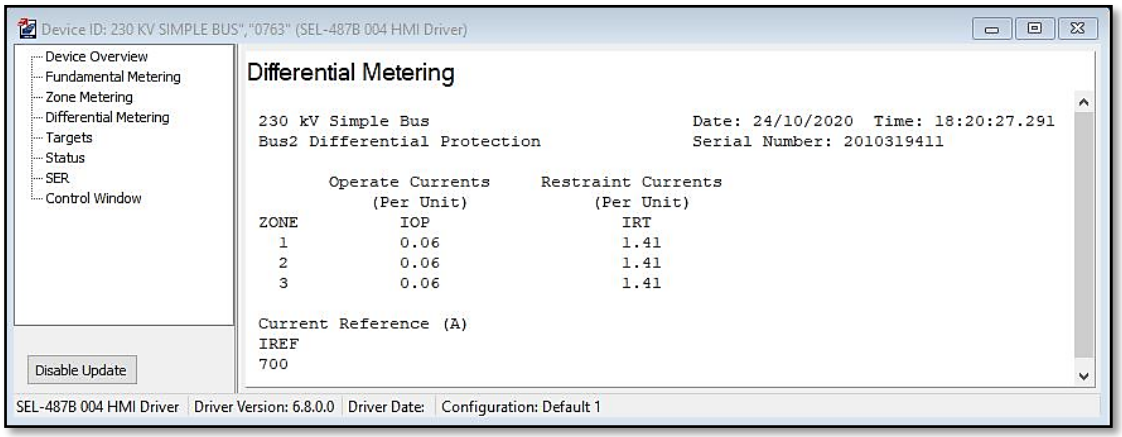

Figure 6.36: **HMI differential and restraint currents monitoring at 420 MW load demand**

Under normal load condition of the initial and the maximum load demand in the system, the differential current must always be greater than the restraining current.

The differential relay element should be set to operate when the operating current (IOP) is greater than the restrained differential element pickup (O87P) setting and the product of the percentage slopes (Slope 1 and Slope 2) and the restraining current (IRT). When the fault occurs, the differential currents usually increases due to the imbalance of the current flow of all the currents to the faulty busbar.

The pickup point or a restrained pickup threshold current setting for most differential relays has no fixed value but is planned from a starting point with a different characteristic curve that increases as the current increases. This characteristic allows for errors in the relaying system that is proportional to the current level. For this reason, the O87P, Slope 1 and Slope 2 values are set to 2 per-unit, 30% and 50% respectively for the first condition. In addition for the second condition, O87P, Slope 1 and Slope 2 values are set to 2.8 per-unit, 42% and 71% respectively.

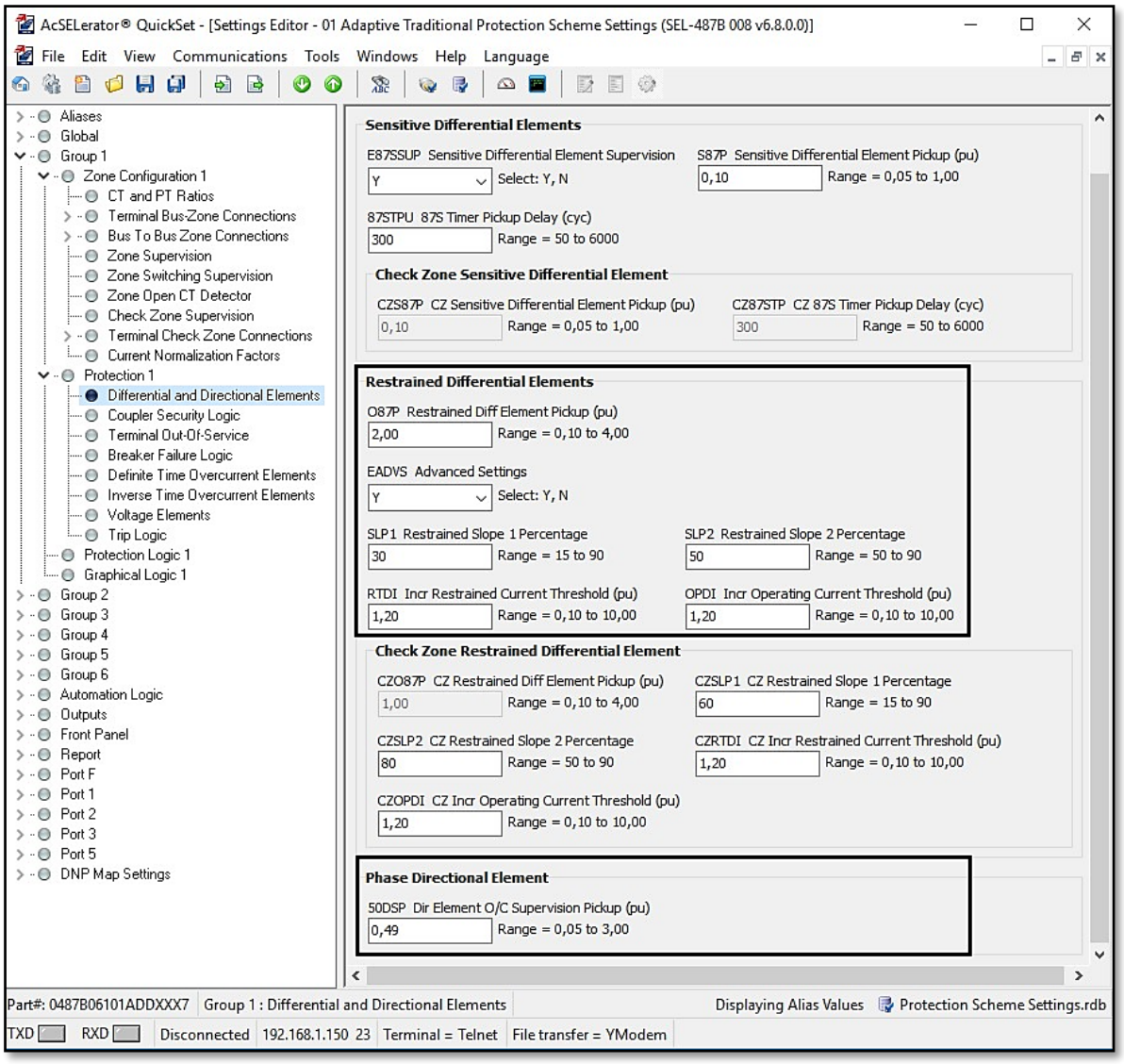

Figure 6.37: **Group 1 filtered differential and phase direction overcurrent element settings**

The directional element threshold setting requires one of the branches to be made a reference branch. In this case, the DLoad1Feeder is made the reference branch because its current is equal to the sum of all currents from other branches. The directional element overcurrent pickup supervision (50DSP) threshold settings for Group 1 and Group 2 are simply set to 0.485 per-unit and 0.645 per-unit respectively.

These values are obtained by calculating the secondary per-unit current for any phase of the dynamic load branch connected to Bus 2 of the system.

Group 1 and Group 2 restrained differential element pickup (O87P), slopes and the directional element overcurrent pickup supervision (50DSP) are shown in Figure 6.37 above on the previous page and in Figure 6.38 below.

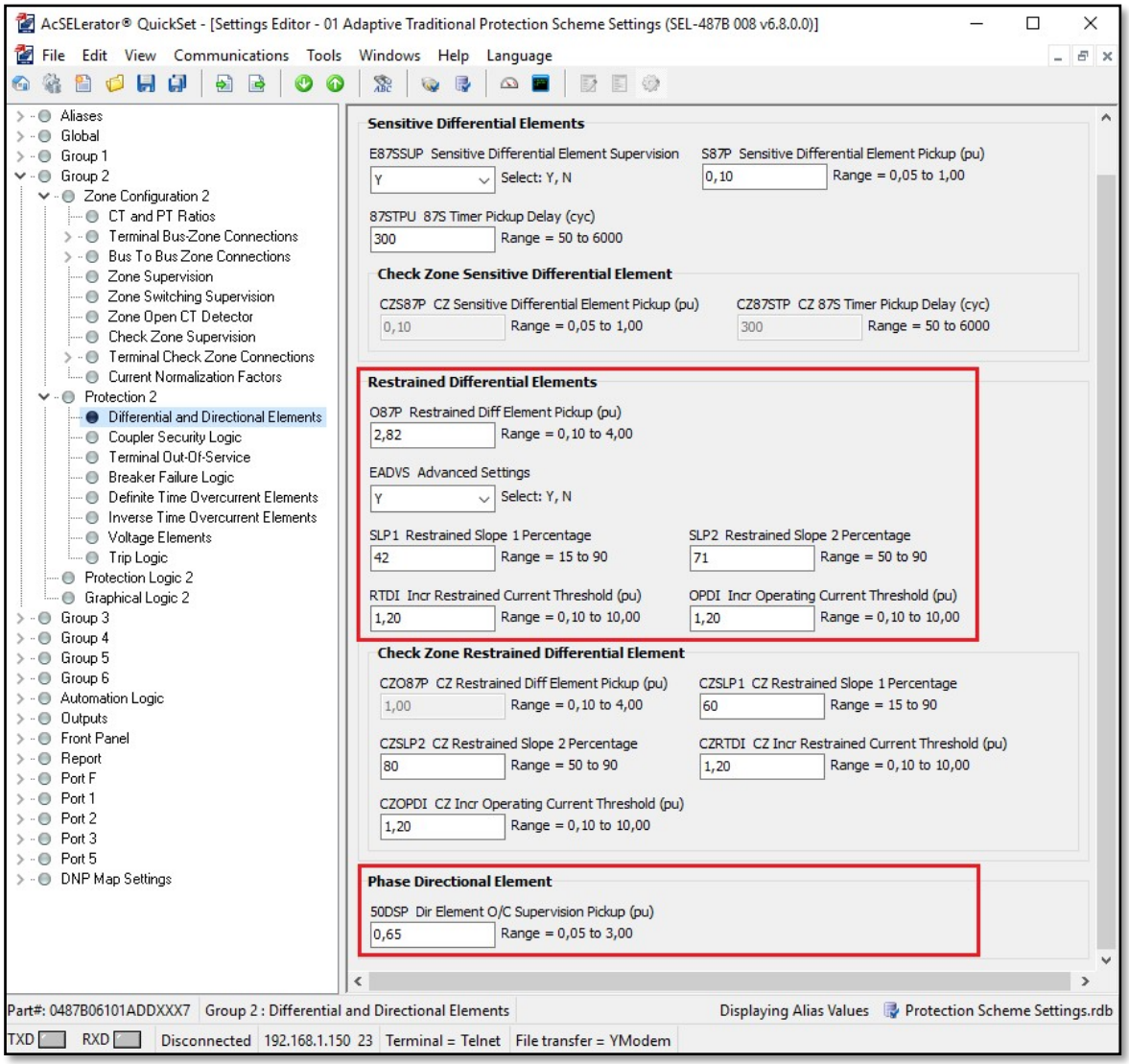

Figure 6.38: Group 2 filtered differential and phase direction overcurrent element settings

6.5.4.2 Group 1 and Group 2 configuration switchover settings

The aim was to have a protection scheme that will automatically change to another group of settings to suit the system requirements. To have such a scheme, the logic was developed within both setting groups of the SEL-487B as shown in Figure 6.39 below. The logic shown in the figure uses the operation of the definite overcurrent pickup word bits (*50RT*, *50YT* and *50BT*) for phases, IR4, IY4 and IB4 of the relay connected to the wind power plant terminal. PB6 and PB5 are pushbuttons found on

the front panel of the SEL-487B relay. To switch to Group 2 settings, any definite time overcurrent elements must be active, or pushbutton 6 (PB6) can be manually pressed. PB5 is for switching back to Group 1 settings and will never work if the current is more than the threshold pickup setting are to follow.

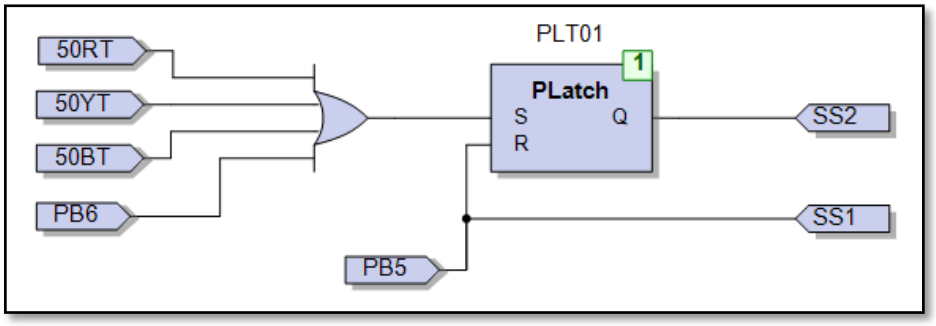

Figure 6.39: SEL-487B relay Group 1 and Group 2 selection logic

When the above logic is designed, it is compiled and mapped to the settings group selection as shown in Figure 6.40 below.

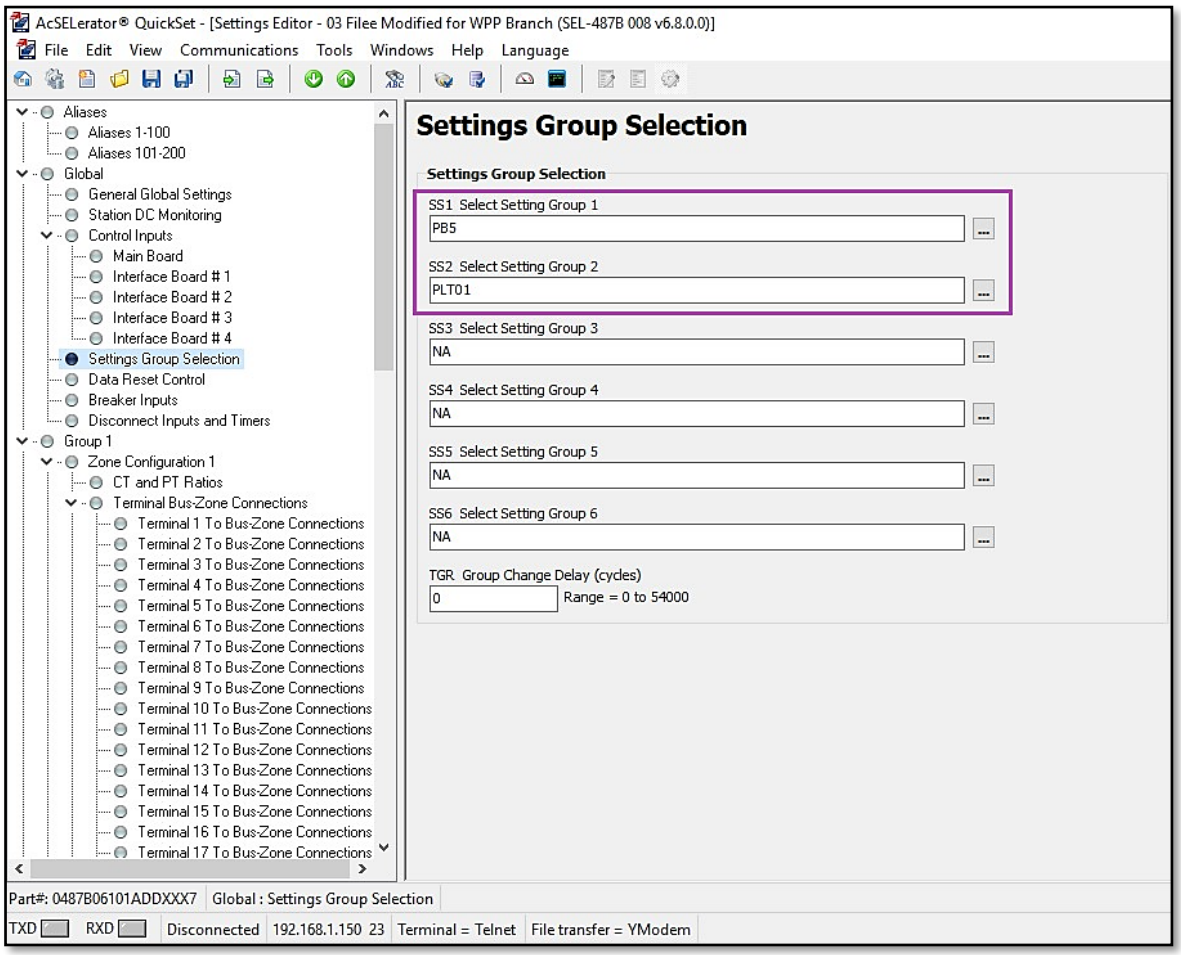

Figure 6.40: Settings group control word bits

The relay word bit *PLT01* in the figure represents the output status of the protection latch which only becomes binary “1” when the pushbutton 6 (PB6) is pressed or any of the definite time overcurrent trip becomes active for 2 seconds.

Because the wind power plant current increases when the load demand increases from 315 MW to 420 MW, the settings are done such that at 50% percent of this transition from the minimum to maximum loading, the relay settings change from Group 1 settings to Group 2 settings. Line currents were monitored on the HMI as recorded in Table 6.4 below.

Table 6.4: Determination of the value of the phase definite time overcurrent pickup for the condition of the load demand transition from 315 MW to 420 MW

WPP branch	315 MW loading	Median		420 MW loading
Line currents	Primary (A)	Primary (A)	Secondary (A)	Primary (A)
IR4	0.6650	86.9795	0.1243	173.2940
IY4	0.6870	86.7315	0.1239	172.7760
IB4	0.8690	87.0175	0.1234	173.1660

The threshold settings for phase definite time overcurrent elements, 50PR4T, 50PY4T and 50PB4T are set accordingly as shown in Figure 6.41 below on the next page for Group 1. The time delay is set to 100 cycles to avoid the definite overcurrent operation due to the overcurrents during the start-up of the system. The same settings are entered for Group 2 settings.

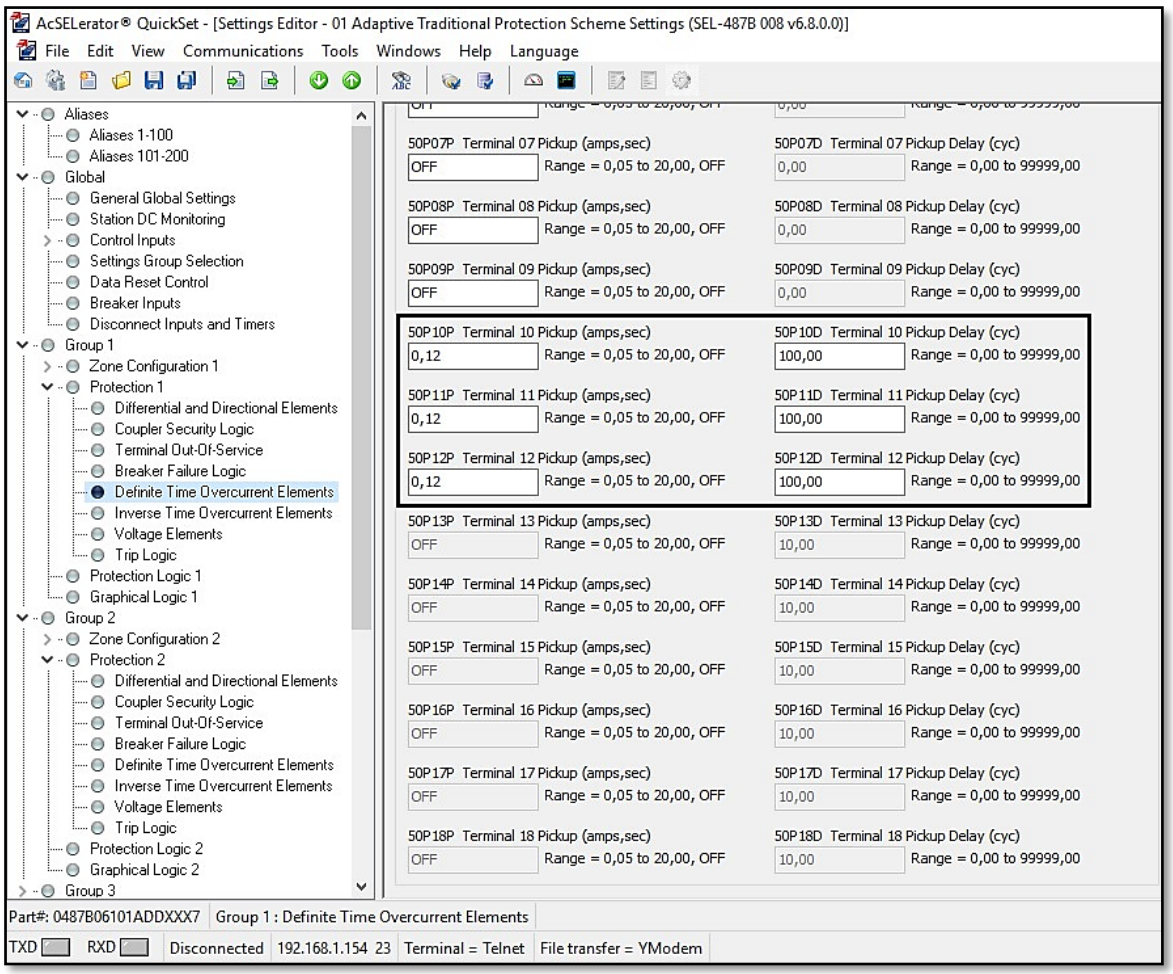

Figure 6.41: **Phase definite time overcurrent pickup settings entered under Group 1 Settings**

The protection scheme's trip logic is defined for elements, 87R1 (87RT), 87R2 (87YT) and 87R3 (87BT) for Zone 1 to Zone 3 differential elements as shown in Figure 6.42 below. The same relay word bits are defined for Group 2 settings.

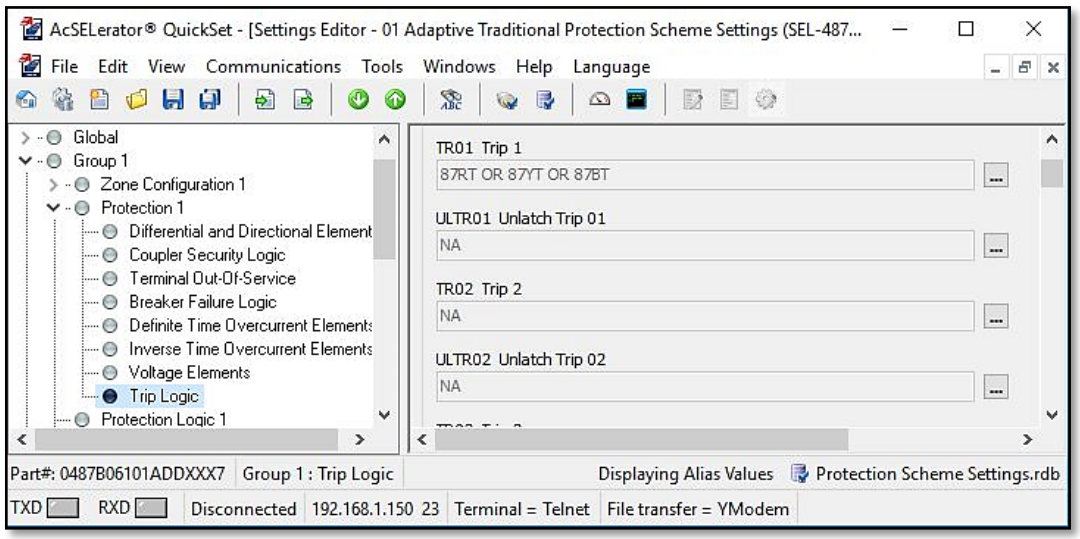

Figure 6.42: **Filtered differential element trip condition for Group 1 settings**

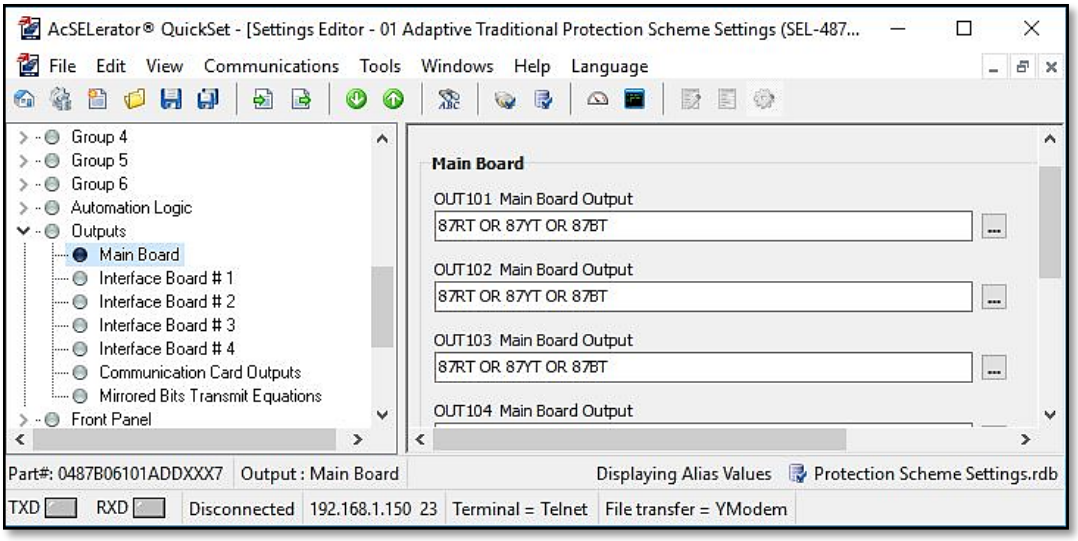

Figure 6.43: **Filtered differential element trip bits for all group settings**

The trip (TR01 Trip 1) logic relay word bits are used for tripping the circuit breaker, they are assigned to the Main Board outputs, OUT101, OUT102 and OUT103 for circuit breakers and are set as shown in Figure 6.43 above. Because there are no specific Group settings for output binary signals, therefore this setting is done once for all group settings.

When the protection scheme is fully configured for the interconnected system, it is then tested. The section below presents the testing and its results for protection scheme based on the two conditions, 315 MW and 420 MW loading.

6.6 Hard-wired protection scheme test

The testing of the developed protection scheme is done using only the Red-phase-to-ground and three-phase faults. This test aims to prove the adaptiveness of the scheme based on the system loading conditions when the current supplied by the wind power plant is very small (approximately equal to zero), and when it supplies larger currents due to its contribution to the system when the load demand has increased. The adaptiveness of the scheme is monitored by looking at the switching of the group settings from Group 1 to Group 2. Group 1 is for faults that occur while the system is operating at the initial load demand of 315 MW, and Group 2 for faults that occur at the increased load demand of 420 MW.

For this test, *Line12RE*, *Line24SE*, *BRK3* currents are monitored because they are the branches that feed the protected busbar. For the results of the waveforms of the currents monitored from these branches, the time when the fault has started and when

it is cleared from the system is analyzed. The time when the trip command arrives at the RTDS simulated system and the time when the virtual circuit breakers operate is looked at. The per-unit voltage at the protected busbar is monitored, as well as the wind power plant receiving-end terminal voltage.

6.6.1 315 MW loading

The simulation cases for this test are run based on the procedure presented in Table 6.5 below. There are two main columns in the table. The first column presents the sequence for system loading, and the second column is for fault simulation.

Table 6.5: Protection scheme test procedure under 315 MW loading

System loading	Fault simulation	
Initial loading (315 MW)	RPh-to-Gnd Fault	3Ph Fault
BRKOneSW, BRKTwoSW, and BRKThreeSW ON, Inputer1SW, Inputer2SW, and Inputer3SW ON DLoadSchedSW OFF, Set simulation case 0.1 secs, Run case and wait until they are up to date, BRKOneSW, BRKTwoSW, and BRKThreeSW OFF.	Select or dial RPh-Gnd position, Set simulation case 100 secs, Inject RPh-Gnd fault and Wait until the plots are up to date, Case 0.1 secs, BRKOnePB, BRKTwoPB and BRKThreePB press, **Target Reset Relay**,	BRKOneSW, BRKTwoSW and BRKThreeSW OFF. Select or dial 3Ph position, Set simulation case 100 secs, Inject 3Ph fault and Wait until the plots are up to date, Case 0.1 secs, BRKOnePB, BRKTwoPB and BRKThreePB press, **Target Reset Relay**,

6.6.1.1 Red-phase-to-ground (RPh-Gnd) fault at Bus 2

The Red-phase-to-ground fault was simulated at Bus 2 while the system was experiencing a load demand of 315 MW. The fault was initiated at 20.012 seconds and got cleared at 20.549 seconds as shown in Figure 6.44 below.

The total duration of the fault is 0.537 seconds, after this time, it was cleared and the busbar was left isolated from the system.

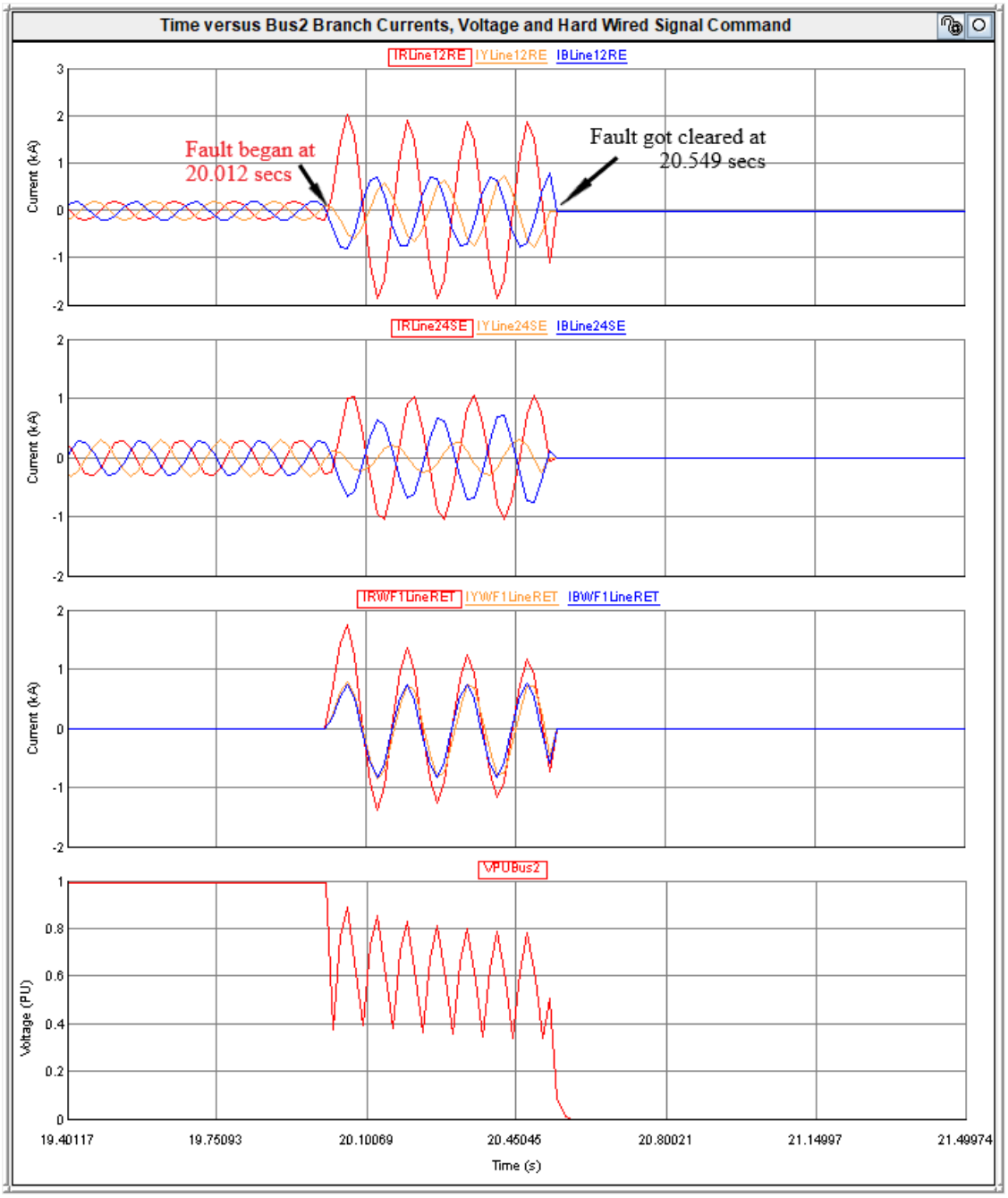

Figure 6.44: **Branch currents and Bus 2 voltage for R-G fault at Bus 2 under 315 MW**

Another waveform is provided in Figure 6.45 below on the next page. In the figure, the upper plot shows the per-unit voltage, and the bottom plot is RMS voltage. Using these plots, the recovery time of the wind power plant receiving-end terminal voltage is analyzed. The disturbance experienced by the wind power plant began at 20.012 seconds and ended at 32.01979 seconds as shown in the plots.

When the faulty busbar was isolated from the system, the wind power plant became free from the fault and remained islanded.

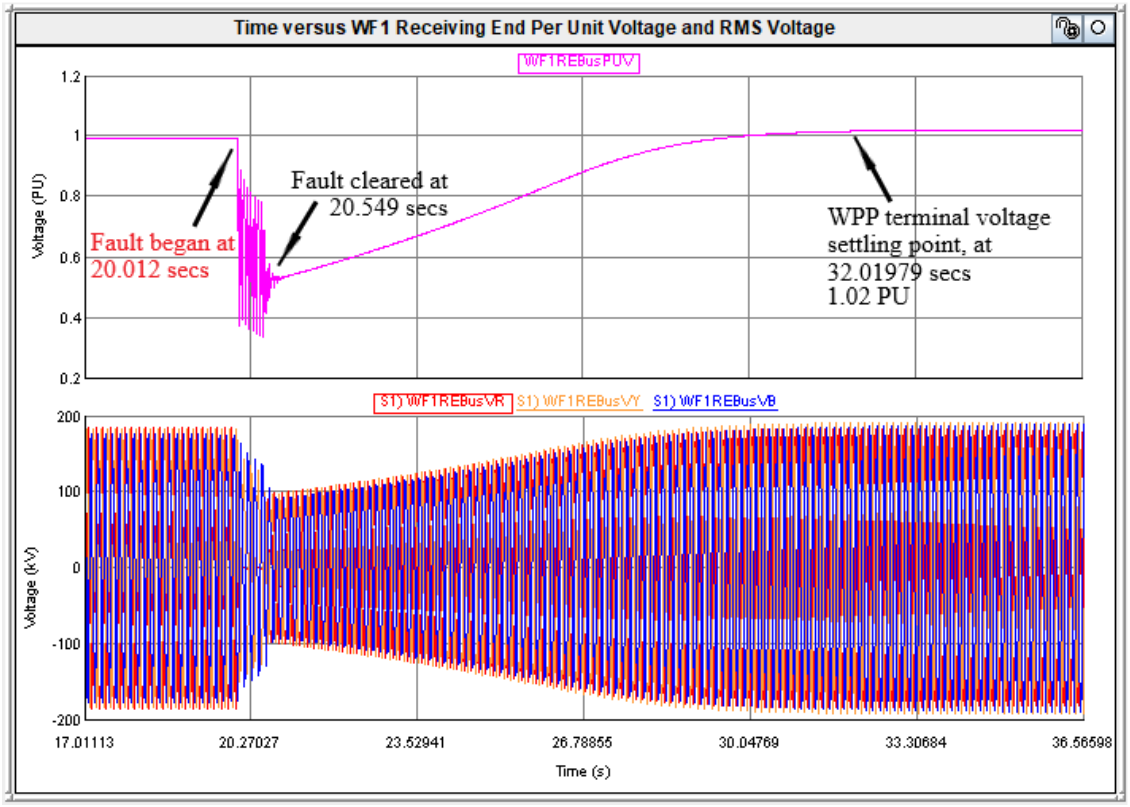

Figure 6.45: **WPP receiving-end voltage for R-G fault at Bus 2 under 315 MW**

After all these events, it took 11.47079 seconds for wind power plant terminal voltage to stabilize. The value at which it is stabilized is 1.02 per unit and is safe for continuous operation of the wind power plant.

The circuit breaker control actions were monitored during the test and the results are shown in Figure 6.46 below on the next page. The trip command was received by the circuit breaker logic at 20.03353 seconds after the fault was detected by the relay, and the circuit breakers operated later at 20.5304 seconds.

The time it took for circuit breakers to open after the trip command was received is approximately 0.4969 seconds.

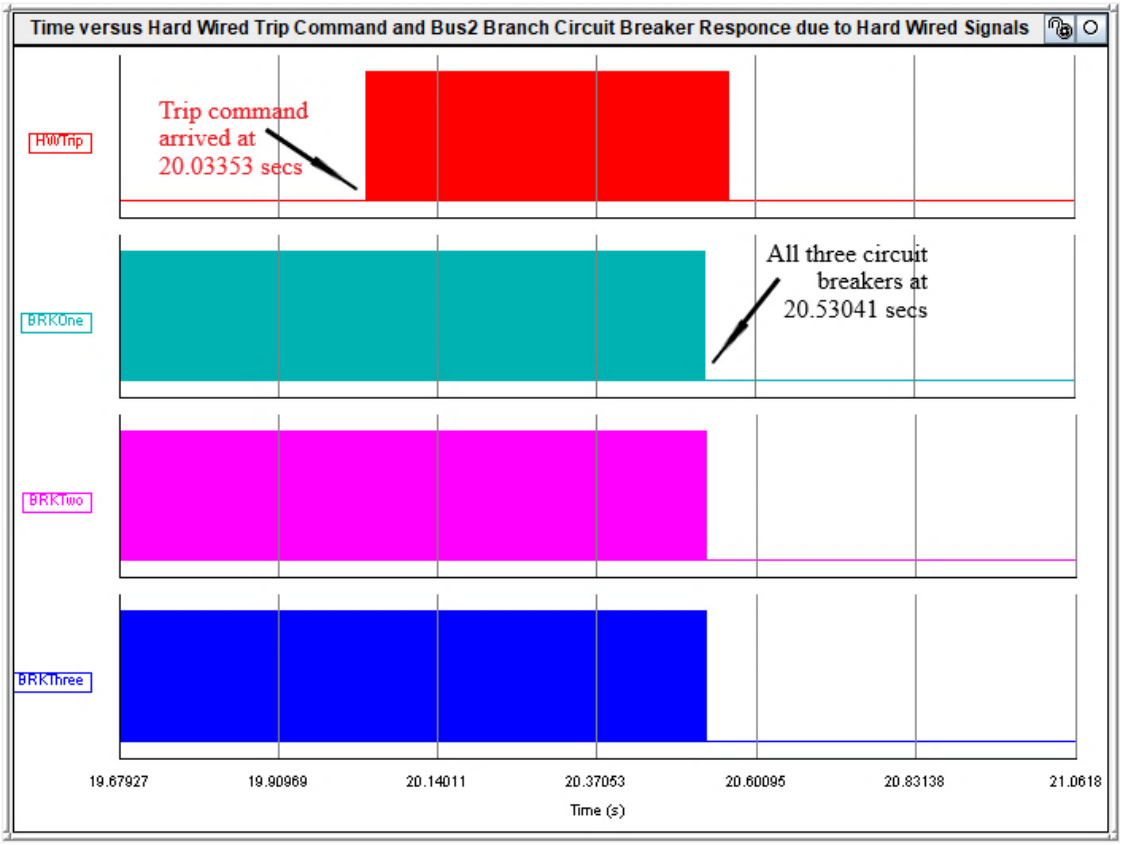

Figure 6.46: CB-received hard-wired trip command for R-G fault at Bus 2 under 315 MW

6.6.1.2 Three-phase (3Ph) fault at Bus 2

The Three-phase fault was simulated at Bus 2 while the system was experiencing a load demand of 315 MW. The fault was initiated at 20.0035 seconds and got cleared at 20.5505 seconds as shown in Figure 6.47 below on the next page.

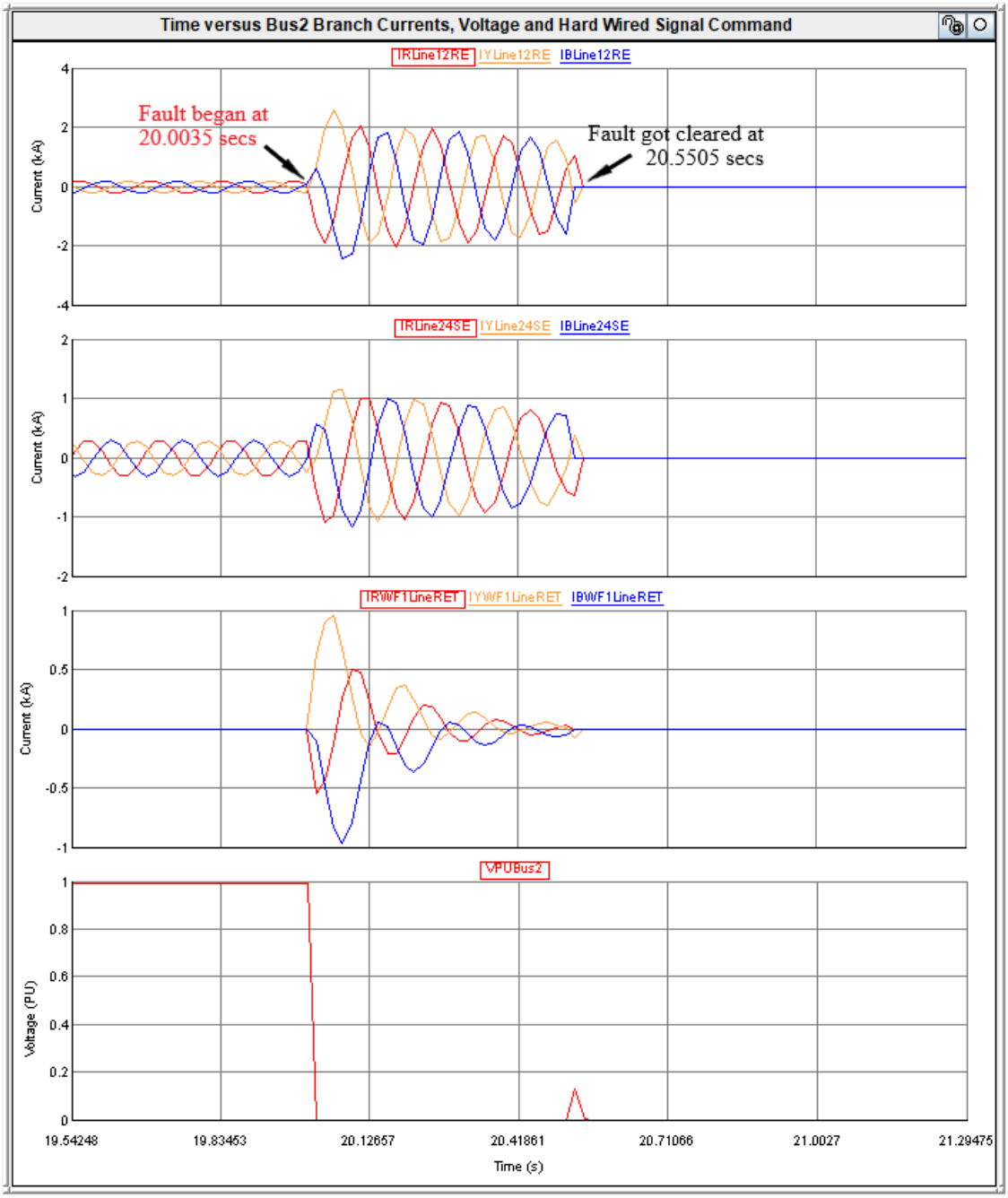

Figure 6.47: **Branch currents and Bus 2 voltage for 3Ph fault at Bus 2 under 315 MW**

The total duration of the fault is 0.547 seconds, after this time, it was cleared and the busbar was left isolated from the system.

Another waveform is provided in Figure 6.48 below on the next page. Using these plots, the recovery time of the wind power plant receiving-end terminal voltage is analyzed. The disturbance experienced by the wind power plant began at 20.0035 seconds and ended at 64.0228 seconds as shown in the plots. When the faulty busbar was isolated from the system, the wind power plant became free from the fault and remained islanded.

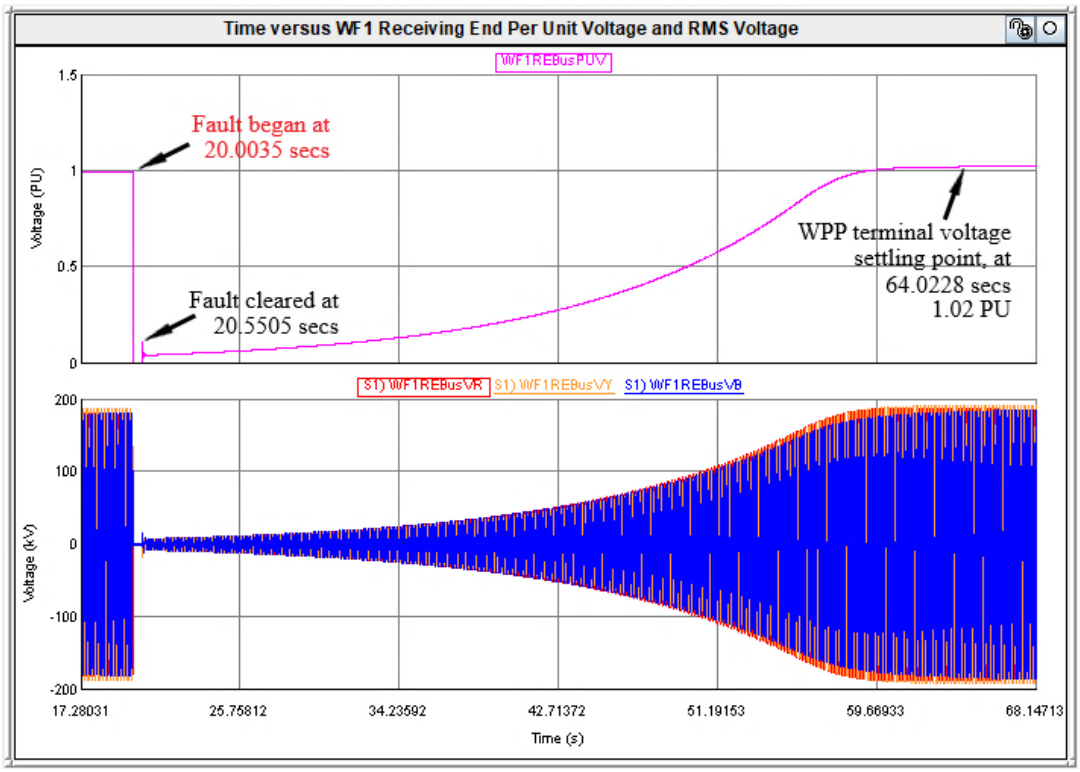

Figure 6.48: **WPP receiving-end voltage for 3Ph fault at Bus 2 under 315 MW**

After all these events, it took 43.4723 seconds for wind power plant terminal voltage to stabilize. The value at which it is stabilized is 1.02 per unit and is safe for continuous operation of the wind power plant.

The circuit breaker control actions were monitored during the test and the results are shown in Figure 6.49 below on the next page. The trip command was received by the circuit breaker logic at 20.0353 seconds after the fault was detected by the relay, and the circuit breakers operated later at 20.5278 seconds.

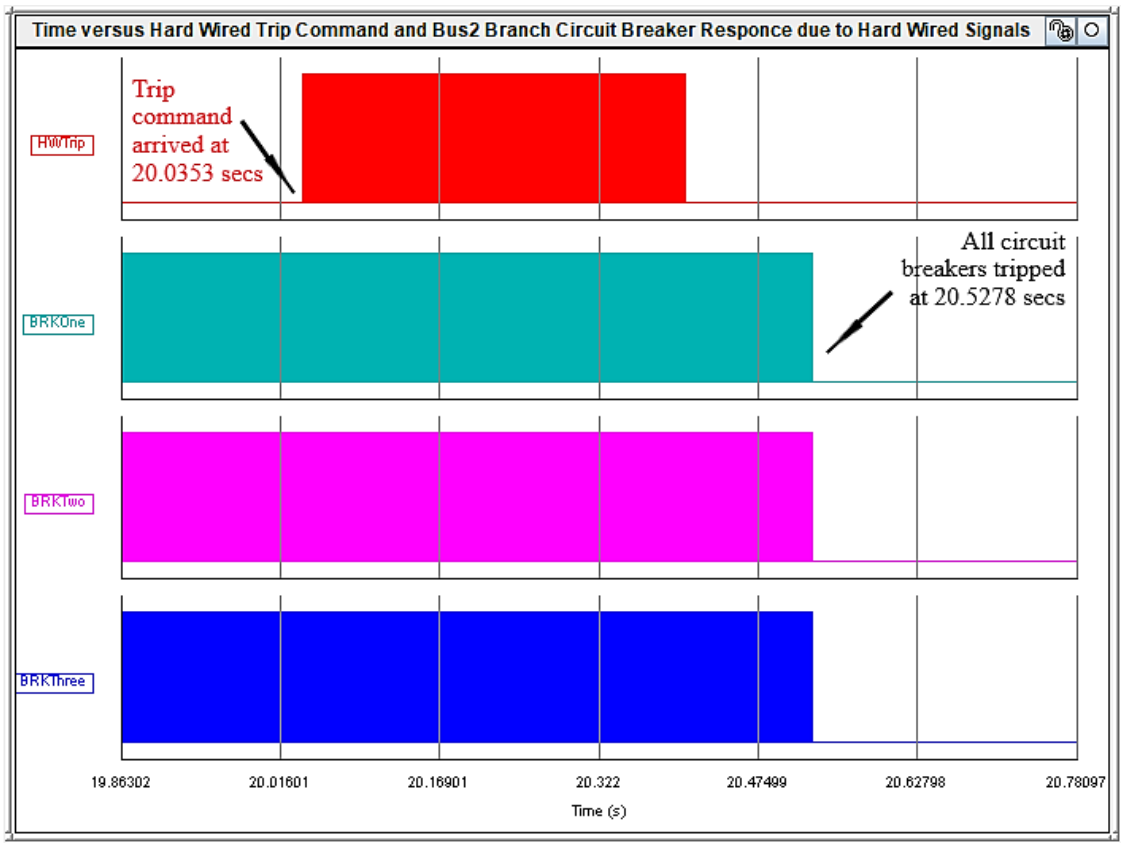

Figure 6.49: CB-received hard-wired trip command for 3Ph fault at Bus 2 under 315 MW

The time it took for circuit breakers to open after the trip command was received is approximately 0.4925 seconds.

6.6.2 420 MW loading

The simulation cases for this test are run based on the procedure presented in Table 6.6 below on the next page. The first column presents the sequence for system loading, and the second column is for fault simulation.

Table 6.6: Protection scheme test procedure under 420 MW loading

System loading	Fault simulation	
Initial loading (420 MW)	RPh-to-Gnd Fault	3Ph Fault
BRKOneSW, BRKTwoSW, and BRKThreeSW ON, Inputer1SW, Inputer2SW, and Inputer3SW ON DLoadSchedSW OFF, Set simulation case 0.1 secs, Run case and wait until plots are up to date, BRKOneSW, BRKTwoSW, and BRKThreeSW OFF. Set simulation case 100 secs. DLoadSchedPB press and wait until plots are up to date.	Set simulation case 0.1 secs, Select or dial RPh-Gnd position, Set simulation case 100 secs, Inject RPh-Gnd fault and Wait until plots are up to date, Case 0.1 secs, BRKOnePB, BRKTwoPB and BRKThreePB press, **Target Reset Relay**,	Select or dial 3Ph position, Set simulation case 100 secs, Inject 3Ph fault and Wait until the plots are up to date, Case 0.1 secs, BRKOnePB, BRKTwoPB and BRKThreePB press, **Target Reset Relay**,

6.6.2.1 Red-phase-to-ground (RPh-Gnd) fault at Bus 2

The Red-phase-to-ground fault was simulated at Bus 2 while the system was experiencing an increased load demand from 315 MW to 420 MW. The fault was initiated at 20.011 seconds and got cleared at 20.549 seconds as shown in Figure 6.50 below on the next page.

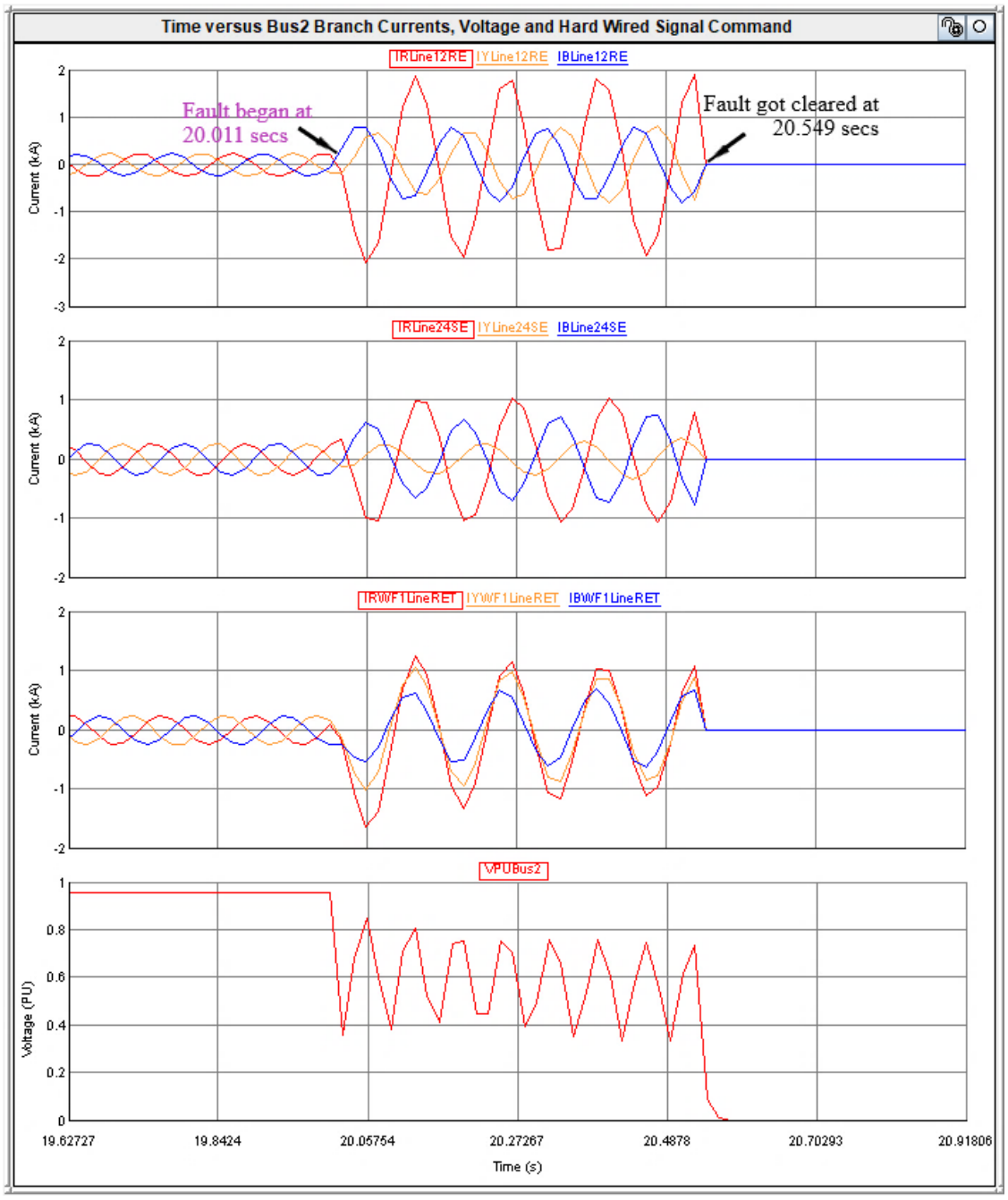

Figure 6.50: **Branch currents and Bus 2 voltage for R-G fault at Bus 2 under 420 MW**

The total duration of the fault is 0.538 seconds, after this time, it was cleared and the busbar was left isolated from the system.

Another waveform is provided in Figure 6.51 below on the next page. Using these plots, the recovery time of the wind power plant receiving-end terminal voltage is analyzed. The disturbance experienced by the wind power plant began at 20.011 seconds and ended at 33.0785 seconds as shown in the plots. When the faulty busbar was isolated from the system, the wind power plant became free from the fault and remained islanded.

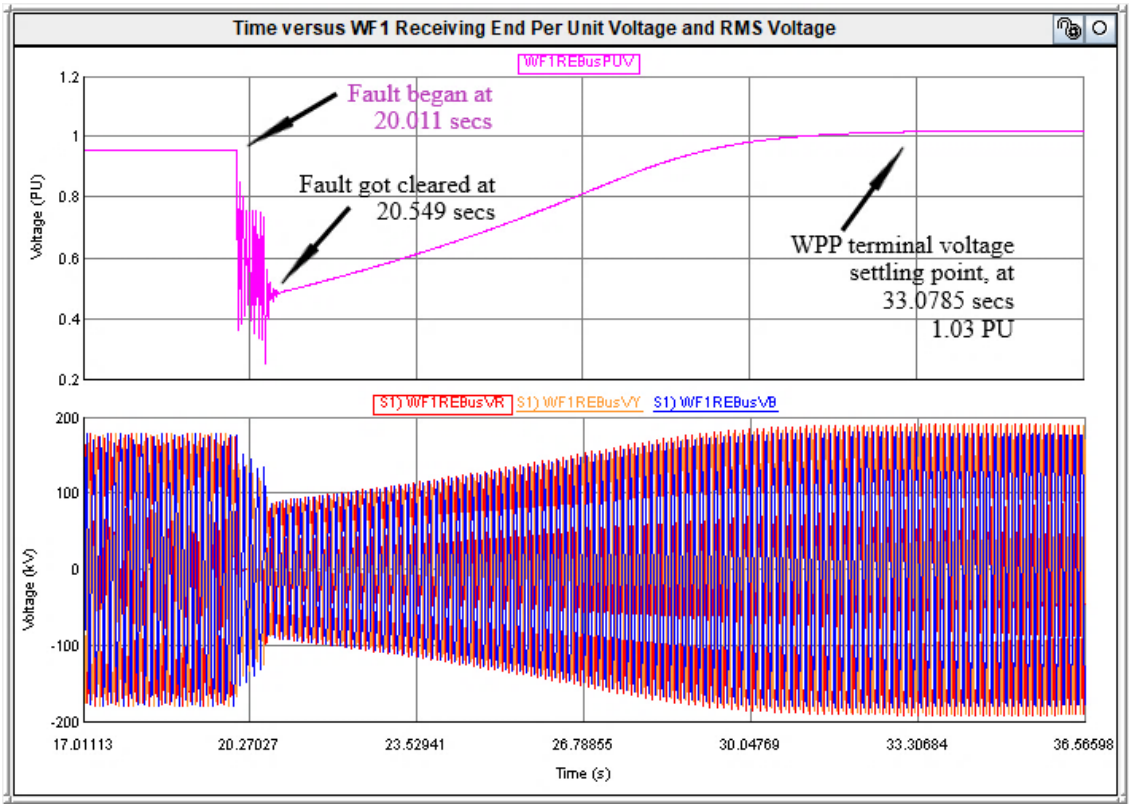

Figure 6.51: WPP receiving-end voltage for R-G fault at Bus 2 under 420 MW

After all these events, it took 12.5295 seconds for wind power plant terminal voltage to stabilize. The value at which it is stabilized is 1.03 per unit and is safe for continuous operation of the wind power plant.

The circuit breaker control actions were monitored during the test and the results are shown in Figure 6.52 on the next page. The trip command was received by the circuit breaker logic at 20.0354 seconds after the fault was detected by the relay, and the circuit breakers operated later at 20.545 seconds.

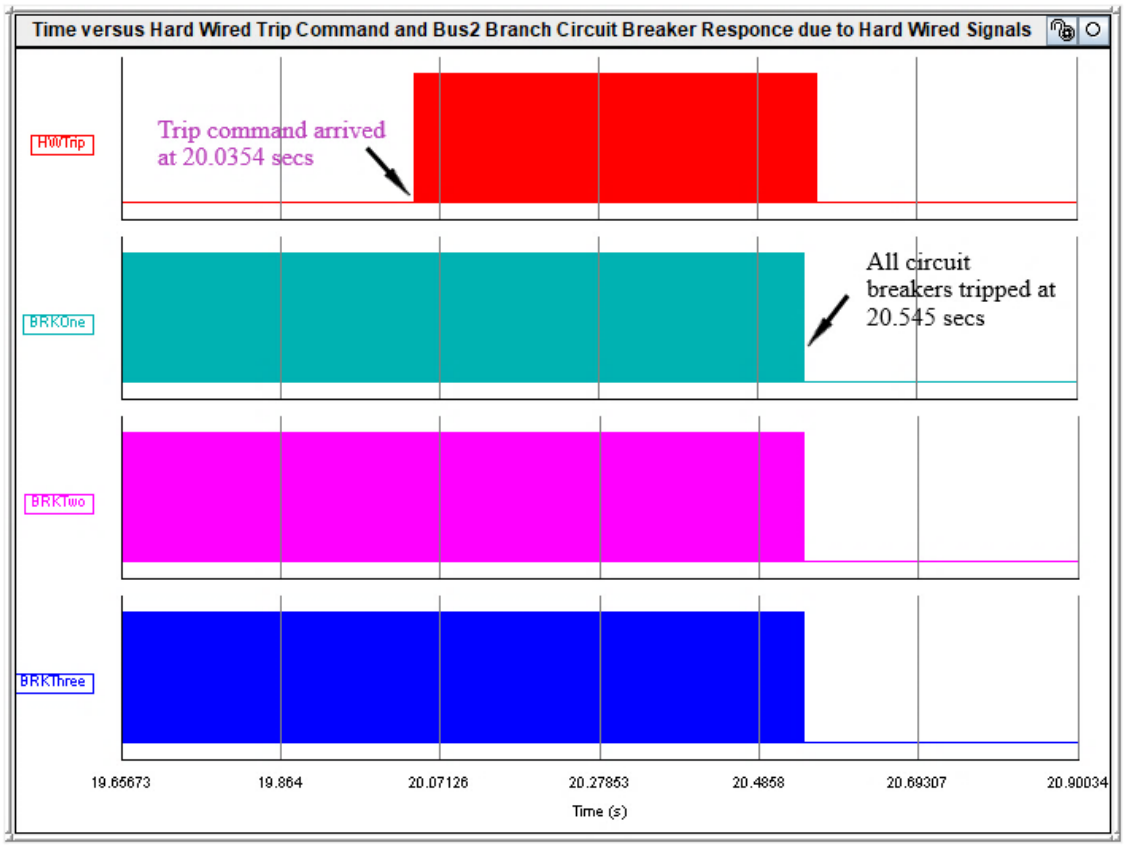

Figure 6.52: CB-received hard-wired trip command for R-G fault at Bus 2 under 420 MW

The time it took for circuit breakers to open after the trip command was received is approximately 0.5096 seconds.

6.6.2.2 Three-phase (3Ph) fault at Bus 2

The Three-phase fault was simulated at Bus 2 while the system was experiencing an increased load demand from 315 MW to 420 MW. The fault was initiated at 20.0051 seconds and got cleared at 20.5475 seconds as shown in Figure 6.53 below on the next page.

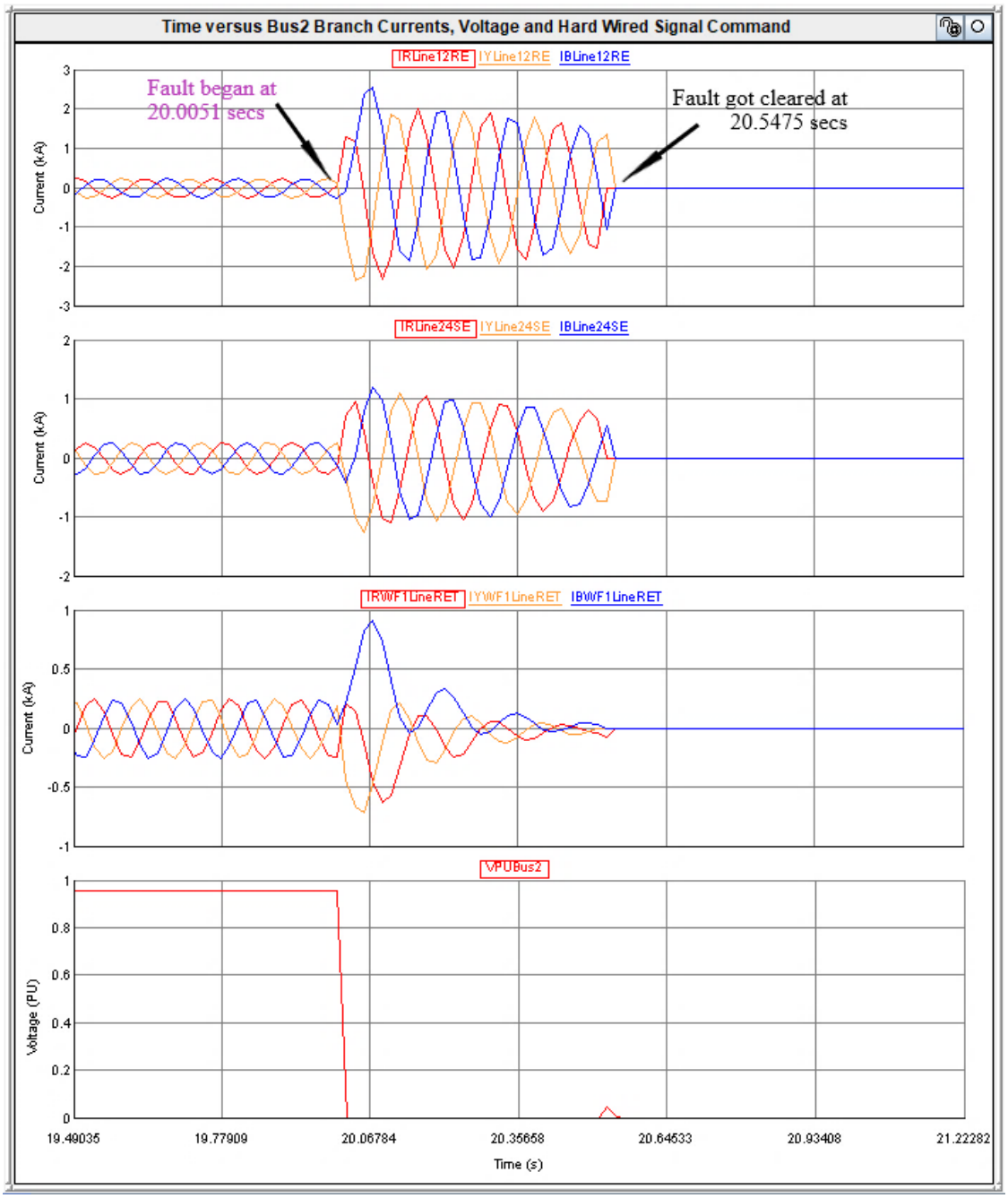

Figure 6.53: **Branch currents and Bus 2 voltage for 3Ph fault at Bus 2 under 420 MW**

The total duration of the fault is 0.5424 seconds, after this time, it was cleared and the busbar was left isolated from the system.

Another waveform is provided in Figure 6.54 below on the next page. Using these plots, the recovery time of the wind power plant receiving-end terminal voltage is analyzed. The disturbance experienced by the wind power plant began at 20.0051 seconds and ended at 65.6402 seconds as shown in the plots. When the faulty busbar was isolated from the system, the wind power plant became free from the fault and remained islanded.

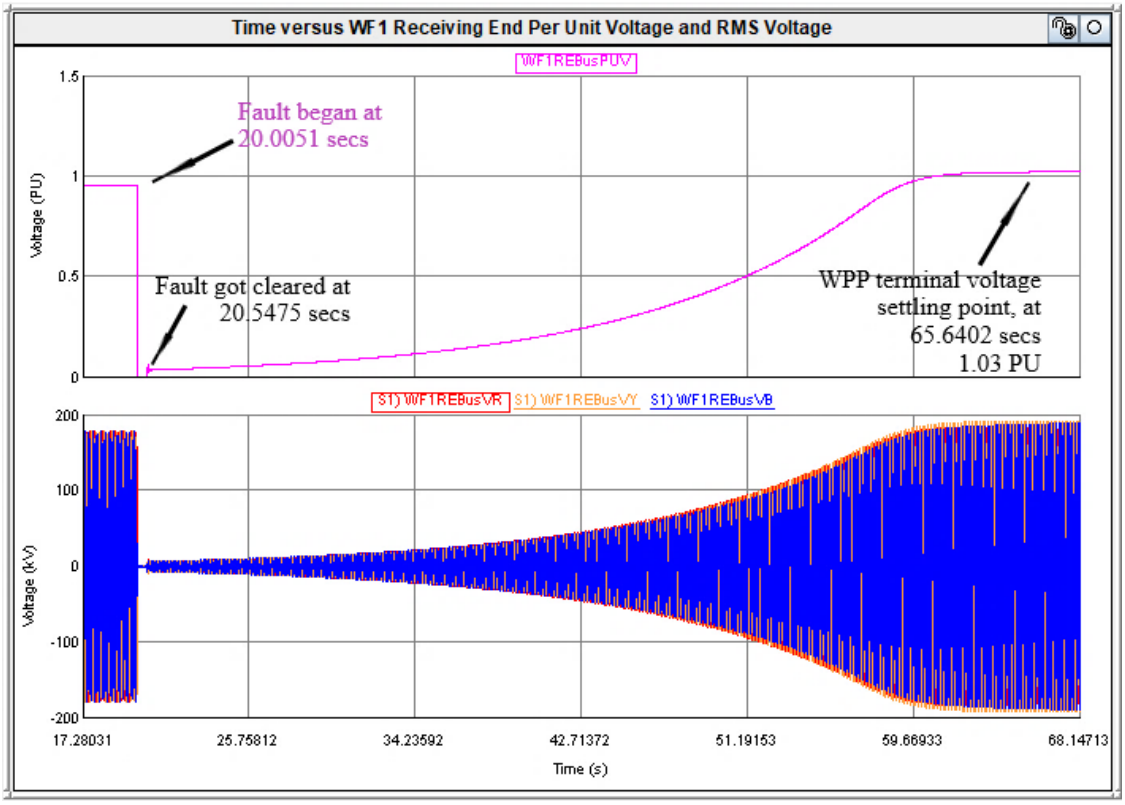

Figure 6.54: **WPP receiving-end voltage for 3Ph fault at Bus 2 under 420 MW**

After all these events, it took 45.0927 seconds for wind power plant terminal voltage to stabilize. The value at which it is stabilized is 1.03 per unit and is safe for continuous operation of the wind power plant.

The circuit breaker control actions were monitored during the test and the results are shown in Figure 6.55 below on the next page. The trip command was received by the circuit breaker logic at 20.035 seconds after the fault was detected by the relay, and the circuit breakers operated later at 20.5294 seconds.

The time it took for circuit breakers to open after the trip command was received is approximately 0.4944 seconds.

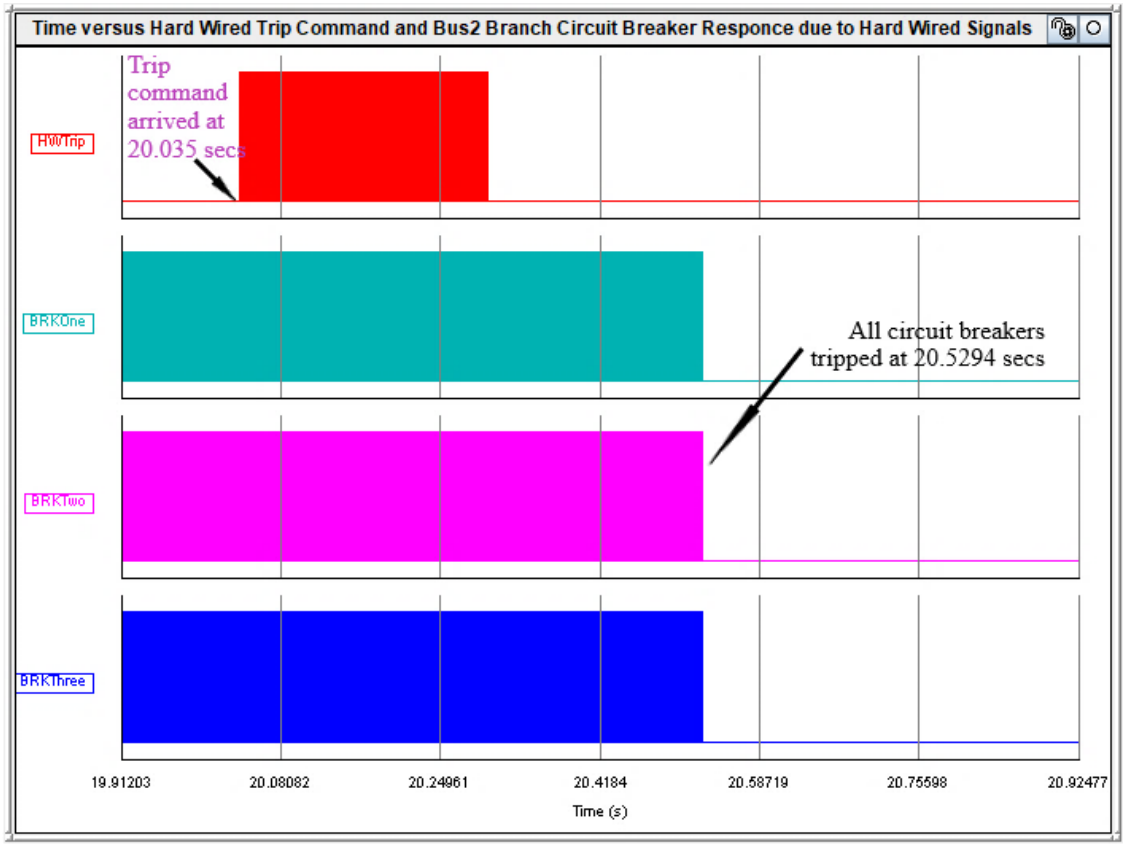

Figure 6.55: CB-received hard-wired trip command for 3Ph fault at Bus 2 under 420 MW

Apart from the protected busbar, the voltages from other busbars were monitored and recorded for statistical analysis and the behaviour of the system after the fault event. These results are shown in Appendix E.

6.7 Summary of results

This section presents in a form of a table (see Table 6.7 below) the summary of results obtained in the previous section.

Table 6.7: Fault event summary

Load condition (MW)	Settings group applied (G1 or G2)	Fault type	Circuit breaker operation in seconds (s)	Duration of fault clearance in seconds (s)
315	G1	R-G	0.4969	0.5370
		3 Ph	0.4925	0.5470
420	G2	R-G	0.5096	0.5380
		3 Ph	0.4944	0.5424

In the above table, the second column indicates the group settings that are applied to the tested types of faults. It is the change from one group to another during the event that proves the adaptability of the scheme. To see the settings group interchange, event reports with monitored currents, voltages and operated and non-operated binary

signals, were extracted from the physical device, The snapshots for these events are attached in Appendix E at the end of this document.

6.8 Conclusion

An adaptive protection scheme was developed, presented and tested in this chapter. It works for conditions of the internal faults at Bus 2. When an instant or sudden increase of the load demand from 315 MW, several times, by intervals of 5 MW per three load points, the protection scheme settings group automatically changes from Group 1 to Group 2 Settings. This is to accommodate the changing current that flows through the protected busbar unit so that the protection can work for both 315 MW and 420 MW load conditions. This is to say, the adaptability of the developed protection scheme has been achieved, though it uses the traditional means of protection, which consists of hard-wired binary outputs to the circuit breakers.

In the case of a real-world scenario, these cables would even be more and this would increase costs for labour and expensive copper. Besides, the commissioning of hard-wired binary outputs is time-consuming.

The IEC 61850 communication standard enables the sharing of status information over a single ethernet cable for subscription by other field devices like circuit breakers. In the perspective of reducing the hard-wired binary outputs from the relay, IEC 61850 standard generic substation event (GSE) control model generic object-oriented substation event (GOOSE), is implemented, configured and tested in the next chapter, to provide means of communication within the developed protection scheme.

CHAPTER SEVEN
THE IMPLEMENTATION OF THE IEC 61850 STANDARD-BASED COMMUNICATION

7.1 Introduction

In power systems, communication is used, whether for protection or to transfer information about the status of the power system network (Kauhaniemi et al., 2014). Protection, control, or monitoring devices consist of a feature known as adaptability. As much as the device's adaptability is based on the design of the device, some adaptive features depend on the type of communication applied. As technology improves, different devices are developed with different capabilities. For instance, the operating time of microprocessor-based protective relays is in real-time (Chandraratne et al., 2019).

The operation and capabilities of the microprocessor-based SEL-487B Protection Automation Control device were presented in Chapter 6, for development of an adaptive protection scheme using the hard-wired methods.

The IEC 61850 standard was mainly designed to provide interoperability between intelligent electronic devices (IEDs) from different vendors. Though it was designed for that, it plays a big role in the performance of functions in a substation but resides in the physical equipment from different vendors. In addition, IEC 61850 reduces hard-wiring from or to the process station to or from the bay substation through the application of a single piece of wire that allows the multicast of information from one device to another.

In this chapter, the advancement of the protection scheme developed in Chapter 6 is done through the application of the communication standard, IEC 61850, by using its generic substation event (GSE) control model generic object-oriented substation event (GOOSE).

The rest of the chapter is organized in sections as follows: Section 7.2 discusses the development of the hardware-in-loop test bench setup for IEC 61850 standard-based protection scheme. Section 7.3 is the testing of the IEC 61850 standard-based protection scheme. Section 7.4 is a summary of the results. Section 7.5 is the conclusion.

7.2 Hardware-in-loop test setup for an IEC 61850 standard-based protection scheme

The hardware-in-loop (HIL) test has already been developed in Chapter 6 and some of the hardware requirements have already been described. In addition, the configuration of the protection scheme settings was done in the chapter, with relay word bits defined in terms of the American National Standards Institute (ANSI). The relay word bits defined in the protection scheme presented in Chapter 6 were used for control of the system modelled on RTDS.

In this chapter, those relay word bits are replaced by the logical nodes (LNs), whose function is to transport data containing status events over Ethernet. To transport the status event messages from the physical device to the RTDS for protection and control, RTDS uses the GTnet cards for this application. The GTnet with GSE firmware in RTDS provides an IEC 61850 GOOSE interface to the simulator to allow a GOOSE-based IED to be simulated for closed-loop testing of the IEC 61850 standard compliant IEDs.

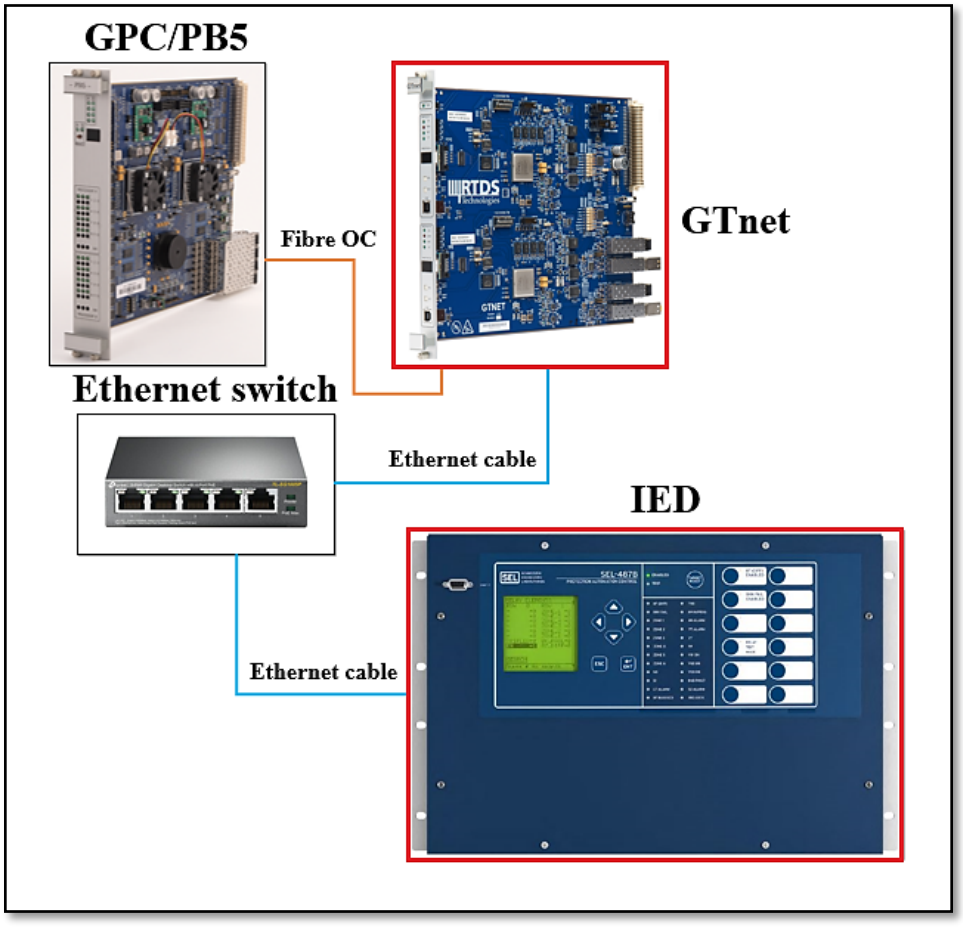

Figure 7.1: IEC 61850 standard-based HIL interface of the IED and RTDS

Figure 7.1 above shows the IEC 61850 standard-based interface of the physical device and the RTDS status information sharing for developed protection scheme.

To complete the IEC 61850 standard-based hardware-in-loop (HIL) test for the scheme, the configuration of the SEL-487B device, RTDS GTnet and some circuit breaker logic was done as presented in sections, 7.2.1 and 7.2.2.

7.2.1 Engineering configuration of GOOSE messages for SEL-487B device

Relay word bits were defined in Chapter 6 for hard-wired binary trip outputs from the relay to the RTDS for control and protection of the RTDS simulated network system. Publishing the status events via Ethernet requires the use of logical nodes (LNs) corresponding to the ANSI relay word bits. Table 7.1 below shows the list of corresponding LNs.

Table 7.1: List of relay word bits and protection logical nodes for SEL-487B device

Data source		Logical node	Attribute	Comment
Original name	Alias name			
P87R1	87RP	D87RPDIF1	Str.general Str.q Str.t	Zone 1 instantaneous differential element picked
P87R2	87YP	D87RPDIF2	Str.general Str.q Str.t	Zone 2 instantaneous differential element picked
P87R3	87BP	D87RPDIF3	Str.general Str.q Str.t	Zone 3 instantaneous differential element picked
87R1	87RT	D87RPDIF1	Op.general Op.q Op.t	Zone 1 restraint differential element picked
87R2	87YT	D87RPDIF2	Op.general Op.q Op.t	Zone 2 restraint differential element picked
87R3	87BT	D87RPDIF3	Op.general Op.q Op.t	Zone 3 restraint differential element picked

The logical nodes (LNs) presented in the above table are used for the configuration of the configured IED description (CID) file for the SEL-487B Protection Automation and Control device. This file is used for configuration of the datasets that are sent through the Ethernet whenever the relay publishes the message containing the status event of the trip to the circuit breakers in the Real-time digital simulators (RTDSs).

To configure the CID file for this relay, various steps were followed, and the snapshots are used to show how the configuration of this file was done. The software, AcSELerator Architect is used for configuration of the substation configuration language (SCL) file. This type of file, which contains all the information pertinent to the

substation, hosts the CID file within it. The CID files within the SCD file contains the information about the device (IED) modelled within the SCD file. Figure 7.2 below shows the main menu of the AcSELerator Architect software. In the figure, the “New Protect” is shown.

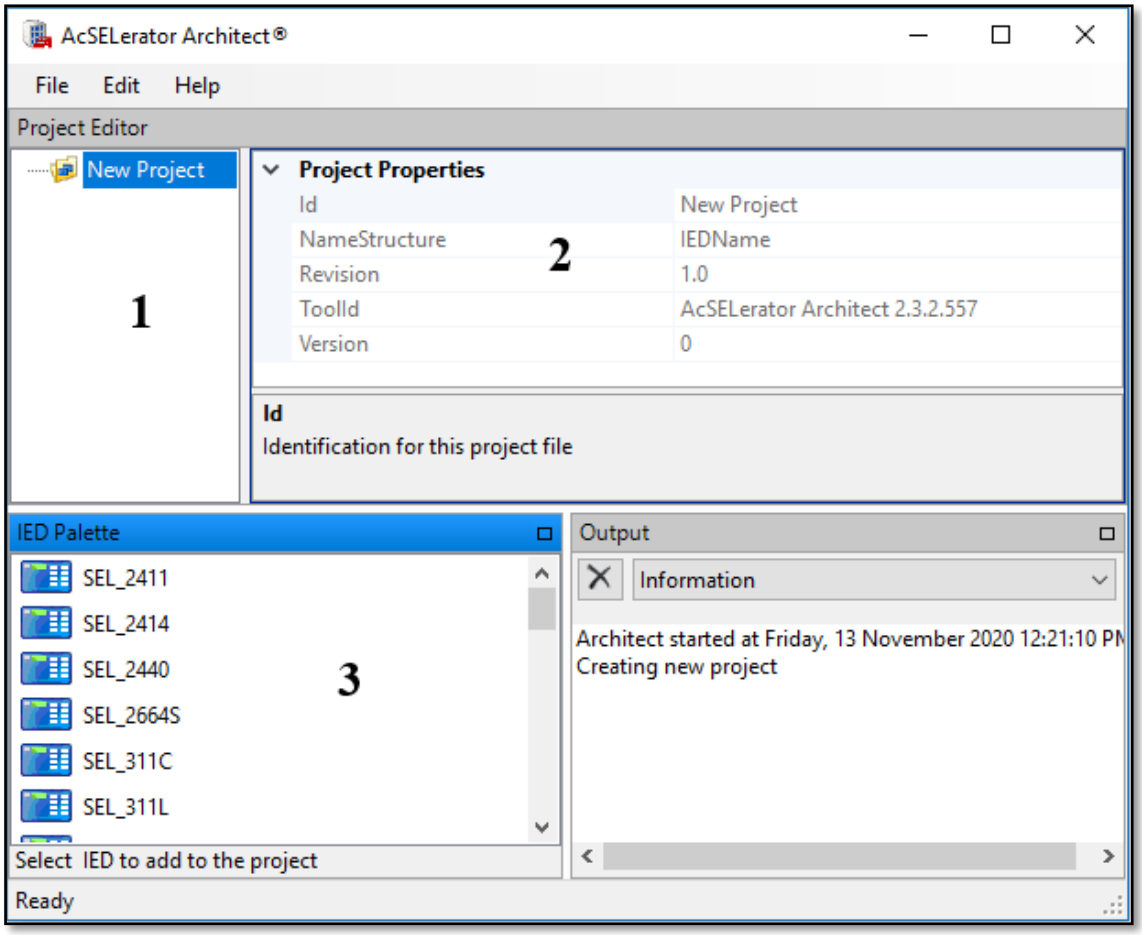

Figure 7.2: AcSELerator Architect main menu

The IED is dragged from the IED Palette and dropped in the New Project as indicated by the arrow in Figure 7.3 below on the next page.

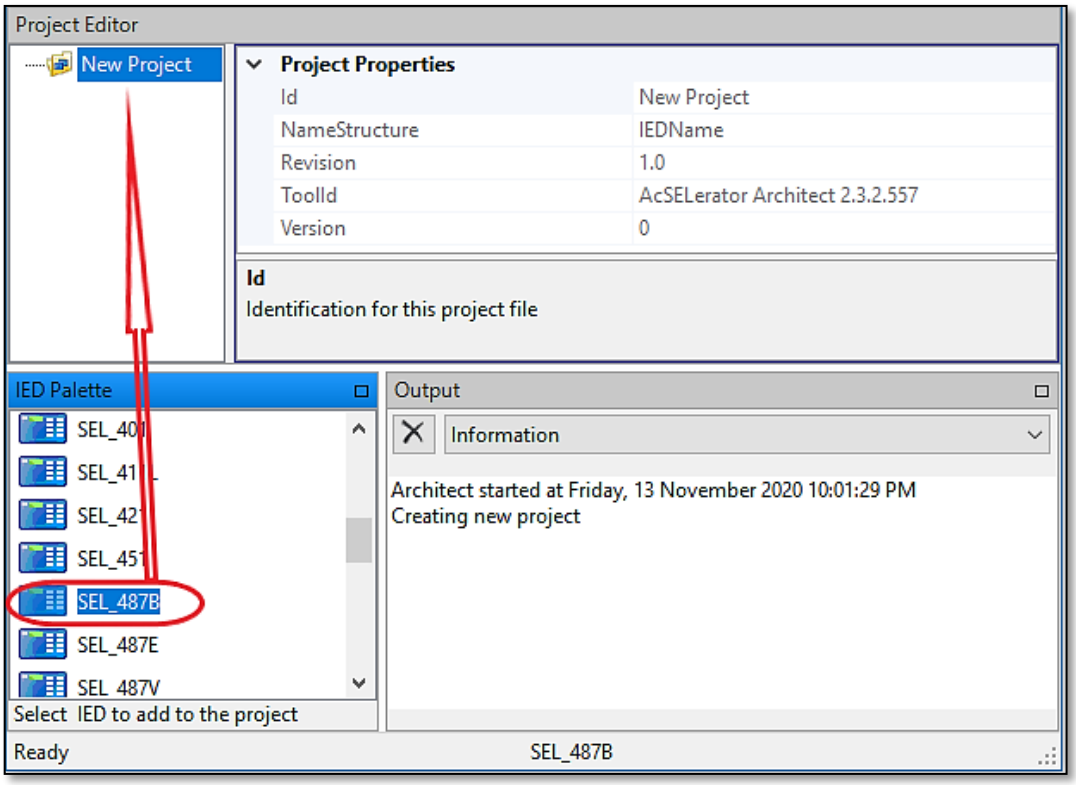

Figure 7.3: AcSELerator Architect – IED

Once the IED is dropped, the window shown in Figure 7.4 below pops up, requiring the definition of the IED ClassFileVersion along with the Description of the device. The SEL-487B relay used for this study belongs to the Blue-highlighted group.

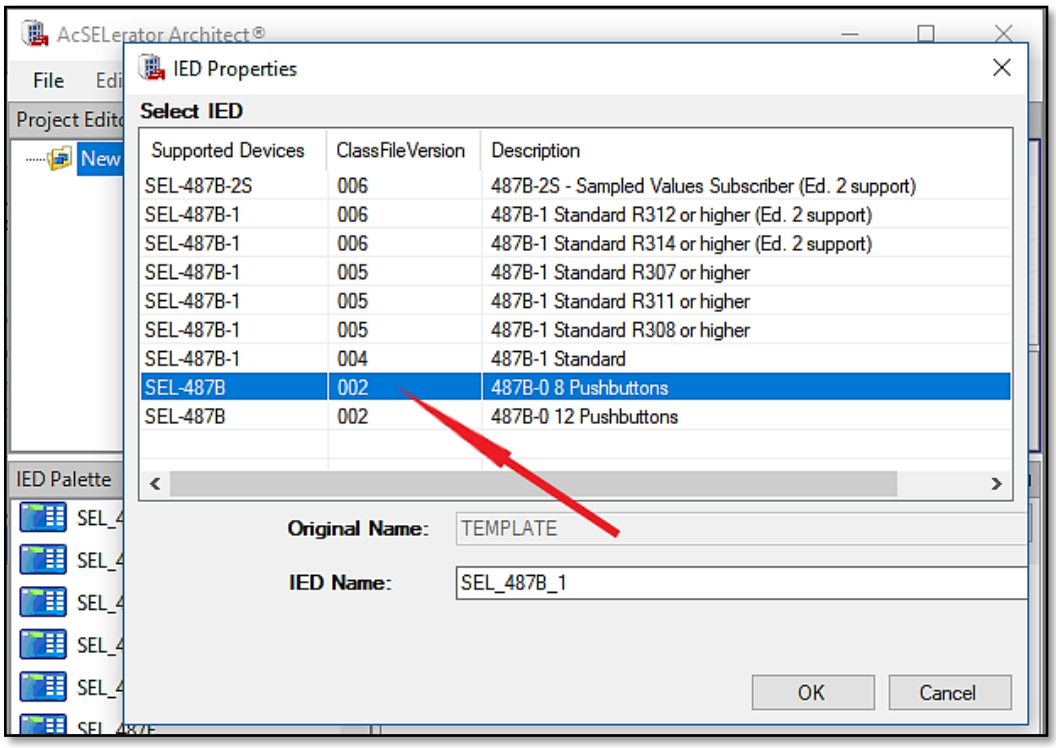

Figure 7.4: IED selection

Once the IED was successfully dropped and defined, it was renamed as shown in figures, 7.5 and 7.6 below and on the next page.

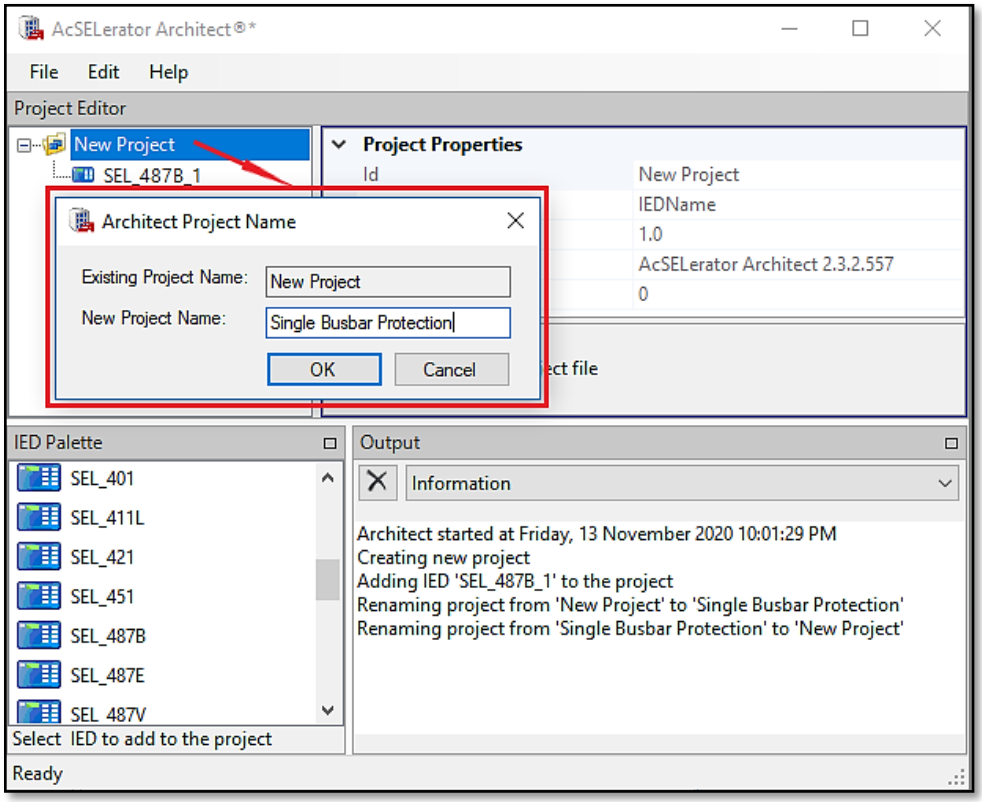

Figure 7.5: Renaming project

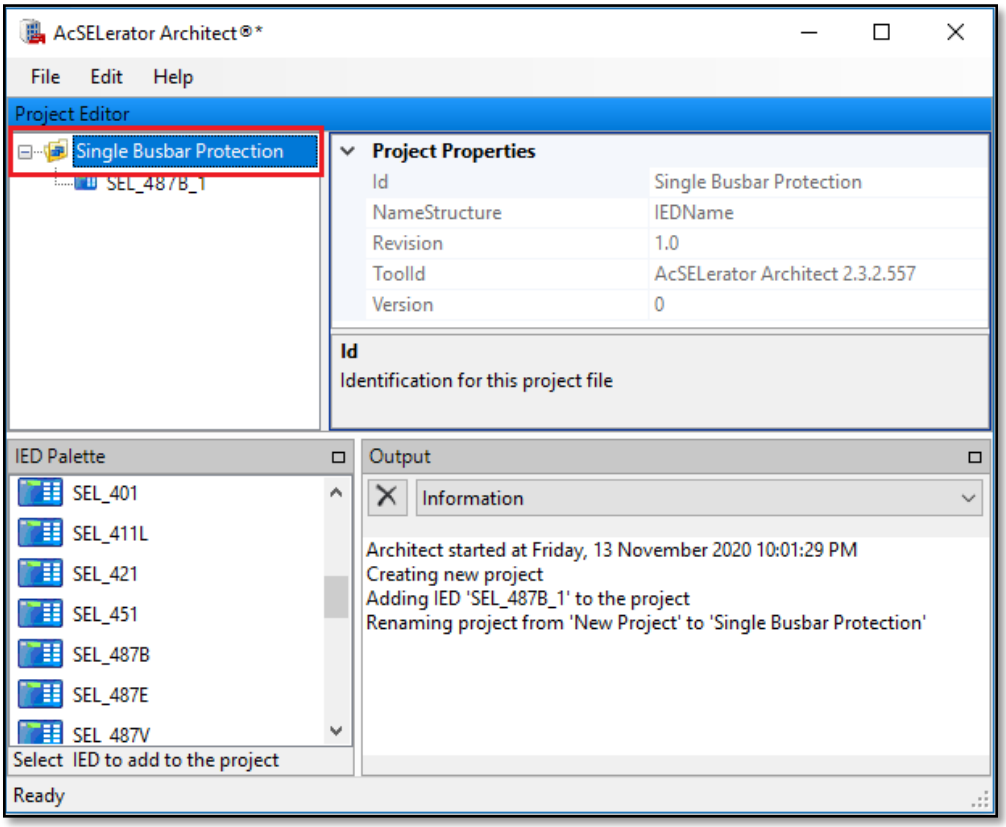

Figure 7.6: Renamed project

IED properties are defined as shown in Figure 7.7 below on the next page for device IP address, Subnet mask and Gateway.

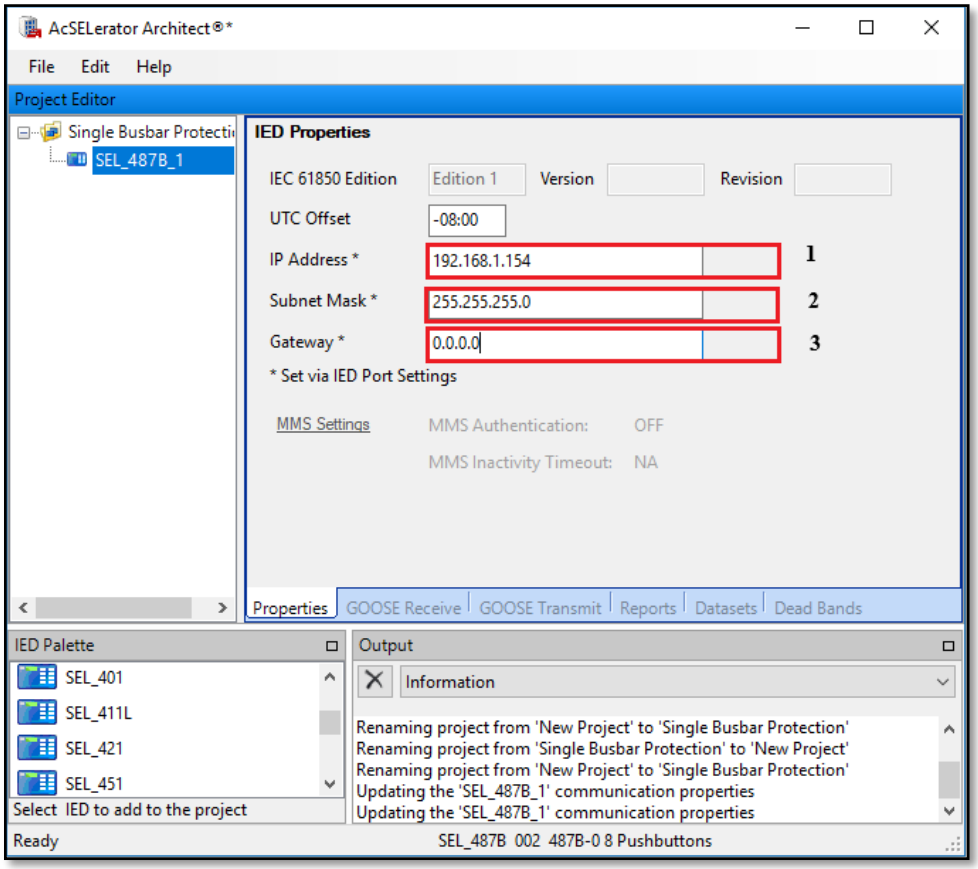

Figure 7.7: Defined IED properties

Once the IED properties were defined, the datasets to be published were defined by clicking on the indicated Zones 1 and 2 in Figure 7.8 below.

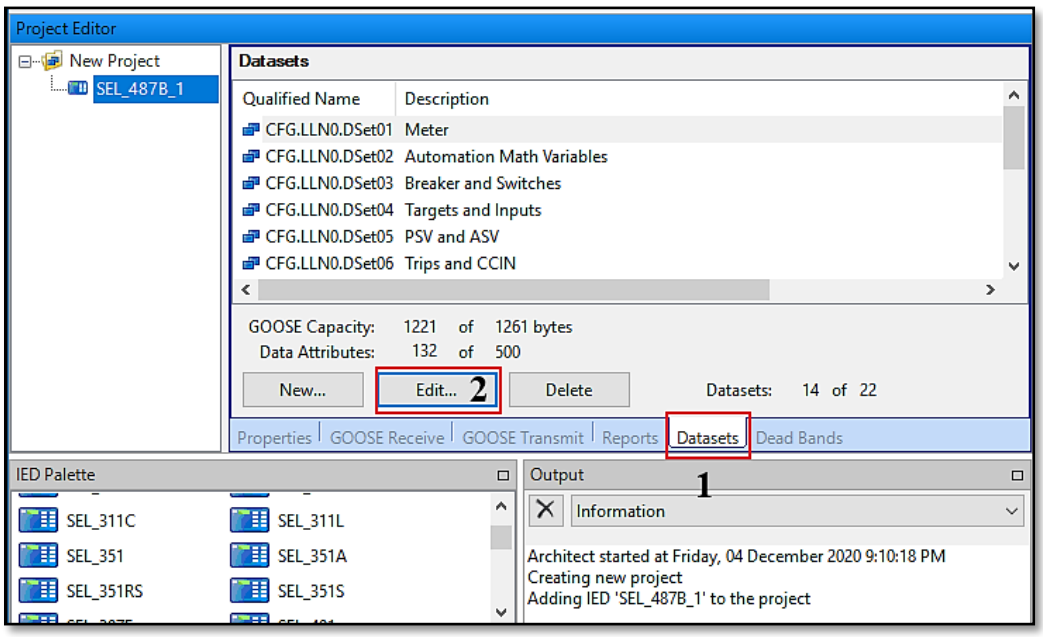

Figure 7.8: Definition of datasets

When the “edit” in Zone 2 is clicked, the window shown in Figure 7.9 below appears, with a list of defined default datasets for the SEL-487B relay.

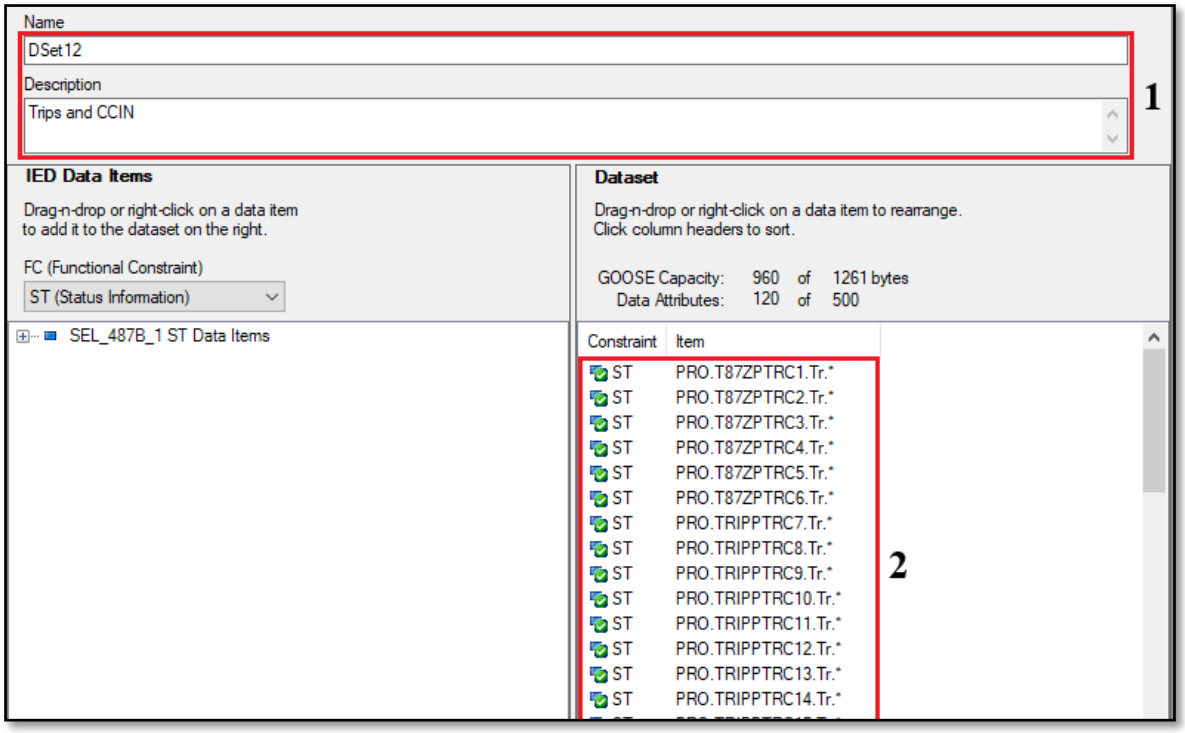

Figure 7.9: Existing data attributes

For the protection scheme used, only the differential element datasets are used. In addition, the name of the defined dataset is renamed and described as indicated in Zone 1 of the figure.

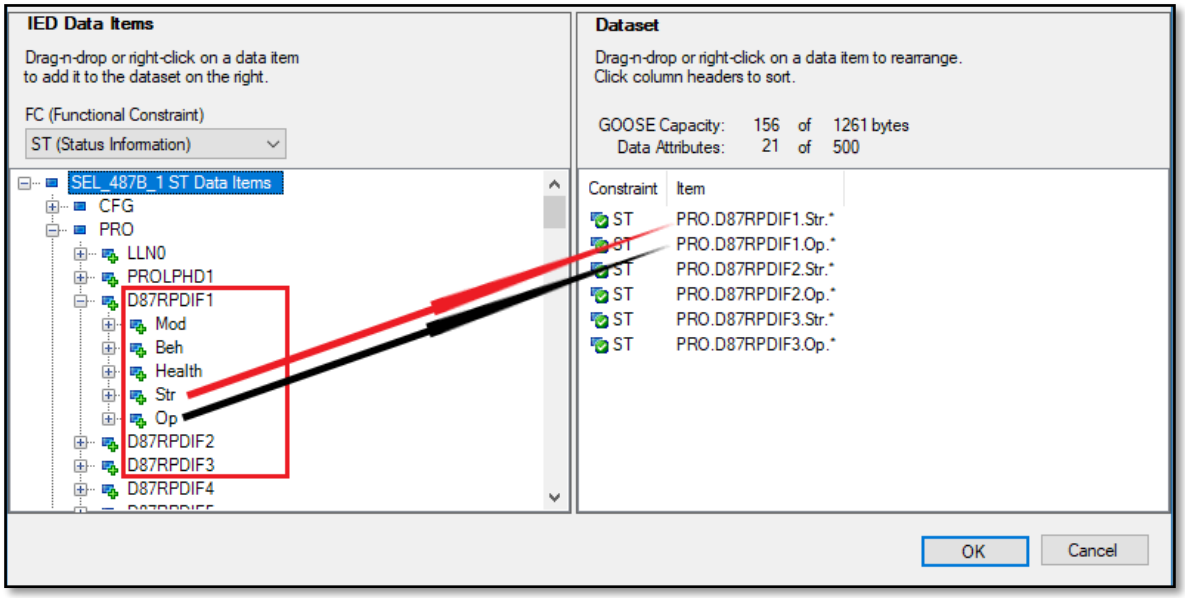

Figure 7.10: Addition of specific data attributes

The new datasets are dragged and dropped in the datasets column as shown in Figure 7.10 above on the previous page for the elements that were indicated in Table 7.1 of this section.

The chosen datasets or attributes are mapped to a GOOSE transmit defined as the logical node (LN) as shown in Figure 7.11 below and Figure 7.12 below on the next page.

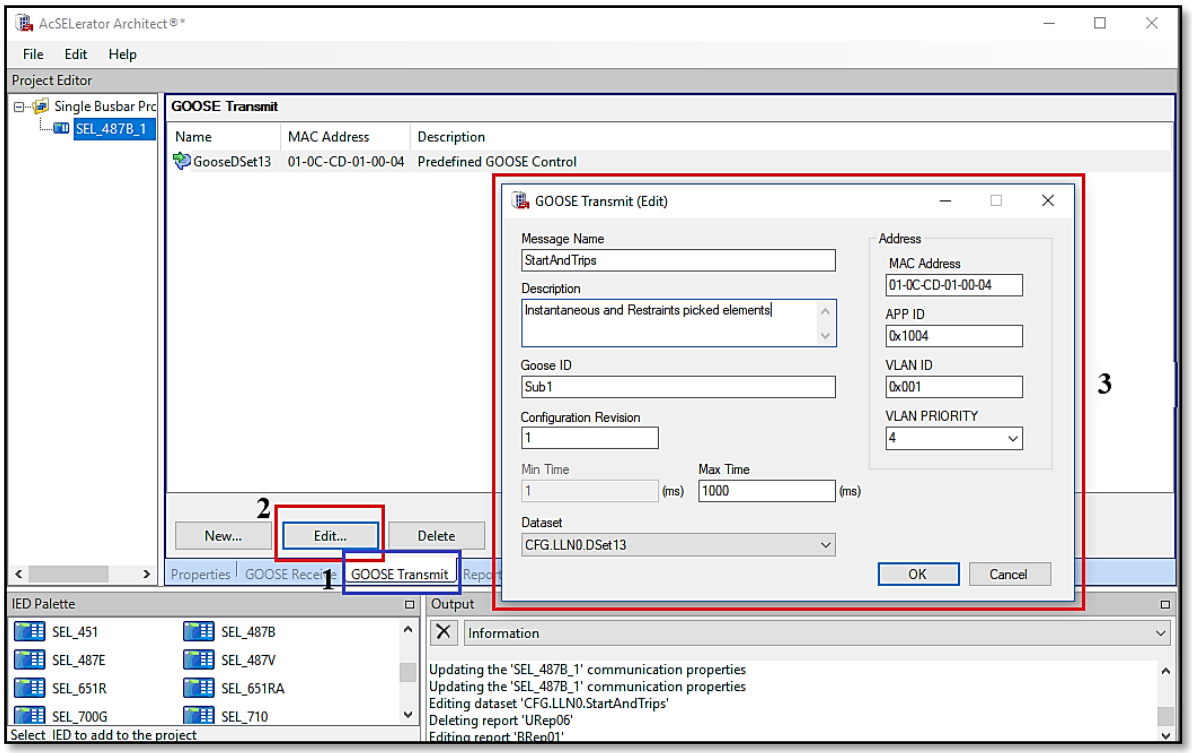

Figure 7.11: GOOSE transmit definition and settings

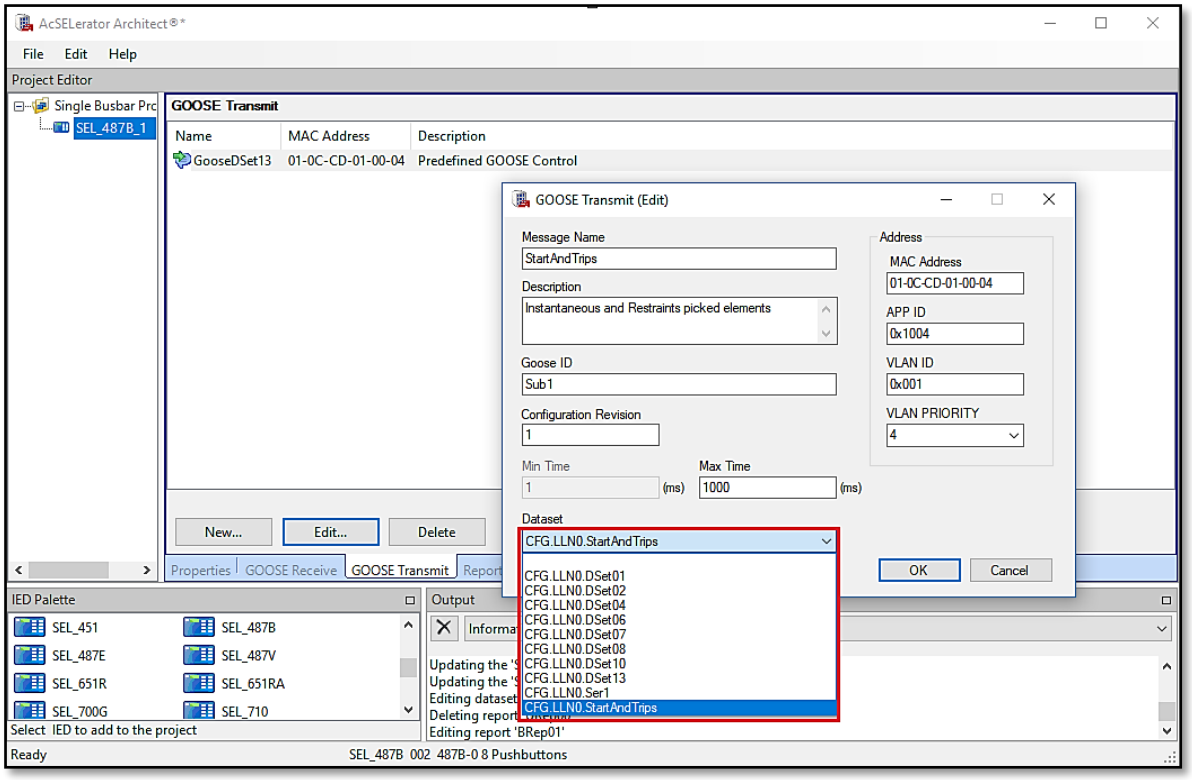

Figure 7.12: Mapping for transportation of data sets over GOOSE transmit

Once the transmission mapping of GOOSE is completed, it appears as shown in Figure 7.13 below, with its defined name, MAC address and description.

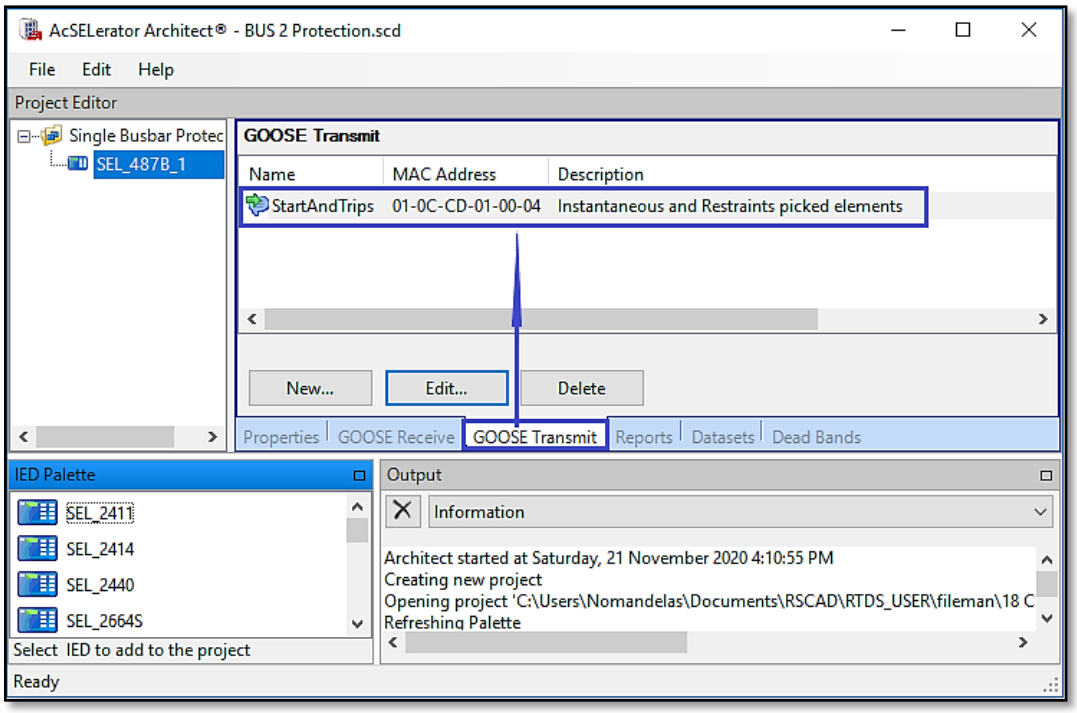

Figure 7.13: Complete transport of the logical node

The SCD file is then saved on the local computer. When the SCD file is saved, the CID which contains the SEL-487B details about the GOOSE messages it should transmit is sent to the IED. But before it is sent, the connection is tested and verified in the terminal command window shown in Figure 7.14 below by pinging the physical IED with the IP address. This confirms the connectivity between the devices and computer.

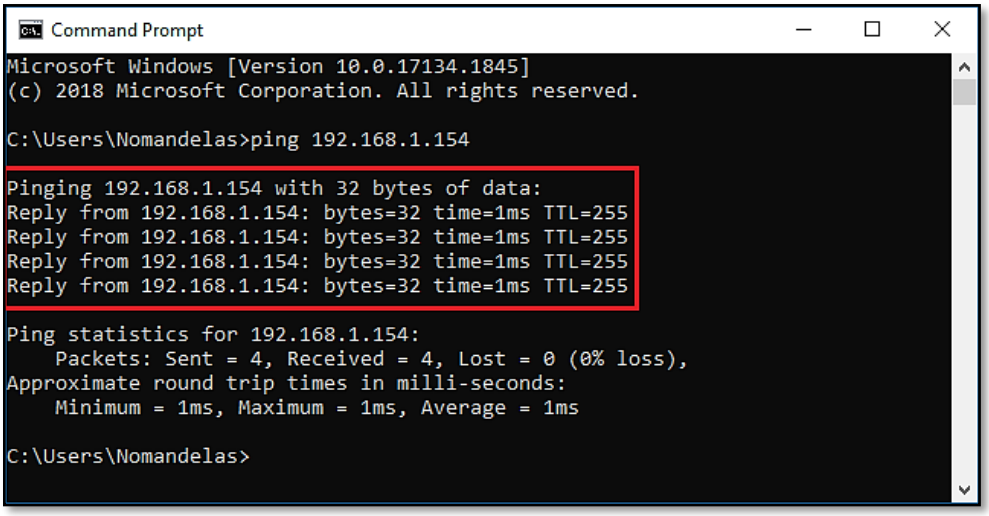

Figure 7.14: Device communication test – device responding

When communication was established between the computer and the relay, the CID file was sent to the physical device as shown in Figure 7.15 below.

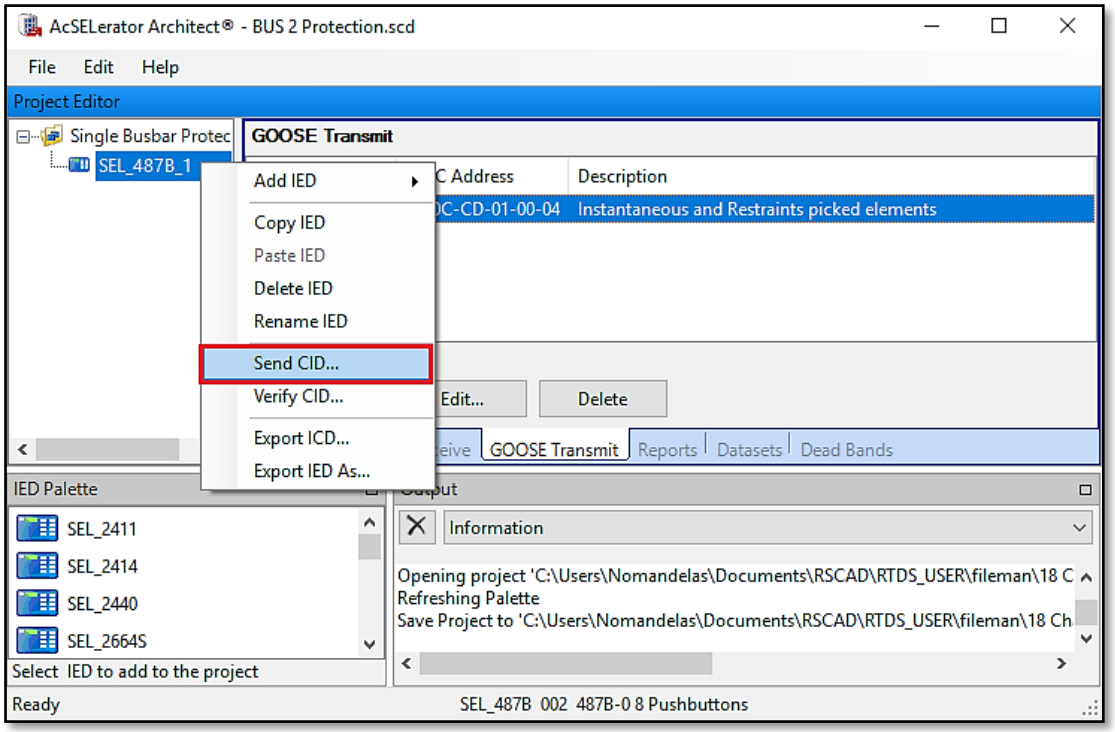

Figure 7.15: Sending of the CID file to the physical IED

When the “Send CID” button is clicked, the network settings confirm window pops up as shown in Figure 7.16 below and the communication network settings are defined.

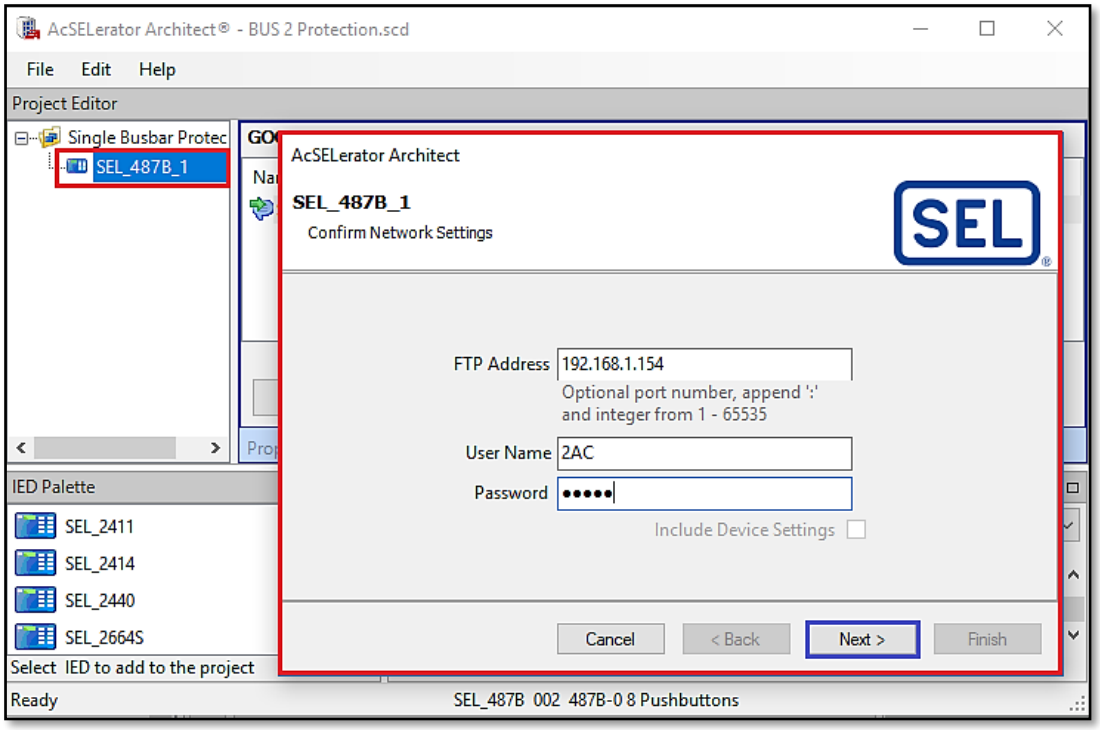

Figure 7.16: Publishing IED network settings confirmation

When the “Confirm Network Settings” is completed, another window pops up and the process is completed by user confirmation until CID file is sent successfuly.

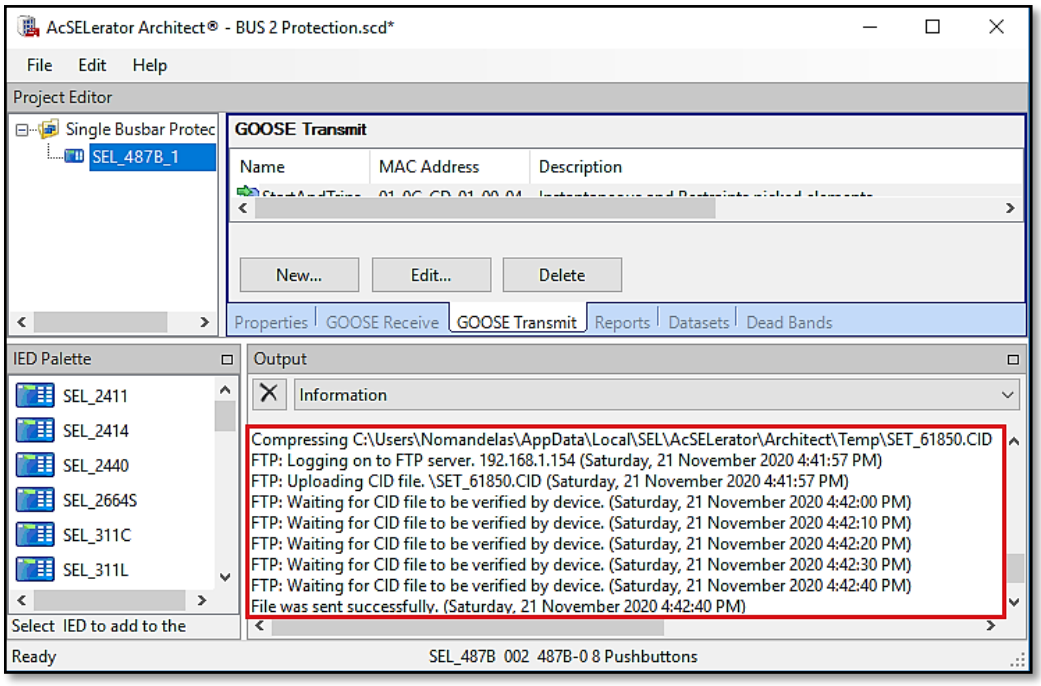

Figure 7.17: CID file sending information

When IED GOOSE settings are successfully sent to SEL-487B, the AcSELerator Architect software displays as shown in Figure 7.17 above on the previous page.

After the settings file was successfully sent to the IED, another software GOOSE Inspector was used to confirm if GOOSE messages are published by the IED as can be seen in Figure 7.18 below. Only six Boolean datasets were set for this IED, and are indicated as Object 1 to Object 6 in the software.

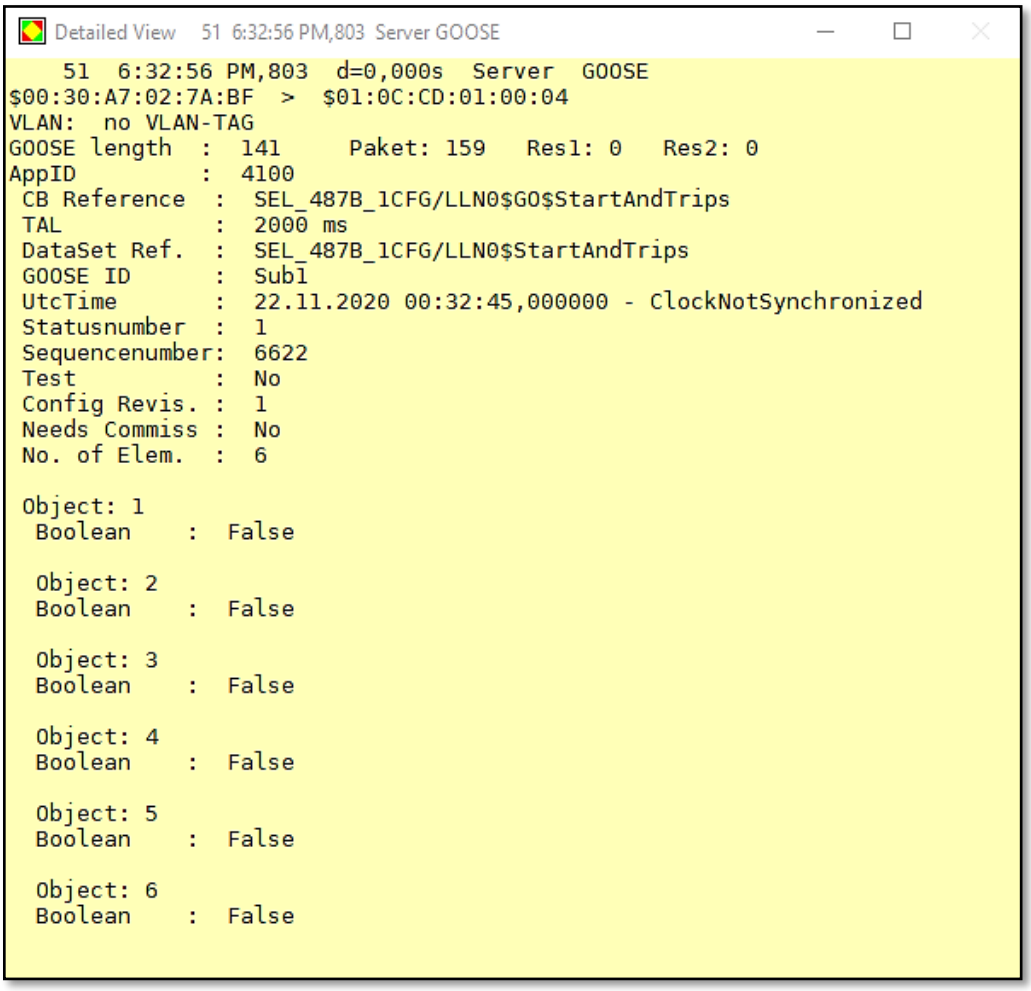

Figure 7.18: GOOSE message datasets

Figure 7.19 below on the next page shows the retransmission of GOOSE messages which approximately updates after every 3 to 4 ms.

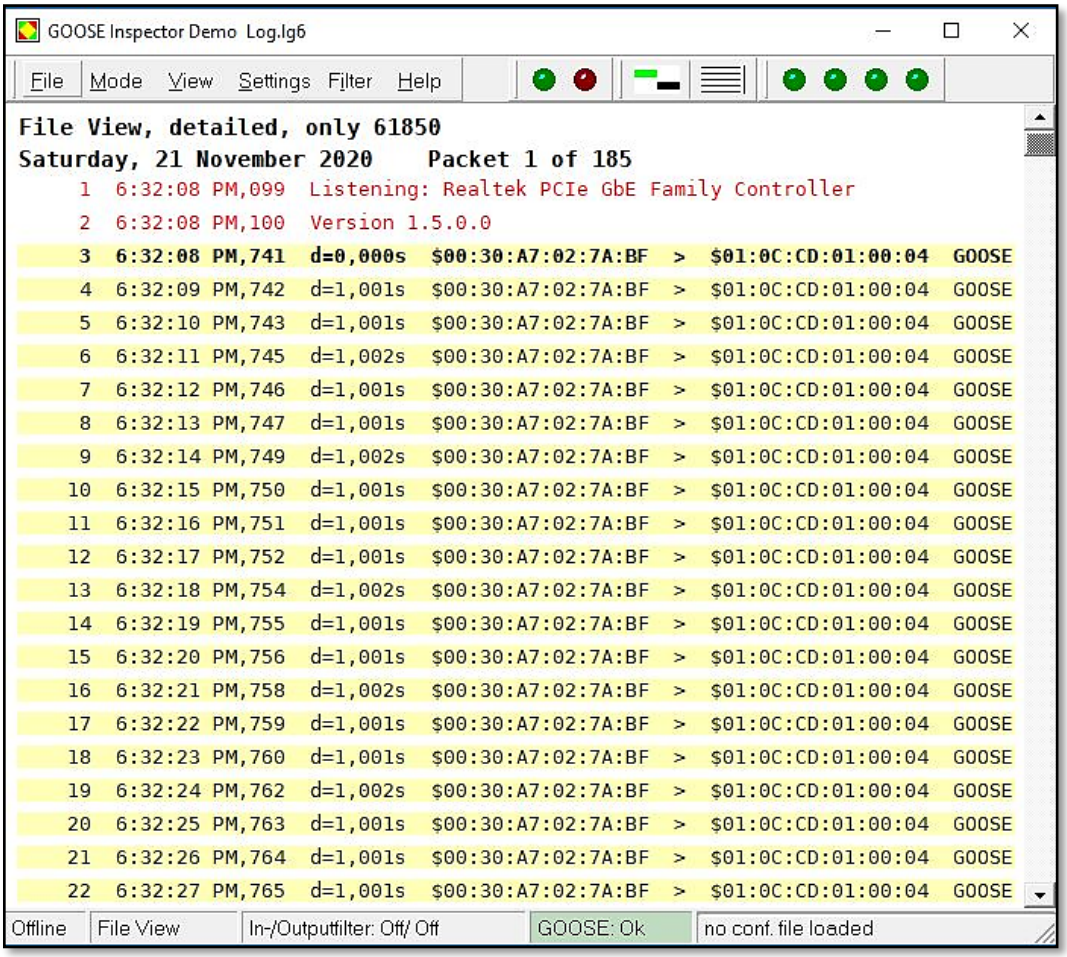

Figure 7.19: Detailed GOOSE message updates

When the configuration of GOOSE is completed for a physical device, the RTDS GTnet GSE is configured for mapping the datasets to the virtual system circuit breakers for trip commands. This is completed in the next part.

7.2.2 Configuration of the RTDS GTnet GSE for GOOSE status event

In this part, the procedure followed to configure GTnet for GOOSE message publishing is discussed in steps. But first, the relationship between the physical device (SEL-487B) and the GTnet component is described. The physical device is linked to the RTDS virtual simulation power system network which consists of three circuit breakers. The GTnet is a virtual device within the RTDS simulation and it performs functions using its internal IEDs.

The IEDs within the GTnet component are GGIOs. The function of a GTnet is to subscribe from the physical device published GSSE/GOOSE messages and use those messages to perform the function of triggering the virtual system circuit breakers for isolation of fault at the busbar. That being said, the RTDS GSE component is exported

from the component library and placed on the RTDS draft as can be seen in Zone 2 of Figure 7.20 below.

To save draft space, the GTnet-GSE component is placed in a drawing box indicated by Zone 1 in the figure. Zone 4 of the figure indicates the protected busbar, Bus 2.

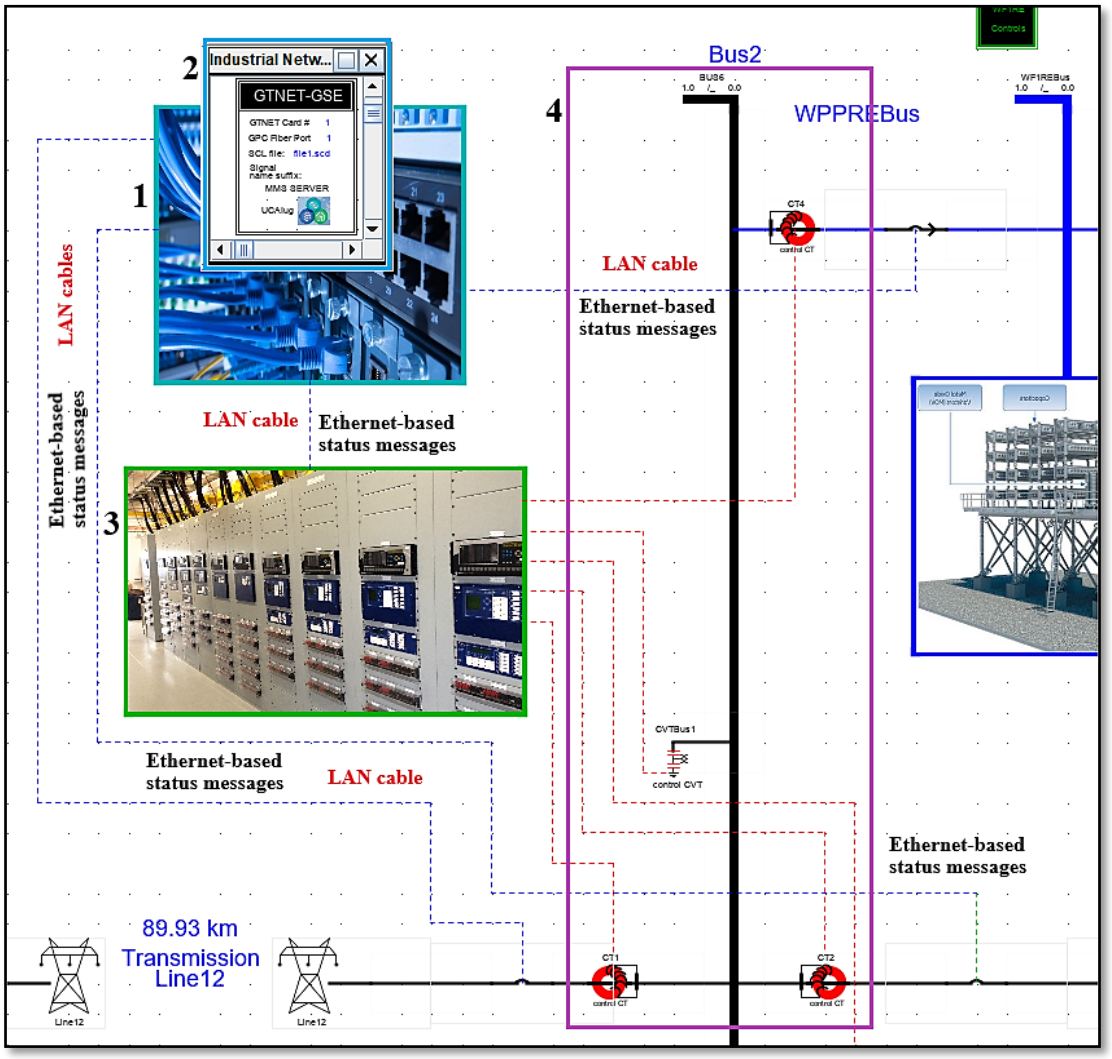

Figure 7.20: GTnet placement

To configure the GTnet-GSE component, the path as shown in Figure 7.21 below on the next page must be completed. The inputs required for GOOSE must be allocated on the SCD file from the template. These are imported from the SCD file created on the IED configuration.

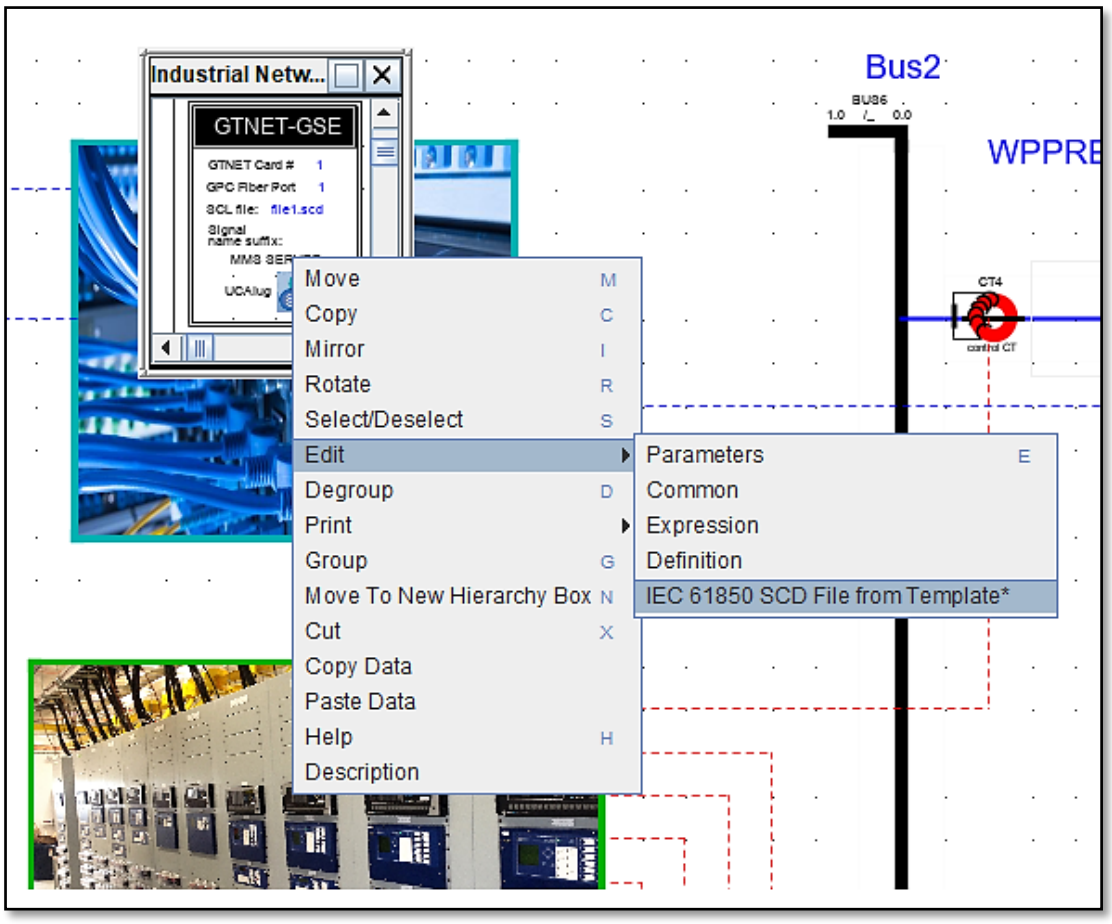

Figure 7.21: GTnet placement – modelling of the IEC 61850 SCD file

After the SCD file is imported, the file contains data attributes (defined by the IEC 61850-7-2) that were created for status sharing. These data attributes are mapped to the lists of messages as shown in Figure 7.22 below on the next page for transport to the virtual circuit breakers for protection and control within the RTDS simulation model.

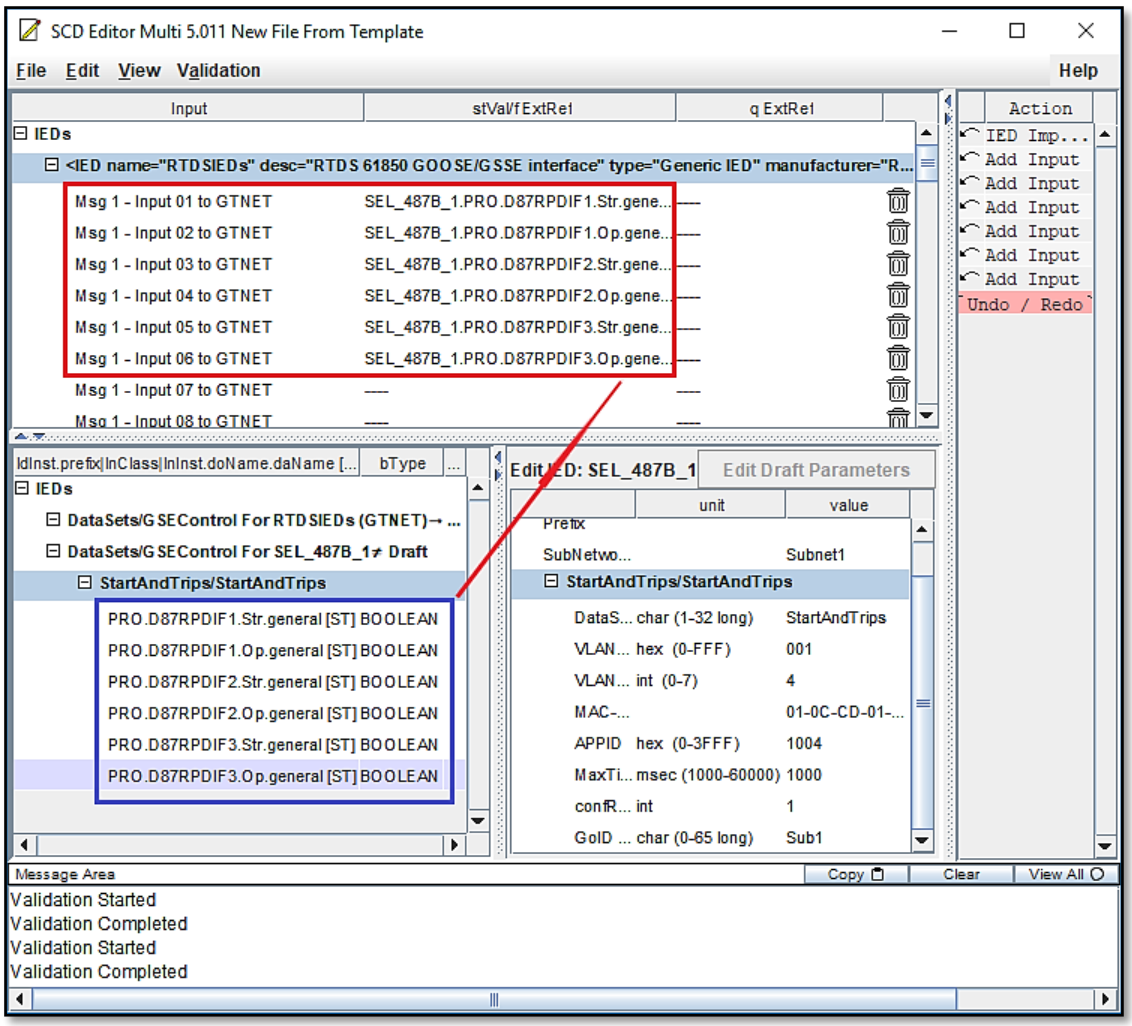

Figure 7.22: **Mapping of the IED datasets for GOOSE transmission by the GTnet IED**

After the mapping of these attributes to the messages, the file must be validated to completed the mapping process.

The GTnet component aims to interface the physical device to the RTDS virtual circuit breakers so that when the status event is shared by the GOOSE publishing IED, the circuit breakers can recognize the command and operate accordingly. This requires further mapping of output signals from the GTnet component. The settings shown in Figure 7.23 below on the next page define GTnet output signals.

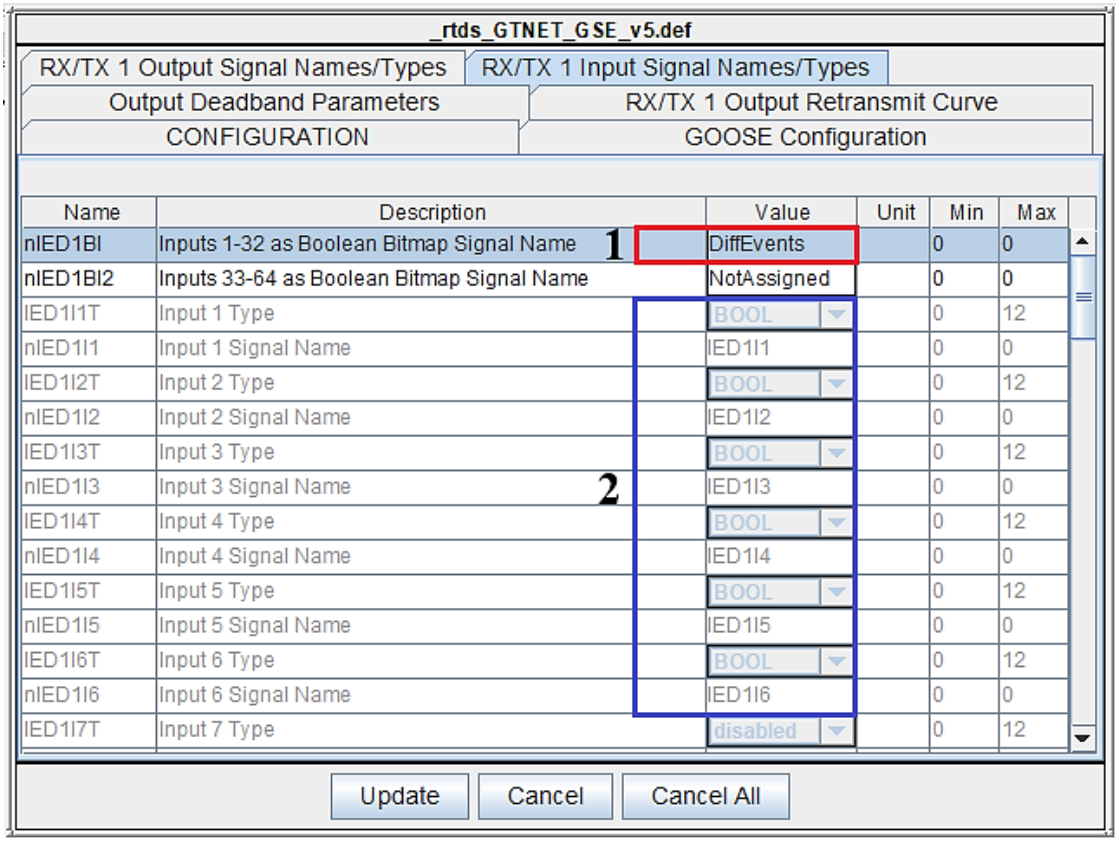

Figure 7.23: Definition of GTnet input signals

The signal word *DiffEvents* is a word command containing all the assigned GOOSE data attributes from the physical external device. These signals are mapped to the GTnet virtual device. The word-to-bit converter exists and is configured on RSCAD, to take the *DiffEvents* signal name and produces the six data attributes corresponding to those that were defined during the GOOSE configuration of the SEL-487B, which the GTnet publishes as *IED1I1*, *IED1I2*, *IED1I3*, *IED1I4*, *IED1I5* and *IED1I6* as can be seen in Zone 2 of the above figure. The signals, *IED1I2*, *IED1I4* and *IED1I6* are differential trips, and the rest are differential pickups.

The differential trip signals are received by the circuit breakers through the word-to-bit converter shown in Figure 7.24 below on the next page and renamed accordingly. The signals *RStEvent*, *YStEvent* and *BStEvent* are start digital bits (1's and 0's) converted from the data attributes published by the GTnet GSE component, whose original publisher is the SEL-487B physical device. The same information applies for operating digital bits (1's and 0's) signals *ROpEvent*, *YOpEvent* and *BOpEvent*.

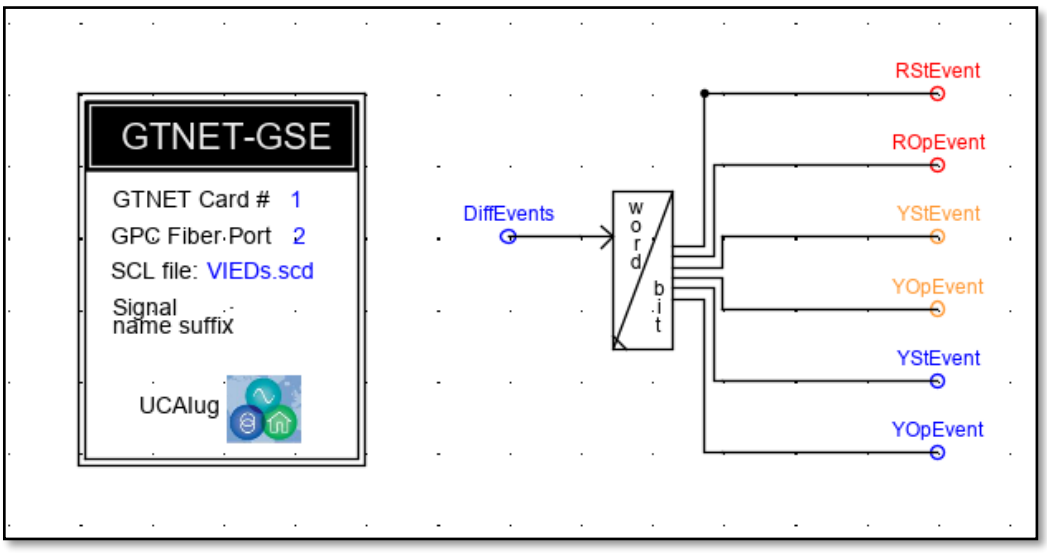

Figure 7.24: GTnet to word-to-bit converter interface

The word-to-bit converter is then connected to the logic (see Figure 7.25 below) that controls the virtual circuit breakers.

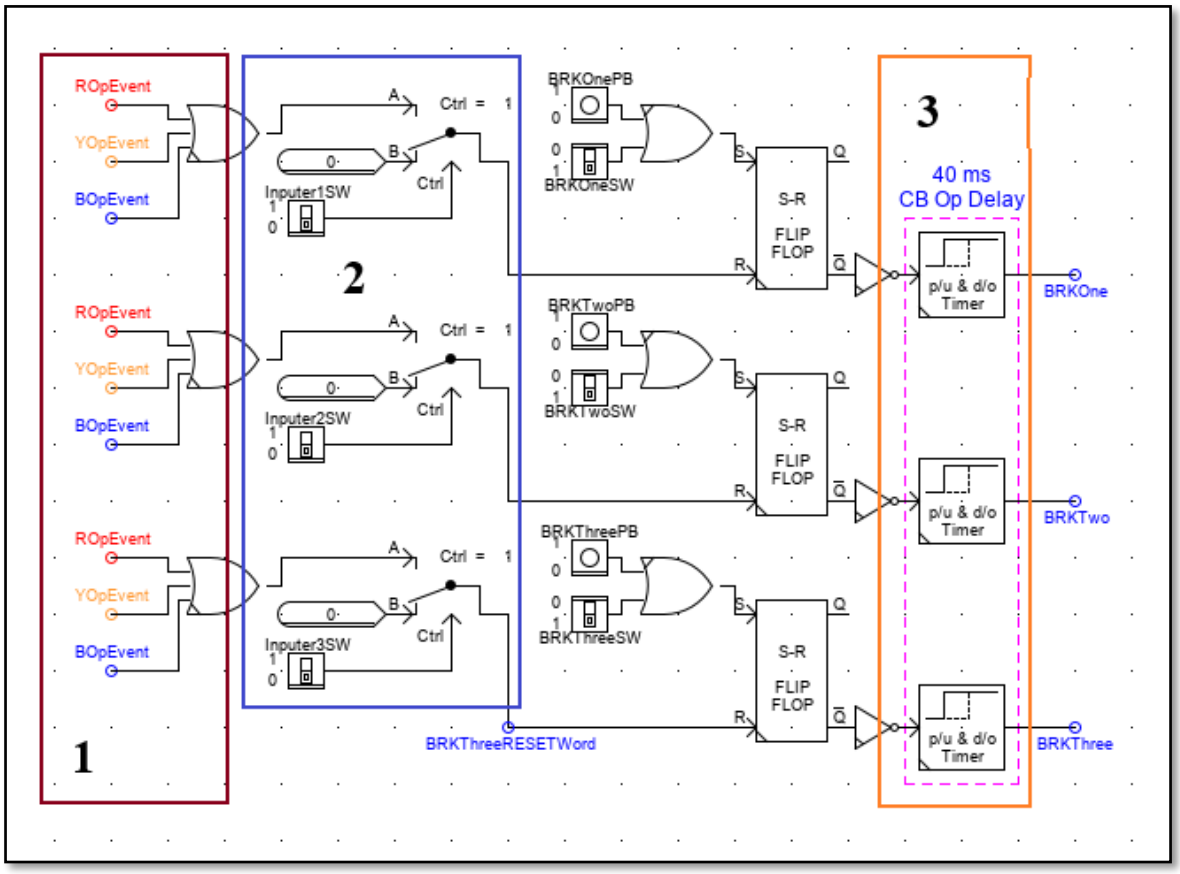

Figure 7.25: Circuit breaker control logic

The operation of smart circuit breakers is usually 40 milliseconds. The timers that are shown in Zone 3 of the circuit breaker logic in the above figure accommodate this delay.

After this setting, the new RTDS SCD file is saved and the RTDS draft file is saved and compiled.

After this simulation, the fault simulation case studies are performed at least for a three-phase fault at busbar 2 (Bus2). This is described in the next section.

7.3 IEC 61850 standard-based protection scheme test

The testing of the developed protection scheme using the IEC 61850 standard generic substation event (GSE) control model generic object-oriented substation event (GOOSE) is described in this section, for two types of faults, Red-phase-to-ground and Three-phase faults at 315 MW and 420 MW loading. The aim of this test is to prove the functionality. The same quantities that were monitored in Chapter 6 are still monitored, in the same order.

7.3.1 315 MW loading

The simulation case under this test is run based on the sequence presented in Table 6.5 in Chapter 6. There are two main columns in the table. The first column presents the sequence for system loading, and the second column is for fault simulation.

7.3.1.1 Red-phase-to-ground (RPh-Gnd) fault at Bus 2

The Red-phase-to-ground fault was simulated at Bus 2 while the system was experiencing a load demand of 315 MW. The fault was initiated at 20.00475 seconds and got cleared at 20.37133 seconds as shown in Figure 7.26 below on the next page.

The total duration of the fault is 0.3666 seconds, after this time, it was cleared and the busbar was left isolated from the system.

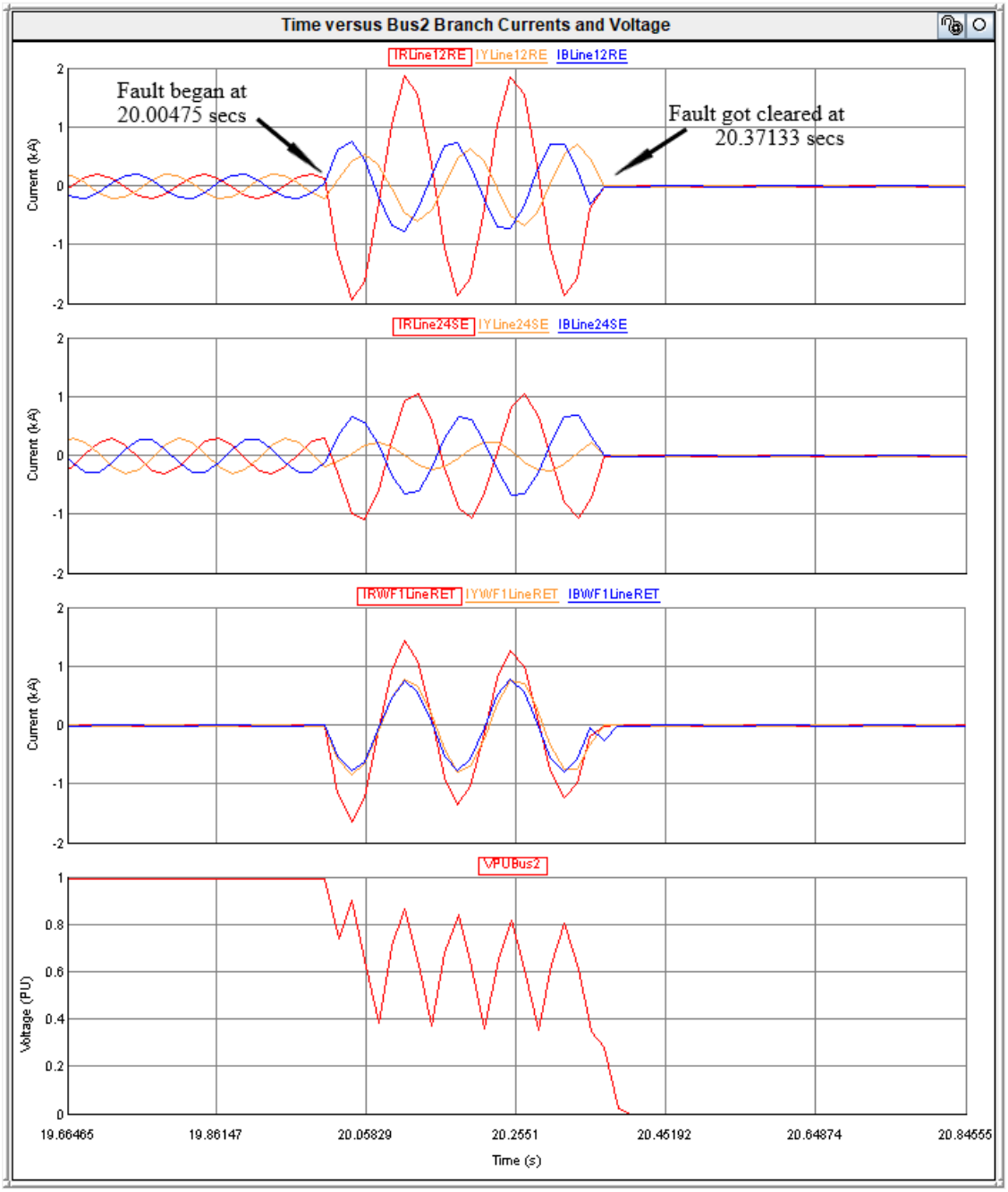

Figure 7.26: **Branch currents and Bus 2 voltage for R-G fault at Bus 2 under 315 MW**

Another waveform is provided in Figure 7.27 below on the next page. In the figure, the upper plot shows the per-unit voltage, and the bottom plot is RMS voltage. Using these plots, the recovery time of the wind power plant receiving-end terminal voltage is analyzed. The disturbance experienced by the wind power plant began at 20.0048 seconds and ended at 32.3518 seconds as shown in the plots.

When the faulty busbar was isolated from the system, the wind power plant became free from the fault and remained islanded.

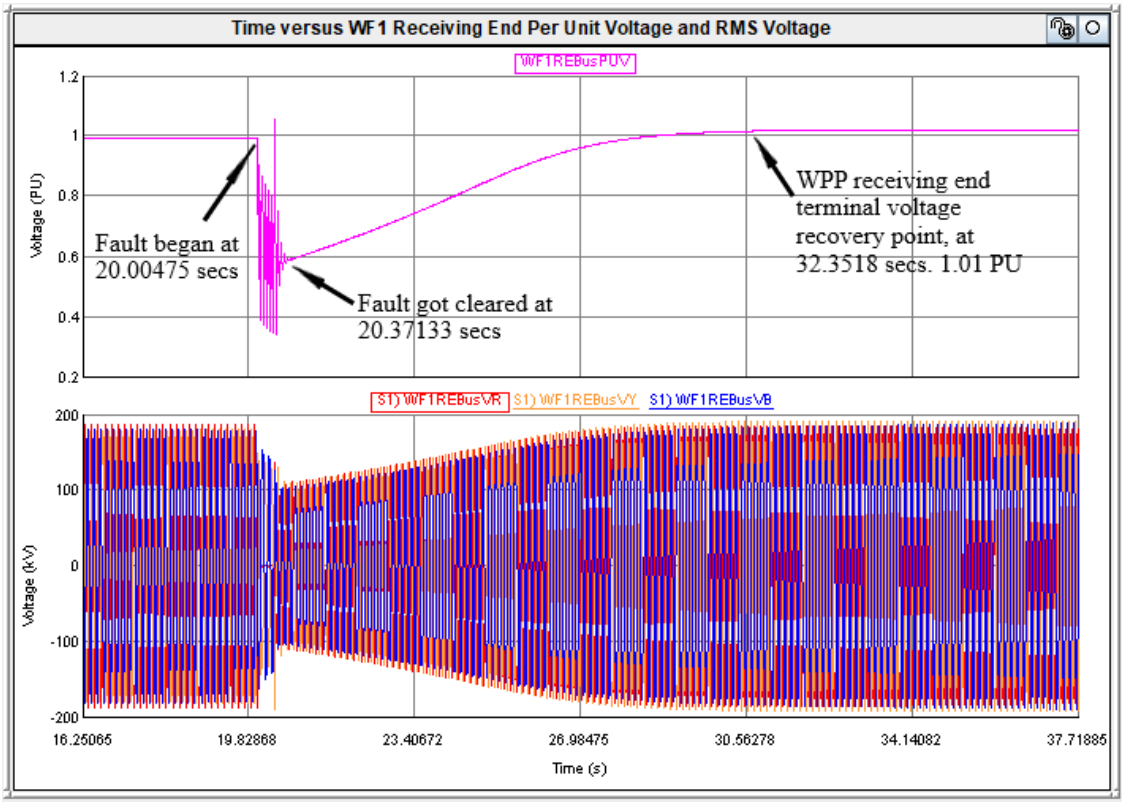

Figure 7.27: **WPP receiving-end voltage for R-G fault at Bus 2 under 315 MW**

After all these events, it took 11.9805 seconds for wind power plant terminal voltage to stabilize. The value at which it is stabilized is 1.01 per unit and is safe for continuous operation of the wind power plant.

The circuit breaker control actions were monitored during the test and the results are shown in Figure 7.28 below on the next page. The trip command was received by the circuit breaker logic at 20.3694 seconds after the fault was detected by the relay, and the circuit breakers operated later at 20.37285 seconds.

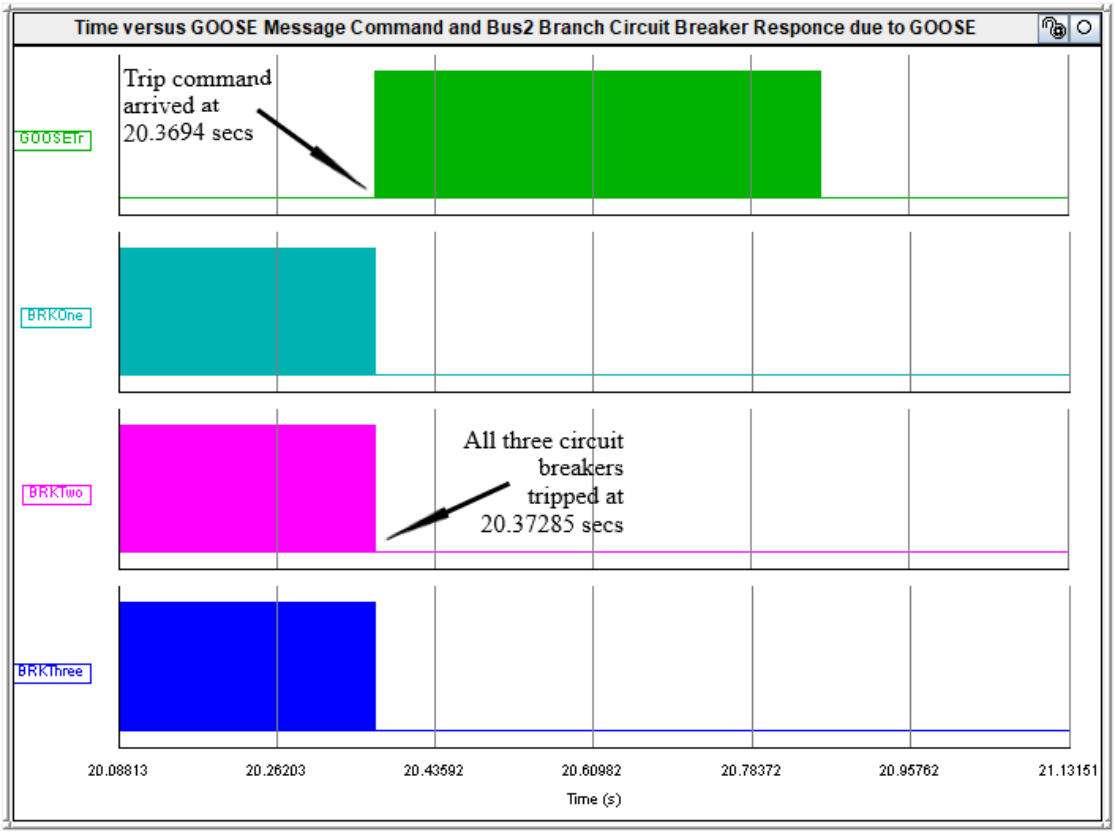

Figure 7.28: CB-received GOOSE trip command for R-G fault at Bus 2 under 315 MW

The time it took for circuit breakers to open after the trip command was received is approximately 3.45 milliseconds.

7.3.1.2 Three-phase (3Ph) fault at Bus 2

The Three-phase fault was simulated at Bus 2 while the system was experiencing a load demand of 315 MW. The fault was initiated at 20.0083 seconds and got cleared at 20.3554 seconds as shown in Figure 7.29 below on the next page.

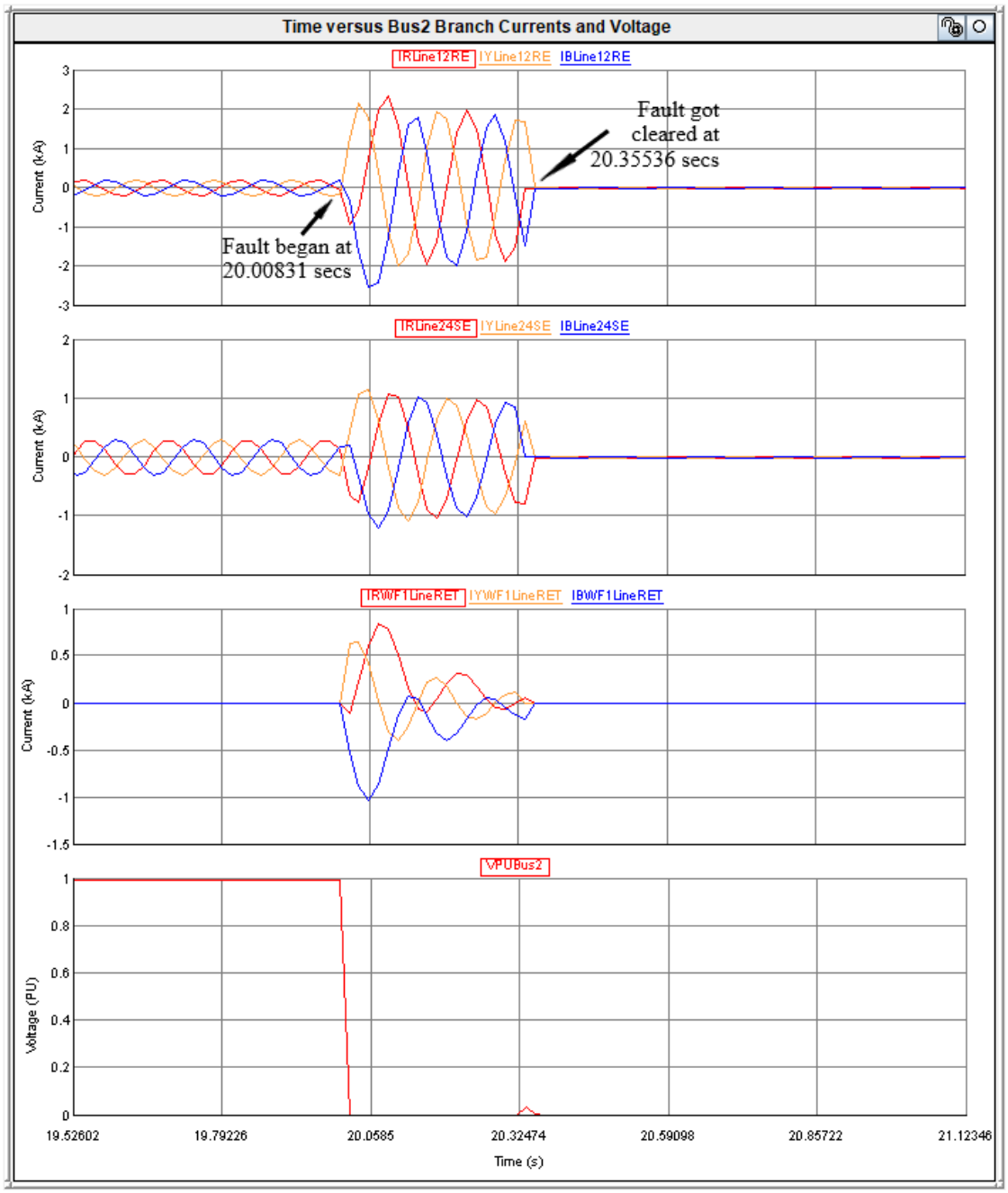

Figure 7.29: **Branch currents and Bus 2 voltage for 3Ph fault at Bus 2 under 315 MW**

The total duration of the fault is 0.3471 seconds, after this time, it was cleared and the busbar was left isolated from the system.

Another waveform is provided in Figure 7.30 below on the next page. Using these plots, the recovery time of the wind power plant receiving-end terminal voltage is analyzed. The disturbance experienced by the wind power plant began at 20.0083 seconds and ended at 49.2846 seconds as shown in the plots. When the faulty busbar was isolated from the system, the wind power plant became free from the fault and remained islanded. After all these events, it took 28.9292 seconds for wind power plant terminal

voltage to stabilize. The value at which it is stabilized is 1.02 per unit and is safe for continuous operation of the wind power plant.

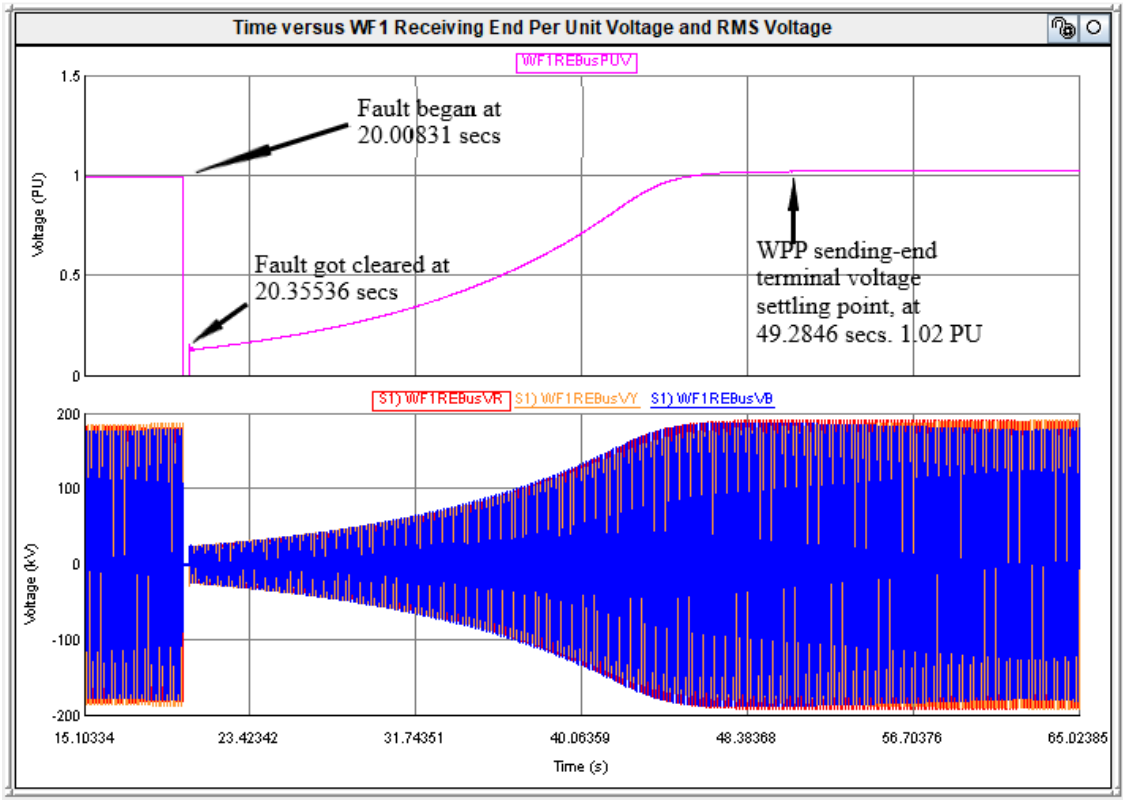

Figure 7.30: WPP receiving-end voltage for 3Ph fault at Bus 2 under 315 MW

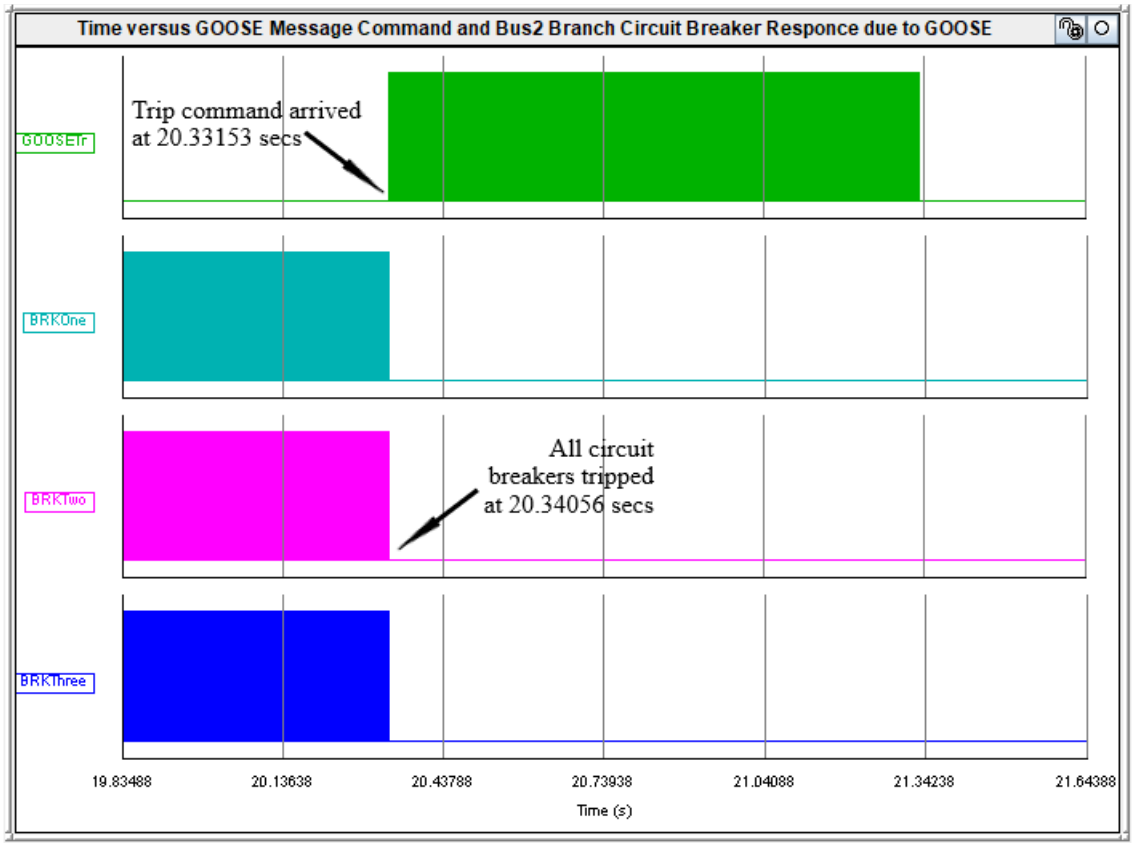

Figure 7.31: CB-received GOOSE trip command for 3Ph fault at Bus 2 under 315 MW

The circuit breaker control actions were monitored during the test and the results are shown in Figure 7.31 above on the previous page. The trip command was received by the circuit breaker logic at 20.3315 seconds after the fault was detected by the relay, and the circuit breakers operated later at 20.3406 seconds. The time it took for circuit breakers to open after the trip command was received is approximately 9.03 milliseconds.

7.3.2 420 MW loading

The simulation case under this test is run based on the sequence presented in Table 6.6 in Chapter 6.

7.3.2.1 Red-phase-to-ground (RPh-Gnd) fault at Bus 2

The Red-phase-to-ground fault was simulated at Bus 2 while the system was experiencing an increased load demand from 315 MW to 420 MW. The fault was initiated at 20.0005 seconds and got cleared at 20.4961 seconds as shown in Figure 7.32 below on the next page.

The total duration of the fault is 0.4956 seconds, after this time, it was cleared and the busbar was left isolated from the system.

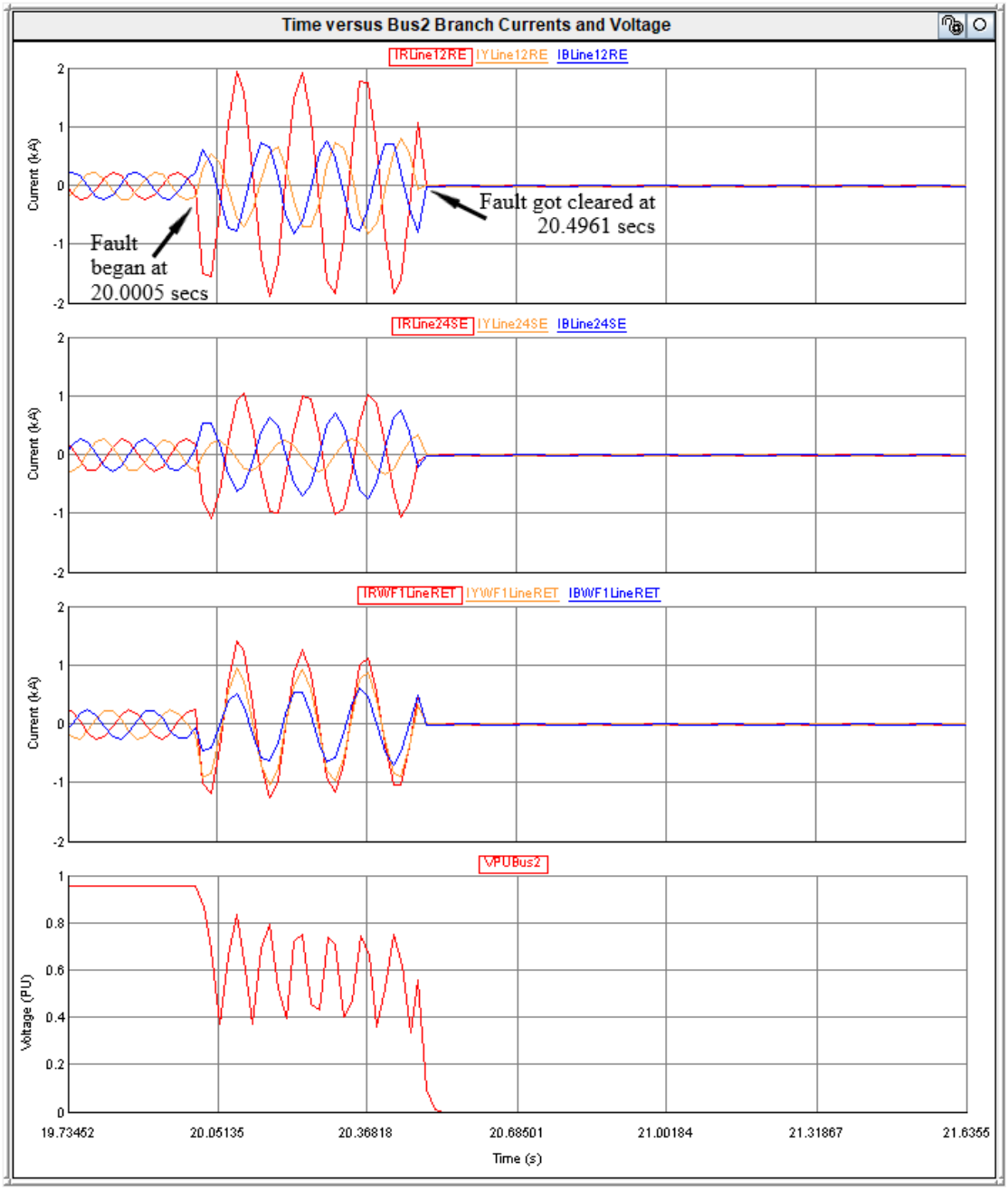

Figure 7.32: **Branch currents and Bus 2 voltage for R-G fault at Bus 2 under 420 MW**

Another waveform is provided in Figure 7.33 below on the next page. Using these plots, the recovery time of the wind power plant receiving-end terminal voltage is analyzed. The disturbance experienced by the wind power plant began at 20.0005 seconds and ended at 32.7118 seconds as shown in the plots. When the faulty busbar was isolated from the system, the wind power plant became free from the fault and remained islanded.

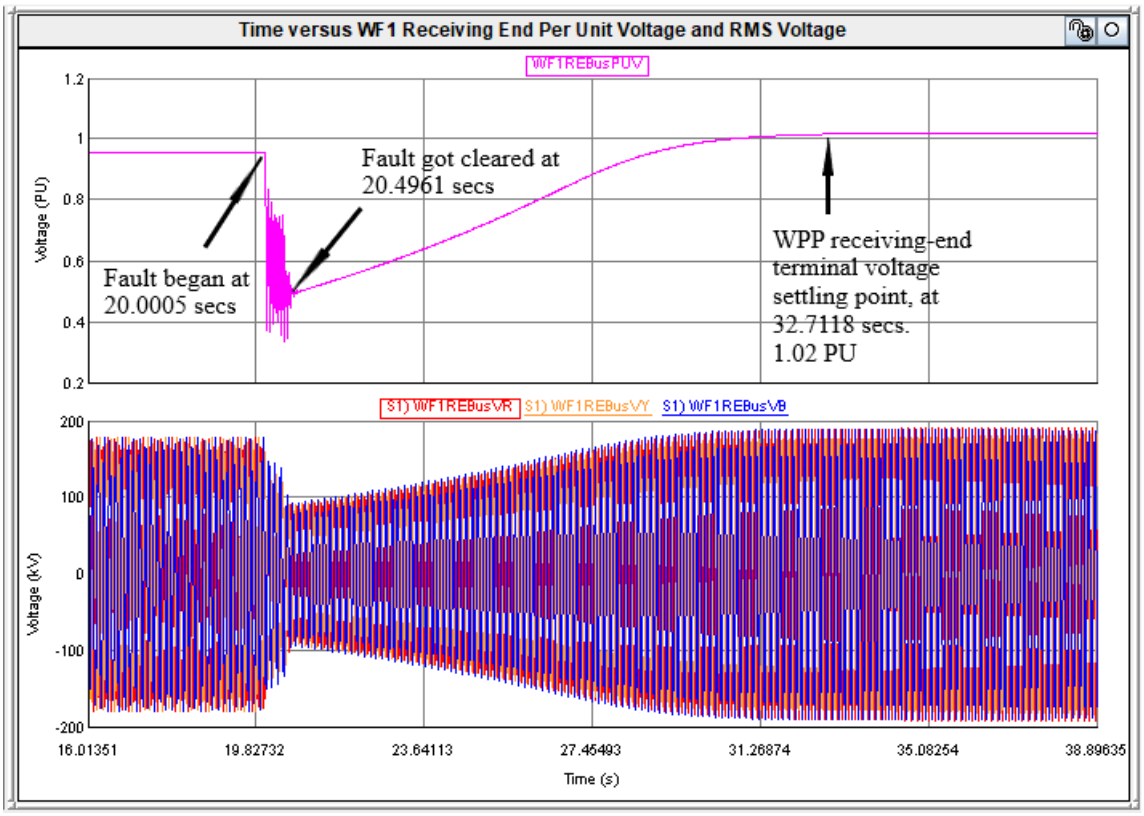

Figure 7.33: **WPP receiving-end voltage for R-G fault at Bus 2 under 420 MW**

After all these events, it took 12.7113 seconds for wind power plant terminal voltage to stabilize. The value at which it is stabilized is 1.02 per unit and is safe for a continuous operation of the wind power plant.

The circuit breaker control actions were monitored during the test and the results are shown in Figure 7.34 below on the next page. The trip command was received by the circuit breaker logic at 20.4869 seconds after the fault was detected by the relay, and the circuit breakers operated later at 20.4988 seconds.

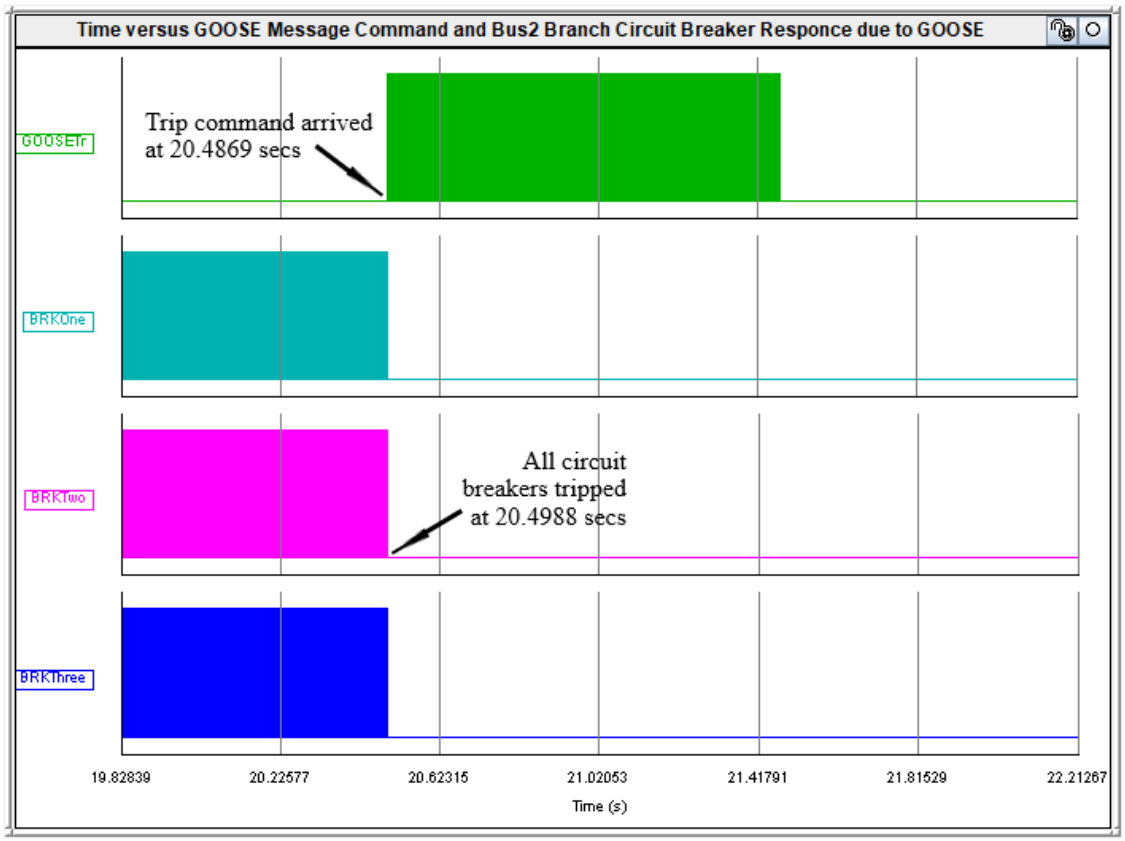

Figure 7.34: CB-received GOOSE trip command for R-G fault at Bus 2 under 420 MW

The time it took for circuit breakers to open after the trip command was received is approximately 11.9 milliseconds.

7.3.2.2 Three-phase-to-ground (3Ph) fault at Bus 2

The Three-phase fault was simulated at Bus 2 while the system was experiencing an increased load demand from 315 MW to 420 MW. The fault was initiated at 20.0018 seconds and got cleared at 20.5306 seconds as shown in Figure 7.35 below on the next page.

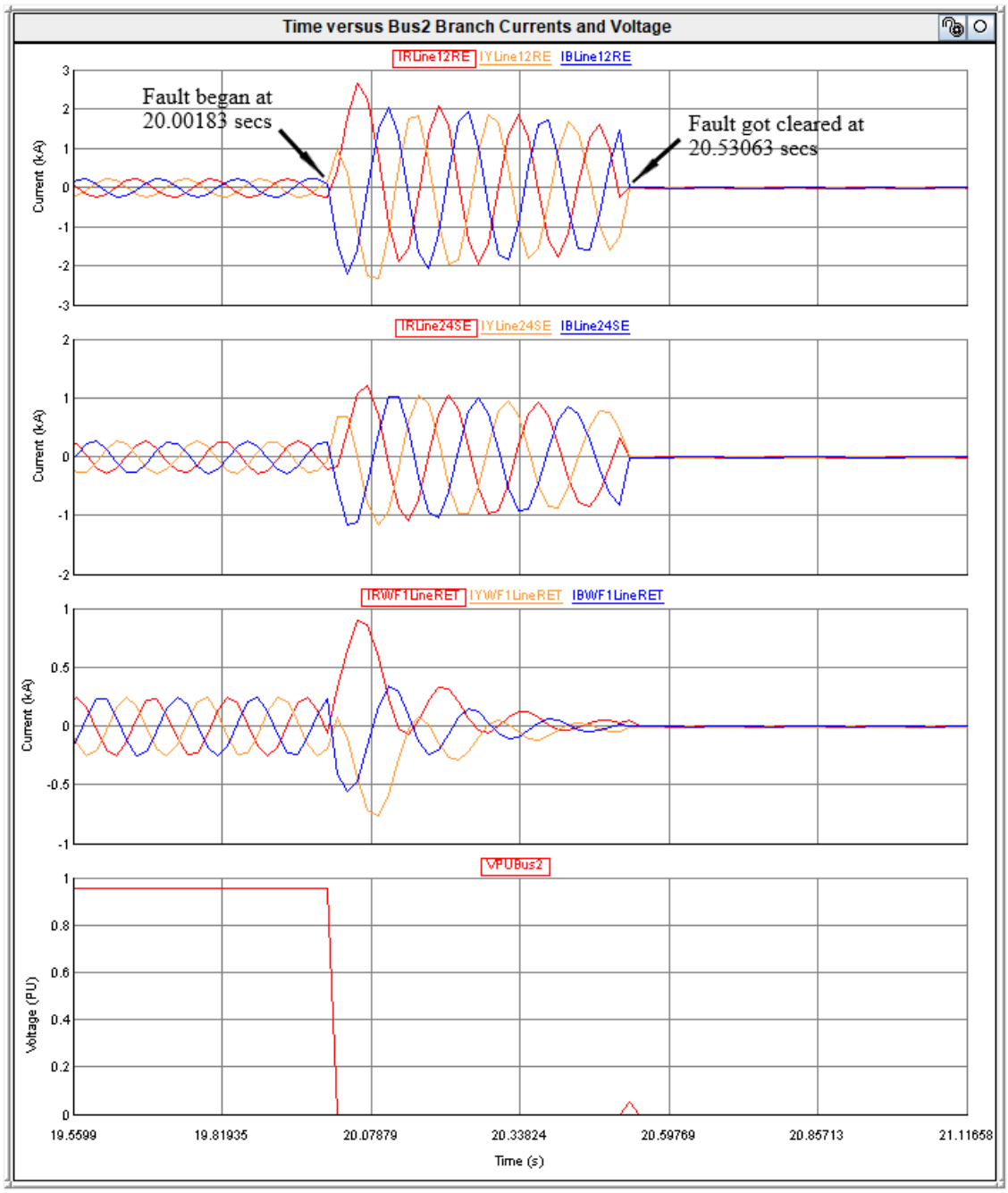

Figure 7.35: **Branch currents and Bus 2 voltage for 3Ph fault at Bus 2 under 420 MW**

The total duration of the fault is 0.5288 seconds, after this time, it was cleared and the busbar was left isolated from the system.

Another waveform is provided in Figure 7.36 below on the next page. Using these plots, the recovery time of the wind power plant receiving-end terminal voltage is analyzed. The disturbance experienced by the wind power plant began at 20.00183 seconds and ended at 63.91097 seconds as shown in the plots. When the faulty busbar was isolated from the system, the wind power plant became free from the fault and remained islanded. After all these events, it took 43.3803 seconds for wind power plant terminal

voltage to stabilize. The value at which it is stabilized is 1.02 per unit and is safe for continuous operation of the wind power plant.

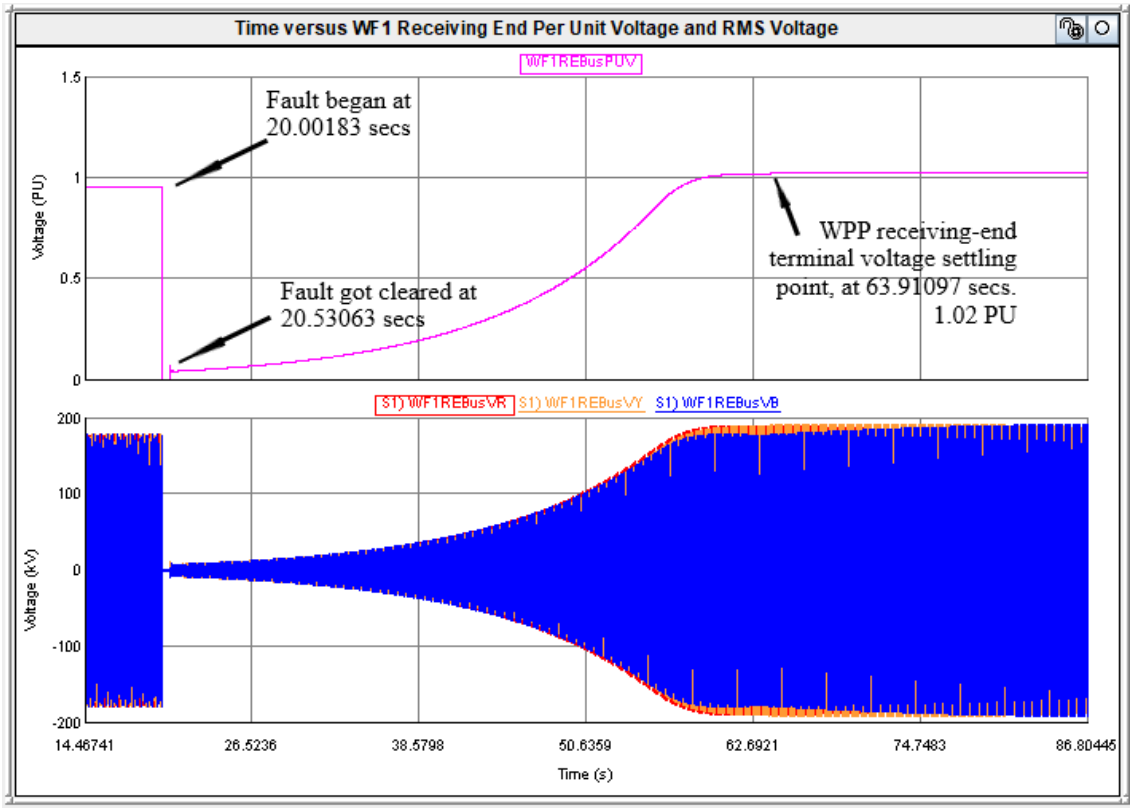

Figure 7.36: **WPP receiving-end voltage for 3Ph fault at Bus 2 under 420 MW**

The circuit breaker control actions were monitored during the test and the results are shown in Figure 7.37 below on the next page. The trip command was received by the circuit breaker logic at 20.52499 seconds after the fault was detected by the relay, and the circuit breakers operated later at 20.529 seconds.

The time it took for circuit breakers to open after the trip command was received is approximately 4.01 milliseconds.

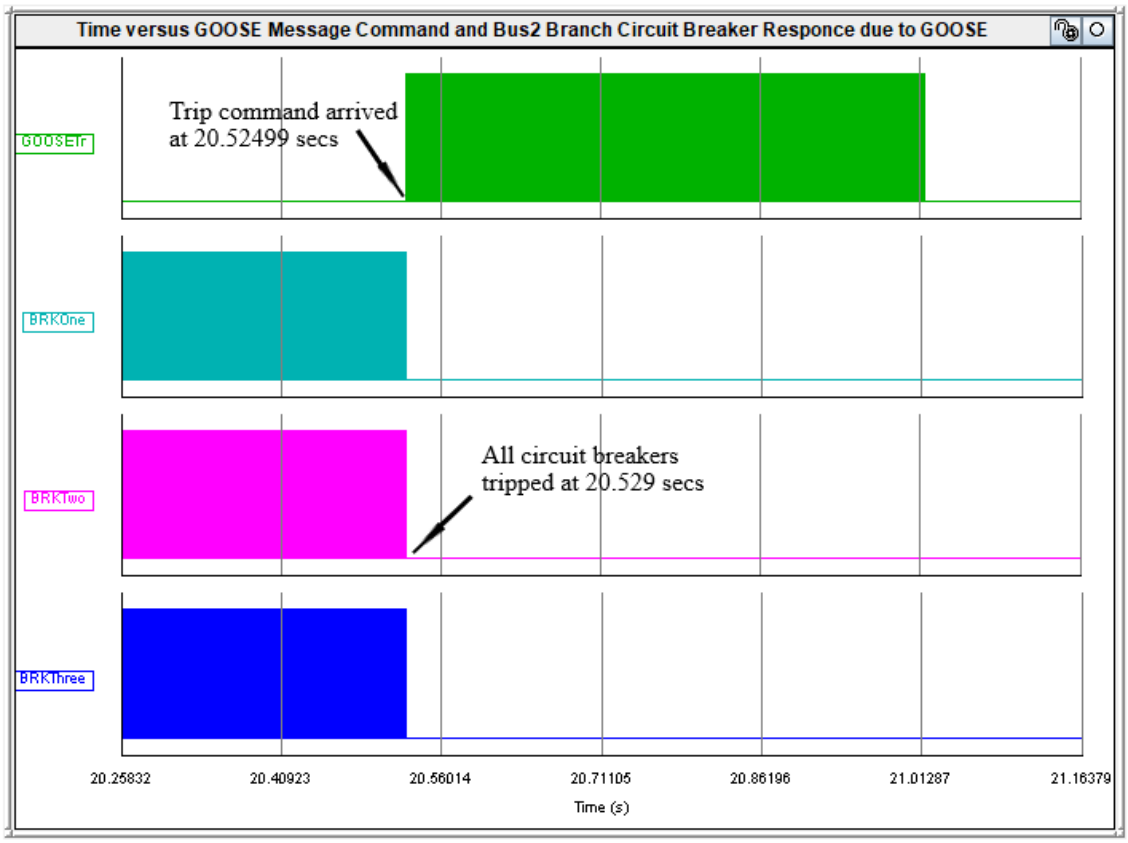

Figure 7.37: CB-received GOOSE trip command for 3Ph fault at Bus 2 under 420 MW

7.4 Summary of results

This section presents in a form of a table (see Table 7.2 below) the summary of results obtained in the previous section.

Table 7.2: Fault event summary

Load condition (MW)	Settings group applied (G1 or G2)	Fault type	Circuit breaker operation in seconds (ms)	Duration of fault clearance in seconds (s)
315	G1	R-G	3.45	0.3666
		3 Ph	9.03	0.3471
420	G2	R-G	11.9	0.4956
		3 Ph	4.01	0.5288

In the above table, the second column indicates the group settings that are applied to the tested types of faults. It is the change from one group to another during the event that proves the adaptability of the scheme. To see the settings group interchange, event reports with monitored currents, voltages and operated and non-operated binary signals, were extracted from the physical device, The snapshots for these events are attached in Appendix F at the end of this document.

7.5 Conclusion

An adaptive protection scheme was developed and tested in Chapter 6 and it worked for conditions of the internal faults at Bus 2 for conditions of the initial loading and proposed loading of the system, which calls for wind power plant operation. In this chapter, the implementation of the IEC 61850 standard is done to replace the hard-wired binary outputs of the relay. The scheme is tested for all the types of faults that were introduced in the previous chapter.

The aim of introducing the communication standard in the protection scheme was to reduce hard-wiring. This hard wiring, in a real power system network, would be implemented using a large number of physical copper wires from the relay's outputs to the circuit breakers situated at the power system process station. That has been achieved and the results obtained from the tests are satisfactory as discussed in Section 7.4.

CHAPTER EIGHT
DELIVERABLES, CONCLUSIONS AND RECOMMENDATIONS

8.1 Introduction

Wind power plant (WPP) integration has become one of the most effective ways of solving voltage stability challenges in the grid. However, this may not be true if the protection scheme used at the point of common coupling fails to provide adaptability.

This thesis focuses on the wind power plant point of common coupling (PoCC) protection scheme, intending to guarantee the effectiveness of wind power plants in overcoming the grid voltage stability challenge. The study involves the design of the protection scheme for a PoCC, and this protection scheme is designed to adapt to the conditions of system operation, that is, when the WPP to the fulfilment of load demand increase and when there is no load increase.

The pre-modelled IEEE Nine-bus system was used as the foundation of the study, and case studies, namely the normal or initial load flows, as well as the load demand increase contingencies of the system, were implemented. Contingencies were used for the investigation of the challenges the power system experiences due to the increased load demand.

The cause of the power system voltage stability challenge was discovered while the load demand contingencies were implemented, and the wind power plant integration was recommended as the most effective practice for a voltage stability challenge in the system. For this reason, the wind power plant was modelled.
The wind power plant was modelled from scratch due to the unavailability of the pre-modelled wind power plants that would suit the selected grid system, while at the same time complying with the grid code requirements.

The modelling and simulations on this thesis were done using the RSCAD and RTDS. The developed protection scheme was tested in the form of a hardware-in-loop (HIL).
In this chapter, the summary of results obtained from the findings due to the deliverables of the thesis is presented. Section 8.2 presents the deliverables of the thesis. Section 8.3 describes the academic and industrial application of this study. Section 8.4 proposes the future research work within the wind power plants and protection schemes involved. Section 8.5 is the reference of the journal sent for publication.

8.2 Thesis deliverables

This section gives a summary of the deliverables undergone to accomplish the study.

8.2.1 Literature review

The literature was done, to effectively explore the challenges power system protection schemes undergo due to the integration of wind power plants into the power systems.

The online digital library, books, and other sources show a lot of concerns raised by the electrical power utilities about the issues wind farms bring to the existing power supply networks. Therefore, they are a part of the material used for the construction of the literature review chapter in this thesis.

This literature reviewed in this thesis focuses on the information presented in peer-reviewed journals and written-books, in the hope that the findings are based more on the complete search and organized breakdown of the raised issues.

8.2.2 Theoretical framework

The theory developed in this thesis explains some of the key concepts of power system voltage stability challenges, models and assumptions made for wind power plants and protection schemes. The online digital library, books and other sources contain theories about the power system protection challenges due to the integration of wind power plants that have been used.

8.2.3 Modelling and simulation of the IEEE Nine-bus system on RSCAD

One of the requirements in power system stability and protection studies is the selection of the power system network model. For this reason, the IEEE Nine-bus system was selected, modelled and simulations cases were conducted for normal load flows and increased load demand contingency when the challenges the power systems undergo in terms of voltage stability were investigated.

8.2.4 Modelling and simulation of the wind power plant on RSCAD

The wind power plant was modelled using the data from Vestas for a wind turbine model, and the literature by the reference (B. Wu, Y. Lang, N. Zargari, 2011) for a squirrel-cage induction generator (SCIG). Load flows were implemented as part of the grid code compliance test using the RSCAD Runtime module.

8.2.5 Modelling and simulation of coupled WPP into the IEEE Nine-bus system

The wind power plant was integrated into the IEEE Nine-bus system. Normal load flows and the increased load demand contingencies were implemented. The load increase

contingency was done to evaluate the wind power plant's contribution in terms of voltage stability improvement.

8.3 Conclusions

This section gives a summary of the conclusions about the study.

8.3.1 The development of a protection scheme for the coupled system

The integration of the wind power plant into the grid has improved the voltage stability, and the proposed amount of load demand was fulfilled. The current flow through the point of common coupling (PoCC) due to initial and increased load demand is not the same, and the difference is too high to be ignored. Because the system has to be operated under both conditions, depending on the system load requirements, the protection scheme was developed, to be effective under these conditions.

The instrument transformers were selected and configured. In addition to that, gigabyte transceiver analog output (GTAO) cards were configured and this was for sampling the virtually simulated power system quantities, namely voltages and currents. From the GTAO card configuration, hardware devices were used, for amplification of analog signals generated by GTAOs. These signals are required for physical protective device interface with RTDS devices for control and protection of the virtual power system simulated in RTDS.

The SEL-487B Protection Automation and Control physical device was configured for an adaptive protection scheme using two settings group to ensure the adaptability of the scheme.

8.3.2 Advancement of the developed protection scheme

The protection scheme summarized in Section 8.2.6 makes use of hard-wired binary output signals to control and protect the coupled power system. This part describes the major steps taken to advance the protection scheme described in Chapter 7.

The binary output signals from hard-wired protective devices use digital contacts and this method is based on the American National Standards Institute (ANSI) codes for protection relay word bits. IEC 61850-7-2 defines the logical nodes (LNs) to replace the hard-wired communicated binary output signals. This method replaces the ANSI code relay word bits with LNs (Umbrella term for data attributes) that are published through Ethernet for use by field devices.

The SEL-487B relay for a protection scheme described in this part, instead of using digital output wires for sending trip signals to RTDS, uses the data attributes that are sent through Ethernet to the RTDS for control and protection of the virtual system. This is how the IEC 61850 Standard-based protection scheme was implemented.

8.3.3 Testing of the developed protection scheme

Two methods of communication were implemented for the designed protection scheme, which are hard-wired and Ethernet-based for control and protection of the power system, and are presented in Chapters, 6 and 7 respectively. In Chapter 6, the protection scheme uses hard-wired binary outputs. In Chapter 7, the Generic Object-Oriented Substation Event (GOOSE) control model is used for communication through Ethernet.

For both communication mediums, Red-phase-to-ground and Three-phase faults are simulated and the results are provided for initial loading and the proposed loading of 420 MW.

8.4 Academic and industrial application

In this thesis, a wind power plant model that can be used by other scholars in their research due to its compliance with the grid code requirements has been developed. The developed protection scheme will be added to one of the practical implementations of the digital protective device tests set up for students in the Protection Technology class. In addition, the test bench setup developed for this study can be used in demonstrations and training for students and industrial people.

The study makes use of Real-time digital simulator (RTDS) devices for its simulations. These devices allow the interface of the physical protective devices with the virtual simulated power systems, and this provides effective testing of the protection devices. As much as the technology grows, in academics, it will be better to apply such a test bench set up to bring into vision how the power systems protection devices work, since this setup mimics the real-world power system protective device response towards power system disturbances, to advance their knowledge.

8.5 Future work

The study focused more on the protection side. The stability of power systems was just used as the foundation to simulate or calculate the voltage instability point. After the determination of the instability point, the decision was made, to integrate the wind power plant into the grid system to improve the busbar voltages, while at the same time fulfilling the required amount of power due to the load demand increase.

The wind power plant consists of the control algorithms, namely proportional integral derivatives (PIDs), Fuzzy controllers, etcetera for optimization of the output power based on the available amount of input power due to wind. The wind power plant modelled in this thesis does not include these control algorithms. Though this does not affect the study, in the future, a wind power plant consisting of these control algorithms will be modelled and this will make it fit in many applications, namely the study where the variation of input power is considered a major factor to the system.

The protection scheme developed in this thesis looks only at the conditions of the increased load demand and changes its settings automatically to the desired configuration that suits the current (in amps) flow at that time. The case whereby the load is decreased is not considered. In the future, the load demand decrease after it has increased will be considered, and the protection scheme to accommodate such a condition will be developed.

8.6 Publication

The paper titled “The Wind Power Plant Modelling for the Conditions of Grid-connected Mode”, by the authors, S. Nomandela, M. Ratshitanga, M.E.S. Mnguni has been submitted for a peer-review to the IEEE Journal on the 10th of November 2020.

BIBLIOGRAPHY

A. Ahmed, M. & Kim, C.-H. 2017. Communication Architecture For Grid Integration Of Cyber-Physical Wind Energy Systems. *Applied Sciences*, 7(10): 1034.

Ahmed, M.A. & Kim, Y.C. 2014. Communication Network Architectures For Smart-Wind Power Farms. *Energies*, 7(6): 3900–3921.

Alcázar, E., Juárez, J., Loza, P. & Altuve, H.J. 2016. Protection System For A Wind Generation Plant In Panama: Challenges And Solutions. In *69th Annual Conference For Protective Relay Engineers*.

Altuve, H.J., Zimmerman, K. & Tziouvaras, D. 2017. Maximizing Line Protection Reliability, Speed, And Sensitivity. In *69th Annual Conference For Protective Relay Engineers, CPRE 2016*. IEEE.

Andrichak, J. & Cardenas, J. 1995. Bus Differential Protection. In *Twenty Second Annual Western Protective Relay Conference*.

Apostolov, A. 2014. The Impact Of Iec 61850 On Transmission And Distribution Substations Busbar Protection. *12th Iet International Conference On Developments In Power System Protection, Dpsp 2014*: 1–6. Https://Www.Mendeley.Com/Catalogue/1378c7f8-029b-30ce-A972-F088889365e3/?Utm_Source=Desktop&Utm_Medium=1.19.8&Utm_Campaign=Open_Catalog&Userdocumentid=%7bb38713d0-2807-48b1-858f-516a07b73370%7d.

B. Wu, Y. Lang, N. Zargari, And S.K. 2011. Power Conversion And Control Of Wind Energy Systems: Appendix B: Generator Parameters. In *Wind Energy*. 319–326. Https://Www.Mendeley.Com/Catalogue/86d24440-161e-3ebf-B2f6-2dfa184879a4/?Utm_Source=Desktop&Utm_Medium=1.19.8&Utm_Campaign=Open_Catalog&Userdocumentid=%7bfc562248-260f-4af1-9b56-1f9291dcaf60%7d.

Bajanek, T. 2014. Overcurrent Protection Relay Model Using IEC 61850-9-2 Sampled Values. *Proceedings Of The 2014 15th International Scientific Conference On Electric Power Engineering, EPE 2014*: 101–106.

Behrendt, K., Costello, D. & Zocholl, S.E. 2010. Considerations For Using High-Impedance Or Low-Impedance Relays For Bus Differential Protection. *2010 63rd Annual Conference For Protective Relay Engineers*.

Brand, K.-P. 2005. The Standard IEC 61850 As Prerequisite For Intelligent Applications In Substations. In *IEEE Power Engineering Society General Meeting, 2004.* IEC: 714–718.

Brand, K., Brunner, C. & Mesmaeker, I. De. 2005. How To Use Iec61850 In Protection And Automation. *Electra*, (222): 11–21.

Brunner, C. 2005. Iec 61850 Process Connection - A Smart Solution To Connect The Primary Equipment To The Substation Automation System. In *15th Power System Computation Conference*. 22–26.

Cai, R. & Su, B. 2011. Study On Protection Of Large Scale Wind Power Integration. *Apap 2011 - Proceedings: 2011 International Conference On Advanced Power System Automation And Protection*, 3: 1718–1722.

Cardenas, J., Muthukrishnan, V., Mcginn, D. & Hunt, R. 2010. Wind Farm Protection Using An Iec 61850 Process Bus Architecture. In *IET Conference Publications*. 3–7.

Chandraratne, C., Woo, W.L., Logenthiran, T. & Naayagi, R.T. 2019. Adaptive Overcurrent Protection For Power Systems With Distributed Generators. *2018 8th International Conference On Power And Energy Systems, ICPES 2018*: 98–103.

Chothani, N. & Bhalja, B. 2011. A New Differential Protection Scheme For Busbar Considering Ct Saturation Effect. *Canadian Conference On Electrical And Computer Engineering*: 000007–000010.

Davidson, I.E. 2017. Introduction To The South African Renewable Energy Grid Code Version 2 . 9 Requirements. *IEEE Africon 2017 Proceedings*: 1263–1267.

Dhivya, S. & Sakthivel, K. 2018. Timing Test Of High Voltage Three Phase Circuit Breaker Using Digital Time Pulse Conversion Method. *International Journal Of Pure And Applied Mathematics*, 119(12): 301–312. www.ijpam.Eu.

Emmanuel Olufemi, O., Rezaei, N., Lutfi Othman, M., Abdul Wahab, N.I. & Hizam, H. 2017. Wind Power Plants Protection Using Overcurrent Relays. *Universal Journal Of Electrical And Electronic Engineering*, 2(8): 311–319.

Fernandes, C., Borkar, S. & Gohil, J. 2014. Testing Of Goose Protocol Of Iec61850 Standard In Protection Ied. *International Journal Of Computer Applications*, 93(16): 30–35.

Gashi, A., Kabashi, G., Kabashi, S., Ahmetaj, S. & Veliu, V. 2012. Simulation The Wind Grid Code Requirements For Wind Farms Connection In Kosovo Transmission Grid. *Energy And Power Engineering*, 04(06): 482–495.

Gupta, G. 2018. *An Analysis And Improvement Of Selected Features Of Power Quality Of Grid-Tied Alternative Energy Systems*. The Cape Peninsula University Of Technology.

Guzmán, A., Qin, B.L. & Labuschagne, C. 2005. Reliable Busbar Protection With Advanced Zone Selection. *IEEE Transactions On Power Delivery*, 20(2 I): 625–629.

Han, A., Zhang, Z. & Yin, X. 2010. The Impacts Of Distributed Doubly-Fed Induction Generators On Smart Distribution Grid Protection. *Modelling, Identification And Control (Icmic), The 2010 International Conference On*: 71–75.

Hughes, R. 2005. Numerical Busbar Protection Benefits Of Numerical Technology In Electrical Substation. *Developments In Power System Protection*, (479): 463–466.

Iec. 2003. Communication Networks And Systems In Substations. *IEC Standard*.

International Electrotechnical Commission. 2004. Communication Networks And Systems In Substations - Part 8-1: Specific Communication Service Mapping (Scsm) - Mappings To Mms (ISO 9506-1 And ISO 9506-2) And To ISO/IEC 8802-3. *IEC*, 1: 131. Https://Webstore.Iec.Ch/Publication/6021.

Jones, D. & Bennett, K. 2012. Wind Farm Collector Protection Using Directional Overcurrent Elements. *Proceedings Of The IEEE Power Engineering Society Transmission And Distribution Conference*: 1–8.

Kanabar, M.G. & Sidhu, T.S. 2011. Performance Of Iec 61850-9-2 Process Bus And Corrective Measure For Digital Relaying. *IEEE Transactions On Power Delivery*, 26(2): 725–735.

Kaneda, K., Tamura, S., Fujiyama, N., Arata, Y. & Ito, H. 2008. Iec61850 Based Substation Automation System. *2008 Joint International Conference On Power System Technology Powercon And Ieee Power India Conference, Powercon 2008*.

Kauhaniemi, K., Voima, S. & Laaksonen, H. 2014. Adaptive Protection Scheme For Smart Grids. In *Iet Conference Publications*. 12.66-12.66. Https://Www.Mendeley.Com/Catalogue/25f5bafc-D987-3b0b-B356-B991f1364b83/?Utm_Source=Desktop&Utm_Medium=1.19.8&Utm_Campaign=Open_Catalog&Userdocumentid=%7bc016a85e-F872-47b6-A22f-A39fdd29a4b7%7d.

Kawady, T.A., Mansour, N.M. & Taalab, A.I. 2008. *Wind Farm Protection Systems: State Of The Art And Challenges*. Intechopen.

Khoddam, M. & Karegar, H.K. 2011. Effect Of Wind Turbines Equipped With Doubly-Fed Induction Generators On Distance Protection. *Apap 2011 - Proceedings: 2011 International Conference On Advanced Power System Automation And Protection*, 2: 1349–1353.

Koshiishi, K., Kaneda, K. & Watabe, Y. 2012. Interoperability Experience With Iec 61850-Based Substation Automation Systems. *Proceedings Of The Ieee Power Engineering Society Transmission And Distribution Conference*: 1–5.

Kundur, P. 1993. *Power System Stability And Control*. First Edition. J. B. Naal & G. L. Mark, Eds. New York: Mcgraw.

Ledesma, P. & Usaola, J. 2001. Minimum Voltage Protections In Variable Speed Wind Farms. *2001 IEEE Porto Power Tech Proceedings*, 4: 240–246.

Li, J., He, J.H., Zhang, H., Xie, F., Bo, Z.Q. & Yip, T. 2011. Research On Adaptive Protection Based On Integrated Protection. *Apap 2011 - Proceedings: 2011 International Conference On Advanced Power System Automation And Protection*, 2: 848–852.

Lin, X.N., Lu, W., Tian, Q., Weng, H. & Liu, P. 2006. A Novel Duplicated Main Protection Scheme Suitable For Both Transmission Lines And Busbars. *2006 IEEE Power Engineering Society General Meeting, Pes*: 1–7.

Liu, J. & Dawalibi, F.P. 2010. Wind Turbine Farm Network Grounding Design Using Integrated Simulation Methods And Techniques. *Proceedings - International Conference On Future Power And Energy Engineering, Icfpee 2010*: 99–102.

Ma, J., Li, J. & Wang, Z. 2010. An Adaptive Distance Protection Scheme For Distribution System With Distributed Generation. *2010 5th International Conference On Critical Infrastructure, Cris 2010 - Proceedings*, (1): 1–4.

Ma, J., Zhang, W., Liu, J. & Thorp, J.S. 2018. A Novel Adaptive Distance Protection Scheme For Dfig Wind Farm Collector Lines. *International Journal Of Electrical Power And Energy Systems*, 94: 234–244. Http://Dx.Doi.Org/10.1016/J.Ijepes.2017.07.008.

Mackiewicz, R.E. 2006. Overview Of Iec 61850 And Benefits. *2006 IEEE PES Power Systems Conference And Exposition, Psce 2006 - Proceedings*, 57(57): 623–630.

Mahmoud, M.S. & Oyedeji, M.O. 2017. Optimal Control Of Wind Turbines Under Islanded Operation. *Intelligent Control And Automation*, 08(01): 1–14.

Marison, G., Gao, B. & Kundur, P. 1993. Voltage Stability Analysis Using Static And Dynamic Approaches. In *IEEE Transactions On Power Electronics*. 1159–1171.

Medeiros, R.P., Costa, F.B. & Silva, K.M. 2016. Power Transformer Differential Protection Using The Boundary Discrete Wavelet Transform. *IEEE Transactions On Power Delivery*, 31(5): 2083–2095.

Mekkanen, M., Virrankoski, R., Elmusrati, M. & Antila, E. 2014. Analysis And Methodology For Measuring The Iec61850 Goose Messages Latency: Gaining Interoperability Testing. *2014 World Congress On Computer Applications And Information Systems, Wccais 2014*: 1–6.

Mnguni, M.E.S. 2014. *Investigation Of The Application Of Iec 61850 Standard In Distribution Busbar Busbar Protection Schemes*. The Cape Peninsula University Of Technology. Https://Cput.Primo.Exlibrisgroup.Com/Discovery/Fulldisplay?Docid=Alma994215435204036&Context=L&Vid=27cput_Inst:Cput&Lang=En&Search_Scope=Myinst_And_Ci&Adaptor=Local Search Engine&Isfrbr=True&Tab=Everything&Query=Any,Contains,Mnguni Busbar&Sortby=Date_D&Facet=Frbrgroupid,Include,9075630023457146882&Offset=0.

Mohan, S.M. & Chatterjee, S. 2010. Busbar Protection - A Review. *Proceedings - 2010 Ieee Region 8 International Conference On Computational Technologies In Electrical And Electronics Engineering, Sibircon-2010*: 755–759.

Moxley, R. & Becker, F. 2018. Adaptive Protection - What Does It Mean And What Can It Do? *71st Annual Conference For Protective Relay Engineers, Cpre 2018*, 2018-Janua: 1–4.

Nahhas, T.A.K. And A.M. 2013. Modelling Issues Of Grid-Integrated Wind Farms For Power System Stability Studies. *Chapter 8*.

Niwas, S., Singh, S., Ostergaard, J. & Jain, N. 2009. Distributed Generation In Power Systems: An Overview And Key Issues. *Citation*. Http://Orbit.Dtu.Dk/Files/5202512/24iec_Paper.Pdf.

Pradhan, A.K. & Joós, G. 2007. Adaptive Distance Relay Setting For Lines Connecting Wind Farms. *Ieee Transactions On Energy Conversion*, 22(1): 206–213.

Ray, S. 2007. *Electrical Power Systems: Concepts, Theory And Practice*. 1st Editio. Prentice-Hall Of India Private Limited, New Delhi.

Reis, C., Andrade, A. & Maciel, F.P. 2009. Voltage Stability Analysis Of Electrical Power System. *Powereng 2009 - 2nd International Conference On Power Engineering, Energy And Electrical Drives Proceedings*, 0: 244–248.

Rekik, M., Abdelkafi, A. & Krichen, L. 2015. Synchronization Of Wind Farm Power System To Utility Grid Under Voltage And Frequency Variations. *International Journal Of Renewable Energy Research*, 5(1): 70–81.

Richter, B. & Lepa, E. 2012. Overvoltage Protection In Wind Power Farms. *2012 31st International Conference On Lightning Protection, ICLP 2012*: 1–5.

Rtds Technologies. 2019a. Excitation System. : 82–83.

Rtds Technologies. 2019b. Governor System. : 01–02.

Saad, S.M., Elhaffar, A. & El-Arroudi, K. 2015. Optimizing Differential Protection Settings For Power Transformers. *2015 Modern Electric Power Systems (Meps)*: 1–6.

Samitier, C. 2017. Utility Communication Networks And Services: Chapter 2: 7–10. Http://Link.Springer.Com/10.1007/978-3-319-40283-3.

Sel. 2018. Sel-487b-1 Bus Differential And Breaker Failure Relay Instruction Manual. : 718.

Sewchurran, S. & Davidson, I.E. 2017. Introduction To The South African Renewable Energy Grid Code Version 2.9 Requirements (Part Ii - Grid Code Technical Requirements).

2017 IEEE Africon: Science, Technology And Innovation For Africa, Africon 2017: 1225–1230.

Siniscalchi-Minna, S., Bianchi, F.D., De-Prada-Gil, M. & Ocampo-Martinez, C. 2019. A Wind Farm Control Strategy For Power Reserve Maximization. *Renewable Energy*, 131: 37–44.

Song, E.Y., Lee, K.B., Fitzpatrick, G.J. & Zhang, Y. 2017. Interoperability Test For Iec 61850-9-2 Standard-Based Merging Units. *2017 Ieee Power And Energy Society Innovative Smart Grid Technologies Conference, ISGT 2017*.

Song, X., Meng, Z., Chang, K., Xue, F. & Zhou, L. 2012. Dynamic Reactive Power Compensation During Fault Conditions For Wind Farms With The Consideration Of Wind Turbine Protection Effects. In *Iet Conference Publications*. 120–120.

Sun, F., Zhang, Y., Faried, S.O., Wheeler, K. & Elsamahy, M. 2018. Impact Of Dfig-Based Wind Farms On Generator Distance Phase Backup Protection. *2017 Ieee Pes Innovative Smart Grid Technologies Conference Europe, ISGT-Europe 2017 - Proceedings*, 2018-Janua: 1–6.

Tart, N., An, W. & French, K. 2010. A Transmission Utility's Experience To Date With Numerical Busbar Protection Systems. *IET Conference Publications*, 2010(558 Cp).

Vasantharathna, S. 2016. *Electric Power Systems*. 5th Editio. John Willey And Sons.

Wang, J., Zhang, B.H., Hao, Z.G., Li, G.H., Bo, Z.Q., Writer, D. & Yip, T. 2011. Fault Features Of Centrally Integrated Wind Farms. *2011 10th International Conference On Environment And Electrical Engineering, EEEIC.EU 2011 - Conference Proceedings*: 2–5.

Wenhao, Z., Lijun, J.I.N. & Shujia, Y.A.N. 2011. An Adaptive Relaying Algorithm For The Protection Of Distribution Networks Integrated With Wind Farms. *2011 International Conference On Advanced Power System Automation And Protection*, 1: 564–567.

Wu, C. & Yu, Q. 2018. Analysis And Countermeasure Of Delay Of Line Differential Protection Caused By Ct Transient Saturation In Faults In Wind Farms. *2018 Chinese Automation Congress (CAC)*: 3209–3212.

Xu, L., Grasset, H., Dong, X., Xu, C. & Xu, R. 2010. A New Method For Busbar Protection Stability Improvement. *IET Conference Publications*, 2010(558 Cp).

Xu, Z.Y., Xu, G., Ran, L., Yu, S. & Yang, Q.X. 2010. A New Fault-Impedance Algorithm For Distance Relaying On A Transmission Line. *IEEE Transactions On Power Delivery*, 25(3): 1384–1392.

Yang, J., Fletcher, J.E. & O'reilly, J. 2010. Multiterminal Dc Wind Farm Collection Grid Internal Fault Analysis And Protection Design. *Ieee Transactions On Power Delivery*, 25(4): 2308–2318.

Zhang, B.H., Guo, D.Y., Huang, R.M. & Wu, W.M. 2013. Single-Phase-To-Ground Fault Detection In Wind Farm Collector Line Using Transient Phase Current Criterion. *IEEE Region 10 Annual International Conference, Proceedings/Tencon*: 1–4.

Zheng, T.Y., Cha, S.T., Crossley, P.A. & Kang, Y.C. 2011. Protection Algorithm For A Wind Turbine Generator Based On Positive- And Negative-Sequence Fault Components. *APAP 2011 - Proceedings: 2011 International Conference On Advanced Power System Automation And Protection*, 2: 1115–1120.

APPENDICES
APPENDIX A
THE IEEE NINE-BUS SYSTEM PARAMETERS

The simulation studies were done based on the IEEE Nine-bus system whose parameters are listed below. The given power flow data of the system is derived using the base of 100 MVA.

A.1 System data

Table A.1, A.2, and A.3 presents the initial power flow data, transmission line, and transformer data. The low-voltage side of each step-up transformer is a delta (mesh) configuration, and the high-voltage side is a star.

Table A.1: Initial power flow data

Bus	Bus type	Voltage (pu)	P_G (MW)	Q_G (MVAr)	P_L (MW)	Q_L (MVAr)
G1Bus	**Slack**	1.040∠0.0°	71.6	27.0	-	-
G2Bus	**PV**	1.025∠9.3°	163.0	6.7	-	-
G3Bus	**PV**	1.025∠4.7°	85.0	-10.9	-	-
Bus1	**PQ**	1.026∠-2.2°	-	-	-	-
Bus2	**PQ**	0.996∠-4.0°	-	-	125.0	50.0
Bus3	**PQ**	1.013∠-3.7°	-	-	90.0	30.0
Bus4	**PQ**	1.026∠3.7°	-	-	-	-
Bus5	**PQ**	1.016∠0.7°	-	-	100.0	35.0
Bus6	**PQ**	1.032∠2.0°	-	-	-	-
Total			319.6	22.8	315.0	115.0

Table A.2: Transmission line data

Line	Length (km)	Resistance (pu)	Reactance (pu)	Susceptance (pu)
12	89.93	0.0100	0.0850	0.1760
13	97.336	0.0170	0.0920	0.1580
24	170.338	0.0320	0.1610	0.3060
36	179.86	0.0390	0.1700	0.3580
45	76.176	0.0085	0.0720	0.1490
56	106.646	0.0119	0.1008	0.2090

Table A.3: Transformer data

Transformer	Resistance (pu)	Inductive reactance (pu)	Tap ratio	Voltage (kV) LV/HV
1	0.0	0.0576	1	16.5/230
2	0.0	0.0625	1	18/230
3	0.0	0.0586	1	13.8/230

A.2 Forceful data

The IEEE Nine-bus system has three generators with their controllers, governors and exciter controllers. Tables A.4 and A.5 show the generator data.

Table A.4: Generator data

Gen	Bus	Per Unit Quantities						
		Xa (pu)	Xd (pu)	Xd' (pu)	Xd"	Xq	Xq'	Xq"
1	**G1Bus**	0.01460	0.1460	0.0608	0.06	0.1000	0.0969	0.06
2	**G2Bus**	0.08958	0.8958	0.1198	0.11	0.8645	0.1969	0.11
3	**G3Bus**	0.13125	1.3125	0.1813	0.18	1.2578	0.2500	0.18

In the above table, Xa, Xd, Xd', Xd", Xq, Xq' and Xq" are stator leakage reactance, D-axis unsaturated reactance, D-axis unsaturated transient reactance, D-axis unsaturated sub-transient reactance, Q-axis unsaturated reactance, Q-axis unsaturated transient reactance, and Q-axis unsaturated sub-transient reactance in per unit.

Table A.5: Generator data

Gen	Bus		Seconds Quantities					
		Ra (pu)	Tdo'	Tdo"	Tqo'	Tqo"	H	D (pu/pu)
1	**G1Bus**	0.000125	8.96	0.01	0.310	0.01	23.64	0.0
2	**G2Bus**	0.000125	6.00	0.01	0.535	0.01	6.40	0.0
3	**G3Bus**	0.000125	5.89	0.01	0.600	0.01	3.01	0.0

In the above table, Ra (pu), Tdo', Tdo", Tqo', Tqo" and H, D (pu/pu) is stator resistance in per unit, D-axis unsaturated transient open-circuit time constant, D-axis unsaturated sub-transient open-circuit time constant, Q-axis unsaturated transient open-circuit time

constant, Q-axis unsaturated sub-transient open-circuit time constant, inertia constant, and synchronous mechanical damping.

A.3 Synchronous generator excitation and propelling model

Synchronous generators require prime for their operation. For a synchronous machine to produce power, it requires the excitation circuits on its rotor windings. This excitation is done using the direct current (DC) source. RSCAD has the component model for the excitation system, it is used to represent field-controlled DC commutator exciters with continuously acting voltage regulators. These voltage regulators use power sources that are not affected by brief transients on the synchronous machine (RTDS Technologies, 2019a). The synchronous generator exciter model is shown in Figure A.1 below.

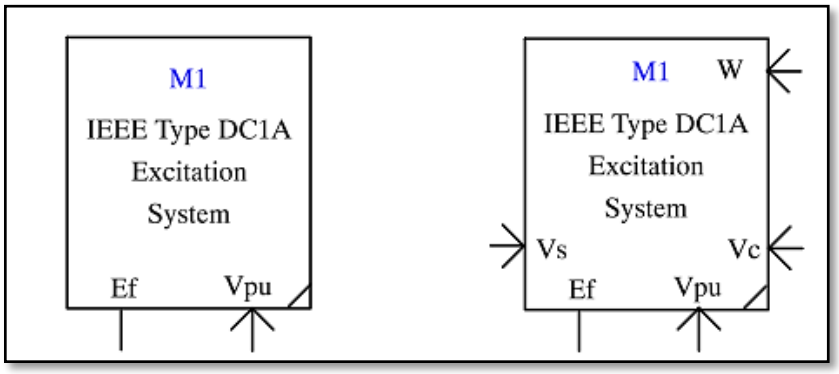

Figure A.1: Synchronous generator exciter model

Some of the parameters shown in the above figure are Ef (per unit field voltage), Vpu (per unit generator stator terminal voltage), Vs (machine output speed) and W (angular rotational speed of the rotor in radians per second). For the synchronous generator rotor to turn, it is driven by the prime mover. RSCAD has a component modelled to represent the prime mover. Figure A.2 shows the synchronous machine governor or propeller model. Tm is the mechanical torque per unit.

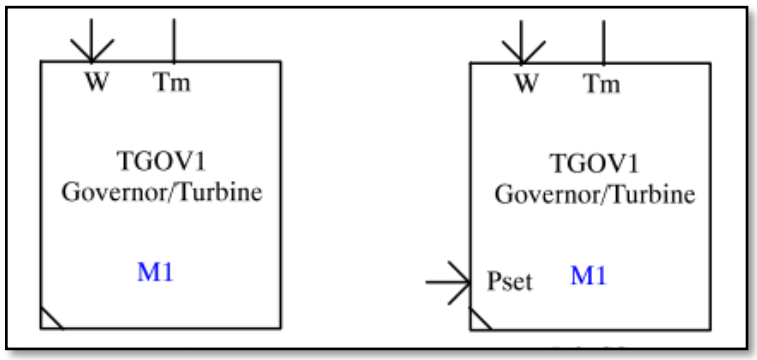

Figure A.2: synchronous machine governor or propeller model

In Table A.6, parameters Ka, Ta, VRmin, VRmax, Ke, Te, Kf, and Tf are gain, minimum controller output, maximum controller output, exciter field resistance line slope margin, exciter time constant, rate feedback gain, and rate feedback time constant.

Table A.6: Exciter data

Gen	Ka	Ta	VRmin	VRmax	Ke	Te	Kf	Tf
1	20.0	0.2	-5.0	5.0	1.0	0.314	0.063	0.35
2	20.0	0.2	-5.0	5.0	1.0	0.314	0.063	0.35
3	20.0	0.2	-5.0	5.0	1.0	0.314	0.063	0.35

In Table A.6, parameters E1, S (E1), E2, and S (E2) are values of E at SE1 (E1), SE at E1 (SE1), E at SE2 (E2) and SE at E2 (SE2).

Table A.7: Exciter data

Gen	E1	S (E1)	E2	S (E2)
1	3.3	0.6602	4.5	4.2662
2	3.3	0.6602	4.5	4.2662
3	3.3	0.6602	4.5	4.2662

Table A.8 shows the parameters of the component model used to drive the synchronous machine model (RTDS Technologies, 2019b). R, T1, Vmax, Vmin, T2, T3, and Dt are permanent droop, governor time constant, maximum valve position, minimum valve position, the time constant of high-pressure fraction, reheater time constant, and turbine damping coefficient.

Table A.8: Governor data

Gen	R	T1	Vmax	Vmin	T2	T3	Dt
1	0.05	0.05	5.00	-5.00	2.1	7.0	0.0
2	0.05	0.05	5.00	-5.00	2.1	7.0	0.0
3	0.05	0.05	5.00	-5.00	2.1	7.0	0.0

APPENDIX B
THE SYSTEM LOAD SCHEDULER

The dynamic loads used makes use of scheduler components that perform the multiplication-by-factor-over-time function. The two most important settings are defined in the load scheduler component, namely the initial power the load must draw, and the time at which the transition from one value to another should occur. Section B.1 shows typical settings.

B.1 Dynamic Load 1 (DLoad1) Typical settings

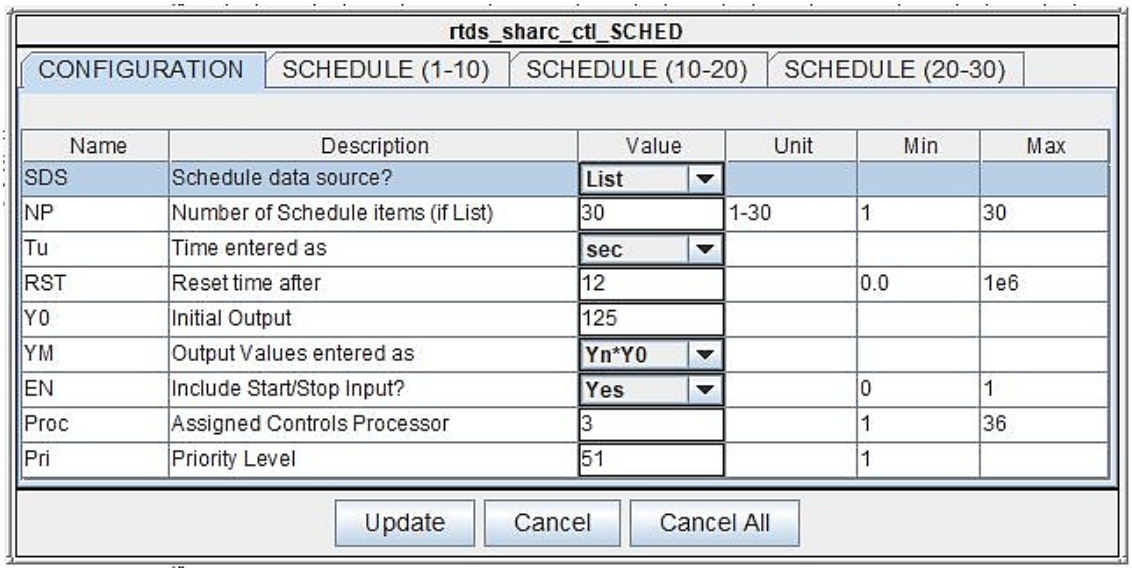

Figure B.1: Dynamic Load 1 scheduler configuration settings

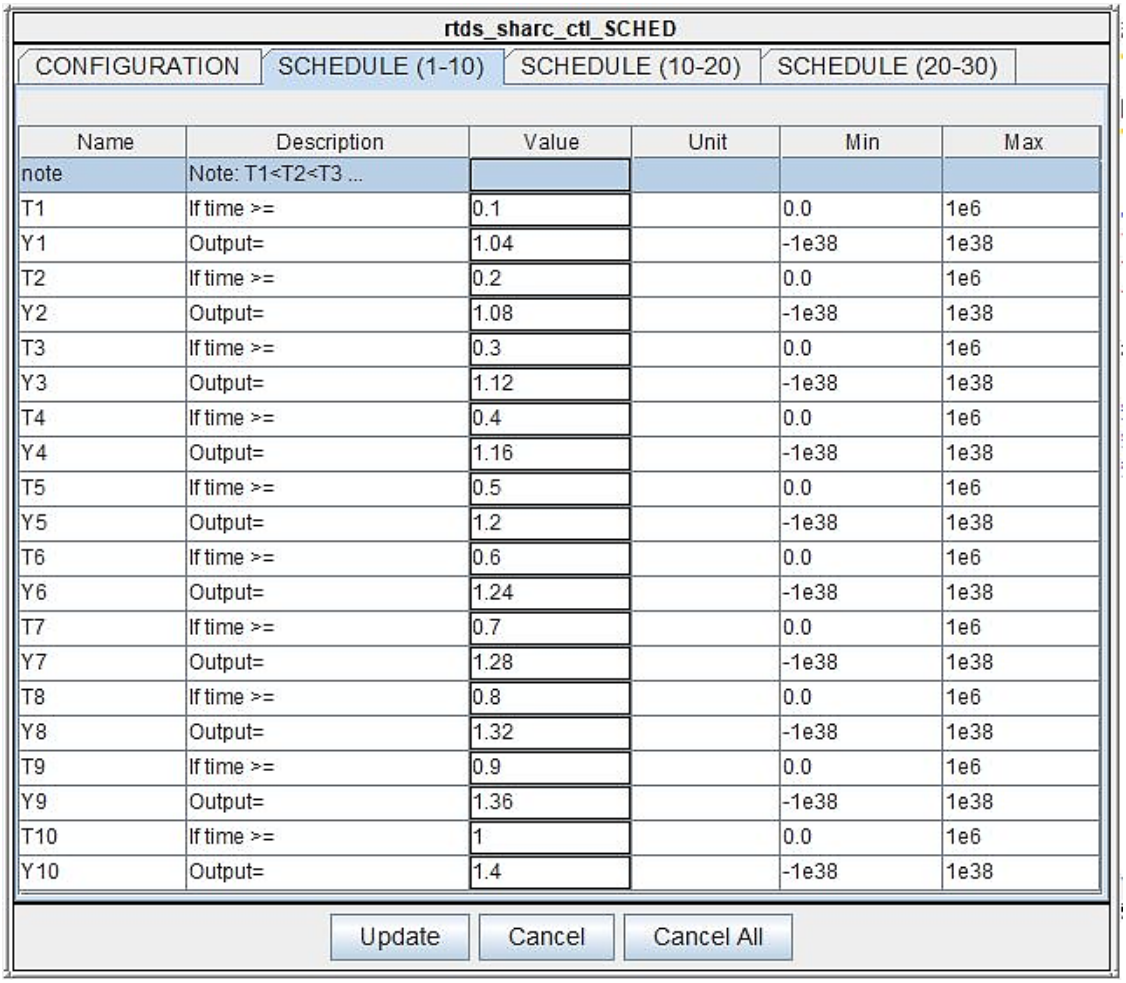

Figure B.2: Dynamic Load 1 (1-10) schedule (time and values) configuration settings

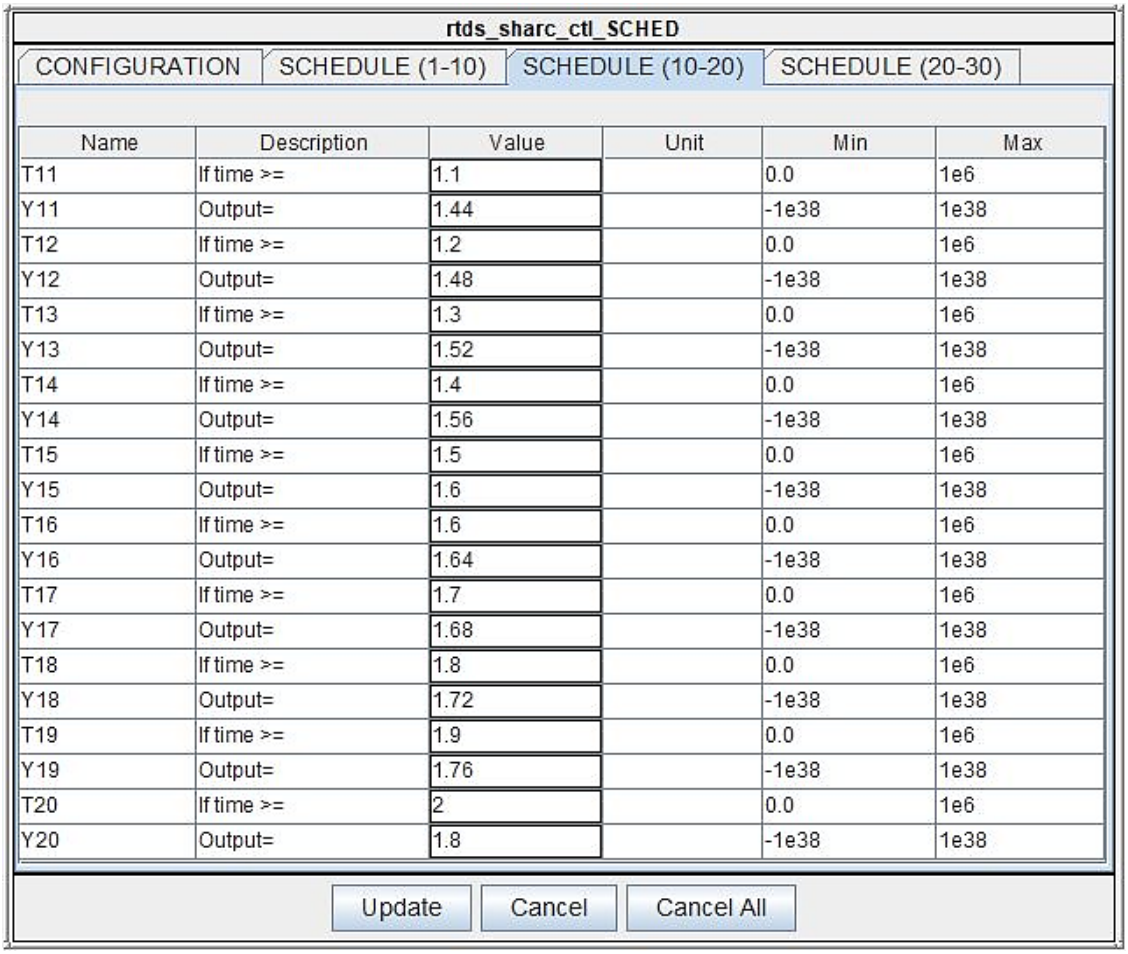

Name	Description	Value	Unit	Min	Max
T11	If time >=	1.1		0.0	1e6
Y11	Output=	1.44		-1e38	1e38
T12	If time >=	1.2		0.0	1e6
Y12	Output=	1.48		-1e38	1e38
T13	If time >=	1.3		0.0	1e6
Y13	Output=	1.52		-1e38	1e38
T14	If time >=	1.4		0.0	1e6
Y14	Output=	1.56		-1e38	1e38
T15	If time >=	1.5		0.0	1e6
Y15	Output=	1.6		-1e38	1e38
T16	If time >=	1.6		0.0	1e6
Y16	Output=	1.64		-1e38	1e38
T17	If time >=	1.7		0.0	1e6
Y17	Output=	1.68		-1e38	1e38
T18	If time >=	1.8		0.0	1e6
Y18	Output=	1.72		-1e38	1e38
T19	If time >=	1.9		0.0	1e6
Y19	Output=	1.76		-1e38	1e38
T20	If time >=	2		0.0	1e6
Y20	Output=	1.8		-1e38	1e38

Figure B.3: Dynamic Load 1 (10-20) schedule (time and values) configuration settings

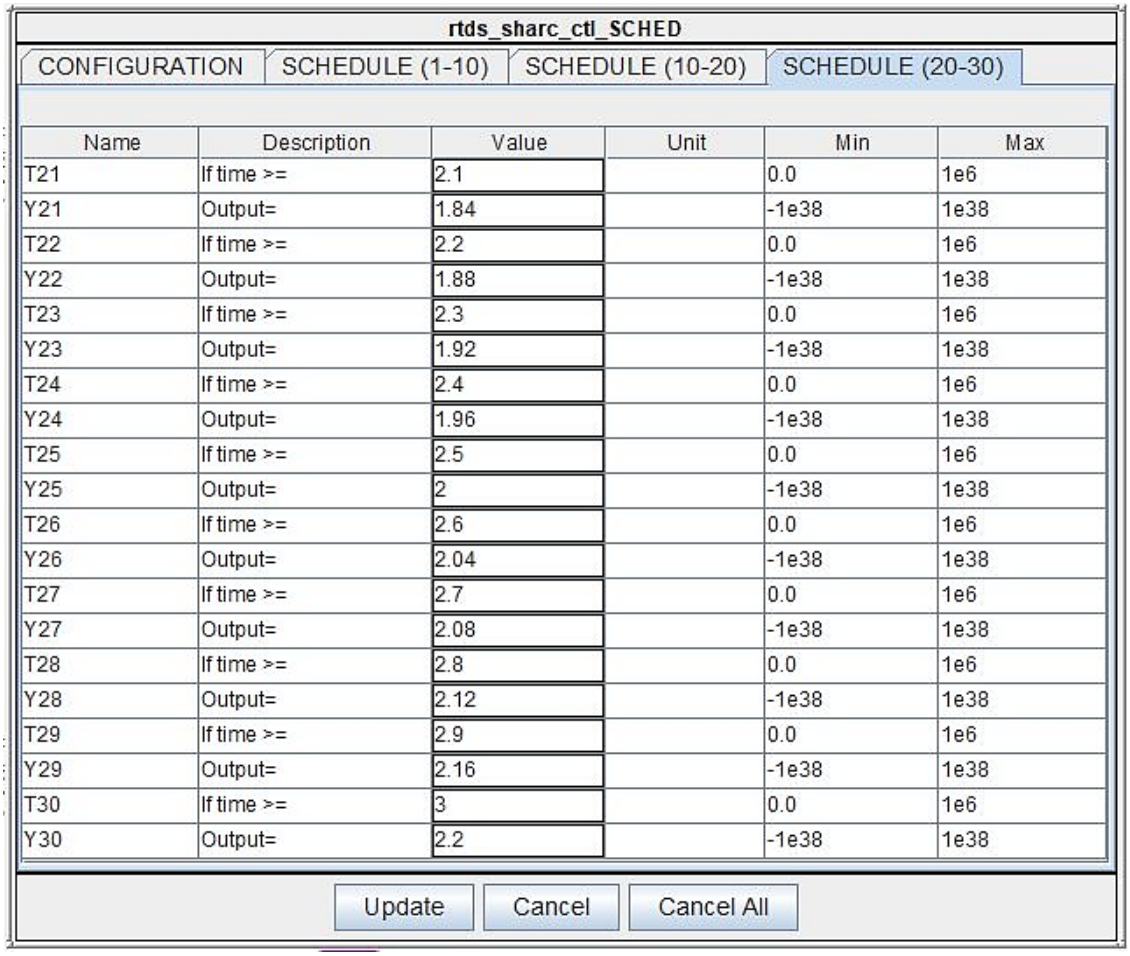

Name	Description	Value	Unit	Min	Max
T21	If time >=	2.1		0.0	1e6
Y21	Output=	1.84		-1e38	1e38
T22	If time >=	2.2		0.0	1e6
Y22	Output=	1.88		-1e38	1e38
T23	If time >=	2.3		0.0	1e6
Y23	Output=	1.92		-1e38	1e38
T24	If time >=	2.4		0.0	1e6
Y24	Output=	1.96		-1e38	1e38
T25	If time >=	2.5		0.0	1e6
Y25	Output=	2		-1e38	1e38
T26	If time >=	2.6		0.0	1e6
Y26	Output=	2.04		-1e38	1e38
T27	If time >=	2.7		0.0	1e6
Y27	Output=	2.08		-1e38	1e38
T28	If time >=	2.8		0.0	1e6
Y28	Output=	2.12		-1e38	1e38
T29	If time >=	2.9		0.0	1e6
Y29	Output=	2.16		-1e38	1e38
T30	If time >=	3		0.0	1e6
Y30	Output=	2.2		-1e38	1e38

Figure B.4: Dynamic Load 1 (20-30) schedule (time and values) configuration settings

APPENDIX C
THE WIND POWER PLANT DATA

The wind power plant (WPP) used makes use of the wind turbine (WT) and the squirrel-cage induction generator (SCIG) whose data is found from reliable sources, namely the Vestas Wind Turbine Broucher and Appendix B for Generator Parameters from the book, Power Conversion of Wind Energy Systems for provided by the reference (B. Wu, Y. Lang, N. Zargari, 2011). The data described above is presented in a form of tables in Section C.1 and C.2.

C.1 Vestas wind turbine operating data and rotor data

Table C.1: Wind turbine operating data

Parameter	Values/specifications
Nominal power (P_{N})	4 MW/4.2 MW
Cut-in-speed (v_{CI})	3 m/s
Nominal speed (v_N)	14 m/s
Cut-out-speed (v_{CO})	25 m/s
Re-cut-in-speed (V_{R-CI})	23 m/s
Wind class	EC IB-T/IEC IIA-T/IEC S-T
Standard operating temperatures	-20 ^{O}C to 45 ^{O}C with de-rating above 30 ^{O}C at 4 MW

Table C.2: Wind turbine operating data

Parameter	Values
Rotor diameter (D_R)	117 m
Swept area (A_S)	10.751 m^2
Minimum turbine angular rotor, ω_{TRMin}	2.1 rpm = 0.22 rad/sec
Nominal turbine angular rotor ω_{TRN}	9.9 rpm = 1.035 rad/sec
Maximum turbine angular rotor ω_{TRMax}	17.7 rpm = 1.85 rad/sec

C.2 Wind turbine generator data

The parameters provided in Table C.3 are referred to the stator side of the squirrel-cage induction generator.

Table C.3: Squirrel-cage induction generator parameters (B. Wu, Y. Lang, N. Zargari, 2011)

Quantities	Parameters	Per-unit parameter values
Rated output power	4.0 MW	-
Rated mechanical power	4.0606 MW	
Rated apparent power	4.842 MVA	
Rated line-to-line voltage	4000 V (rms)	
Rated phase voltage = Base voltage	2309.4 V (rms)	
Rated stator current = Base current	698.88 A (rms)	
Rated stator frequency	50 Hz	
Rated power factor	0.8261	
Rated rotor speed	1510.5 rpm	
Rated slip	-0.007	
Number of pole pairs	2	
Rated mechanical torque	25.671 kN.m	
Rated stator flux linkage	7.3917 Wb (rms)	
Rated rotor flux linkage	6.7114 Wb (rms)	
Stator winding resistance	22.104 mΩ	0.0067
Rotor winding resistance	23.1515 mΩ	0.0069
Stator leakage inductance	1.698 mH	
Stator leakage reactance	j0.53344 Ω	j0.1615
Rotor leakage inductance	1.698 mH	
Rotor leakage reactance	j0.53344 Ω	j0.1615
Magnetizing inductance	33.597 mH	
Magnetizing reactance	j10.5548 Ω	j3.1946
Base flux linkage	7.3511 Wb (rms)	
Base impedance	3.3044 Ω	
Base inductance	10.518 mH	
Base capacitance	963.29 u.F	

APPENDIX D
SEL-487B ALIAS AND INPUT CONTACT SETTING PARAMETERS

One of the primary settings within the Protection Automation and Control device is that of assigning contacts to the selected logics and declaring terminal terminal-to-bus elements. Section D.1 provides the figure with evidence using a single snapshot of how these settings were done.

D.1 Assign input contacts. (Typical Example for all terminals)

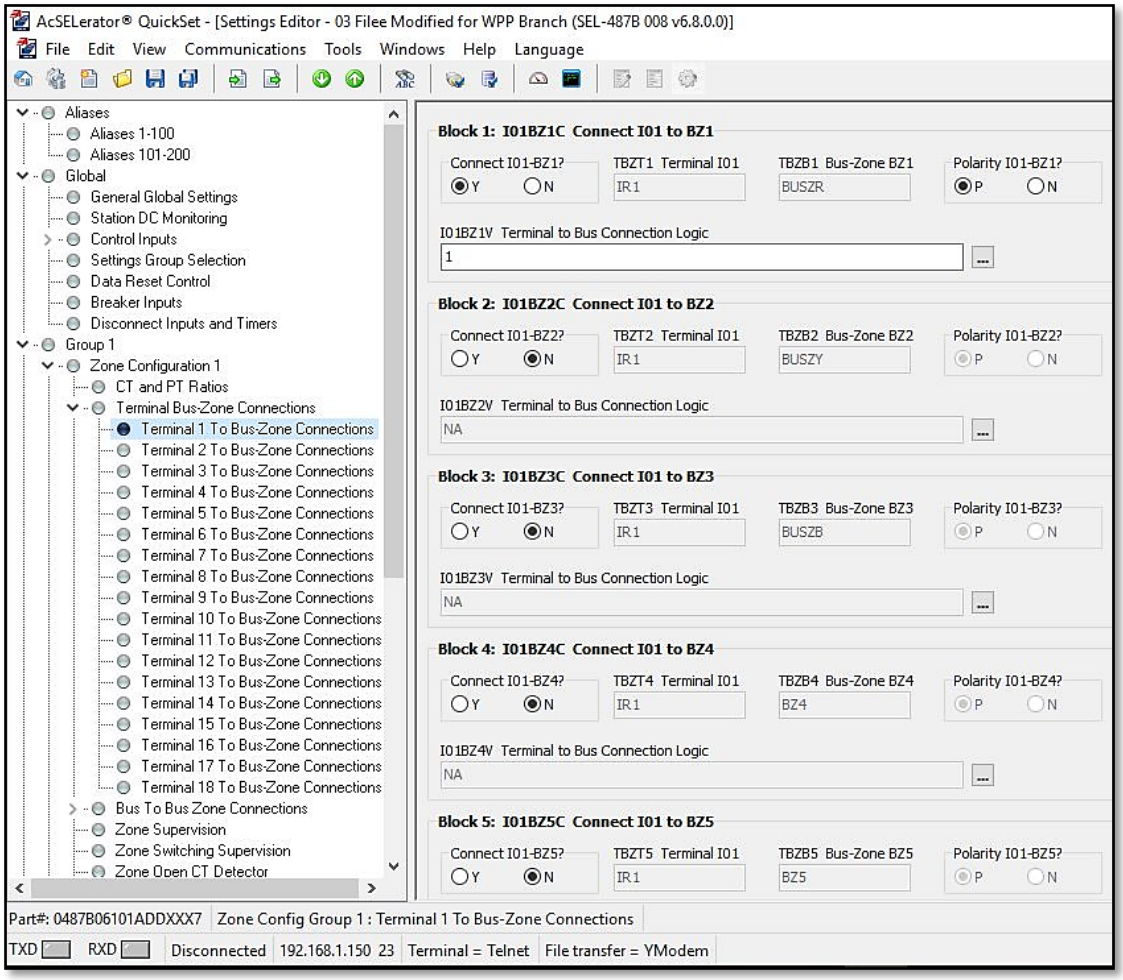

Figure D.1: Terminal 1 to bus-zone connections

APPENDIX E
EVENT REPORTS FOR FAULTS AT BUS 2 DUE TO HARD-WIRED TRIP SIGNAL

The results shown in even figures, E.1 to E.8 indicate separately the relay word bits for Zone 1-2 instantaneous differential element picked (87RP, 87YP and 87BP) and Zone 1-2 restraint differential element picked (87RT, 87YT and 87BT). The phase definite overcurrent pickup (50RP, 50YP and 50BP) and their trip bits, 50RT, 50YT and 50BT are are recorded. The switching-over between two settings groups, Group 1 and Group 2 depends on the operation of the trip bits. If any of the phase trip bits are active, Group 2 settings apply and are indicated by the word bit SG2 in even figures. Otherwise SG1 for Group 1 settings.

E.1 Events extracted at 315 MW loading

E.1.1 Red phase to ground fault

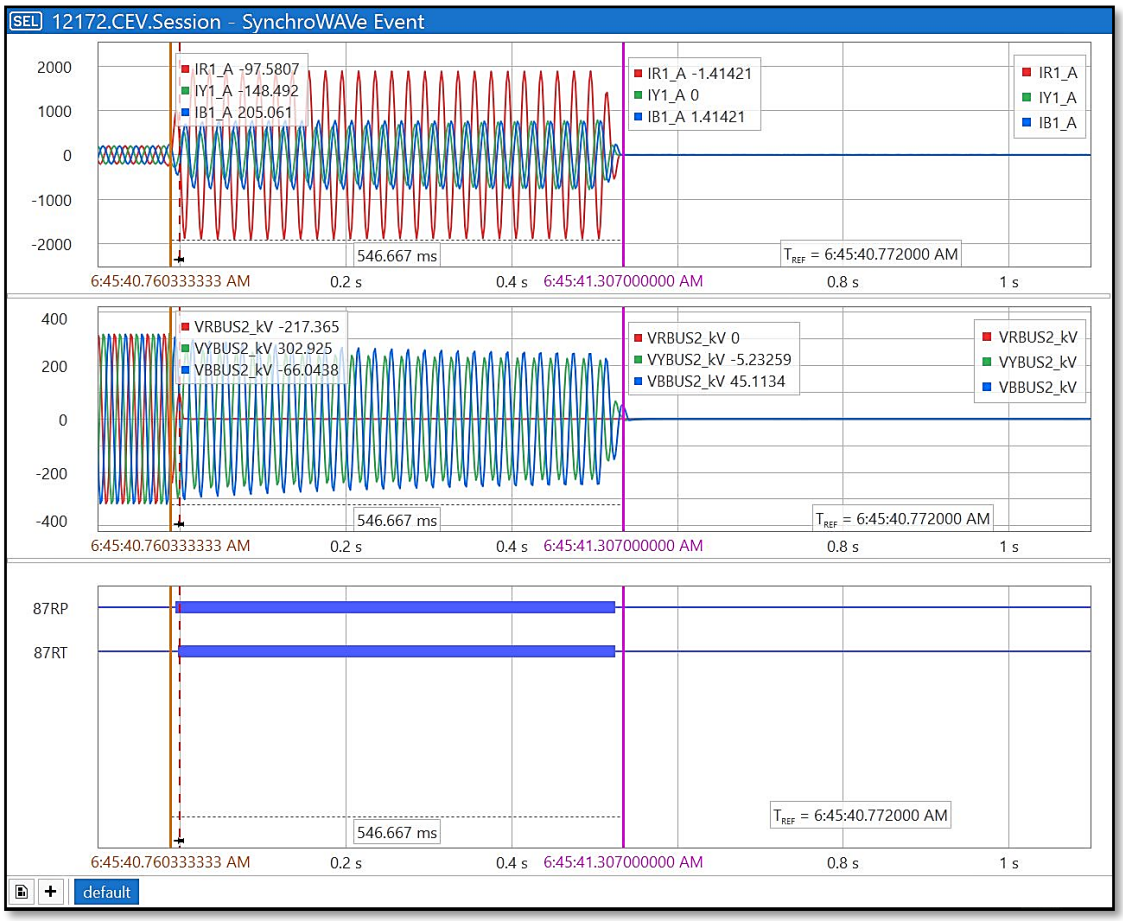

Figure E.1: Event for Red-phase-to-ground fault at Bus 2 – analogs and digitals

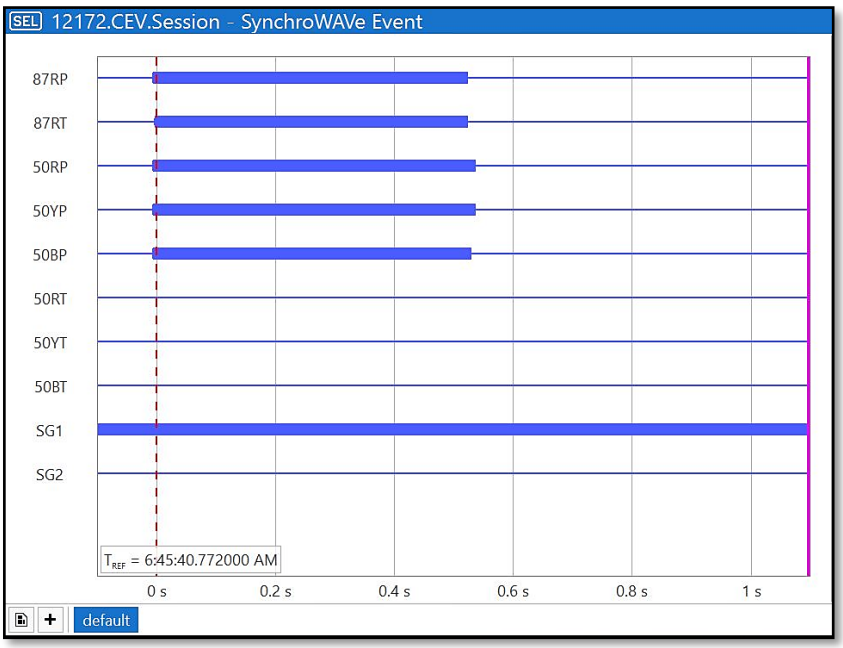

Figure E.2: Event for Red-phase-to-ground fault at Bus 2 – group 1 settings operated

E.1.2 Three-phase fault

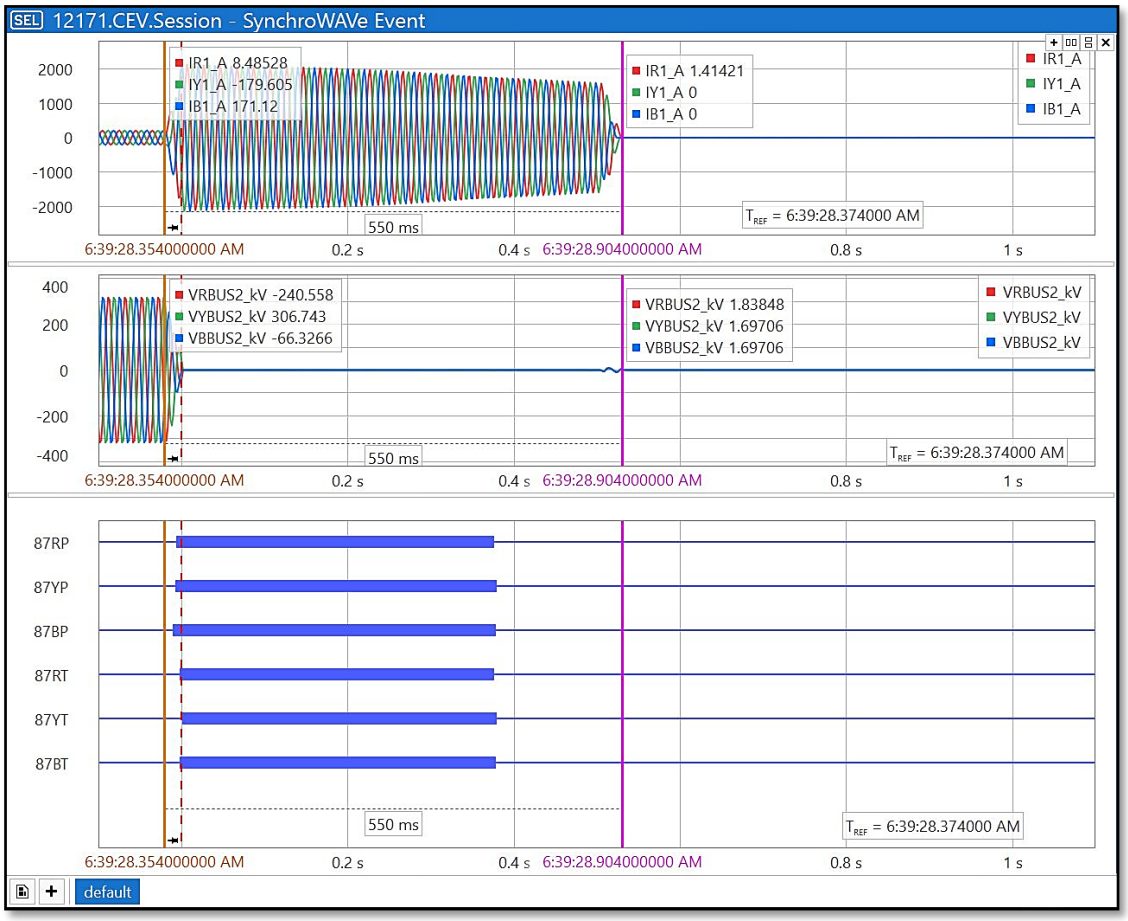

Figure E.3: Event for three-phase fault at Bus 2 – analogs and digitals

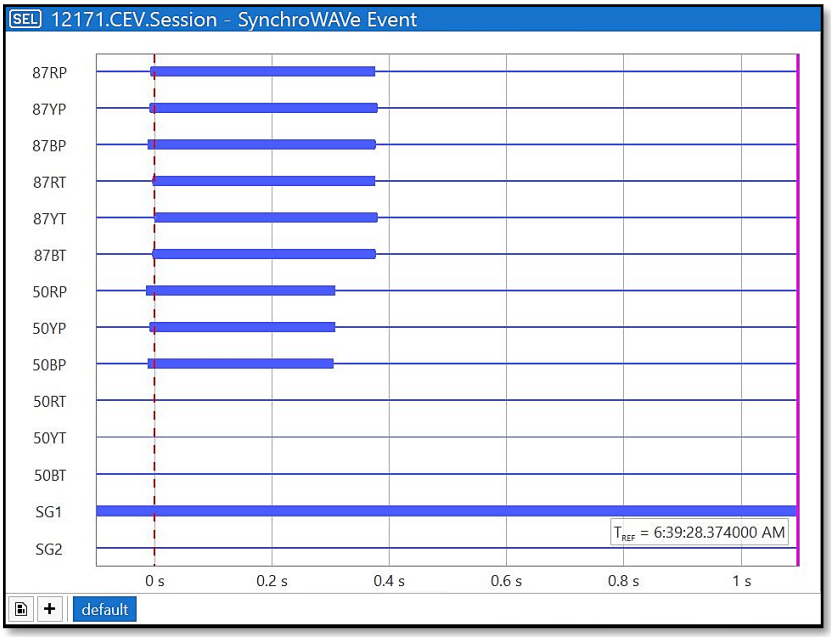

Figure E.4: Event for three-phase fault at Bus 2 – group 1 settings operated

E.2 Events extracted at 420 MW loading

E.2.1 Red phase to ground fault

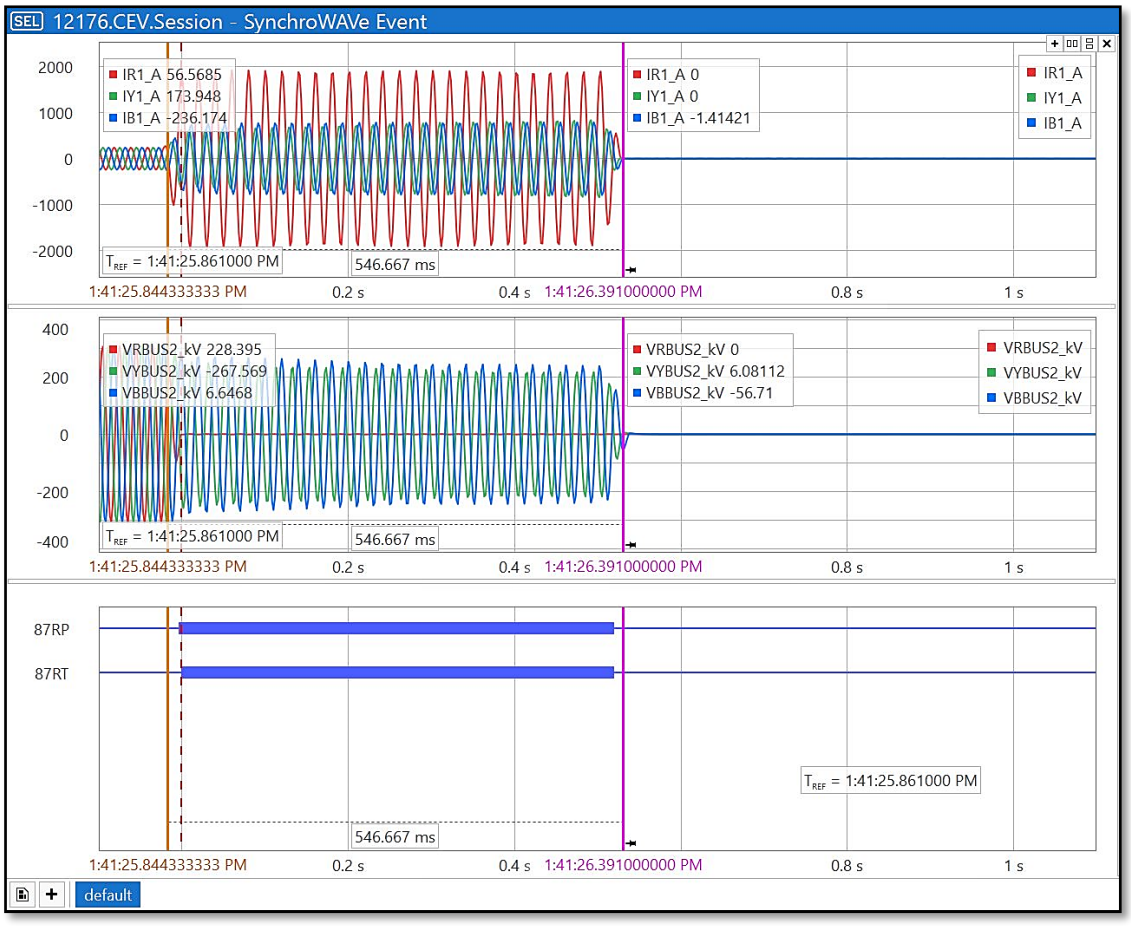

Figure E.5: Event for Red-phase-to-ground fault at Bus 2 – analogs and digital

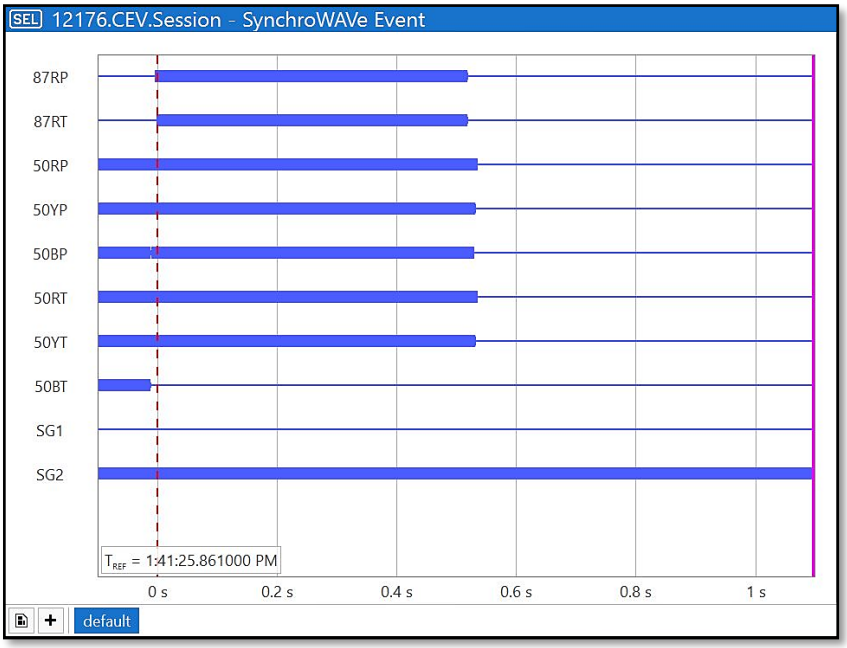

Figure E.6: Event for Red-phase-to-ground fault at Bus 2 – group 2 settings operated

E.2.2 Three-phase fault

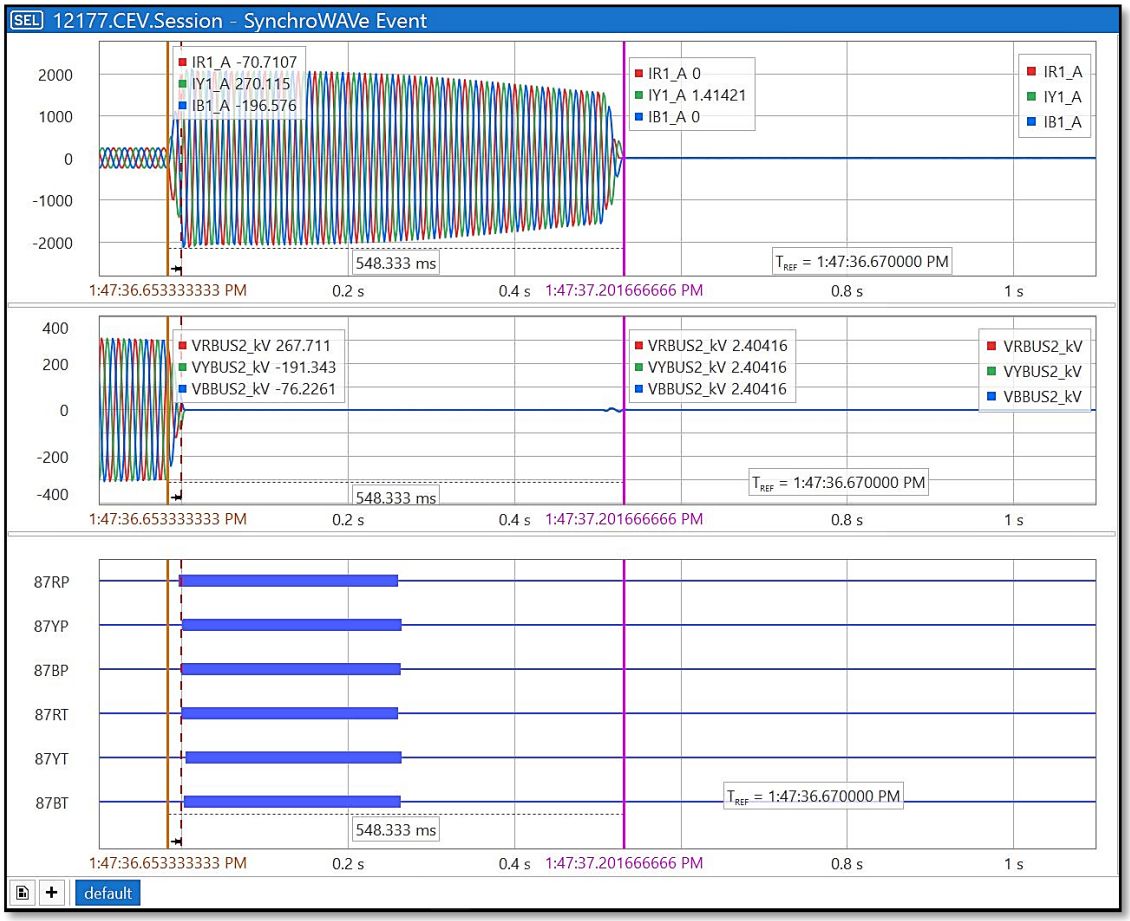

Figure E.7: Event for three-phase fault at Bus 2 – analogs and digitals

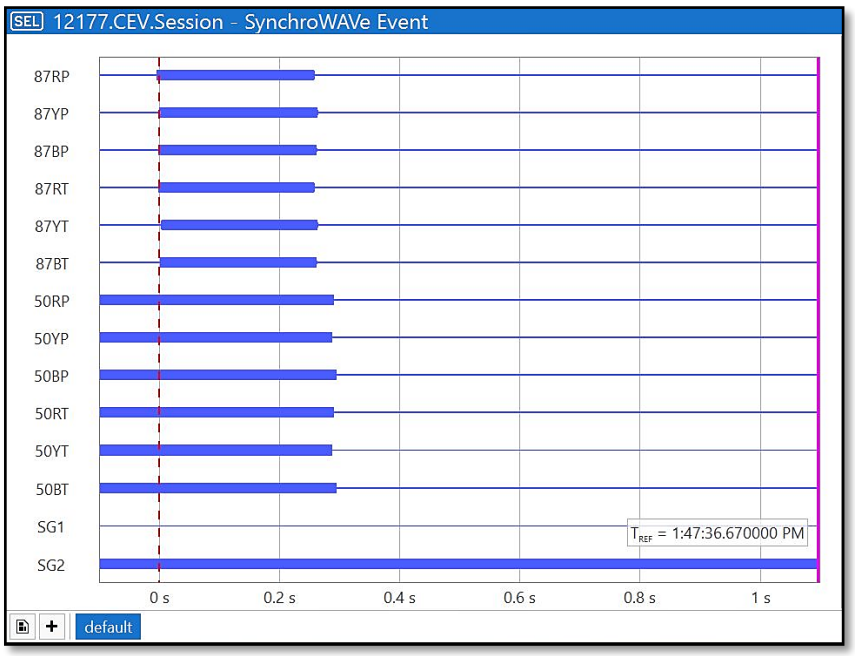

Figure E.8: Event for three-phase fault at Bus 2 – group 2 settings operated

APPENDIX F
EVENT REPORTS FOR FAULTS AT BUS 2 DUE TO GOOSE TRIP SIGNAL

The results provided in this appendix are those that are obtained when the protection scheme uses the GOOSE control model to operate the circuit breakers. The switching-over between two settings groups, Group 1 and Group 2 depends on the operation of the trip bits. If any of the phase trip bits are active, Group 2 settings apply and are indicated by the word bit SG2 (or GRP2SET) in even figures (F.2 to F.8). Otherwise SG1 (or GRP1SET) for Group 1 settings. GRP1SET and GRP2SET are aliases for SG1 and SG2. This is because the relay word bits SG1 and SG2 were renamed (aliased) at the later stage.

F.1 Events extracted at 315 MW

F.1.1 Red phase to ground fault

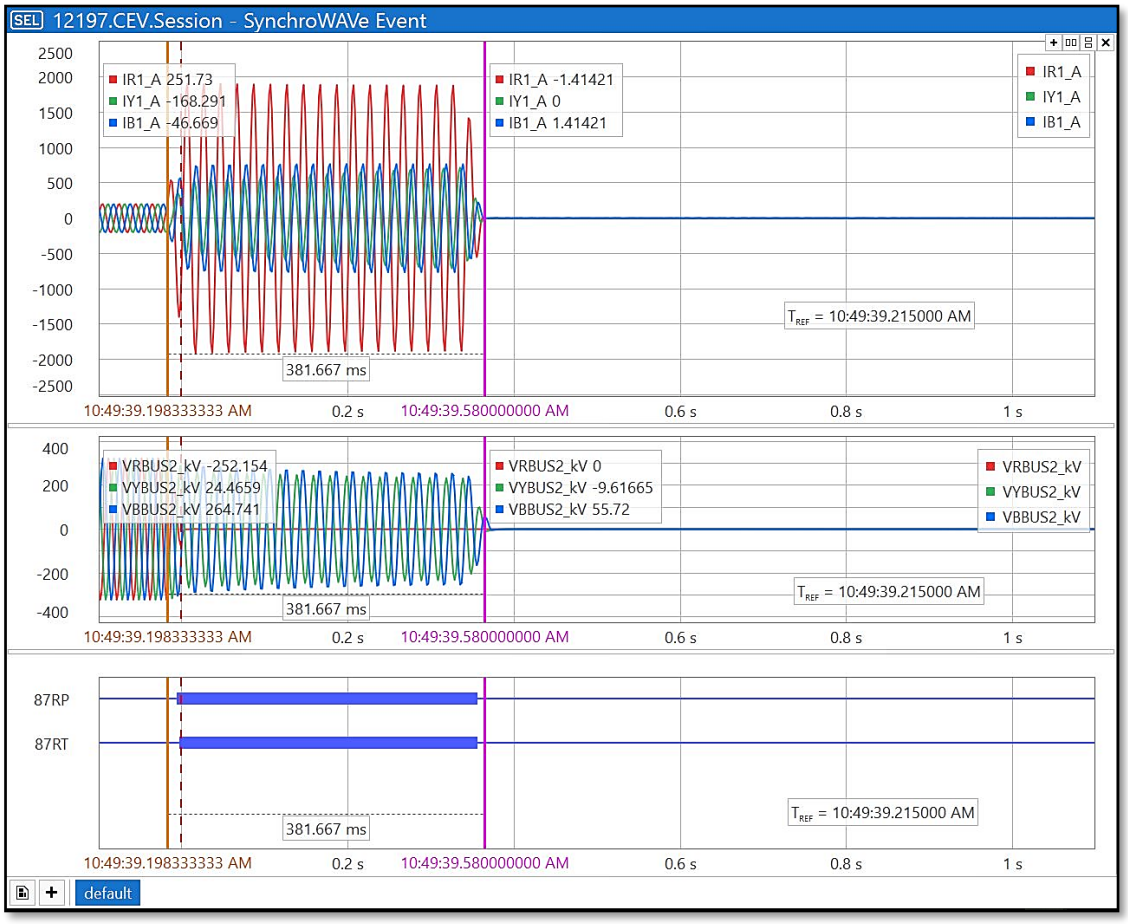

Figure F.1: Event for Red-phase-to-ground fault at Bus 2 – analogs and digitals

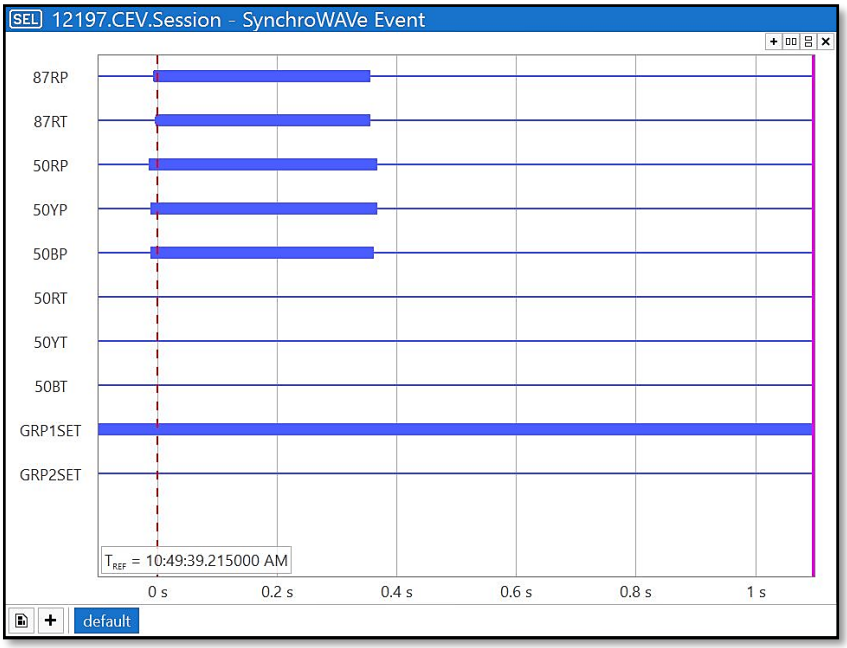

Figure F.2: Event for Red-phase-to-ground fault at Bus 2 – group 1 settings operated

F.1.2 Three-phase fault

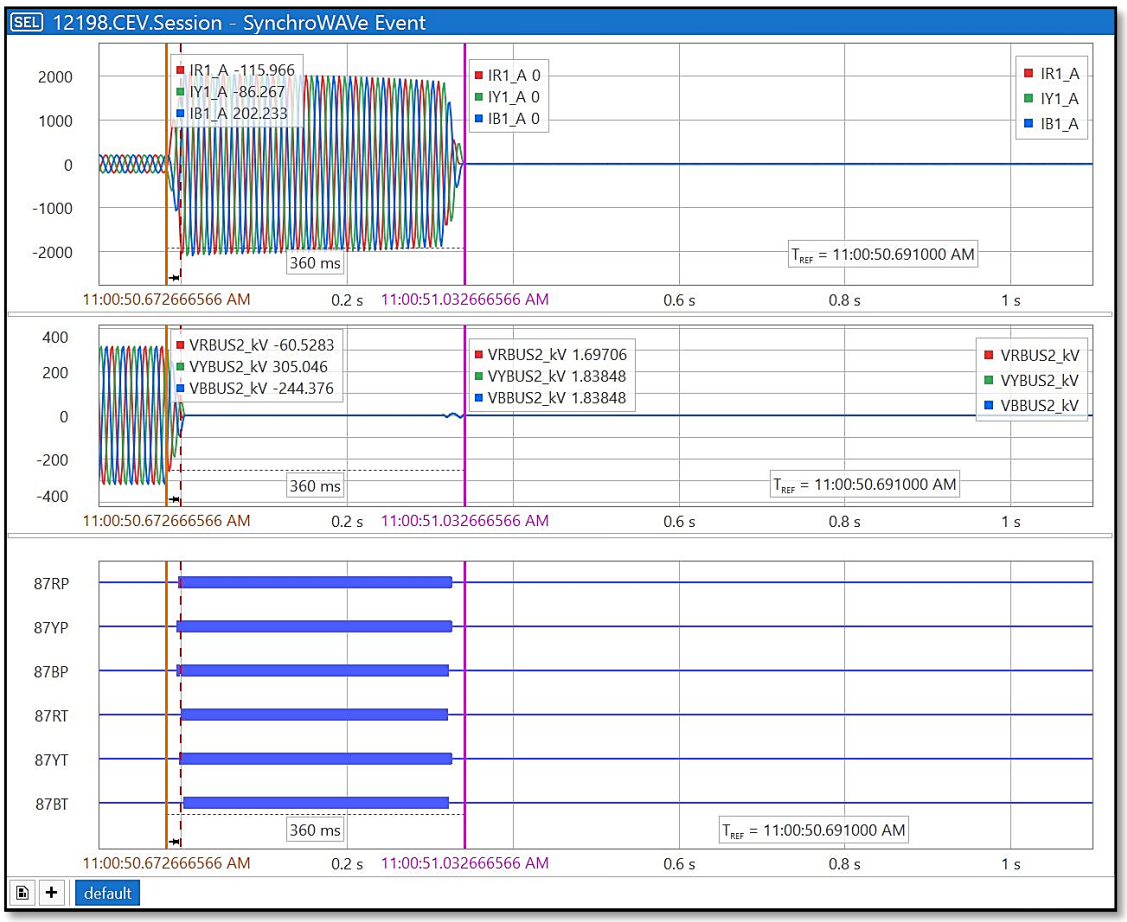

Figure F.3: Event for three-phase fault at Bus 2 – analogs and digitals

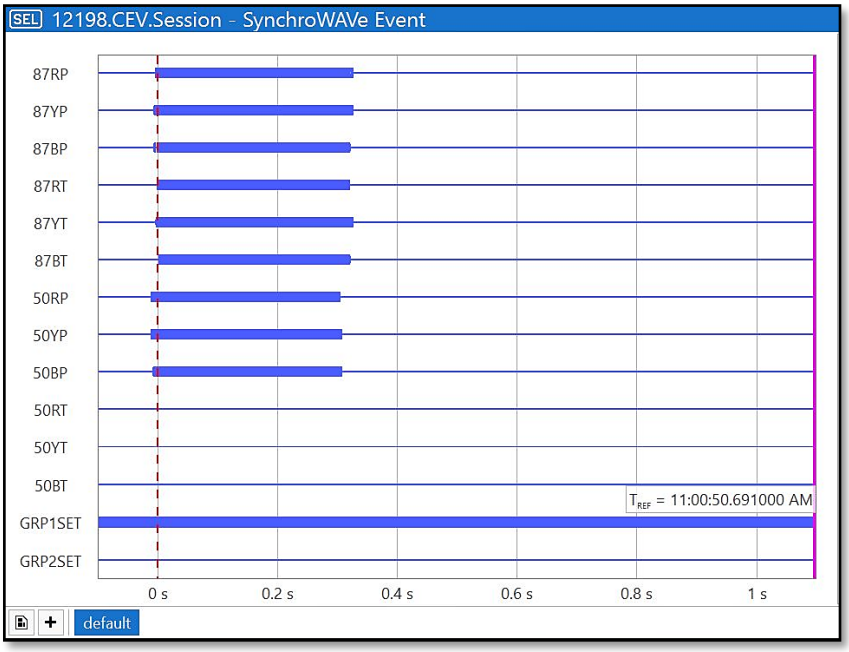

Figure F.4: Event for three-phase fault at Bus 2 – group 1 settings operated

F.2 Events extracted at 420 MW

F.2.1 Red phase to ground fault

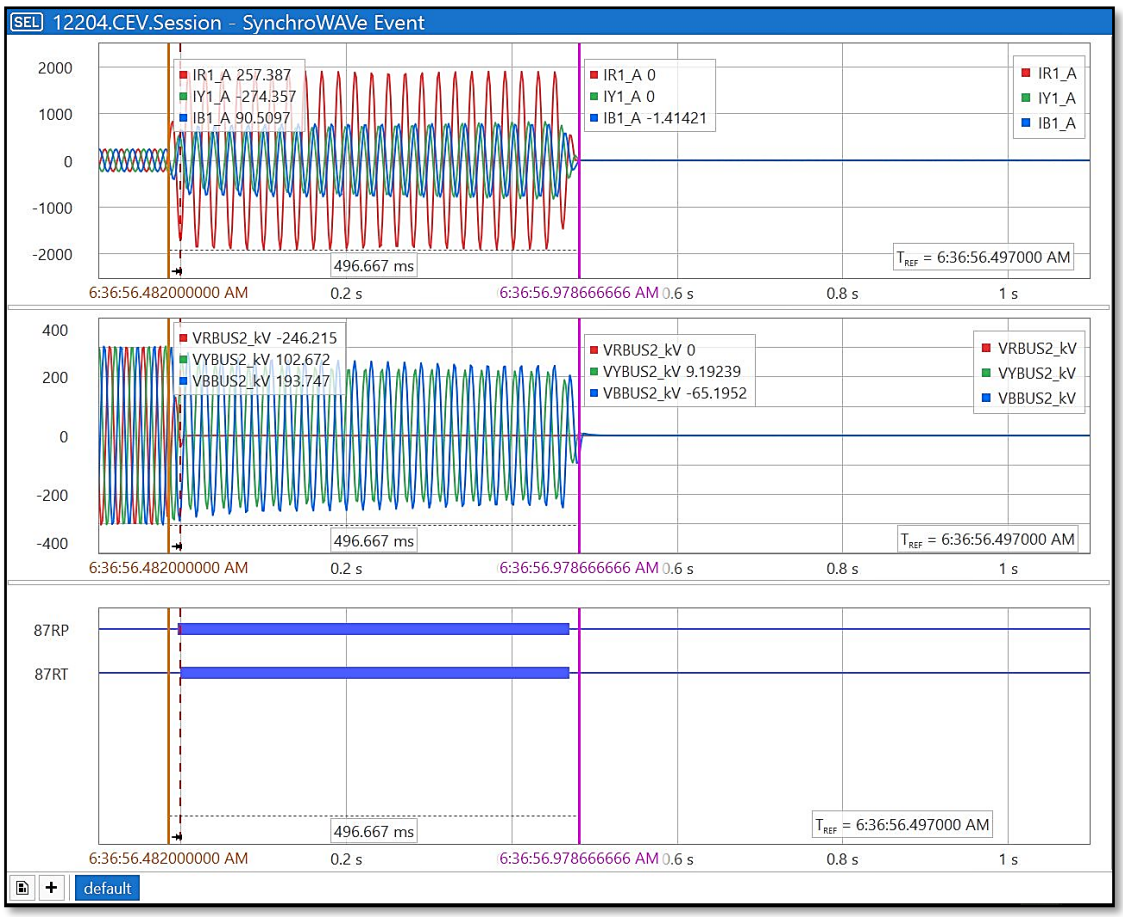

Figure F.5: Event for Red-phase-to-ground fault at Bus 2 – group 2 settings operated

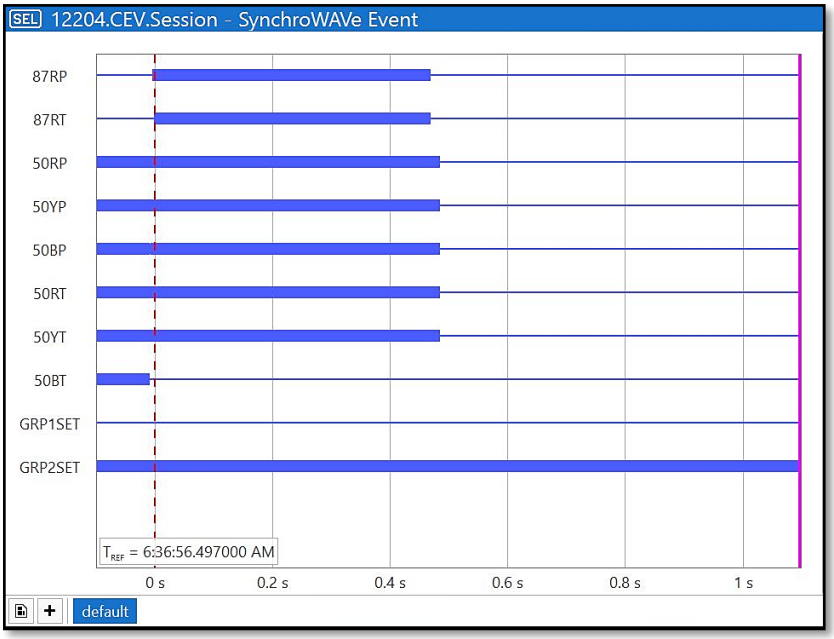

Figure F.6: Event for Red-phase-to-ground fault at Bus 2 – group 2 settings operated

F.2.2 Three-phase fault

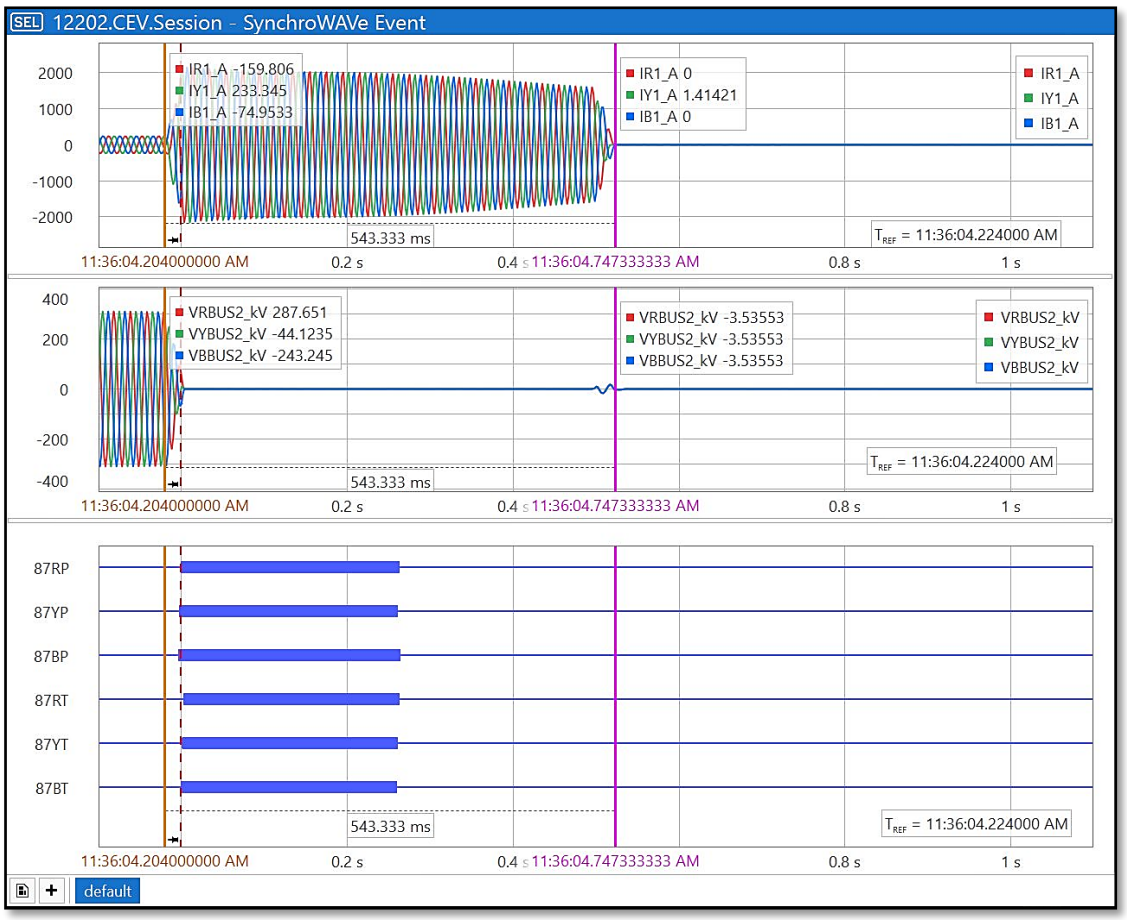

Figure F.7: Event for three-phase fault at Bus 2 – analogs and digitals

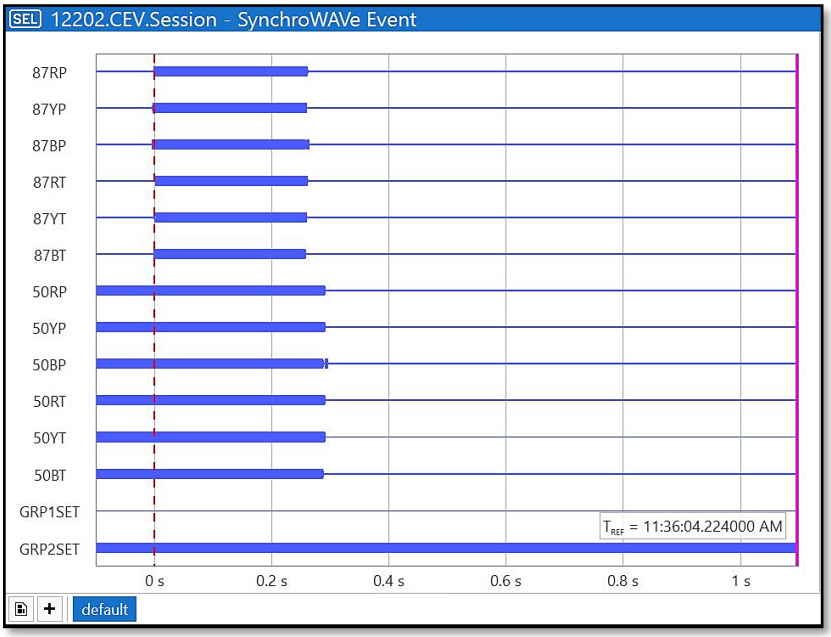

Figure F.8: Event for three-phase fault at Bus 2 – group 2 settings operated

APPENDIX G
THE HARDWARE-IN-LOOP (HIL) TEST BENCH SET-UP

The test bench setups were done for the developed common point of coupling (PoCC) protection scheme in Chapters 6 and 7. In Chapter 6, the relay's binary output trip signals were done using the hard-wired signals for control of virtual circuit breakers in the real-time digital simulator devices where the virtual power system network is simulated.

For both cases, the physical intelligent electronic device (IED) receives analogue currents using copper wires for both phase voltages and currents. As output feedback to the RTDS for control and protection, the test in Chapter 6 made use of three sets of binary output trip signal wires as shown in Figure G.1.

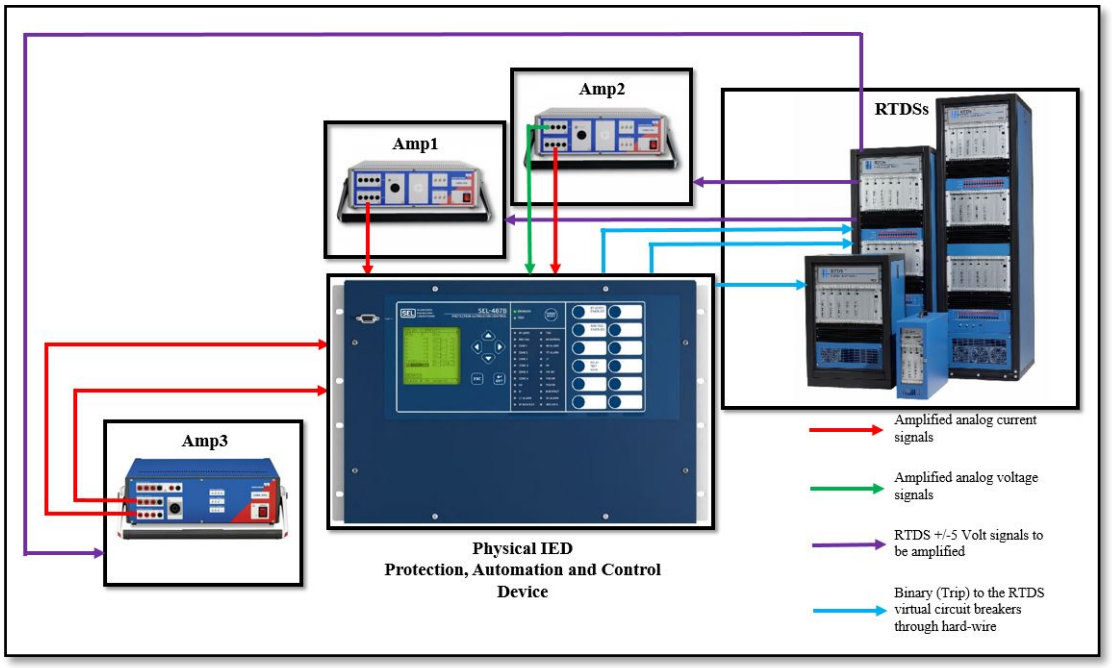

Figure G.1: The HIL test bench setup for the developed protection scheme test in Chapter 6

In the figure, Amp 3 measures the currents flowing through the branches, DLoad1 branch and wind power plant supply branch. The relays use this current as the reference. Amp 1 measures from the Line12RE branch, and Amp 2 measures the current at Line24SE and voltage at Bus 2.

The system in Chapter 7 is the same as the one in the above figure, except for the outputs from the relay to the RTDS, that are sent via Ethernet.